

# Radiofluorination of amines via hypervalent iodonium (III) ylides, reduction & activating group approach

Gaute Grønnevik



Master thesis in Chemistry

Department of Chemistry, University of Oslo, Norway

Faculty of Mathematics and Natural Sciences

May 2017

© Gaute Grønnevik

2017

Radiofluorination of amines via hypervalent iodonium(III) ylides, reduction & activating group approach

<http://www.duo.uio.no/>

Print: Reprosentralen, University of Oslo

# Abstract

Radiofluorination of basic amines are a well-known challenge in  $^{18}\text{F}$ -radiochemistry, and deactivated arenes are a particular challenge for radiolabeling in general. Current methods are often insufficient to label tertiary amines. Various approaches such as transition metal-mediation have been investigated for radiolabeling electron rich arenes, but these methods are often absent in clinical radiopharmaceutical chemistry due to non-cGMP compliance.  $\lambda^3$ -iodoarenes share some reactivity with heavy metals, but do not share their toxicity and environmental damage. The goal of this work is develop a route for radiofluorinating deactivated aryl rings by using interconversion of amide/amine functional groups, as the proximity of amides facilitate arene deactivation while also functioning as unconventional protective groups in the oxidizing synthesis step.

By applying literature procedures the ylides of hypervalent iodonium (III) iodanes were obtained, synthesized as precursors for radiochemical incorporation of  $^{18}\text{F}$ . Literature procedures for synthesizing fragments of compounds of radiopharmaceutical interest (such as anilines, N-methyl-1-phenylmethamamines and indoles) were successful. A high yielding method was developed for drying, reducing and purifying n.c.a.  $^{18}\text{F}$ -labeled 4-fluoro-N,N-dimethylaniline. Radiolabeling the deactivated aniline achieved an overall RCY of 36% (decay corrected), with 90 minutes passing from start to achieving a purified compound. Synthesis of N-(4-fluorophenyl)-N-methylformamide to a secondary amine by hydrolysis was also successful.

Applying developed conditions to achieve successful labeling and reduction on other analogs was moderately too successful. However, with an increase in temperature and time moderate to good results were yielded. Iodonium ylides proved sensitive to light and air, and the age of iodonium ylides heavily influenced the results. Iodonium ylides were heavily favored as a leaving group compared to nitro group typical for  $\text{S}_{\text{N}}\text{Ar}$  reactions in radiofluorination.





# Preface

The present work was performed at the Department of Chemistry at the University of Oslo from August 2015 to May 2017 in the research group of Associate Professor Patrick Riss. This work is part of a scientific poster presented at the 22<sup>nd</sup> International Symposium on Radiopharmaceutical Sciences (ISRS) and a manuscript for publication is in preparation.

I would like to give my sincere thanks to my supervisors; Associate Professor Patrick Riss and PhD candidate Jimmy Erik Jakobsson for taking a genuine interest for teaching me chemistry during this time period, for great suggestions, feedback and helpful discussions.

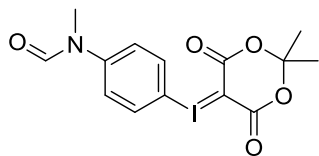
The compound used for method development was synthesized by, and the method development was done in a joint effort with another member of the research group, Jimmy Erik Jakobsson (JEJ). I would like to thank Osamu Sekiguchi for helping with the mass spectroscopy analysis, and Frode Rise for help with NMR analysis. You have both been more than accommodating when asked for help.

I would like to thank the people who have read through the thesis, and to thank my family, friends, office mates, colleagues and girlfriend.

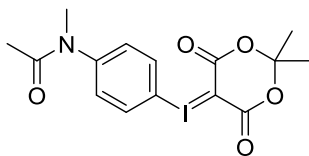
# Table of content

1	Introduction .....	11
1.1	Radioactive decay and decay characteristics .....	11
1.2	On the synthesis of radiotracers.....	15
1.3	Introduction of the radiotracer .....	17
1.3.1	Production of <sup>18</sup> Fluorine.....	17
1.3.2	Methods of <sup>18</sup> F-fluorine introduction routinely used .....	19
1.3.3	Radiofluorination using hypervalent iodonium(III).....	22
1.3.4	Amines and amides in radiopharmaceuticals .....	28
1.3.5	Biologically important compounds of substructures.....	31
2	Aim of study.....	33
3	Results and discussion.....	35
3.1	Designing the synthesis and developing a method for radiofluorination .....	35
3.2	Method development for radiofluorination .....	38
3.2.1	Drying agent and elution screening.....	38
3.2.2	Reducing agent and additive screening .....	41
3.2.3	Solvent screening .....	42
3.2.4	Temperature and reducing agent equivalent screening .....	44
3.2.5	Application to other analogs .....	46
3.2.6	Hydrolysis .....	48
3.3	Activity loss and method application .....	51
3.4	Iodonium ylide yield and appearance .....	55
3.4.1	Radiochemical conversion of ylides .....	56
3.5	Iodonium ylide degradation.....	57
3.6	Competition experiment .....	61
4	Experimental Section .....	63
4.1	General.....	63
4.2	Radiochemical procedures.....	64
4.3	Organic procedures.....	65
5	Conclusions and outlook .....	79
	Bibliography.....	80

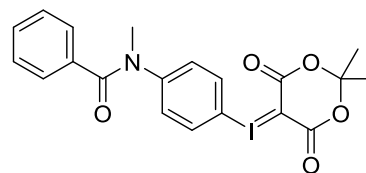
# Important compounds in thesis



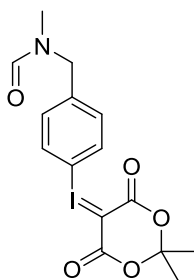
1a)



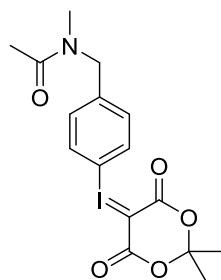
2a)



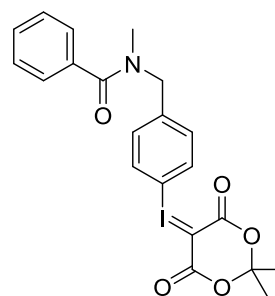
3a)



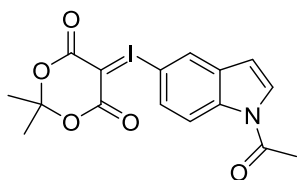
4a)



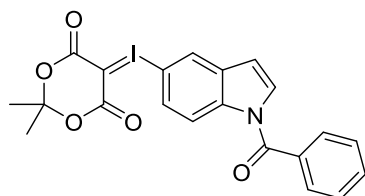
5a)



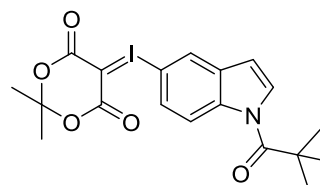
6a)



7a)



8a)



9a)

# Abbreviations

MeOH – Methanol

MeOD - Deuterated Methanol

EtOH – Ethanol

AcN - Acetonitrile

DCM – Dichloromethane

DCE – Dichloroethane

DME - Dimethoxyethane

DMSO - Dimethylsuloxide

PhMe - Toluene

mCPBA - meta-Chloroperoxybenzoic Acid

DMAP – 4-*N,N*-Dimethylaminopyridine

PhSiH<sub>3</sub> – Phenylsilane

PPh<sub>3</sub> – Triphenylphosphine

HMPT - Hexamethylphosphorous triamide

VB<sup>iPr</sup> – Verkade S Base, 2,8,9-Triisopropyl-2,5,8,9-tetraaza-1-phosphabicyclo[3,3,3]undecane

9 BBN – 9-borabicyclo[3.3.1]nonane

Crypt-222 - Kryptofix<sup>®</sup>-222 / K<sub>222</sub> - 4, 7, 13, 16, 21, 24-hexaoxa-1-10-diazabicyclo[8.8.8]hexacosane

PhCH<sub>2</sub> – Benzyl group

Bz – Benzoyl group

Piv – Pival(o)yl group

Et – Ethyl group

CH<sub>3</sub>CO – Acetyl group

CHO – Formyl group

TMEDA - Tetramethylethylenediamine

Eq. - Equivalents

S<sub>N</sub>Ar - Nucleophilic Aromatic Substitution Reaction

S<sub>N</sub>2 – One-step nucleophilic substitution reaction

Conventional or stoichiometric - Reactions without artificial radionuclides

RCY - Radiochemical Yield, the yield of a radiochemical separation expressed as a fraction of the activity originally present (IUPAC definition).

cGMP - Current Good Manufacturing Practice

Hot / Hot chemistry – Using radioactive isotopes

Cold / Cold chemistry – Using non-radioactive isotopes

EC - Electron Capture

NMR – Nuclear Magnetic Resonance

MS – Mass Spectrometry

HR-MS – High-Resolution Mass Spectrometry

*m/z* – Mass-to-Charge ratio

ESI - Electrospray ionization

QTOF – Quadruple Time Of Flight

TOF – Time Of flight

n – Replicate(s)

ppm – Parts Per Million

HBA – Hydrogen Bond Acceptor

HBD – Hydrogen Bond Donor



# 1 Introduction

## 1.1 Radioactive decay and decay characteristics

The smallest form a chemical can be is an atom. It consists of a nucleus and surrounding electrons. The nucleus is again subdivided into one or more positively charged particles, protons denoted by  $Z$ , and an equal or similar number of uncharged particles, neutrons denoted by  $N$ . The neutron has an approximate mass equal to the proton. The proton number defines the chemical element and is equal to the number of electrons in an uncharged atom. The neutron defines which isotope or nuclide the element is in. The nucleus ( $Z + N$ ) has a positive charge coming from the proton, which is surrounded by negatively charged electrons. Electrons are attracted to the nucleus by columbic attraction forces. The nuclei are kept together by a residual strong force. As the positive charge of the protons repels each other, the electrically neutral neutrons help the atom to stabilize by reducing the electrostatic repulsion of the protons.

A radioactive or unstable nuclide aims to stabilize itself by emitting the excess energy, either as gamma radiation, creating a new particle (alpha or beta particle) or by transferring its energy to a surrounding electron. The reason a nuclide undergoes beta decay can be either too high or too low neutron to proton ratio, compared with the ratio required for stability. Too many protons to neutrons can result in the release of a  $\beta^+$  particle, while the opposite can cause release of a  $\beta^-$  particle. While the  $\beta^-$  particle is identical to an electron with regards to both mass and charge, the  $\beta^+$  (positron) is an antiparticle to an electron. They are identical in mass, but opposite in charge. A third beta decay called electron capture (EC) is also possible. In an EC a proton - rich nucleus absorbs an electron from inner (K or L) shell, transmuting a proton to a neutron within the nucleus. As the vacancy in the electron shell is filled by electrons in the upper shell, a detectable x-ray is released.

The positron decay has been of a particular interest in medicinal imaging, forming the basis of positron emission tomography - PET. Positron decay is the conversion of a proton in the original nucleus (mother) into a neutron in the product (daughter), leaving the atomic mass number unchanged. Positron decay is an isobaric process characterized by a neutron deficient isotope emitting a  $\beta^+$  particle and an electron neutrino,  $\nu_e$ . The decay of a nuclide is dictated from the law of mass-energy equivalence, famously formulated by Einstein  $E = mc^2$ . Positron

emission is favored if the energy of the mother-to daughter decay energy is larger than 1.022 MeV. The daughter needs to balance its charge, creating one electron (511 keV) and one positron (511 keV).

The energy of the  $\beta^+$  particle declines as it passes through matter. When the  $\beta^+$  particle has lost almost all its energy, it interacts with electron shells of the surrounding matter and a particle-antiparticle annihilation process will occur. As the positron-electron pair annihilates the mass is converted into two energy photons of 511 keV (one electron mass each), travelling approximately  $180^\circ$  from each other. Combining a positron emitting nuclide with a biologically active molecule creates a biological radiotracer. By following an injection of a radioactive dose into a subject, the radioactivity distribution of the radiation emissions can be used to create a computerized reconstruction in 2D or 3D images. This allows for studying the behavior of the drug molecule. The detection of these emissions, the principle of a PET scan is shown in Figure 1, courtesy of Wikipedia.<sup>1</sup> These can be detected within the patient using data from multiple coincidence detectors in a circular gantry.<sup>2-3</sup>

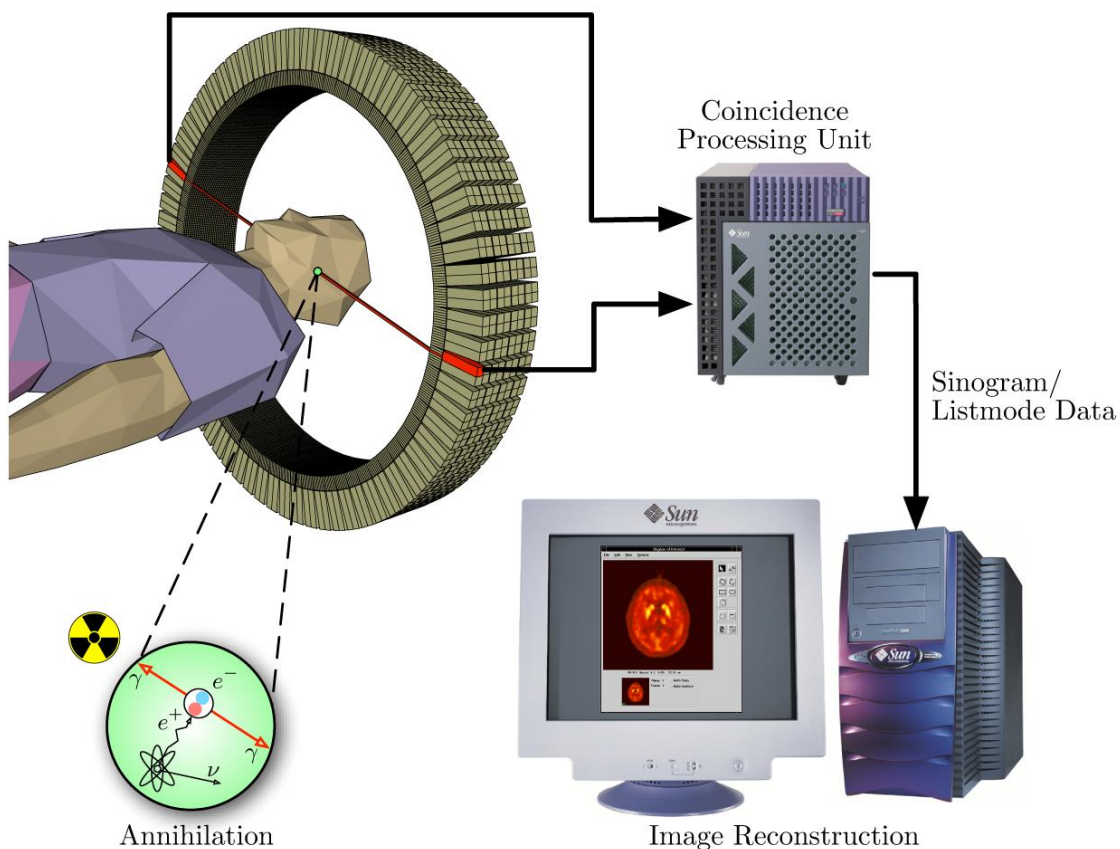


**Figure 1** The radionuclide is accumulated within the patient, and as it decays by positron emission the photons are detected in coincidence by scanners in a circular gantry. The signal is registered and processed before a final image is reconstructed by a computer.

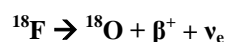


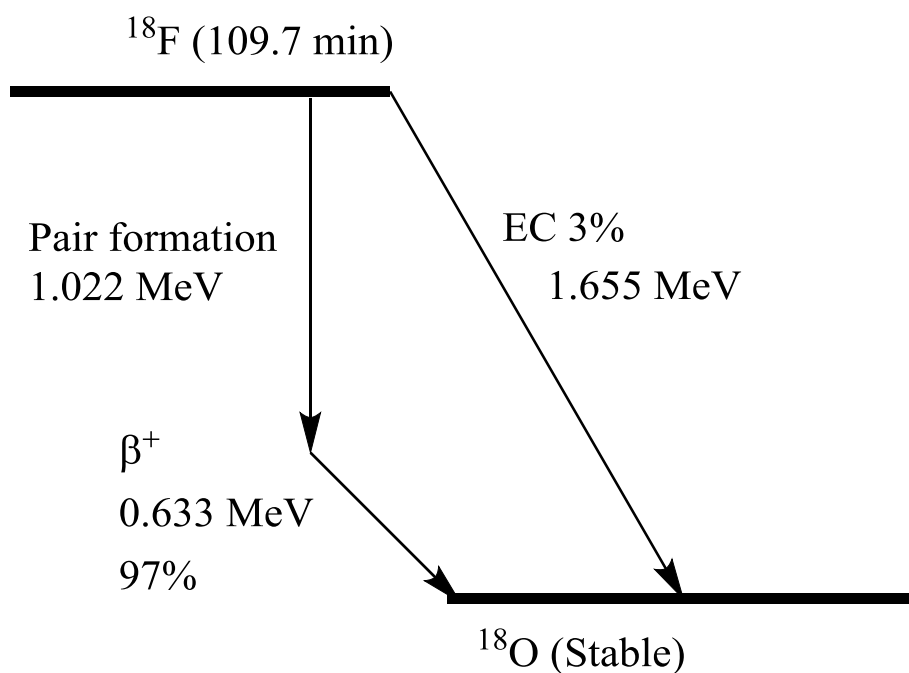
The technology for detecting photons emitted from radiolabeled compounds forms the basis of positron emission tomography (PET) and single photon emission computed tomography (SPECT). With SPECT the radiation is detected using a NaI scintillation detector with collimation, while PET uses high density detectors with a coincidence circuit, which greatly increase the imaging quality and the resolution. Even though magnetic resonance imaging (MRI) and computerized tomography (CT) can provide detailed anatomical images, non-invasive PET imaging techniques permit high resolution imaging of metabolic and chemical processes. The probe is accumulated within the body in precise regions of interest and the radioactive labeled material can be observed.<sup>4</sup> The usage of radioisotopes as a tool for adsorption, distribution, metabolism and excretion (ADME) studies has extensively advanced biochemistry and metabolism studies.

While there are several isotopes emitting positrons in clinical use such as <sup>13</sup>N ( $t_{1/2} = 9.97$  min), <sup>15</sup>O ( $t_{1/2} = 2.04$  min), and <sup>68</sup>Ga ( $t_{1/2} = 67.6$  min) the most commonly used isotopes used for labeling in PET remain <sup>18</sup>F ( $t_{1/2} = 109.8$  min) followed by <sup>11</sup>C ( $t_{1/2} = 20.4$  min).

As the most used radionuclide in PET, <sup>18</sup>F is an important radionuclide in the field of molecular imaging. This isotope decays with 97% positron emission and 3% electron capture (EC), depicted in Scheme 1. The energy of the decay is split between the neutrino and the  $\beta^+$  particle, ranging from 0 keV up to maximum energy of 0.63 MeV.

**Equation 1: The decay of the unnatural isotope <sup>18</sup>F. It decays to the stable isotope, <sup>18</sup>O by releasing the excess energy either by electron capture (3%) or positron emission (97%).**





**Scheme 1** The decay of  $^{18}\text{F}$  can occur in two ways: by electron capture (EC), where it decays directly to the ground state and occurs in 3% of  $^{18}\text{F}$  decay. It can also decay by undergoing an electron-positron pair formation, and allows a maximum of 0.63 MeV transferred to the positron, which happens in 97% of  $^{18}\text{F}$  decays.

The energy released in a nuclear reaction is called the Q-value. As a nuclide decays by positron emission, the energy is split between the positron and the neutrino. The average energy transferred to the beta particle of several nuclides decays, their half-life and maximum positron travel range in water (tissue) can be found in Table 1.

**Table 1: Physical characteristics of commonly used PET radionuclides, including the half-life, mode of decay, average beta energy and the range of this beta decay in water/tissue.**

Isotope	Half-life	Decay mode	Average beta energy (keV)	Max positron range in water/tissue (mm)
$^{11}\text{C}$	20.4 min	99.8% $\beta^+$ / 0.24% EC	385	3.8
$^{18}\text{F}$	109.7 min	96.9% $\beta^+$ / 3.1% EC	242	2.4
$^{15}\text{O}$	122.2 s	99.9% $\beta^+$ / 0.01% EC	735	7.6
$^{13}\text{N}$	9.97 min	99.8% $\beta^+$ / 0.2% EC	491	5
$^{68}\text{Ga}$	67.7 min	88.9% $\beta^+$ / 11.1% EC	890	8.9

$^{18}\text{F}$  is the used radionuclide in medicinal imaging and techniques of introducing it into molecules have been substantially investigated, largely motivated by the successful use of the glucose analog 2- $^{18}\text{F}$ fluoro-2-deoxy-d-glucose ( $^{18}\text{F}$ FDG) in clinical oncology and medicinal chemistry. This is due to its manageable half-life and excellent decay characteristics, as shown in Table 1. It is also easily produced in large quantities and with high specific activity. Even after a promising pharmaceutical has been discovered, there has been a concomitant need to investigate routes of incorporating an  $^{18}\text{F}$  or  $^{11}\text{C}$  isotope into the molecule. The  $^{18}\text{F}$  labeling differentiates from traditional fluorine chemistry and stems from the production of the artificial isotope. Typically it is produced by bombarding enriched  $^{18}\text{O}$  water with high energy protons using a cyclotron or a linear particle accelerator. So far the  $^{18}\text{F}$  isotope has shown a lot of promise for radiolabeling.

## 1.2 On the synthesis of radiotracers

Since its discovery the usage of radioisotopic tracer techniques have transformed the development of medicine and science. In just under a century, the metabolic fate of strychnine was estimated by counting the amount of frogs the excreted urine killed<sup>5</sup>. In modern times the localization and expression of a receptor in tissue can be analyzed, accurate within a few mm. These leaps in science and technology are however often overshadowed and underappreciated by a public phobia of radioactivity, being unaware of the low dose radiation our bodies are naturally exposed to. Moreover many studies which demonstrate health benefits (and not just absence of harm) of low dose radiation exposure have been avoided by the general public<sup>6-7</sup>.

In a lot of the radiochemical synthesis and radiolabeling reactions the radiation exposure is greatly increased, and the safety aspects of working with radioactive material must be taken into consideration. ALARA/ALARP, an acronym for As Low As Reasonably Achievable/Practicable is the most fundamental of these. The safety aspects dictates avoiding manipulations exposes the worker to large doses of radiation, e.g. because they require a lot of time or tedious. The safety aspect, together with several other unique requirements translates directly into the synthesis of the labeling precursor. Since the radioisotopes of interest for PET have a half-life typically ranging from minutes to hours, the introduction of the radioisotope should be performed in one step, with all following reactions being short (rule of thumb is within 4 half-lives). The chemistry should ideally also be under mild conditions, with a reaction stoichiometry compatible with very small amounts of radionuclide. The

reaction profile should be thoroughly investigated to avoid any unforeseen and unwanted incidents, and be able to translate into regulatory approval for clinical radiopharmaceutical manufacture.

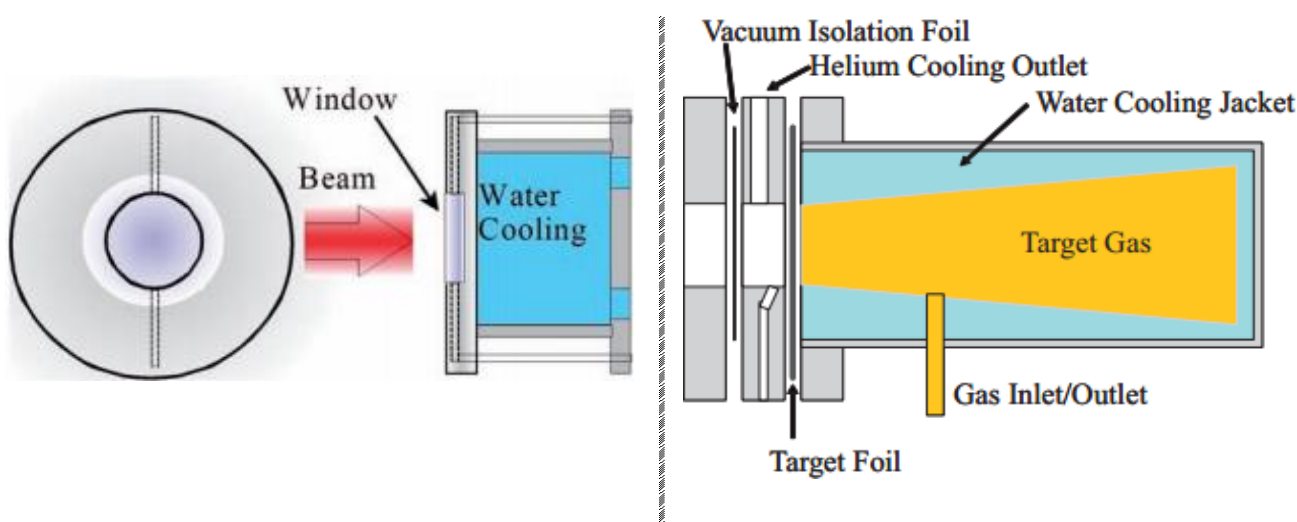
As final goal of the radiopharmaceutical is injection into a patient and investigation of its pathway, the PET radiochemistry must comply with cGMP standards. These criteria include purity of the product, high specific activity and it should have acceptable amounts of non-toxic byproducts. After the synthesis of the radiopharmaceutical it has to undergo several quality controls before it deemed suitable for human use. The purification on the radiopharmaceutical must be rapidly achievable using HPLC and/or solid-phase extraction (SPE) cartridges, followed by sterile filtration. With a continuous decline of product, the radiochemical yield must be sufficiently high after several hours of necessary quality control and transport from manufacturing site to clinic. Methods should be automatable and adaptable to single-use consumables or synthesis modules used in sterile manufacturing. This is important as it helps with facilitating the radiopharmaceutical production to GMP compliance. This again translates into an increase in the productions robustness.<sup>8-9</sup>

As soon as the radiotracer is injected into the blood, the tracer meets an array of adversity from a metabolizing biological environment. In order to be used as a PET radiotracer in medicinal imaging, the tracer candidate needs to meet several criteria depending on the biological pathway to be studied. Investigation of the biological behavior is the key to the prediction of the effectiveness of the radiotracer. Extensive biological characterization is state-of-the-art in radiotracer applications. While some of these criteria are general for all pharmaceuticals, such as safe for administration at the administered dose, others like a lack of troublesome radiometabolites are specific for radiopharmaceuticals. With a large part of the human genes being expressed in the central nervous system, the sensitivity and spatial resolution of PET has found large appliance to study drug binding and pharmacodynamic effects in the human brain.<sup>10</sup> Pike reviewed the specific factors that affect radiopharmaceuticals without a recognized transporter system to pass through the blood brain barrier.<sup>11</sup>

## 1.3 Introduction of the radiotracer

### 1.3.1 Production of $^{18}\text{F}$ Fluorine

With limitations from metabolic exposure and laboratory synthesis as key criteria for a successful radiotracer, it is possible to discuss the chemistry of radiolabeling compounds intended for biological studies. Incorporation of non-radioactive fluorine in pharmaceuticals is well known, and is often associated with an increase in biological half-life and drug potency. Fluorine containing drugs can provide dramatic improvement in pharmacokinetic and bioavailability studies, and it is estimated that ~20% of prescribed pharmaceuticals contain fluorine.<sup>12</sup> Traditional fluorine chemistry has been dominated by the usage of fluorine gas, alkali metals and harsh conditions. The fluorine has often been too reactive ( $\text{F}_2$ ), or too unreactive ( $\text{KF}$ ).<sup>13</sup> To enable optimal development in pharmaceuticals the labeling techniques should have the possibility to incorporate the radioactivity into any structure scaffold and in the correct position of the structure. Arenes and heteroarenes are privileged in the area of  $^{18}\text{F}$  labeling due to metabolic robustness. On the subject of labeling arenes with fluorine there are two major pathways; electrophilic and nucleophilic fluorine substitution reactions.



**Scheme 2** Schematic diagrams of a liquid and gaseous target used for producing radioisotopes. The left diagram shows a liquid target, constructed from silver as it is used to produce  $^{18}\text{F}$  from  $^{18}\text{O}$  enriched water. The right diagram shows a typical gas target, where the beam coming from the left is scattered by the interactions between the charged particles and target. The gas chamber has been cut at an angle to account for beams scattering<sup>14</sup>.

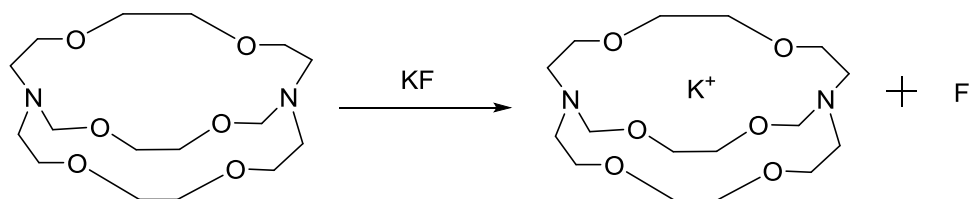
The route of how the used positron emitter has been produced for directly affects its suitability for labeling. Two different targets used in  $^{18}\text{F}$ -production are shown in Scheme 2. Other than the interactions of the charged particles with the matter, factors like stopping power and range of the beam, energy straggling, heat transfer with efficient cooling and beam scattering play important roles in radionuclide production.<sup>14</sup> The chemical form of the radionuclide production is also a major targetry assessment, where the half-life of the produced radioisotope accompanies the assessment. All high specific activity and no-carrier-added  $^{18}\text{F}$ -fluorine is currently produced using enriched  $^{18}\text{O}$  water as a target. Most isolation of  $^{18}\text{F}$ -fluoride is done by using an ion exchange resin or quaternary methyl ammonium (QMA) anion exchange resin, which allow a recovery efficiency greater than 95%<sup>15</sup>

Fluorine-18 used in electrophilic fluorination reactions are produced from a gaseous target of  $^{18}\text{O}_2$  in a  $^{18}\text{O}(\text{p}, \text{n})^{18}\text{F}$  reaction. The fluorine produced will, without the presence of other nearby fluorine atoms to bond with, be adsorbed to the walls in the target holder. This is difficult to release within its half-life, and thus creates a need for free  $^{19}\text{F}$  atoms. The need for  $^{19}\text{F}$  in the target gas in order to create  $\text{F}_2$  creates an unavoidable amount of non-radioactive fluorine (called carrier fluorine) in the product. Thus already in the  $^{18}\text{F}$  production the maximum theoretical RCY of the radioisotope is of lower molar radioactivity and specific activities (radioactivity per amount of substance, i.e. Bq/mol; radioactivity per mass unit, Bq/g).

The electrophilic  $^{18}\text{F}$  fluorination reactions have in common that the final specific activity (SA) and the final RCY in the product are lower than for nucleophilic reactions, as the result of the unavoidable addition of  $^{19}\text{F}$ , non-radioactive carrier fluorine. The electrophilic radiofluorination reactions are useful for investigations of metabolic processes that do not involve saturable ligand protein binding. It is not widely used and electrophilic fluorination is sometimes not suited for investigation of biochemical processes as the regioselectivity is low and extensive purification is required to separate the fluorinated isomers.<sup>16-18</sup> The SA is of critical importance when working with low capacity systems (like ligand-receptor binding), where a low SA can result in saturation of the receptors and a decrease of positron signals.<sup>18</sup>

A common source for  $^{18}\text{F}$  as nucleophilic reagents is  $^{18}\text{F}^-$  (aq.), produced by proton bombardment of  $^{18}\text{O}$ -enriched  $\text{H}_2^{18}\text{O}$ . The produced  $^{18}\text{F}^-$  will then be in an aqueous solution with less than 10000  $^{19}\text{F}$  atoms present in the aqueous solution per each of the  $^{18}\text{F}$  isotope. This is referred to as no-carrier added fluorine and can provide products with high specific

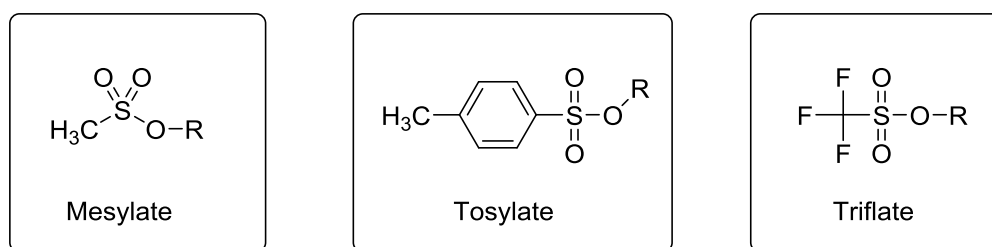
activity. Though the fluoride ion is a strong nucleophile it will form hydrogen bonds with surrounding water molecules. This will lead to a high degree of solvation which reduces the obtained  $^{18}\text{F}^-$  to a poor nucleophile<sup>18</sup>. The nucleophilicity is improved by the addition of a phase-transfer reagent such as Kryptofix-222®, followed by removal of water.<sup>19</sup> The function of Kryptofix-222® is depicted in Scheme 3, where it leaves the fluoride molecule naked and reactive.



**Scheme 3** The nucleophilicity of fluoride can be improved by adding the phase-transfer cryptate complex Kryptofix-222®

### 1.3.2 Methods of $^{18}\text{F}$ -fluorine introduction routinely used

The labeling pathway of nucleophilic substitution is typically divided into aromatic and aliphatic substitutions. The aliphatic substitutions proceeds in a  $\text{S}_{\text{N}}2$  mechanistic fashion with adequate leaving groups such as, mesylate, tosylate, triflate or halogens, as shown in Scheme 4.



**Scheme 4** Common leaving groups in aliphatic substitution reactions used in radiochemistry.

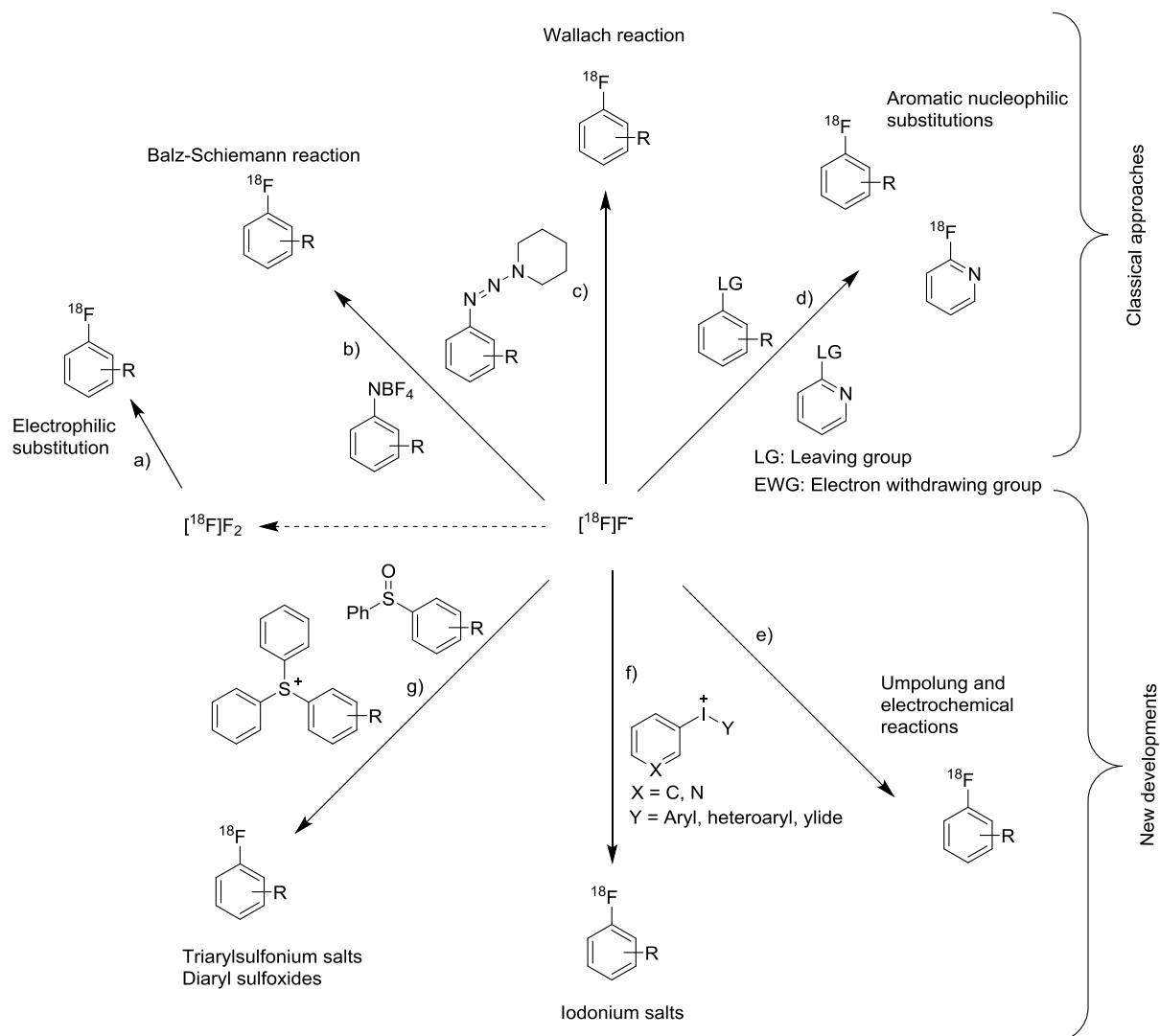
The labeling often occurs on aryl rings as these are more metabolically stable. The direct nucleophilic substitution (Scheme 5 d, redrawn from Ermert<sup>20</sup>) with  $^{18}\text{F}^-$  is a convenient one-step pathway of labeling a wide range of aromatic compounds, given the aromatic ring is

activated (electron poor) by a suitable electron-withdrawing group (such as CHO, COCH<sub>3</sub>, COOMe, NO<sub>2</sub>, CN, etc.) in ortho or para positions to the displacement<sup>19</sup>.

Trimethylammonium salts and the nitro group as the most common leaving groups.<sup>21</sup> The temperatures used for aromatic fluorination of trimethylammonium groups are lower (100 - 110 °C) compared to the nitro group (120 - 180 °C).<sup>18</sup> The electron-withdrawing groups need to be removed from the final product if they are not desirable. By doing this the RCY could be significantly reduced.<sup>21</sup> Typical S<sub>N</sub>Ar reactions for <sup>18</sup>F labeling require heating at high temperatures (>100 °C) with a polar aprotic solvent such as DMF or DMSO. These conditions may prevent more sensitive functional groups and limit the substrate scope to thermally stable starting materials. The direct nucleophilic substitution is often used, but it does not allow labeling on many molecules, e.g. peptides or proteins.

The Balz-Schiemann reaction (a thermal decomposition of an aryl diazonium salt) and Wallach reaction (a thermal decomposition of an aryl triazene) are shown in Scheme 5 b) and c). These methods have also been adapted to successfully introduce <sup>18</sup>F into aryl rings, but the procedures are often limited by their lack of radiospecificity, low RCY or high amounts of side products.<sup>18, 22</sup> As the drive for easier, time-efficient methods of fluorine incorporation persists iodonium salts (Scheme 5 f) and transition metal mediated radiofluorination have showed to be promising labeling methods for radiolabeling (Scheme 5 e).<sup>18, 23</sup> The usage of transition metals have allowed for reactions unavailable by traditional chemistry and has a lot of success in introducing fluorine in organic molecules. However, the ultimate aim is to simplify late-stage <sup>18</sup>F-fluorination and the usage of transition metals is accompanied by metal toxicity and purification issues, which does not always translate well into cGMP clinical chemistry.<sup>24</sup> Another recent method established is usage of triarylsulfonium salts (Scheme 5 g). The reactions are applicable to a range of aryl precursors, given the aryl ring bears an electron withdrawing group in para-position of the <sup>18</sup>F-fluorine. These reactions are relatively mild, rapid and efficient and may give access to potentially labeling synthons.<sup>20, 25</sup>



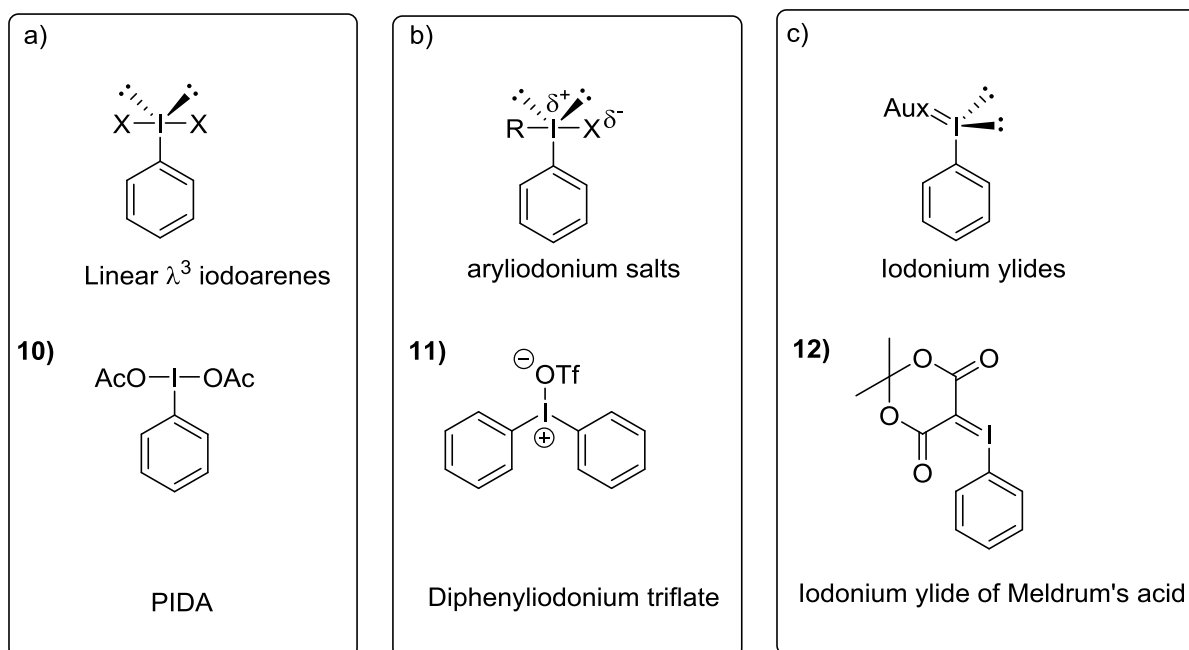


**Scheme 5** An overview of various pathways for aromatic  $^{18}\text{F}$ -labelling. The traditional methods like Balz-Schiemann and Wallach reactions are not commonly used in radiofluorination, but aromatic nucleophilic substitution reactions are. Iodonium and triarylsulfonium salts, diaryl sulfoxides, umpolung and electrochemical reactions are all promising radiofluorination methods in development.

### 1.3.3 Radiofluorination using hypervalent iodonium(III)

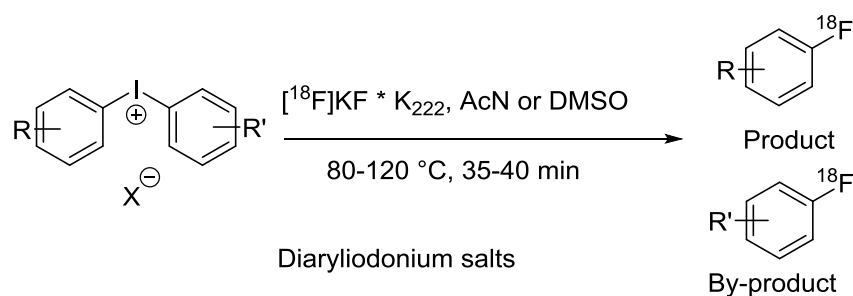
Iodine,  $^{53}\text{I}$ , was earliest isolated from sea weed ash in 1881 and has played an important role in inorganic, organic and biochemistry from early antiseptic tinctures to treatment of radiation exposure.<sup>26</sup> It is the heaviest among the stable halogens, and differs from others in its group by occurring in many oxidation states. While typically in the monovalent state, it allows the formation of stable polycordinate, multivalent bonds. Polyvalent iodonium species were first described in 1886, 75 years after the discovery of iodine. The multivalent organoiodonium compounds have been valued for their availability and selectivity even under mild conditions. Iodine (III) ( $\lambda^3$ -iodanes) resemble the reactivity to heavy metal species like Hg(II), Tl(III) and Pb(IV), but is not associated to the toxic and environmental problems related to heavy metals.<sup>26</sup> The use of hypervalent iodonium as an environmentally sustainable alternative to heavy metals has gained attention recently<sup>27</sup>. Aryliodonium salts were well known to react with a variety of nucleophiles, including halide anions such as  $\text{Cl}^-$ ,  $\text{Br}^-$  and  $\text{I}^-$ . Aryliodonium salts were comprehensively described in 1914.<sup>29-30</sup>

The interest in polyvalent organic iodonium species came and went, before a renaissance occurred in the early 1980s.<sup>30</sup> Motivated by the good decay properties of  $^{18}\text{F}$ , the use of diaryliodonium salts to produce aryl fluorines by radiofluorination was first described by Pike and Aigbirhio in 1995.<sup>23,31</sup> Iodine in the  $\lambda^3$ -iodane form has 10 electrons and an overall geometry of a distorted trigonal bipyramid with two heteroatom ligands in axial positions. In equatorial positions there are both electron pairs and the least electronegative carbon, R. Different species of  $\lambda^3$ -iodanes are shown in Scheme 6. The hypervalent bond in  $\lambda^3$ -iodanes is highly polarized and longer than a normal covalent, and this is responsible for their high electrophilic reactivity.<sup>32-33</sup>



**Scheme 6 Structures of hypervalent iodine(III) species with examples of compounds where they are found. From left to right: Linear  $\lambda^3$ -iodoarenes, as found in PIDA. Aryliodonium salts, found in diphenyliodonium triflate and iodonium ylides, as found in ylides of Meldrum's acid.**

Diaryliodonium salts and  $^{18}\text{F}$  together with crypt-222 gives a fast and convenient way of fluorinating aryl rings outlined in the Scheme 7. The basis for hypervalent iodine chemistry arises from the strong electrophilic nature of iodine, creating a position in the molecule susceptible to nucleophilic attacks. The reductive elimination of hypervalent iodine back to its normal valency is considered the key element to the reactivity of hypervalent iodine. Iodonium salts have been attributed to having the ability of a “hyperleaving group”. Diaryliodonium salts are stable and the most investigated iodine(III)-compounds.<sup>19, 30</sup>

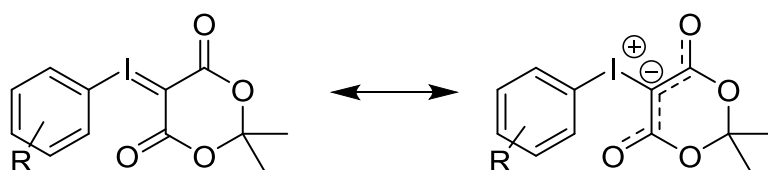


**Scheme 7 A simplified radiofluorination of diaryliodonium salts with  $\text{K}_{222}$ . The iodonium salt is heated in the presence of  $^{18}\text{F}$ -fluoro-crypt<sub>222</sub>-complex in a polar, aprotic solvent to give the desired product.**

The use of arylodonium and diaryliodonium derivatives as precursors is becoming increasingly popular in PET chemistry. This is due to their efficiency in introducing  $^{18}\text{F}$  in fast and convenient aromatic nucleophilic substitution reactions with exceptional high reactivity in a one-step reaction without toxic transition metals or ligands.

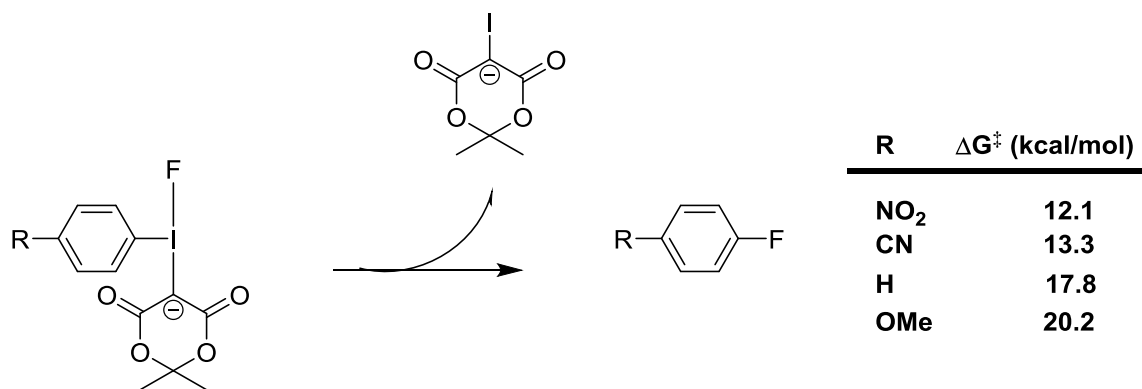
The regioselectivity of the fluorination of diaryliodonium is guided both by electronic and steric features of the two aryl rings, but the reactions of hypervalent iodonium have been found to be mechanistically more intricate than computed binding energies suggest.<sup>34</sup>

The use of iodonium ylides as a PET labeling precursor was initially described in a patent.<sup>16</sup> Iodonium ylides show several advantages for radiofluorination in comparison to diaryliodonium salts, foremost having a lack of auxiliary arene and counterion.<sup>35-36</sup> The iodonium ylide,  $\text{ArI}^+-\text{CX}_2$  (where X represents an electron withdrawing substituent) contains strong electron withdrawing substituents. This creates a carbon with a carbanionic character, creating a positive and negative charge within the neutral molecule as shown in Scheme 8.<sup>37</sup>



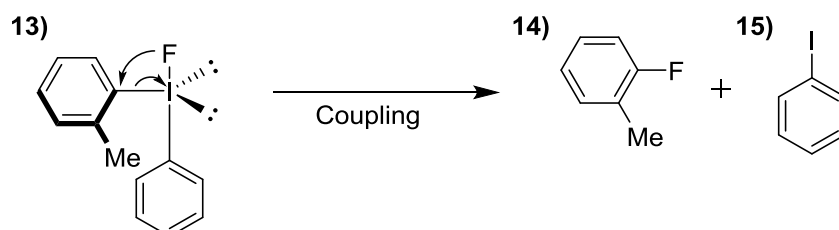
**Scheme 8: The carbanionic character of Meldrum's acid based iodonium ylides. The electron withdrawing oxygens provide an artificial negative charge on the carbon alpha to the iodonium.**

The charge of the carbon directs the attack of the nucleophile exclusively toward the aromatic ring of the arene group of iodonium ylides. Substituents on the aryl ring which alter the steric and electronic configuration affect how easily the fluorine is introduced (see Scheme 9). Similar to arylodonium salts used together with the nucleophilic no-carrier added  $^{18}\text{F}^-$ , iodonium ylides allow for labeling of electron rich aryl rings. Iodonium ylides have however been claimed to be regiospecific, in contrast to aryl iodonium salts.<sup>16</sup>



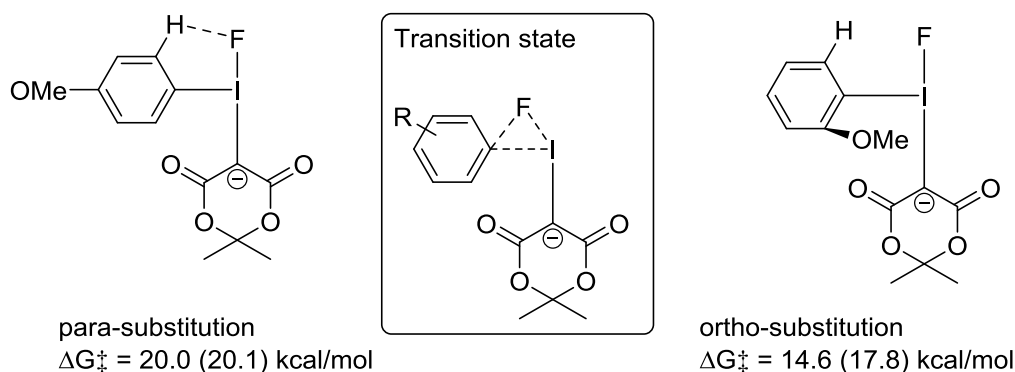
**Scheme 9** The predicted effect from arene electronics on a reductive elimination reaction.<sup>36</sup>

With asymmetrical iodonium salts the nucleophilic substitution is guided towards the more electron deficient aryl ring, while being directed additionally by an observed “ortho” effect. These reactions favor the coupling of the nucleophile with the ortho-substituted aryl ligand, even when the aryl ligand is more electron rich than the other.<sup>19, 38</sup> This benefit has been attributed to the conformation of two lone pairs in equatorial position, as shown in Scheme 10.



**Scheme 10** Visualization of the improved reactivity due to the steric interaction referred to as the ortho-effect.

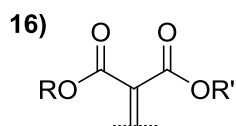
The reductive elimination benefits from the steric interactions of ortho-substituents, shown in Scheme 11. This is predicted to reduce the energy barrier as the reductive elimination proceeds through an out-of-plane transition state and avoids an energetic cost of rotating the arene prior to the reductive elimination. The effect has recently been computed to originate from a sterically induced destabilization from the ground state of ortho-C-H...F interaction.<sup>36</sup> This methodology provides challenges in the design and synthesis of precursor, but has been promising for aromatic radiofluorination.



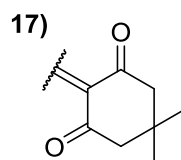
**Scheme 11 Reduction of energy barrier for a reductive elimination reaction due to the ortho-effect, calculated by Rotstein *et al.*<sup>36</sup>**

While arylidonium salts have enabled direct  $^{18}\text{F}$ -fluorination into both electron poor and electron rich arenes in several positions, the introduction has shown to be increasingly more difficult for labeling radiotracers of a higher molecular weight and complexity.<sup>39</sup>

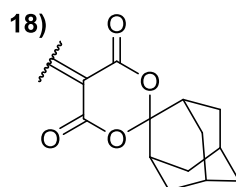
Different iodonium ylides successfully used for radiofluorination are exemplified in Scheme 12. Practical application of iodonium ylides are limited by their poor solubility and are unstable even at ambient conditions.<sup>17</sup> Iodonium ylides produced from Meldrum's acid has shown an increase in stability has given their iodonium ylides formed increased attention and made them attractive for use as labeling precursors in  $^{18}\text{F}$  labeling.<sup>40-41</sup> Meldrum's acid was discovered in 1908 (by Meldrum<sup>42</sup> and structurally misidentified for the next 40 years<sup>43</sup>), has been shown to have an unusually low pKa value of 4.97 compared to what would be expected from similar acids such as dimedone (pKa: 5.23) and dimethyl malonate (pKa ~13). It also has a remarkable electrophilicity.<sup>44</sup> These abnormalities can be speculated to give Meldrum's acid the fitting properties to act as a ligand in a broad range of reactions.<sup>45</sup>



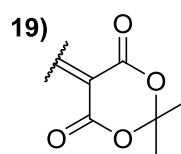
Malonic ester derivatives  
R and R' = Me, i-Pr, Et, t-Bu etc



5,5-dimethylcyclohexane-1,3-dione  
(dimedone)



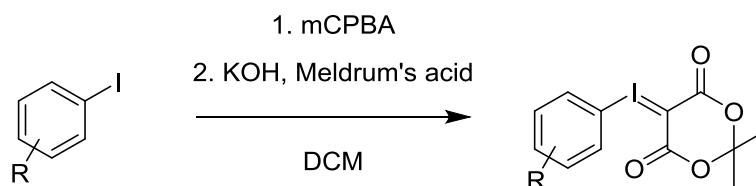
spiroadamantyl-1,3-dioxane-4,6-dione  
(SPIAd)



2,2-dimethyl-1,3-dioxane-4,6-dione  
(Meldrum's acid)

**Scheme 12 Examples of different ylides successfully used for radiofluorination.**

A simplified two-step, one pot procedure of making [2-(2-dimethyl-1,3-dioxane-4,6-dione)]-ylides (**19**) from aryl iodides was described by Cardinale and Ermert<sup>40</sup>, and is shown in Scheme 13. In the procedure the aryl iodide is first oxidized with *m*-chloroperoxybenzoic acid (mCPBA) in DCM, before KOH and Meldrum's acid are added to the reaction mixture affording the iodonium ylide in moderate yields. This method has already been used for the radiosynthesis of L-6-[<sup>18</sup>F]fluoro-L-DOPA, a useful PET imaging agent for mapping dopamine related brain disorders. Iodonium ylides have also been applied to drugs involved in serotonin related diseases.<sup>46</sup> Dopamine transporters ligands such as L-6-[<sup>18</sup>F]fluoro-L-DOPA are often the standard of care (together with SPECT) for the diagnosis of Parkinson's disease and other dopamine related disorders.<sup>19</sup>

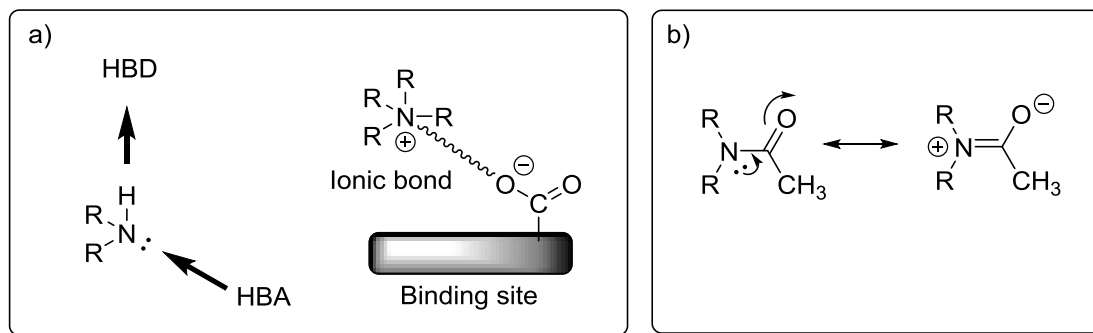


**Scheme 13 A simplified reaction for the described two-step, one pot procedure for producing iodonium ylides using Meldrum's acid.**

Aryliodonium salts have been used in the Riss group at the University of Oslo with a particular interest of incorporating <sup>18</sup>F-fluorine ion into potential imaging agents.

### 1.3.4 Amines and amides in radiopharmaceuticals

Functional groups of amines and amides are extremely important in medicinal chemistry and in many drugs due to their binding roles. The lone pair of the nitrogen atom can act as a hydrogen bond acceptor, and primary and secondary amines have N-H groups that can act as a hydrogen bond donor. The lone pair in aromatic and heteroaromatic amines interacts with aromatic rings, and these amines only act as a hydrogen bond donor. While interacting with their binding site the amine may be protonated and thus function as a hydrogen bond donor or creating a strong ionic bond with a binding site, shown in Scheme 14 a).



**Scheme 14** the possible interactions and binding roles of amines and amides. b) The charge on the amide nitrogen makes it unable to participate in hydrogen or ionic bonding.

The carbonyl oxygen on amides can act as a hydrogen bond acceptor while the nitrogen cannot. The N-H group of primary and secondary amines allow for hydrogen bond donation. Amides are however planar compared with amines, which can result in a loss of binding activity due to the nitrogen being unable to participate in a hydrogen or ionic bond, shown in Scheme 14 b).<sup>47</sup>

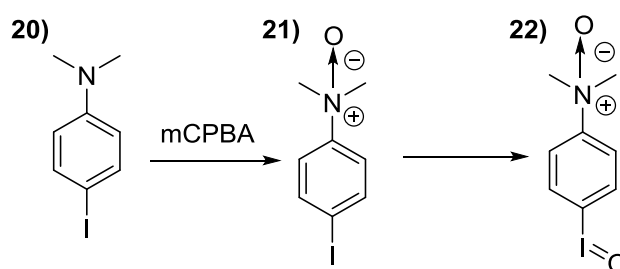
The cleavage of the nitrogen-carbon bond when injected into an organism is an important process in drug metabolism. Promoted by a vast and complex metabolic environment, a small modification of molecule could alter the function of xenometabolites significantly. One particular example is metabolism of xenometabolites by de-methylation. The metabolite has little interference with the measurements, but metabolism of compounds containing N,N-dimethylamino and N,N-dimethylamido groups can influence the measurements. Mono-



methylation of these can result in radiometabolites with similar structure and properties as the designed radiotracer, resulting in confusing quantitative measurements.<sup>11</sup>

Complex labeling precursors often contains one or several areas that are considered reactive, and often more reactive than preferred. Oxidation reactions increases molecules oxidation state and lose electrons, while a reduction decreases the oxidation state with a gain of electrons. A change of the oxidation state results in different molecular attributes.

A setback to the synthetic method of making iodonium ylides is its incompatibility with certain functional groups. Amines, phosphanes and thioethers are prone to oxidize from the conditions used in both the synthesis of the precursor and in radiochemical labeling, as mCPBA does in Scheme 15. Protic functional groups can protonate the anionic ylide-ligand, leading to degradation.



**Scheme 15: The mCPBA oxidation without any amine protection with a co-ordinate bond between the nitrogen and oxygen.**

The most common way of dealing with reactive groups is using protective groups, where a well-known and reliable reaction is conducted to couple the reactive area to the protective group, making the area less reactive. By protecting sensitive groups, compounds which were otherwise inaccessible or unstable become available. If this is correctly the protective group can be removed by a reliable reaction, returning the areas sensitivity again and often in high yield. Both the protection and de-protection of functional groups increase the synthesis by two non-productive steps.<sup>48</sup>

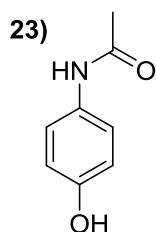
A good protective group should be easily introduced and mask the reactivity of the functional group. It should also be easily removed when the protection is no longer required. Common functional groups that often require protection include alcohols, amines, ketones, aldehydes and carboxylic acids. The choice of protection requires careful consideration in the synthetic

strategy. Molecules with a range of functional groups may require several different protective groups.

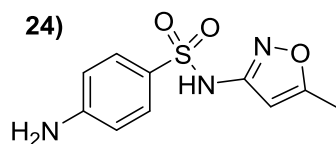
In the work presented amides are used as unconventional protective groups. The two most common reducing agents are  $\text{LiAlH}_4$  and  $\text{NaBH}_4$ , and replacement of hydrogens with alkyl or alkoxy groups have led to a variety of different reducing agents with a wide array of reducing abilities, chemoselectivity and stereoselectivity.<sup>49</sup> An investigation of reducing agent is always necessary to avoid unwanted side reactions. While being the strongest reducing agent commonly used, the time consuming work-up from  $\text{LiAlH}_4$  reduces the practicality of it while working with radioisotopes with a short half-life. Several of the borane species decomposes in the presence of water due to hydrolysis, making the reduction vulnerable to moisture.

### 1.3.5 Biologically important compounds of substructures

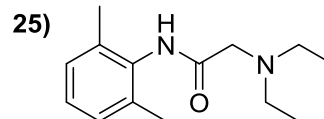
The aniline, benzyl amines and indole compounds are fragments of clinically relevant pharmaceuticals. Examples of pharmaceuticals where these are fragments are shown in Scheme 16, Scheme 17 and Scheme 18.



Paracetamol

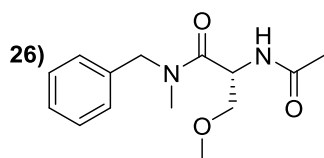


Sulfamethoxazole

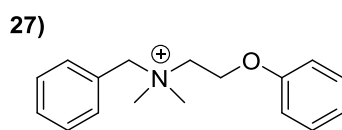


Lidocaine

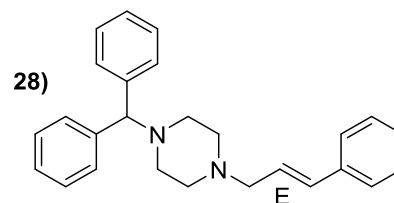
**Scheme 16: From left to right: 23) Paracetamol, pain and fever medication. 24) Sulfamethoxazole, an antibiotic. 25) Lidocaine, a local anesthetic and ventricular tachycardic medication.**



Lacosamide / Vimpat

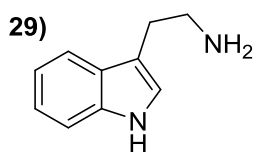


Bephenium hydroxynaphthoate

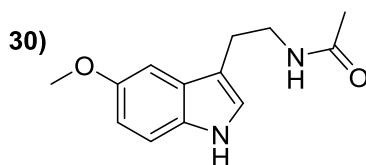


Cinnarizine / Stugeron

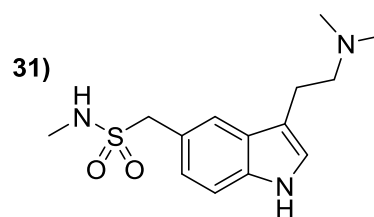
**Scheme 17: From left to right: 26) Lacosamide, a seizure and diabetic neuropathic pain medicament. 27) Bephenium hydroxynaphthoate, an antiparasitic drug. 28) Cinnarizine, an antihistamine.**



Tryptamine



Melatonin



Sumatriptan / Imitrex

**Scheme 18: From left to right: 29) Tryptamine, a neurotransmitter. 30) Melatonin, a sleep and wakefulness hormone. 31) Sumatriptan, a migraine medicament.**



## 2 Aim of study

The radiolabeling of deactivated arenes is considered a very difficult labeling challenge in radiochemistry, and basic amine functional group has been a longstanding challenge in  $^{18}\text{F}$ -radiochemistry. Conventional methods have often been insufficient to label the aniline scaffold. We aim to circumvent this challenge by radiolabeling amides prior to reducing the compound to its amine analog. By applying this to N-methyl-1-phenylmethamphetamine and indole scaffolds we aim to determine the scope and versatility of this method. The fragment compounds of clinically relevant radiopharmaceuticals were synthesized to demonstrate the utility of late stage  $^{18}\text{F}$  introduction in biologically expressive molecules, on which an *in vivo* pharmacokinetic investigation could be carried out.

The ultimate goal of this study is to synthesize a series of  $^{18}\text{F}$ -labeled electron rich amines that would prove difficult to fluorinate by conventional methods. The  $^{18}\text{F}$  introduction is to be performed using iodonium ylides. This can be divided into a series of sub-goals

- Develop a synthetic route and a library series of N-methylaniline, N-methyl-1-phenylmethamphetamine and indole iodonium ylides with a variety of substrates analogs, together with their non-radioactive analogs for HPLC identification and detection.
- Develop a synthetic strategy for introducing  $^{18}\text{F}$ -fluorine into the arene amides prior to a functional group reduction to amines.
- Further develop the reduction and functional group interconversion by optimizing solvent, additives and kinetics.

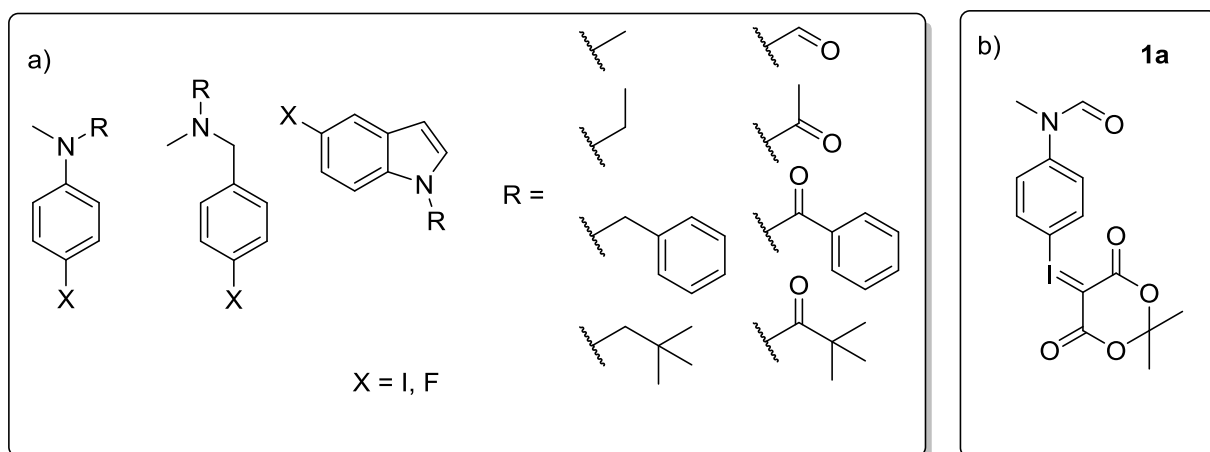


## 3 Results and discussion

### 3.1 Designing the synthesis and developing a method for radiofluorination

The aim of this study is to make radiofluorinated electron rich amines by  $^{18}\text{F}^-$ -incorporation using  $\lambda^3$ -iodonium ylides and an activating group approach. The amines were chosen from carbon skeletons of known biologically active compounds. N-methylanilines, N-methyl-1-phenylmethanamines and indoles (found in Scheme 19 a) were all considered valid substructures and chosen for their pharmaceutical interest.

While not a classical protective group, we hope to demonstrate the amide/amine interconversion can function to protect amines in  $^{18}\text{F}$ -radiochemistry. By using precursors with a different molecular entity, we gain the electronic character of amides as a conjugated system. The carbonyl (C=O) of the amide delocalizes electrons from the aryl ring, which changes the electronic character and makes the introduction of fluorine into the aryl ring easier than on corresponding amines. By applying well-known reductive conditions, a one-step reaction can provide the desired amine product without sacrificing the RCY substantially.

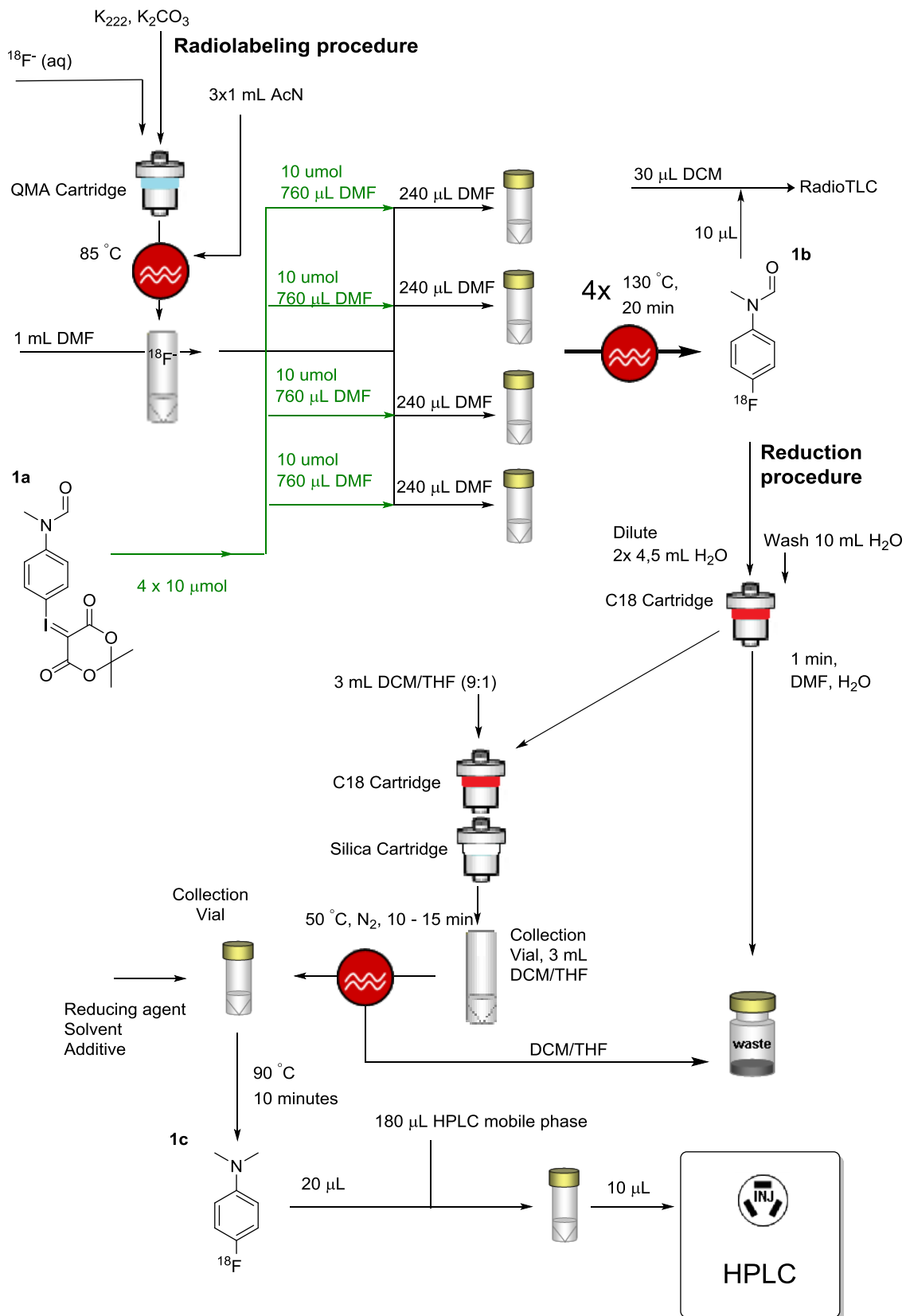


**Scheme 19 a) The substructures used for the synthesis of the iodonium ylides and the reference compound of the cold product. b) The iodonium ylide utilized for the reduction screening and optimization.**

An initial method where  $^{18}\text{F}$ -fluorine was incorporated into a test compound needed to be developed prior to testing the versatility of said method. Compound **1a**) (found in Scheme 19 b) was used in the screening (unless specified otherwise). Prior to any experimental work, a synthetic and radiolabeling strategy needed to be devised. Literature procedures were available for synthesis of a library of the compounds found in Scheme 19 a. For varying the amide moiety, N-methylanilines, N-methyl-1-benzylamines and indoles were chosen to allow an investigation of the effect these had on the iodonium ylide formation, labeling and reduction. Producing a non-radioactive analog was also required for exact HPLC detection and identification.

A simplified one pot synthesis of the ylides starting from the corresponding iodo-substituted starting materials was used from Cardinale & Ermert<sup>19</sup>, together with literature procedures for azeotropic drying of aqueous  $^{18}\text{F}$ -fluorine followed by fluorine incorporation into the target molecule. The trapping of the radiolabeled compound on the cartridge, removal of water and reduction conditions needed to be experimentally investigated and optimized. The effect of the different screening conditions was investigated by varying one parameter under investigation while keeping the other conditions the same. After developing the drying method so far as fair results were yielded, the screening started with an investigation of the reducing agent with a presumptive catalyst, followed by solvent effects in the reduction step and kinetics by varying temperature and time. **All radioactivity measurements are decay-corrected, unless specified otherwise.**





**Scheme 20** A general outline of the radiochemistry procedure: The  $^{18}\text{F}^-$  is trapped, mixed with  $\text{K}_2\text{CO}_3$  and  $\text{K}_{222}$  before being re-dissolved and added to vials containing iodonium ylides. After labeling the desired compound is trapped on cartridges, before either being hydrolyzed or reduced.

## 3.2 Method development for radiofluorination

### 3.2.1 Drying agent and elution screening

Literature procedures were available for preparation of the  $^{18}\text{F}$ -fluoride ion-crypt<sub>222</sub> cryptate complex. The DMF and free  $^{18}\text{F}^-$  needed to be separated from the compound after the labeling. The amount of the aromatic compound trapped on cartridges is shown in only two cartridges, the Sep-Pak C18 and the Chromabond® HR-P, as these were the only available cartridges which were successful in trapping the desired compound. Using a tC18 cartridge for trapping the compound was investigated, but the cartridge failed to successfully trap the desired compound in a reasonable yield. Both the C18 and the Chromabond® HR-P were reverse phase solid phase extraction based, where a nonpolar solvent would disrupt the binding interaction and elute the compound. The Chromabond® HR-P trapped the desired compound very well, while the C18 trapped a fair amount. The C18 Cartridge had a marked price of less than one tenth of the Chromabond® HR-P. As only a fair amount was required the C18 cartridge was used for the trapping of the compound.

Impurities on the hydrophobic SPE cartridge were removed by diluting the reaction mixture with water. The water needed to be removed prior to the reduction. The water removal is shown in Table 2.

**Table 2** The content of the C18 cartridge was eluted together with undesired water. The removal of water is shown below, drying agent, elution solution used, with activity stuck in the drying agent and the subsequent yield of the reduction.

Drying agent	Na <sub>2</sub> SO <sub>4</sub> cartridge <sup>a)</sup>	MgSO <sub>4</sub> cartridge <sup>a)</sup>	MgSO <sub>4</sub> cartridge <sup>a)</sup>	MgSO <sub>4</sub> cartridge <sup>a)</sup>	Silica cartridge	Silica cartridge	Azeotropic drying
Solvent	THF	THF	Pentane	DCM	DCM	THF/DCM	AcN
Stuck C18 cart. (%)	3	5 +/- 3	23	2 +/- 0.2	2	2 +/- 0.6	5
Stuck drying agent (%)	10	12 +/- 10	15	19 +/- 14	11	15 +/- 9	NA
n =	1	2	1	2	1	2	1
Yield (%)	0%	0%	0%	0%	30	86 +/- 9	68

a) Self-made cartridges

The self-made cartridges were made using the drying agent in barrel from an empty syringe, with cotton and Celite in the bottom of the syringe. The removal of water was unsuccessful in several attempts. By using a non-polar solvent as pentane or DCM the water could be displaced and pushed through the cartridge, but pentane failed to elute the desired compound from the C18 cartridge. This may also pentane failing to dissolve the compound. The DCM eluted a large amount of the compound from both the MgSO<sub>4</sub> and silica cartridge, but the subsequent reduction failed when using the MgSO<sub>4</sub> cartridge. The initial reductions were carried out using 9 BBN, a reducing agent quenched by water. The absence of desired product from the self-made cartridges could indicate not enough drying agent used, or that the industrial made cartridges are tighter packed than readily achievable. An azeotropic drying of the collected solution was also attempted. The procedure removed enough water to give fair yields, but much of the labeled compound was lost to evaporation. The DCM/Silica combination gave a successful reduction, but in poor yield. The elution solutions were varied, and are shown in Figure 2. A good yield was obtained with 10 vol% THF in DCM, which proved to be the elution solution of choice as it eluted a large amount of the compound without eluting substantial amounts of water.

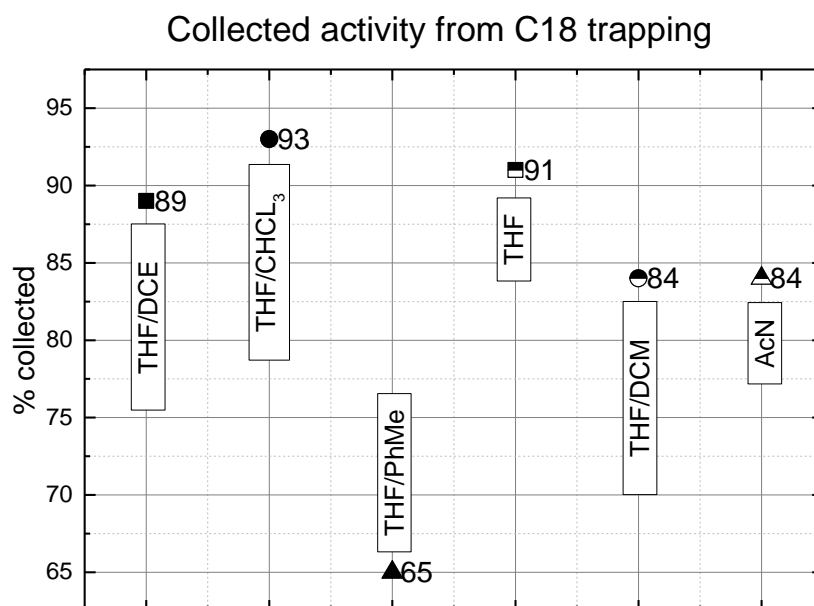


**Figure 2 shows the activity eluted versus the activity trapped in the C18 & silica cartridge using various elution solutions. From left to right: DCE/THF, THF/CHCl<sub>3</sub>, THF/PhMe, THF, THF/DCM solution and AcN.**

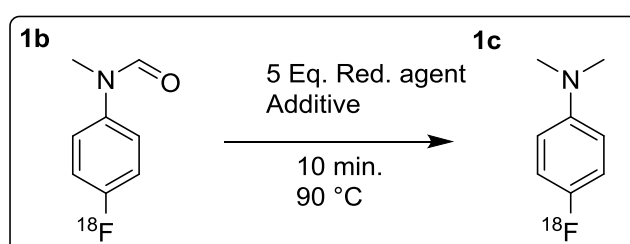
An investigation into the ideal elution solution for the C18-trapped compound is shown in Figure 2. The THF/PhMe eluted the least amount of trapped compound, and from the figure and the amount of compound lost to the C18 cartridge in Table 2 it appears as if PhMe is unsuited for this use. The reason PhMe was unsuited can be attributed to solubility issues, similar to pentane. The elution by AcN was for azeotropic drying and did not use a subsequent drying cartridge after the C18 trapping. While most of the solutions eluted the desired compound in large amounts, the reduction failed to provide any yields (determined by radioTLC) on several of the solutions including THF/DCE, THF/CHCl<sub>3</sub>, THF, and PhMe. This would indicate that the solutions were insufficient in purifying the desired compound, eluting water from the cartridge to quench the reducing agent in subsequent steps.

The desired properties of the elution solutions would exclusively elute the trapped compound, which a non-polar solvent could achieve. It would be ideal with a solvent non-polar enough to elute through the C18 cartridge, while being polar enough to elute through the silica cartridge. The solutions mixtures tested were all with 10 vol% THF in the solutions. The 10% THF in DCM became the solution of choice as both of these are easily evaporated and were efficient

in eluting the compound. THF and DCM are also beneficial as they both form a weak azeotrope with water.

### 3.2.2 Reducing agent and additive screening

Table 3 shows the conditions and yields of attempting the reduction with different reducing agents with an appropriate additive. All reductions were attempted on **1b** with 5 equivalents reducing agent at 90 °C for 10 minutes (see Scheme 21).



**Scheme 21** The reaction screening varying different reducing agents and presumptive catalyst.

**Table 3** The yield from different silanes and boranes with a presumptive catalyst is defined in the table below, with conditions used in the reduction. Triphenylphosphine = PPh<sub>3</sub>, VB<sup>iPr</sup> = Verkade's base, HMPT = hexamethylphosphoramide.

Entry	Red. agent	Catalyst	Solvent	Yield	n =
1	Polysilane	NHC	DMF	0	1
2	Polysilane	NHC	THF	0	1
3	Ph.Silane	NHC	DMF	0	1
4	Ph.Silane	NHC	THF	0	1
5	Pinacolborane	NHC	THF	1 +/- 0	2
6	9 BBN	NHC	THF	77+/-7	3
7	9 BBN	PPh <sub>3</sub>	THF	81+/-3	3
8	9 BBN	VB <sup>iPr</sup>	THF	79+/-3	3
9	9 BBN	HMPT	THF	76+/-9	3
10	9 BBN	NA	THF	92+/-2	3
11	BH <sub>3</sub> • SMe <sub>2</sub>	NA	THF	90+/-1	3

From Table 3 it is apparent the silanes gave no useful reduction yield. N-heterocyclic carbene (CAS 244187) was investigated as it is well known to beneficially react with boranes; the properties of PPh<sub>3</sub> have a reducing character; HMPT has been reported to beneficial in

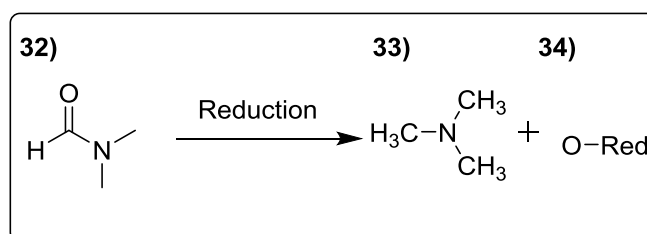
accelerating S<sub>N</sub>2-reactions; Verkade's base was investigated for the reported activating effect. These additions gave detrimental or no effect.<sup>50</sup> This can also be interpreted that the reduction is robust enough to withstand addition of phosphorous containing Lewis bases. The best initial yield was achieved using 9 BBN as a reducing agent with a NHC additive. Several other additives were then screened for the reduction with one vial in the series was used as a control sample with no additive was added. The catalyst was found to be inefficient in the reaction, yielding even less than without any addition of additive. This could be the additive sticking to or hindering the reactive part in reaching the desired configuration with the amide. All subsequent reductions were performed without additive.

### 3.2.3 Solvent screening

The reduction of **1b**) was carried out in different solvent systems, as shown in Table 4. All reductions were carried out at 90 °C for 10 minutes using 9 BBN (without catalyst). The 9 BBN was dissolved in THF. This resulted in all solvents being a mixture of the solvent tested and approximately 19-20 vol% THF from the dissolved reducing agent.

**Table 4** The result of attempting the reduction in a variety of different solvents is shown below, with other conditions. To the right: the reduction of DMF for the negative control, where DMF is reduced to N-N-dimethylamine and carbon dioxide. iPr<sub>2</sub>O = diisopropyl ether.

Entry	Solvent	yield	n =
1	THF	92+/-2	3
2	DCE	89+/-2	3
3	DME	87+/-2	3
4	AcN	67+/-3	3
5	iPr <sub>2</sub> O	92+/-0	3
6	DMF	0	2



Ethereal solvents were selected as these are known to be good in combination with boranes. THF and AcN were of particular interest as polar, aprotic solvents often used in radiochemistry. A negative control was conducted to confirm the reaction gave no yield when no yield was expected. This outcome indicated that amide reduction of the desired compound is taking place in the solvents other than DMF, and the reducing agent is being consumed by DMF when it is used as solvent. The iodonium ylide dissolved in DMF had 275 equivalents of amide coming from DMF per equivalent reducing agent. As expected, the negative control yielded no result.

While several of the solvents used provided high yields of the reductions, the reactions performed in DME differed from the rest. While promoting a high yield, the peak believed to be the intermediate state (see Scheme 22 a) in the HPLC elution profile appeared strongly in all reactions except DME, where it was almost absent. The separation of reductions done in DME thus increased substantially, thought to simplify purification by HPLC. The chromatograms with and without the intermediate peak are shown in Figure 3.

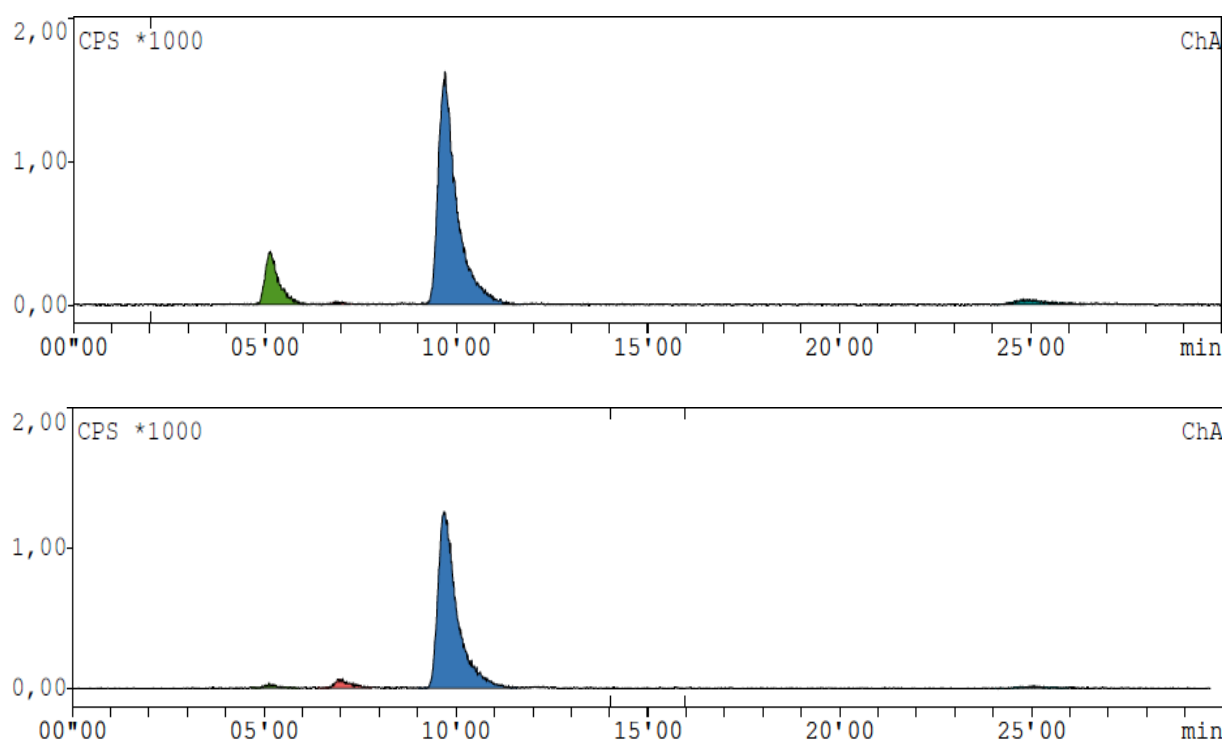
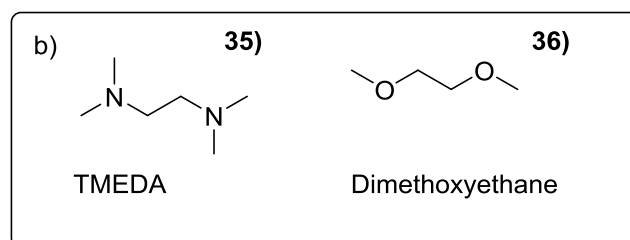
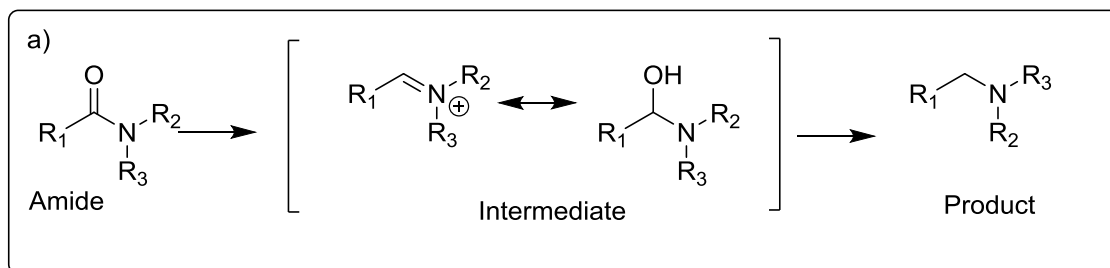


**Figure 3** The figure depicts the effect a moderate amount of DME solvation had on the resulting HPLC chromatogram. The top chromatogram is carried out in pure THF, while the bottom chromatogram was solved in 38% THF in DME.

It was hypothesized that the DME increased the reaction rate of the reduction reaction so that the main product of the reaction shifted from an intermediate product on further to form the desired product. A reaction was designed where a small amount of DME (10 Eq.) in was added prior to the reduction in a THF solution. This was designed to investigate if only trace amounts of DME was required to remove the intermediate peak, but the reaction still showed the chromatogram with the same ratio as pure THF.



**Scheme 22 a) The believed progress from the initial amide to the intermediate states before producing the amine product b) The structures of tetramethylethylenediamine (TMEDA) and dimethoxyethane (DME).**

With the intermediate reaction product in mind (see Scheme 22 a) alternative conditions were investigated. Instead of using neat DME a structurally similar compound TMEDA (10 Eq.) was added prior to the reduction in THF (See Scheme 22 b). The TMEDA was added to facilitate the reaction in a similar manner as DME. Instead this hindered the reduction, yielding only 17% compared to the THF standard yield of 92%.

### 3.2.4 Temperature and reducing agent equivalent screening

Table 5 shows the yields and conditions of attempting milder conditions for reducing **1b**). The conditions were modified by varying the reducing agent stoichiometry relative to the iodonium ylide used. Here 3, 5 and 10 equivalents were used. The influence of temperature and reaction time was also investigated. All reductions were attempted using 9 BBN and the yield quantified by radioHPLC.



**Table 5 presents the effect of attempting the reduction in milder conditions, such as less reducing equivalents, lower temperatures or less time.**

Entry	Eq.	Solvent	Temp. (°C)	Time (min)	Yield (%)	n =
1	3	THF	90	10	52+/-2	3
2	5	DME	75	10	70+/-3	2
3	5	DME	60	10	45+/-4	2
4	5	DME	90	1	31	1

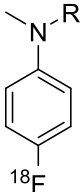
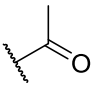
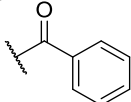
The reduction yield was found to be heavily influenced by both temperature and equivalents of reducing agent. This was somewhat counterintuitive since n.c.a. product would be even less than the initial amount of precursor, calculated to be in the pico-mol range before the reduction stage. The added reducing agent would be equivalent to the iodonium ylide precursor, and one equivalent reducing agent before the reduction would be in around  $5.0 \times 10^{11}$  excess of the fluorinated amide. Alternating between  $5 \times 10^{11}$  (1 Eq.),  $25 \times 10^{11}$  (5 Eq.) and  $50 \times 10^{11}$  (10 Eq.) effective equivalents should have no effect on the rate of the reduction. Table 5 shows the opposite of this.

The yield was significantly lower when the reducing agent equivalents or temperature were decreased, and a fair amount of the compound was reduced already within the first minute of the reduction. While assuming there would be some species of the formamide without the radiofluorine (like H- or I-substituents instead of  $^{18}\text{F}$ ) also present in the solution, these species could not account for such a consumption of the reducing agent. Due to the extent of the reducing agent inefficient we surmised that the underlying reason was water left in the reaction vials, and using more drying agent could allow for using less reducing agent equivalents. An investigation into purification of the intermediate by HPLC could also yield a reduction of equivalents. When lower temperature was investigated a substantial drop in yield was observed. This indicates the speed of the reduction is strongly correlated with the increase in energy/heat. Given the short half-life of  $^{18}\text{F}$ , higher reaction temperature was clearly favorable due to higher yields in a shorter period of time. Before applying these temperatures to other compounds an investigation into heat sensitive functional groups would need to be conducted.

### 3.2.5 Application to other analogs

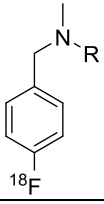
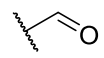
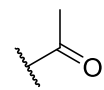
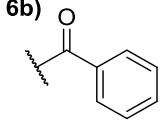
After optimization, high radionuclide incorporation and high yield for the reduction were achieved. Hence, the method was applied to amide analogs in order to establish the substrate scope of the method. The yields and conditions for other 4- $^{18}\text{F}$ fluoro-N-methylamides are found in Table 6.

**Table 6** The radiofluorination and reduction conditions effect on larger substrates of the phenyl-N-methylamides is expressed below.

		4- $^{18}\text{F}$ -fluoro-N-methylamides						
		Entry	Red. Agent	Eq.	Solvent	Temp. ( $^{\circ}\text{C}$ )	Time (min)	Yield (%)
R = <b>2b)</b> 	1	9 BBN	5	THF	90	10	10	1
	2	$\text{BH}_3 \cdot \text{SMe}_2$	10	THF	90	10	3	1
	3	9 BBN	10	38% THF /DME	120	20	47	1
	4	9 BBN	26	THF	120	20	57	1
R = <b>3b)</b> 	5	9 BBN	5	THF	90	10	1	1

Applying the initial conditions to **2b** drastically decreased the radiochemical incorporation yield for all amides. Increasing the reaction temperature, time and reduction equivalents yielded a moderate amount of product, as seen in entry 3 & 4. The  $\text{BH}_3 \cdot \text{SMe}_2$  was unsuccessful in reducing the acetyl analog, where the 9 BBN proved to be a superior reducing agent for the substrate. Both reducing agents gave poor yields at the conditions initially tested. The increase in temperature, time and equivalents gave a fair yield. It could be speculated the bulkier substituents complicates the reduction sterically, increasing the energy barrier required. Reduction of **3b** was unsuccessful at the standard conditions, yielding a mere 1%. Applying the harsher conditions to the **3b** was not attempted. The conditions were also attempted for the 1-4- $^{18}\text{F}$ -fluoro-N-methylmethanamides, as shown in Table 7, with yields determined by radioHPLC

**Table 7** The radiofluorination and reduction conditions effect on various subspecies of benzyl-N-methylamides is shown below.

1-(4-[ <sup>18</sup> F]fluorophenyl)-N-methylmethanamide								
	Entry	Red. Agent	Eq.	Solvent	Temp. (°C)	Time (min)	Yield (%)	n =
R = <b>4b</b> 	1	9 BBN	5	20% THF in DME	90	10	67+/-10	7
R = <b>5b</b> 	2	9 BBN	5	20% THF/DME	90	10	10	1
	3	9 BBN	25	THF	120	20	73	1
R = <b>6b</b> 	4	9 BBN	5	THF	90	10	0	1
	5	9 BBN	25	THF	120	20	81	1

The first attempt of reducing the **5b** resulted in a substantial yield reduction, seen in entry 2, Table 7. The reduction was drastically improved by applying higher temperature, indicating that the drop in yield is mainly affected by a reduced rate of reaction. There is a distinct reduction in yield which can be attributed to the carbon spacer between the nitrogen and the aryl ring. The effect could be attributed to the fluorinated aryl ring, where the inductive effects of the carbon spacer could severely impact the delocalization of aryl electrons to the amide. Adding more equivalents of the reducing agent (26 Eq.) and performing the reaction at higher temperatures (120 °C) increased the amount of desired product from 10% to 57%. The **6b** gave higher yield than **5b**, which is the opposite of the expected result. When the reduction was attempted on **6b**, the iodonium ylide batch was fresh compared to the other iodonium ylides used. The impaired yield is also an effect of screening the method using one of the smallest and simplest amide, as it is believed to be more easily reduced and the conditions used to reduce it would be the mildest conditions.

### 3.2.6 Hydrolysis

It was attempted to hydrolyze the N-(4-fluorophenyl)-N-methylformamide and N-(4-fluorobenzyl)-N-methylformamide in order to further vary the functional group alterations possible for the designed compounds, and is shown in Table 8. The compounds were dissolved in H<sub>2</sub>O/Dioxane at 100 °C, with the yield determined by radioHPLC.

**Table 8 The yield from amide hydrolysis using various concentrations of HCl at different reaction times.**

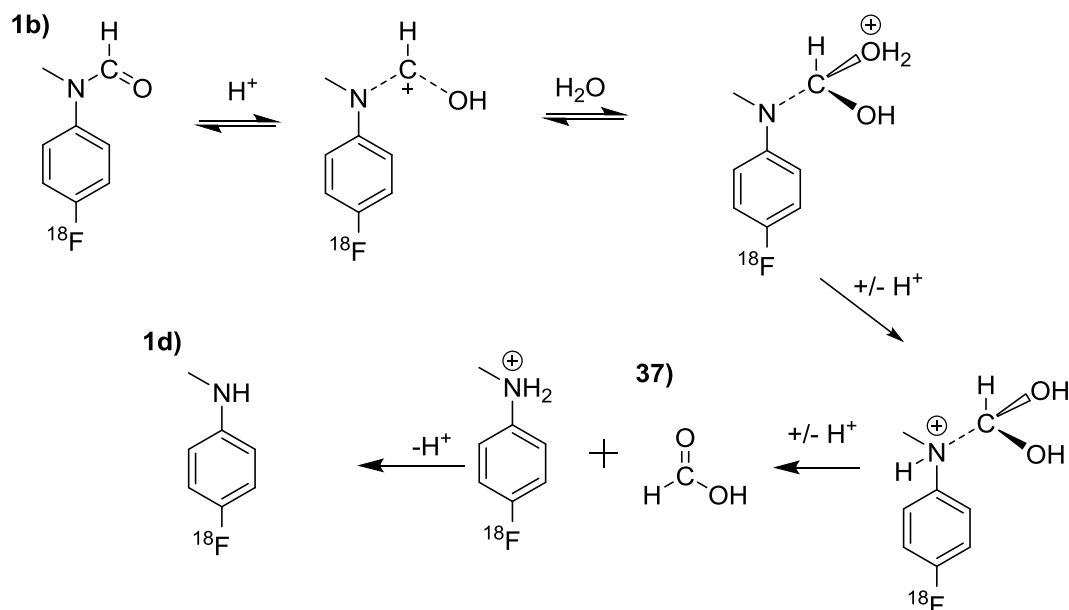
Conditions	Time (min)	Yield (%)	n =
10% HCl	10	78 +/- 1	3
18.5% HCl	10	82	1
10% HCl	25	78	1
18.5% HCl	25	84 <sup>a)</sup>	1
10% HCl	10	79 <sup>b)</sup>	1
10% HCl	10	61 +/- 5 <sup>c)</sup>	3

a) restarted reaction (10+15 min)

b) addition of 5 eq. cold compound

c) N-(4-fluorobenzyl)-N-methylformamide

Table 8 shows the results of hydrolyzing **1b**) with HCl in water-dioxane, x:y. A 10 minute hydrolysis with 10% HCl yielded 78% after 10 minutes. It was investigated if the reaction had not proceeded completely by increasing the hydrolysis reaction time 25 minutes by restarting the reaction. This gave an insignificant yield improvement. There is a slight yield improvement by using 18.5% HCl compared with 10%, but the increase is small enough to be attributed as statistical variation. **4b**) yielded 61% compared to 78% of the **1b**), indicating a more difficult hydrolysis. The neutralization of the hydronium ion and the amine formation is highly exergonic. Reversibility of the reaction came to mind as an explanation of the yield being less than expected.



**Scheme 23** the proposed pathway for acid hydrolysis of N-(4-[<sup>18</sup>F]fluorophenyl)-N-methylformamide, where an acid A-H increases the polarity of the carbonyl group creating a tetrahedral intermediate before forming an amine.

There was hypothesized that the hydrolysis reaction proceeded as equilibrium pushed far to the amine product, shown in Scheme 23. This was investigated by an addition of 5 eq. cold product in a 10% HCl solution, with similar conditions to the first entry in Table 8. In accordance to Le Chatelier's principle the addition would change the final concentration, resulting in more amount of final product. With sufficient time the radioactive tracer should behave like the bulk, HCl and water is in excess and equilibrates. The equilibrium yield for the reaction is typically calculated by Equation 2.

**Equation 2** The equilibrium equation used to calculate the hydrolyzed amine.

$$K = \frac{[\text{Hydrolyzed amine}] * [\text{carboxylic acid}]}{[\text{Starting amide}] * [\text{H}_2\text{O}]}$$

As the water would be in excess, the calculated yield ( $K = 29.7$ ) would be increased to 88% by adding 5 equivalents cold product. The reaction yielded 79%, which would not indicate an equilibrium being the yield limiting factor. This is supported by the HPLC chromatogram (shown in Figure 4) there is a large increase in the UV signal for the sample where cold compound was added, yet the yield determined by radioHPLC is the same as the reaction without cold compound.

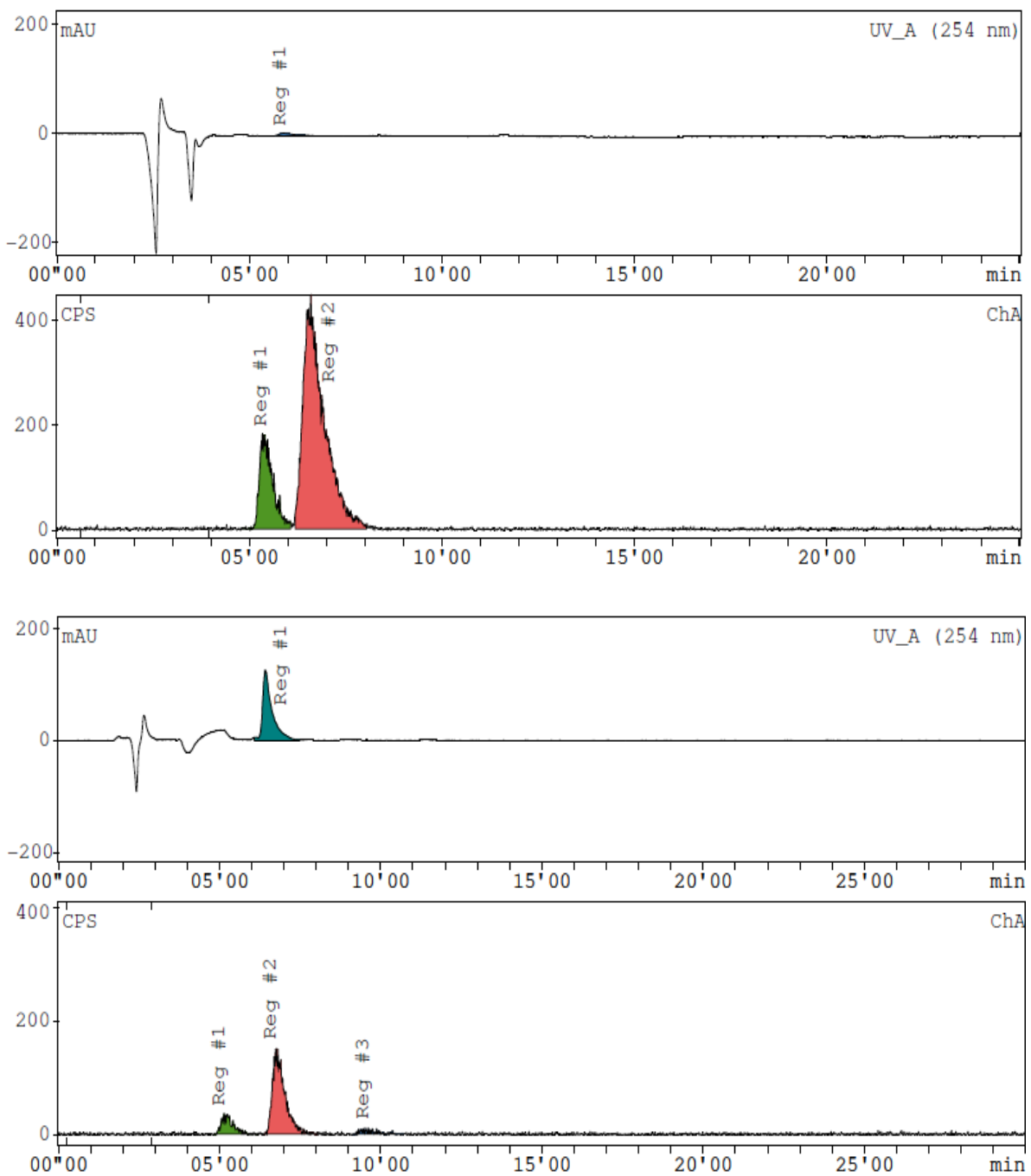


**Figure 4 shows the effect of adding 5 equivalents cold product. The yield determined by radioHPLC is the same (79%), while the solution with 5 equivalents cold product shows a large increase in the UV signal.**

### 3.3 Activity loss and method application

The initial loss of activity from being stuck to the vial, the average RCC and average trapping yields are shown in Table 9. The data was collected while labeling compound **1a**). An activity balance was made over the reaction to estimate the overall isolated yield of the method. The results are shown in Table 9.

**Table 9** The loss of activity from the first stages of the method, where much of the activity is as free  $^{18}\text{F}$ .

	Avg. (%)	n =
Average labeling yield	87 +/- 10	114
Stuck to vial	15 +/- 9	18
Average trapping yield using C18 cartridge	66 +/- 3	3
Average trapping yield using Chromabond ® HR-P cartridge	82 +/- 3	3

The average labeling yield is the average of all the  $^{18}\text{F}$ -fluorine incorporation. The RCC was determined by radioTLC for the N-(4-fluorophenyl)-N-methylformamide. While a chromatographic radiochemical yield of 87 +/- 10% was found, 15 +/- 9% of the starting activity were retained in the vial after transfer of the reaction mixture. This loss was composed of the dead volume; tiny droplets of reaction mixture retained in the vial as well as adsorption of fluoride ion to the borosilicate surface of the vial. In practice, the dead volume loss can be dealt with by dilution. The adsorption is not a problem when using e.g. Sigradur reaction vessels, which are common radiofluorination equipment. The amount of compound trapped in the cartridge versus the total amount of labeled compound is calculated by Equation 3, and is referred to as the trapping yield. The trapping yield was found to be 66 +/- 3% on C18 cartridges, and by applying the same conditions to the Chromabond ® HR-P cartridge the trapping yield was improved to 82 +/- 3%. The cost of the cartridges and the quantity of trappings performed argued for the cheaper option.

**Equation 3** shows the calculation of the trapping yield.

$$\text{Trapping yield} = \frac{(\text{Activity C18 Cart.} + \text{Activity Si Cart.} + \text{Collected activity})}{(\text{Activity}_{\text{start}} - \text{Activity}_{\text{empty vial}}) * \text{RCC}}$$

A considerable amount of the activity eluted through the C18 cartridge, and some stuck to the silica cartridge. This is thought to be a mixture between labeled compound and some free  $^{18}\text{F}$ , and is shown in Table 10 and visualized in Scheme 24.

In order to correct for losses an activity balance was kept over the course of the method. Identifying where and when activity was lost could suggest how different strategies than those applied could improve the final yield, and when action should be taken. Glassware and consumables were counted and the activity was corrected using Equation 4. The individual percentage of activity in the C18 cartridge, silica cartridge, evaporated and amount left before reduction is detailed in Table 10.

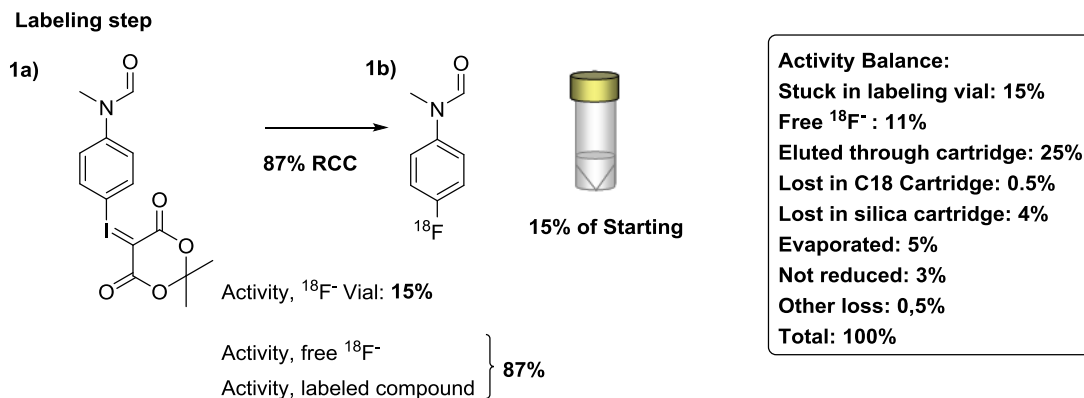
**Equation 4 the equation for decay correction.**

$$\text{Activity after time}(t_1) = A_{start} * 2^{\left(\frac{t_1}{t_{1/2}}\right)}$$

**Table 10 shows the loss of activity after the labeled compound has been trapped, both with regards to amount of labeled compound and initial activity.**

After trapping			
	% of trapped compound	% of total Activity	n =
Stuck in C18 cartridge	1 +/- 0.8	0.6 +/- 0.3	11
Stuck in Chromabond cartridge	6 +/- 4	4 +/- 2	2
Stuck in silica cartridge	8 +/- 9	4 +/- 5	7
Evaporated	10 +/- 6	5 +/- 3	45
Purified intermediate	81 +/- 23	39 +/- 17	45
Reduced species	75 +/- 1	36 +/- 0.5	10

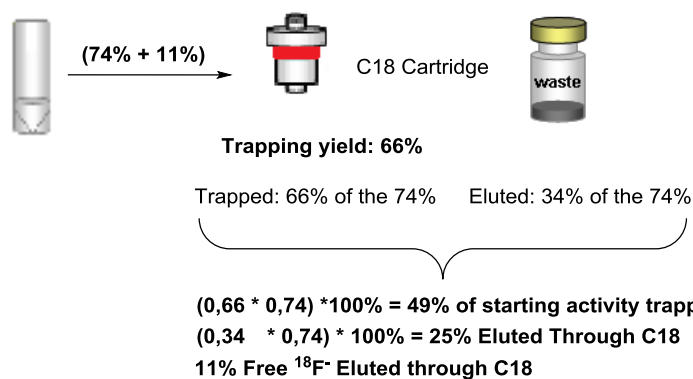




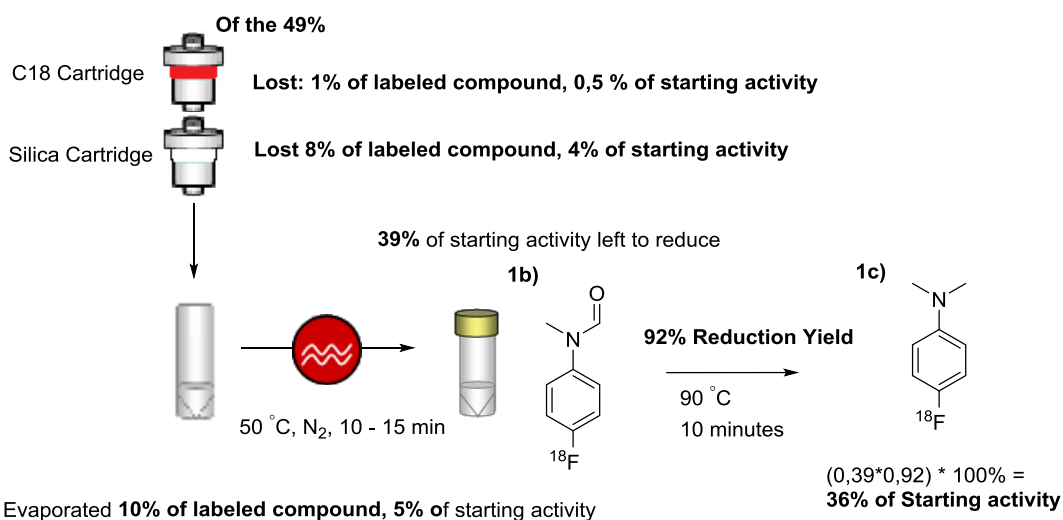
$$(0,87 * 0,85) * 100\% = 74\% \text{ Labeled compound}$$

$$100\% - 74\% - 15\% = 11\% \text{ Free } ^{18}\text{F}^-$$

**Trapping step**



**Elution, drying and reduction**



**Scheme 24 A graphic flow scheme of the method, depicting where the labeled compound and the decay-corrected activity is lost throughout the reaction. In the labeling step 74% of the activity is from the labeled compound, continues on to the C18 cartridge, together with 11% free  $^{18}\text{F}$ . 66% of the 74% is trapped, with a large amount of compound lost through elution. Of the trapped compound, 1% is lost to the C18 cartridge, 8% to the silica cartridge and 10% lost from evaporation. 36% of the initial activity remains after the last step.**

The activity balance shows where the loss of activity and compound occurs in the method. A small loss of 1% of the activity is lost to the C18 cartridge, meaning the elution is successful in eluting the trapped compound. Most of the activity trapped in the cartridges occurs from the labeled compound, but some free  $^{18}\text{F}^-$  would also be trapped. TLC analysis of the eluted mixture confirms no presence of  $^{18}\text{F}^-$ , the activity stuck in the silica cartridge is thought to be composed by the free  $^{18}\text{F}^-$  and a minor loss of compound. The eluted solution was dried using 50 °C and a stream of  $\text{N}_2$ . This also causes a loss of 10% the trapped compound (believed to be volatile to some extent) leaving 39% of the starting activity (or 81% of the trapped compound) to be available for reduction. The average reduction yield (determined by HPLC) was found to be 92% in THF. The balance of the activity from the labeled compound is visualized in Scheme 24. The major loss of compound (25%) occurs from the elution, which can be improved by using cartridges better designed for trapping the compound in question. With the activity balanced and decay corrected a total of 36% of the starting activity remains available after the reduction and purification. The required starting activity for a normal patient injection is also calculated below.

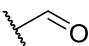
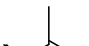
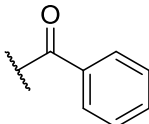
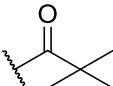
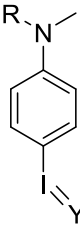
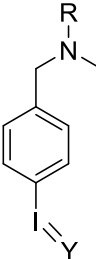
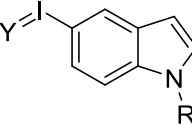
The total reaction time was calculated to: 15 minutes for preparation of reactive  $^{18}\text{F}$ -fluoride ion-crypt-222 cryptate complex, 20 minutes for labeling, 5 minute cartridge handling, 10 minute evaporation, 10 minutes reduction and 30 minutes HPLC purification. This would mean the 43% of the starting activity is lost to 90 minutes decay.

The standard IV injection dose is roughly 10 - 20 mCi / 370 – 740 MBq per patient. The required starting activity for 1 dose with 36% of initial activity left after method (found in Table 10): 1.0 – 2.1 GBq. If applying the method to an actual injection the Chromabond ® HR-P Cartridge or another cartridge superior to the C18 trapping would be used. If a Chromabond ® HR-P Cartridge was used 42% of the initial starting activity would be left after the reduction, and the required starting activity would be 0.9 – 1.8 GBq.

### 3.4 Iodonium ylide yield and appearance

Ylides were obtained via an initial oxidation of the corresponding iodides, followed by an addition of Meldrum's acid. The reaction mixture was filtered using a filter paper (55 mm) before the solvent was removed and the crude was re-dissolved in a small amount of DCM. The product was precipitated by adding distilled hexanes. The appearance and yield of the iodonium ylides synthesized for this thesis is found below in Table 11.

**Table 11 lists the yield and appearance of the precipitation of the different iodonium ylides from the different substructures, Y = iodonium ylide.**

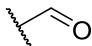
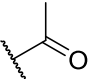
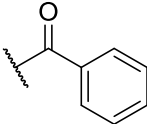
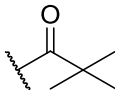
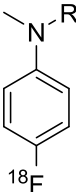
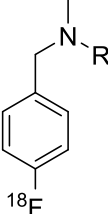
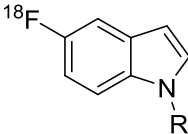
R =					
	Number	<b>1a)</b>	<b>2a)</b>	<b>3a)</b>	NA
	Yield (%)	22	22	20	NA
	Appearance	Colorless solid	Colorless solid	Yellow solid	NA
	Number	<b>4a)</b>	<b>5a)</b>	<b>6a)</b>	NA
	Yield (%)	10	29	22	NA
	Appearance	Yellow solid	Colorless solid	Colorless solid	NA
	Number	NA	<b>7a)</b>	<b>8a)</b>	<b>9a)</b>
	Yield (%)	NA	38	18	34
	Appearance	NA	Colorless solid	Colorless solid	Yellow-white solid

The precipitation yields from the various iodonium ylides are found in Table 11, where the Y represents iodonium ylides of Meldrum's acid. The yields are poor, but coherent with the expected yields of Cardinale and Ermert<sup>19</sup>. The increase in yield for **7a)** may come from precipitation of the compounds at -20 °C instead of room temperature. The 1H-indole-1-carbaldehyde could not be synthesized, so was instead **9a)** synthesized.

### 3.4.1 Radiochemical conversion of ylides

The amount of  $^{18}\text{F}$  fluorine successfully incorporated into the different substructures is found in Table 12, and was determined by radioTLC

**Table 12** The radiochemical incorporation of the different species of N-(4- $^{18}\text{F}$ )fluorophenyl-N-methylamides and N-(4- $^{18}\text{F}$ )fluorobenzyl)-N-methylamides are shown. The indoles gave provided no fluorine incorporation.

R =									
		Avg. (%)	n =	Avg. (%)	n =	Avg. (%)	n =	Avg. (%)	n =
Number		<b>1b)</b>		<b>2b)</b>		<b>3b)</b>		NA	
		87 +/- 10	114	90 +/- 4	4	84 +/- 2	2	NA	NA
Number		<b>4b)</b>		<b>5b)</b>		<b>6b)</b>		NA	
		88 +/- 9	7	51 +/- 3	2	80 +/- 8	4	NA	NA
Number		NA		<b>7b)</b>		<b>8b)</b>		<b>9b)</b>	
		NA	NA	NA	5	NA	2	NA	2

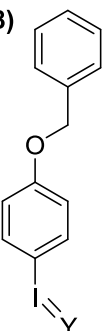
The large amount of samples of the **1b)** comes from the reduction condition screening. Even with a high amount of replicates (n = 114) the standard deviation is relatively large. The high deviation may originate from the iodonium ylides being unstable or small contaminations in the reaction. There are also multiple steps before the radiolabeling, so some deviation must be expected. It is not known whether iodonium ylides are unstable with regards to radiolysis. As the standard deviation is compared with the total average, small deviations would affect a poorer yield even more. The N-(4-fluorophenyl)-N-methylamides all gave good RCC, and are within the standard deviations of each other. Regarding compound **4b)**, the original labeling

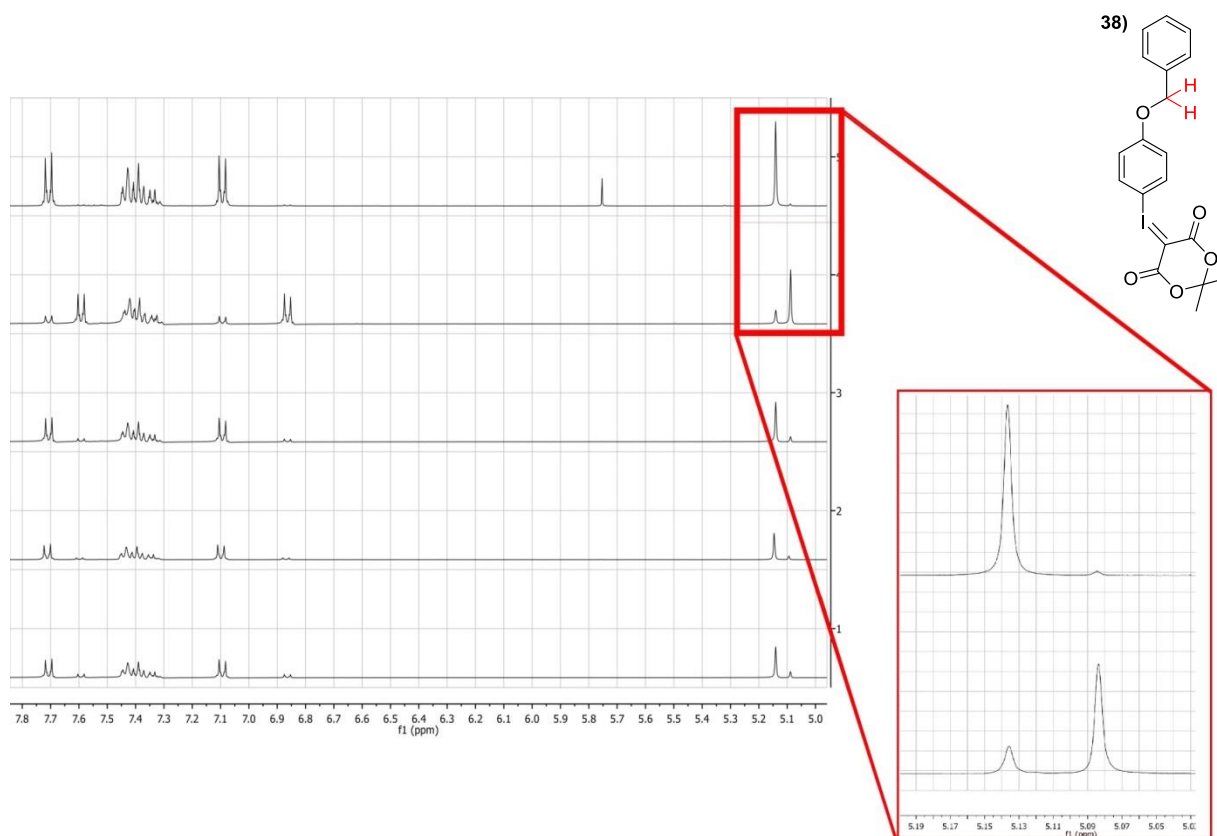
gave 24% (+/- 7, n = 2). Compound **6b**) also gave a much lower yield of 7% (+/- 1, n = 2). Suspecting degradation of the iodonium ylide, it was remade which gave a RCC similar to the N-(4-fluorophenyl)-N-methylamide series. The degraded iodonium ylide had been stored at -20 °C while being protected from light for a few months before use. It would seem apparent that a requirement for successfully radiolabeling with iodonium ylides is a reasonably fresh batch. **5b**) was less successful in incorporating  $^{18}\text{F}$ , indicating that compounds with might have degraded to some extent. None of the compounds with an indole carbon skeleton gave any RCC. This was investigated and is further discussed in the comments of Table 14.

### 3.5 Iodonium ylide degradation

The stability of iodonium ylides has been important when discussing the applicability of the ylides for radiolabeling. An NMR study of a small amount of iodonium ylide is shown in Table 13 and visualized in Scheme 25 where a  $^1\text{H}$ -NMR analysis was carried out on an iodonium ylide. The sum of the integrals used to determine the amount of intact ylide **38** can be found in Table 13. The amount is compared with the age and storage of the iodonium ylide. The iodonium ylide used for this experiment was synthesized by JEJ.

**Table 13** The relative degradation of the iodonium ylides with the age and exposure.

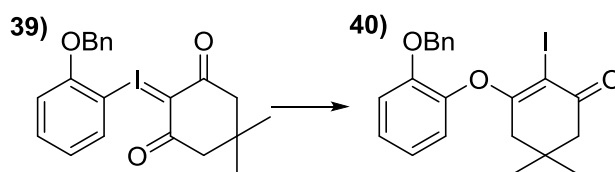
38)		Exposure	Age (weeks)	Purity (% , 5.14/(5.14 + 5.09 ppm))
		NA	Fresh	98
Light & air	1	67		
Air	1	94		
Air	2	89		
Air	4	84		



**Scheme 25** The stacked <sup>1</sup>H-NMR spectra of an iodonium ylide stability test are shown above, with an enlarged cut-out of the reference peaks used to determine the degradation. From top to bottom: Fresh ylide, 1 week old stored in air and room temperature, 1 week old stored in room temperature, 2 weeks old stored in room temperature and 4 weeks old stored in room temperature.

The time points of the analysis was just after its synthesis, after one week with the iodonium ylide exposed to sunlight and room temperature and after 1, 2 and 4 weeks with exposure to room temperature but shielded from light. The decomposition is moderate degradation from storage in room temperature and major (33%) when exposed to light together with ambient atmosphere. The table shows trend of continuous degradation with prolonged temperature exposure. It can also be deduced that exposure to both sunlight and room temperature increases the rate of degradation significantly. The <sup>1</sup>H-NMR signals in the table are assigned to the benzylic protons between the oxygen and the aryl ring shown in Table 13 and Scheme 25. There are several other NMR shifts with the same product:degraded product ratio as used in Table 13. With the degradation there are also an ingrowth of signals with an unequal ratio compared to those in Table 13, subtle in the iodonium ylides only exposed to room

temperature, but more apparent in the ylide exposed to light. This could indicate that iodonium ylides have several pathways in which it can degrade.



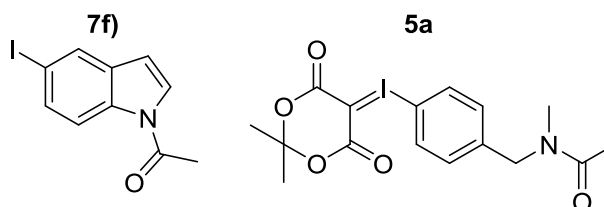
**Scheme 26** A structural decomposition of the ylide reported by Rotstein *et al.*<sup>36</sup> The structural decomposition could also be present on ylides by Meldrum's acid.

There has a reported route of decomposition of a dimeric iodonium ylide, structurally similar to the iodonium ylides of Meldrum's acid. It is not known if the iodonium ylide of Meldrum's acid degrades in a similar fashion to the one shown in Scheme 26.

The impact an iodinated indole precursor had on the RCC was investigated and is shown in Table 14.

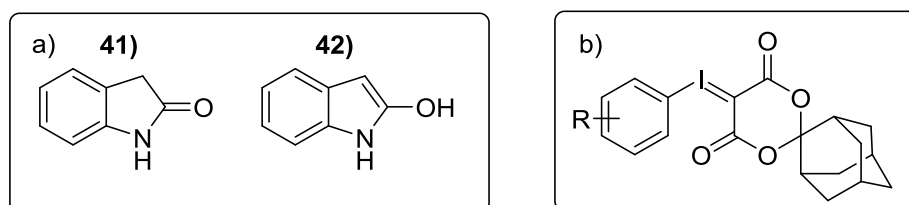
**Table 14** The radiochemical incorporation yield of an iodonium ylide with a given amount of indole in the reaction vial with a visual representation of the two compounds to the right.

<b>7f</b>	<b>5a</b>	RCC (%)	n =
Eq.			
1	0	91	1
0	1	0	1
1	1	56	1
1	2	20	1



The reason for poor radiochemical conversion of indoles after the labeling reactions needed to be investigated. Rotstein *et al.*<sup>36</sup> have previously labeled Boc-protected indole in the 5-position using a SPIAd-ylide (shown in Scheme 27 b), with 8% (+/- 4) conversion yield. The radiolabeling was attempted using a replicated procedure as described (using tetraethylammonium bicarbonate as elution base instead of  $K_2CO_3$ ). Iodonium ylides were also resynthesized followed by an attempted radiofluorination, still providing no RCC. An experiment was designed where **5a** was labeled in the presence of **7f**. The presence of the indole was significantly deterrent for the iodonium ylide labeling, where more indole gave less desired product. It can be hypothesized that the double bond of the indole is oxidized by

the iodonium ylide, as hypervalent iodonium(III) species such as PIDA has been used oxidize indoles, shown in Scheme 27 a.<sup>51-52</sup>



**Scheme 27 a) Oxidized indole tautomers. b) A SPIAd-ylide used by Rotstein *et al.***

The obvious question is how Rotstein *et al* managed to label the indole carbon skeleton in the same position. The labeling temperature may have been lower for indoles, thus labeling with less oxidizing conditions. It is stated that the N-Boc indole is spontaneously de-protected during radiofluorination, which would make the indole less electron rich thus less prone to oxidation. An experiment where two indoles, one with and one without N-Boc protection were labeled would provide valuable information regarding this hypothesis. An NMR experiment was conducted where the labeling conditions were replicated of an indole ylide. There was an ingrowth of a degradation product, but the experiment was inconclusive with regards to what product was being formed.

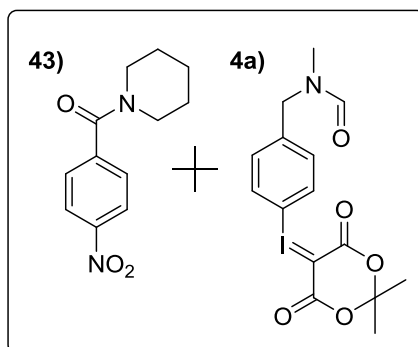


### 3.6 Competition experiment

An experiment with two closely related amides with different leaving group (nitro vs iodonium ylide) was carried out. The aim of these experiments was to investigate the rate of fluorination these, and is found in Table 15.

**Table 15** The radiochemical conversion obtained from two different leaving groups with the two amides illustrated to the right.

Yield (%)		n
<b>4a)</b>	<b>43)</b>	=
95	NA	1
NA	13	1
<b>4a) + 43)</b>		2
89	3	



The RCC was determined by radioTLC. The iodonium ylide individually yielded 93%, and 13% for reacting **43**) individually. When both **4a**) and **43** were reacted in the same vial (and competing for  $^{18}\text{F}$ -fluorine) the yield dropped to 89% for the iodonium ylide and to 3% for the p-nitro. The radiolabeling experiment was carried out on each amide individually prior radiolabeling both in the same vial, for an indication of the preferred leaving group. With the added competition the iodonium ylide maintained 94% of its original yield, while the yield of the nitro group was reduced to a mere 23% of its original yield. The nitro compound would benefit more from the carbonyl group of the amide, being closer to the aromatic ring than the iodonium ylide. That both compounds provide yields would suggest that iodonium ylides react faster with the limited amount of fluorine in the reaction mixture compared with the nitro-group. As the reaction progressed this would leave even less fluorine to react, leaving the iodonium ylide substitution increasingly more as the dominant route. These overall findings are in correlation with the hypothesis of iodonium ylides serving as better leaving group compared to a regular  $\text{S}_{\text{N}}\text{Ar}$ -substitution of the  $\text{NO}_2$ .



## 4 Experimental Section

### 4.1 General

All reagents and solvents, unless specified otherwise, were used as delivered from commercial suppliers without any further purification.

Milli-Q water was used. Argon gas was used to perform reactions under inert atmosphere. NMR-solvents were used as delivered from suppliers. Thin layer chromatography was performed on 60 F<sub>254</sub> silica coated gel from Merck. Flash chromatography was performed manually on silica gel from Merck (Silicagel 60, 0.040-0.063 mm). <sup>18</sup>F was delivered by Norsk Medisinsk Syklotronsenter AS (NMS).

<sup>1</sup>H, <sup>13</sup>C and <sup>19</sup>F NMR experiments were recorded in Chloroform-*d*, MeOH-*d*<sub>4</sub> or DMSO-*d*<sub>6</sub> using either a Bruker Avance AVIII400, AVII400, AVII600 or AVIIHD800 instrument. Residual solvent was used to calibrate the spectra. Chemical shifts ( $\delta$ ) are given in parts per million (ppm) and coupling constants (*J*) are given in Hertz (*Hz*). Multiplicities are abbreviated as: s – singlet; d – doublet; t – triplet; m – multiplet; br. Broad. All spectra were recorded at room temperature (approximately 20 °C). The HPLC detectors used were Raytest Gabi Star as a radio detector and Agilent 1100/1200 DAD as UV monitor. RadioTLC was detected by Raytest miniGita beta detector GML.

Mass spectra were obtained on a micromass QTOF II spectrometer by Osamu Sekiguchi.

## 4.2 Radiochemical procedures

### Radiolabeling of iodonium ylides

An anion exchange resin (Accell<sup>tm</sup> plus QMA Carbonate cartridge) was conditioned with water (5 mL) and air was passed through the cartridge. The aqueous <sup>18</sup>F-fluoride solution was trapped on the exchange resin, and subsequently eluted with (K<sub>2</sub>CO<sub>3</sub> (1.84 mg, 13.3 μmol per reaction vial) Kryptofix<sub>222</sub> (10 mg, 27 μmol per reaction vial) dissolved in a 1 mL solution of 3:7 H<sub>2</sub>O:AcN. The mixture was azeotropically evaporated to dryness with AcN (3 x 1 mL) under a stream of N<sub>2</sub> at 85 °C. The white residue was re-dissolved in DMF (1 mL), used around 100 MBq in each reaction vial.

The appropriate iodonium ylide (9 – 10 μmol) was dissolved in DMF and added to the K<sub>2</sub>CO<sub>3</sub>-<sup>18</sup>F-K<sub>222</sub> solution. The reaction vial was closed and heated to 130 °C for 20 minutes. The vials were allowed to reach room temperature, before a small sample (10 μL) was diluted with DCM (30 μL) and analyzed via radioTLC.

### Reduction

A C18 cartridge was conditioned with water (5 mL), MeOH (5 mL) and air was passed through the cartridge. The content of the reaction vial was diluted in water (9 mL) and passed through the cartridge, followed by water (10 mL). A silica cartridge was conditioned with DCM (5 mL) and air was passed through the cartridge. The silica cartridge was connected underneath the C18 cartridge, and the contents eluted with a THF:DCM solution (1:9 – 1:19 THF:DCM, 2.5 – 3.5 mL). The content of the vial was evaporated at 50 °C under a stream of N<sub>2</sub> until dryness, typically 10 - 15 minutes. Reducing agent (3 - 26.6 Eq.), additive and solvent were added to a total end volume of 500 μL. The vial was capped and the solution was heated to 90 °C for 10 minutes. The vials were allowed to reach room temperature, before a small sample (20 μL) was diluted with HPLC buffer solution (180 μL) and analyzed via radioHPLC.

## Hydrolysis

A C18 cartridge was washed with water (5 mL), MeOH and air was passed through the cartridge. The content of the reaction vial was diluted in water (9 mL) and passed through the cartridge, followed by water (10 mL). The contents were eluted with dioxane (1.5 – 3.0 mL) into a reaction vial containing HCl, with a final HCl concentration of 10% or 18.5% HCl. The vial was capped and the solution was heated to 100 °C for 10 minutes. The vials were allowed to reach room temperature, quenched with 3.3M NaOH until a neutral pH was obtained. A small sample (20 µL) was diluted with HPLC buffer solution (180 µL) and analyzed via radioHPLC.

## 4.3 Organic procedures

### Typical procedure A (Iodonium ylide formation)

In a light protected, inert atmosphere, amide<sup>a)</sup> was dissolved in DCM (5 mL) followed by an addition of mCPBA<sup>b)</sup> in DCM (2 mL). The reaction mixture was kept at 40 °C for 80 minutes, until a major conversion to an intermediate was shown on TLC. The reaction mixture was cooled in a water bath to 15 °C before addition of KOH<sup>c)</sup> and Meldrum's acid<sup>d)</sup>. The reaction progress was monitored via appearance of a new spot on TLC analysis. After 20 minutes the solution was diluted with DCM (10 mL), passed through a filter paper (55 mm) and washed with DCM (10 mL). The solvent was removed under reduced pressure.

### Typical procedure B

Amide<sup>a)</sup> was added dropwise to a slurry of 60% NaH<sup>b)</sup> in DMF<sup>c)</sup> at 0 °C under inert atmosphere. Evolution of gas ceased, and the reaction mixture was allowed to reach room temperature. Reagent<sup>d)</sup> was dropwise added and the reaction mixture was left for several hours at room temperature<sup>e)</sup>. The reaction was monitored by TLC analysis. The solution was diluted in H<sub>2</sub>O (10 mL), washed with NaHCO<sub>3</sub> (sat., 10 mL) and extracted using EtOAc (3x15 mL). The combined organic phases were dried over Na<sub>2</sub>SO<sub>4</sub>, and the solvent was removed under reduced pressure.

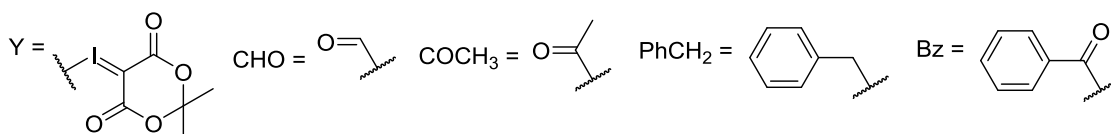
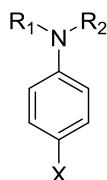
### Typical procedure C

To amine<sup>a)</sup> in solvent<sup>b)</sup> was added triethylamine<sup>c)</sup> and DMAP<sup>d)</sup> under inert atmosphere. Reagent<sup>e)</sup> was added, and the reaction mixture was heated overnight at 50 °C<sup>f)</sup>. The reaction was followed by TLC analysis. The mixture was added H<sub>2</sub>O (10 mL), NaHCO<sub>3</sub> (Sat., 10 mL), and extracted using EtOAc (3x15 mL). The combined organic phases were dried over Na<sub>2</sub>SO<sub>4</sub>, filtered and removed under reduced pressure.

**1a)**: X = Y, R<sub>1</sub> = CHO, R<sub>2</sub> = Me  
**1b)**: X = F, R<sub>1</sub> = CHO, R<sub>2</sub> = Me  
**1c)**: X = F, R<sub>1</sub> = R<sub>2</sub> = Me  
**1d)**: X = F, R<sub>1</sub> = Me, R<sub>2</sub> = H  
**1e)**: X = I, R<sub>1</sub> = R<sub>2</sub> = H  
**1f)**: X = I, R<sub>1</sub> = CHO, R<sub>2</sub> = H  
**1g)**: X = I, R<sub>1</sub> = CHO, R<sub>2</sub> = Me

**2a)** = Y, R<sub>1</sub> = COCH<sub>3</sub>, R<sub>2</sub> = Me  
**2b)**: X = F, R<sub>1</sub> = COCH<sub>3</sub>, R<sub>2</sub> = Me  
**2c)**: X = F, R<sub>1</sub> = Et, R<sub>2</sub> = Me  
**2d)**: X = I, R<sub>1</sub> = COCH<sub>3</sub>, R<sub>2</sub> = H  
**2e)**: X = I, R<sub>1</sub> = COCH<sub>3</sub>, R<sub>2</sub> = Me

**3a)**: X = Y, R<sub>1</sub> = Me, R<sub>2</sub> = Bz  
**3b)**: X = F, R<sub>1</sub> = Me, R<sub>2</sub> = Bz  
**3c)**: X = F, R<sub>1</sub> = H, R<sub>2</sub> = PhCH<sub>2</sub>  
**3d)**: X = I, R<sub>1</sub> = H, R<sub>2</sub> = Bz  
**3e)**: X = I, R<sub>1</sub> = Me, R<sub>2</sub> = Bz



**Compounds 1b), 1f) and 1g) were synthesized by JEJ. 1d) and 1e) were purchased.**

### **N-(4-((2,2-dimethyl-4,6-dioxo-1,3-dioxan-5-ylidene)-1,3-iodanyl)phenyl)-N-methylformamide (1a)**

Following **typical procedure A**, the crude was dissolved in DCM (10 mL) and precipitated in hexanes (20 mL) yielding **1a** in 24% (49 mg, 0.12 mmol) as a white solid. **a) 0.131 g, 0.50 mmol of amide 1g) b) 115 mg, 0.66 mmol mCPBA c) 0.218 g, 3.9 mmol KOH d) 95 mg, 0.66 mmol Meldrum's acid.** <sup>1</sup>H NMR (400 MHz, DMSO-*d*<sub>6</sub>) δ 8.65 (s, 1H), 7.82 – 7.77 (m, 2H), 7.47 – 7.42 (m, 2H), 3.21 (s, 3H), 1.57 (s, 6H). <sup>13</sup>C NMR (101 MHz, DMSO) δ (162.8;162.1), 144.1, (133.7;122.9), 128.7, 127.6, 111.4, 102.7, 58.3, 30.5, 25.6. **MS** (ESI, MeOH) *m/z*: 425.981 [M + Na]<sup>+</sup>. **HRMS** (MeOH): Calculated for C<sub>14</sub>H<sub>14</sub>INO<sub>5</sub> [M + Na]<sup>+</sup> 425.9815, found 425.9808 (Δ 0.0007 ppm).

### **4-fluoro-N,N-dimethylaniline (1c)**

To **1d** (98 mg, 0.78 mmol) dissolved in DCE (4 ml) was added formaldehyde (44 μL, 1.2 mmol), ZnCl<sub>2</sub> (13 mg, 0.95 mmol) and MeOH (2mL). The reaction mixture was left to stir for several hours until TLC analysis indicated some consumption. The reaction mixture was added H<sub>2</sub>O (10 mL) NaOH (2M, Aq., 10 mL) and extracted with EtOAc (3x15 mL). The combined organic phases were dried over Na<sub>2</sub>SO<sub>4</sub>, and the solvent evaporated under reduced pressure. The crude was purified using flash column chromatography with 1:4 hexanes:DCM affording **1b** in 25% (18 mg, 0.20 mmol) as a yellow-green oil. <sup>1</sup>H NMR (400 MHz, Chloroform-*d*) δ 6.99 – 6.91 (m, 2H), 6.72 – 6.65 (m, 2H), 2.90 (s, 6H). See Dong et al<sup>53</sup> for reference <sup>1</sup>H-NMR and <sup>13</sup>C-NMR <sup>19</sup>F NMR (377 MHz, Chloroform-*d*) δ -129.0 (s). **MS** (ESI, MeOH) *m/z*: 140.087 [M + H]<sup>+</sup> **HRMS** (MeOH): Calculated for C<sub>8</sub>H<sub>10</sub>FNH<sup>+</sup> [M + H]<sup>+</sup> 140.0875, found 140.0869 (Δ 0.0006 ppm)

### **N-(4-((2,2-dimethyl-4,6-dioxo-1,3-dioxan-5-ylidene)-1,3-iodanyl)phenyl)-N-methylacetamide (2a)**

Following **typical procedure B**, the crude was dissolved in DCM (10 mL) and precipitated in hexanes (20 mL) yielding **2a** in 22% (84 mg, 0.22 mmol) as a white solid. **a) 0.25 g, 0.89 mmol of amide 2e) b) 247 mg, 1.43 mmol mCPBA c) 0.44 g, 7.8 mmol KOH d) 170 mg, 1.18 mmol Meldrum's acid.** <sup>1</sup>H NMR (600 MHz, DMSO-*d*<sub>6</sub>) δ 7.81 (d, *J* = 8.2 Hz, 2H), 7.44 (d, *J* = 8.1 Hz, 2H), 3.17 (s, 3H), 1.85 (br., 3H), 1.58 (s, 6H). <sup>13</sup>C NMR (151 MHz, DMSO-*d*<sub>6</sub>) δ 163.3, 146.8, 133.8, 129.9, 103.3, 58.4, 55.4, 37.1, 27.4, 26.1, 22.9. **MS** (ESI, MeOH) *m/z*: 439.997 [M + Na]<sup>+</sup>. **HRMS** (MeOH): Calculated for C<sub>15</sub>H<sub>16</sub>INO<sub>5</sub> [M + Na]<sup>+</sup> 439.9971, found 439.9966 (Δ 0.0005 ppm).

### **N-(4-fluorophenyl)-N-methyl-acetamide (2b)**

To a solution of **1d** (85 mg, 0.68 mmol) in THF (4 mL) was added acetic anhydride (0.71 μL, 0.75 mmol) at 0° C. The solution was allowed to reach room temperature and left to stir for several hours. TLC analysis indicated some conversion. The reaction mixture was added H<sub>2</sub>O (10 mL), basified with saturated NaHCO<sub>3</sub> (10 mL) and extracted with EtOAc (3x15 mL). The organic phase was dried over Na<sub>2</sub>SO<sub>4</sub> and the solvent removed under reduced pressure. The crude was purified by flash column chromatography (1:1 EtOAc:Hexanes) yielding **2b** in 54% as a yellow-white solid. <sup>1</sup>H NMR (400 MHz, Chloroform-*d*) δ 7.16 (m, 2H), 7.09 (m, 2H), 3.22 (s, 3H), 1.84 (s, 3H). <sup>13</sup>C NMR (101 MHz, Chloroform-*d*) See Lindstad et al<sup>54</sup> for reference <sup>1</sup>H-NMR, <sup>13</sup>C-NMR, <sup>19</sup>F-NMR. **MS** (ESI, MeOH) *m/z*: 190.064 [M + Na]<sup>+</sup>. **HRMS** (MeOH): Calculated for C<sub>9</sub>H<sub>10</sub>FNONa<sup>+</sup> [M + Na]<sup>+</sup> 190.0746, found 190.0639 (Δ 0.0005 ppm)

### **N-ethyl-4-fluoro-N-methyl-benzenamine (2c)**

To a closed microwave vial equipped with **2b** (0.30 mmol, 50 mg) dissolved in THF (2 mL) was added 1,3-Bis(2,6-diisopropylphenyl)-1,3-dihydro-2H-imidazol-2-ylidene (1 mg, 2.6 μmol) from THF (0.25 mL). The reaction vial was flushed with argon and 0.5 M 9-BBN in THF (2.4 μL, 1.2 mmol) was added. The reaction vial was heated to 90 °C for 10 minutes. TLC analysis indicated full conversion. The solution was cooled to room temperature and quenched with H<sub>2</sub>O (0.5 mL). The solution was diluted with H<sub>2</sub>O (10 mL), basified via addition of NaOH (10 mL, 2M), and extracted using EtOAc (3x15 mL). The combined organic phases were dried over Na<sub>2</sub>SO<sub>4</sub> and the solvents were removed under reduced pressure. The crude was purified using 1:9 MeOH:CHCl<sub>3</sub> flash column chromatography yielding **2b** in 67% (31 mg, 0.20 mmol) as brown oil. <sup>1</sup>H NMR (400 MHz, Chloroform-*d*) δ 6.98 – 6.88 (m, 2H), 6.70 – 6.62 (m, 2H), 3.34 (q, *J* = 7.1 Hz, 2H), 2.86 (s, 3H), 1.10 (t, *J* = 7.1 Hz, 3H). <sup>13</sup>C NMR (101 MHz, Chloroform-*d*) δ 155.5 (d, *J*<sub>CF</sub> = 235 Hz), 146.2, br., 115.6 (d, *J*<sub>CF</sub> = 22 Hz), 114.1 (d, *J*<sub>CF</sub> = 7 Hz) 47.8, 38.2, 11.2. <sup>19</sup>F NMR (377 MHz, Chloroform-*d*) δ -129.6. **MS** (ESI, MeOH) *m/z*: 154.103 [M + H]<sup>+</sup>. **HRMS** (MeOH): Calculated for C<sub>9</sub>H<sub>12</sub>FNH<sup>+</sup> [M + H]<sup>+</sup> 154.1032, found 154.1027 (Δ 0.0005 ppm)

### **N-(4-iodophenyl)-acetamide (2d)**

To 4-iodoaniline (**1e**) (3.01g, 13.8 mmol) dissolved in THF (6 ml) was added acetic anhydride (1.5 mL, 16 mmol). The reaction mixture was left to stir for several hours until major conversion was indicated by TLC. The reaction mixture was diluted with H<sub>2</sub>O (10 mL), washed with saturated NaHCO<sub>3</sub> (10 mL), and extracted with EtOAc (3x15 mL). The



combined organic phases were dried over Na<sub>2</sub>SO<sub>4</sub>, and the solvents removed under reduced pressure. The crude was recrystallized from EtOH affording **2d**) in 87% (3.12 g, 11.9 mmol) as white crystals. <sup>1</sup>H NMR (400 MHz, DMSO-*d*<sub>6</sub>) δ 10.00 (s, 1H), 7.64 – 7.57 (m, 2H), 7.45 – 7.37 (m, 2H), 2.03 (s, 3H). See Knauber et al<sup>55</sup> for reference <sup>1</sup>H-NMR and <sup>13</sup>C-NMR. **MS** (ESI, MeOH) *m/z*: 283.954 [M + Na]<sup>+</sup> **HRMS** (MeOH): Calculated for C<sub>8</sub>H<sub>8</sub>INONa<sup>+</sup> [M + Na]<sup>+</sup> 283.9549, found 283.9543 (Δ 0.0006 ppm)

#### ***N*-(4-iodophenyl)-*N*-methyl-Acetamide (2e)**

Following **typical procedure B**, the crude was recrystallized from EtOH affording **2e**) in 73% (0.78 g, 2.84 mmol) as pale, yellow solids. a) **1.01g, 3.83 mmol of amide 2d**) b) **256 mg, 6.40 mmol NaH** c) **8 mL DMF** d) **0.36 mL, 5.8 mmol methyl iodide** e) **the reaction mixture was left for several hours.** <sup>1</sup>H NMR (400 MHz, Chloroform-*d*) δ 7.81 – 7.65 (m, 2H), 7.02 – 6.86 (m, 2H), 3.23 (s, 3H), 1.87 (s, 3H). See Knauber et al<sup>55</sup> for reference <sup>1</sup>H-NMR and <sup>13</sup>C-NMR. [M + Na]<sup>+</sup>. **HRMS** (MeOH): Calculated for C<sub>9</sub>H<sub>10</sub>FNONa<sup>+</sup> [M + Na]<sup>+</sup> 190.0644, found 190.0639 (Δ 0.0005 ppm)

#### ***N*-(4-((2,2-dimethyl-4,6-dioxo-1,3-dioxan-5-ylidene)-1,3-iodanyl)phenyl)-*N*-methylbenzamide (3a)**

Following **typical procedure A**, the crude was dissolved in EtOAc (10 mL) and precipitated in pentane (20 mL) yielding **3a**) in 20% (67 mg, 0.14 mmol) as a yellow solid. a) **236 mg, 0.7 mmol of 1g**). b) **196 mg, 1.13 mmol mCPBA** c) **335 mg, 6.0 mmol KOH** d) **175 mg, 0.122 mmol Meldrum's acid** <sup>1</sup>H NMR (400 MHz, DMSO-*d*<sub>6</sub>) δ 7.70 – 7.55 (m, 2H), 7.31 – 7.20 (m, 7H), 3.36 (s, 3H), 1.53 (s, 6H). <sup>13</sup>C NMR (101 MHz, DMSO-*d*<sub>6</sub>) δ 169.5, 162.8, 146.6, 135.8, 133.1, 129.7, 129.2, 128.1, 127.9, 112.8, 102.7, 58.0, 37.7, 25.6. **MS** (ESI, MeOH) *m/z*: 502.012 [M + Na]<sup>+</sup>. **HRMS** (MeOH): Calculated for C<sub>20</sub>H<sub>18</sub>INO<sub>5</sub>Na<sup>+</sup> [M + Na]<sup>+</sup> 502.0128, found 502.0122 (0.0006 Δ ppm)

#### ***N*-benzyl-4-fluoro-*N*-methylaniline (3b)**

To **1d**) (0.108 g, 0.862 mmol) dissolved in DMF (1 ml), was added K<sub>2</sub>CO<sub>3</sub> (105 mg, 0.75 mmol) and benzyl bromide (8.7 μL, 107 μmol). After the addition the reaction temperature was increased to 80° C and the temperature was held for 1 hour. TLC indicated consumption of starting material, and the mixture was cooled to room temperature. The reaction mixture was diluted with H<sub>2</sub>O (10 mL) washed with NaHCO<sub>3</sub> (5 mL), followed by extraction by EtOAc (3x15 mL). The combined organic layers were dried over Na<sub>2</sub>SO<sub>4</sub>, and the solvents removed under reduced pressure. The residue was purified by flash column chromatography using 1:9 EtOAc:Hexanes affording **3b**) in 27% (0.23 mmol, 49 mg) as a brown oil. <sup>1</sup>H NMR (400 MHz, Chloroform-*d*) δ 7.42 – 7.14 (m, 5H), 7.01 – 6.84 (m, 2H), 6.76 – 6.57 (m, 2H), 4.49 (s, 2H), 2.98 (s, 3H). See Wang et al<sup>56</sup> for reference <sup>1</sup>H-NMR and <sup>13</sup>C-NMR. <sup>19</sup>F NMR (377 MHz, Chloroform-*d*) δ -129.1 (m). **MS** (ESI, MeOH) *m/z*: 216.118 [M + H]<sup>+</sup>. **HRMS** (MeOH): Calculated for C<sub>14</sub>H<sub>14</sub>FNH<sup>+</sup> [M + H]<sup>+</sup> 216.1188, found 216.1184 (0.0004 Δ ppm)

#### ***N*-(4-fluorophenyl)-*N*-methylbenzamide (3c)**

Following **typical procedure C**, the crude was purified by flash column chromatography using a gradient from 1:3 EtOAc/Hexanes to 1:1 EtOAc:Hexanes affording **3c**) in 75% (68.1 mg, 0.30 mmol) as yellow white crystal a) **50 mg, 0.40 mmol of amine 1d**) b) **4 mL THF** c) **0.11 mL, 0.80 mmol triethylamine** d) **No DMAP** e) **0.93 mL, 0.80 mmol benzoyl chloride** f) **stirred in room temperature overnight.** <sup>1</sup>H NMR (400 MHz, Chloroform-*d*) δ 7.35 – 7.09 (m,

5H), 7.09 – 6.95 (m, 2H), 6.95 – 6.81 (m, 2H), 3.45 (s, 3H). See Kato et al<sup>57</sup> for reference <sup>1</sup>H-NMR and <sup>13</sup>C-NMR. <sup>19</sup>F NMR (377 MHz, Chloroform-*d*) δ -114.9 (m). **MS** (ESI, MeOH) *m/z*: 252.080 [M + Na]<sup>+</sup>. **HRMS** (MeOH): Calculated for C<sub>14</sub>H<sub>12</sub>FNONa<sup>+</sup> [M + Na]<sup>+</sup> 252.0801, found 252.0795 (0.0006 Δ ppm)

### **N-(4-iodophenyl)benzamide (3d)**

To **1e** (3.0 g, 13.7 mmol) dissolved in THF (15 mL) together with triethylamine (1.92 mL, 13.7 mmol) was added benzoyl chloride (1.6 mL, 13.7 mmol). The reaction mixture was refluxed for 6 hours. After cooling to room temperature the reaction mixture was basified to pH 8-9 by aqueous KOH (2M, 9 mL) and the reaction mixture was further left for 30 min. The solids were filtered off yielding **3d** in 61% (2.72 g, 8.4 mmol) as a white crystalline powder. <sup>1</sup>H NMR (400 MHz, DMSO-*d*<sub>6</sub>) δ 10.32 (s, 1H), 7.98 – 7.91 (m, 2H), 7.74 – 7.67 (m, 2H), 7.66 – 7.62 (m, 2H), 7.62 – 7.56 (m, 1H), 7.56 – 7.48 (m, 2H). See Xu et al<sup>58</sup> for reference <sup>1</sup>H-NMR and <sup>13</sup>C-NMR. **MS** (ESI, MeOH) *m/z*: 345.970 [M + Na]<sup>+</sup>. **HRMS** (MeOH): Calculated for C<sub>13</sub>H<sub>10</sub>INONa<sup>+</sup> [M + Na]<sup>+</sup> 345.9705, found 345.9699 (Δ0.0006 ppm)

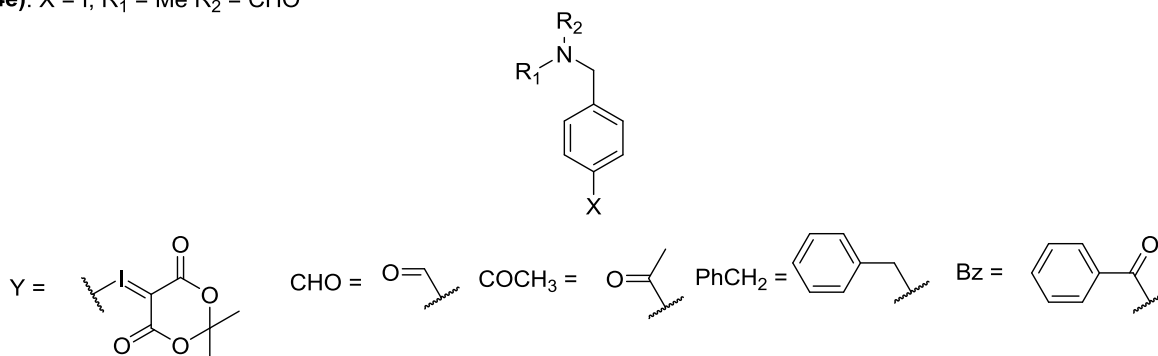
### **N-(4-iodophenyl)-N-methylbenzamide (3e)**

Following **typical procedure B**, the crude was recrystallized from MeOH affording **3e** in 72% (992 mg 2.94 mmol) as pale yellow-white solids. **a) 1.38 g, 4.1 mmol of amide 3d b) 246 mg, 6.2 mmol NaH c) 7 mL DMF d) 0.77 mL, 12 mmol methyl iodide** <sup>1</sup>H NMR (400 MHz, Chloroform-*d*) δ 7.51 – 7.41 (m, 2H), 7.21 (ddd, *J* = 8.4, 7.0, 1.5 Hz, 3H), 7.17 – 7.07 (m, 2H), 6.75 – 6.65 (m, 2H), 3.39 (s, 3H). <sup>13</sup>C NMR (101 MHz, Chloroform-*d*) δ 170.6, 144.9, 138.4, 135.7, 130.0, 128.8 (d, *J* = 4.7 Hz), 128.1, 91.2, 38.4. **MS** (ESI, MeOH) *m/z*: 359.986 [M + Na]<sup>+</sup>. **HRMS** (MeOH): Calculated for C<sub>14</sub>H<sub>12</sub>INONa<sup>+</sup> [M + Na]<sup>+</sup> 359.9862, found 359.9856 (Δ 0.0005 ppm)

**4a):** X = Y, R<sub>1</sub> = Me, R<sub>2</sub> = CHO  
**4b):** X = F, R<sub>1</sub> = Me, R<sub>2</sub> = CHO  
**4c):** X = F, R<sub>1</sub> = R<sub>2</sub> = Me  
**4d):** X = F, R<sub>1</sub> = H, R<sub>2</sub> = Me  
**4e):** X = I, R<sub>1</sub> = Me, R<sub>2</sub> = CHO

**5a):** X = Y, R<sub>1</sub> = Me, R<sub>2</sub> = COCH<sub>3</sub>  
**5b):** X = F, R<sub>1</sub> = Me, R<sub>2</sub> = COCH<sub>3</sub>  
**5c):** X = F, R<sub>1</sub> = Me, R<sub>2</sub> = Et  
**5d):** X = I, R<sub>1</sub> = Me, R<sub>2</sub> = COCH<sub>3</sub>

**6a):** X = Y, R<sub>1</sub> = Me, R<sub>2</sub> = Bz  
**6b):** X = F, R<sub>1</sub> = Me, R<sub>2</sub> = Bz  
**6c):** X = F, R<sub>1</sub> = Me, R<sub>2</sub> = PhCH<sub>2</sub>  
**6d):** X = I, R<sub>1</sub> = Me, R<sub>2</sub> = Bz



**Compound 4d)** was purchased.

#### N-(4-((2,2-dimethyl-4,6-dioxo-1,3-dioxan-5-ylidene)-1,3-iodanyl)benzyl)-N-methylformamide (**4a**)

Following **typical procedure A**, the crude was dissolved in DCM (10 mL) and precipitated in hexanes (20 mL) yielding 10% (0.11 mmol, 46 mg) of **4a**) as yellow solids. **a) 289 mg, 1.05 mmol of 4e) b) 270 mg, 1.56 mmol mCPBA c) 416 mg, 7.42 mmol KOH d) 191 mg, 1.32 mmol Meldrum's acid** <sup>1</sup>H NMR (400 MHz, DMSO-*d*<sub>6</sub>) δ 8.21 (d, *J* = 50.5 Hz, 1H), 7.82 – 7.73 (m, 2H), 7.44 – 7.27 (m, 2H), 4.50 (s, 2H), 2.74 (d, *J* = 89.2 Hz, 3H), 1.57 (s, 6H). <sup>13</sup>C NMR (101 MHz, DMSO-*d*<sub>6</sub>) δ (166.4;165.8); (162.9;162.8); (140.0;139.7); (132.84;132.78); (130.07;130.05); (115.1;114.7), 102.7, 57.9, (51.5;46.2); (33.8;28.9); (26.0;25.6). **MS** (ESI, MeOH) *m/z*: 439.997 [M + Na]<sup>+</sup>. **HRMS** (MeOH): Calculated for C<sub>15</sub>H<sub>16</sub>I NONa<sup>+</sup> [M + Na]<sup>+</sup> 439.9971, found 439.9965 (0.0006 Δ ppm)

#### N-(4-fluorobenzyl)-N-methylformamide (**4b**)

A neat mixture of acetaldehyde (0.07 mL, 0.3 mmol) and acetic anhydride (0.14 mL, 0.20 mmol) was heated to 85° C for 30 min. The mixture was added to **4e**) (108 mg, 0.78 mmol) dissolved in THF (2 mL). The mixture was left to react for 30 minutes. TLC indicated some conversion. The solution was diluted in H<sub>2</sub>O (10 mL), washed with NaHCO<sub>3</sub> until gas formation ceased, and extracted with EtOAc (3x15 mL). The combined organic phases were dried using Na<sub>2</sub>SO<sub>4</sub>, and the solvents removed under reduced pressure. The crude was purified by flash column chromatography (1:1 EtOAc:Hexanes) yielding 18% (24 mg, 0.14 mmol) of **4b**) as a white yellowish powder. <sup>1</sup>H NMR (400 MHz, Chloroform-*d*) δ 8.20 (d, *J* = 53.4 Hz, 1H), 7.25 – 7.11 (m, 2H), 7.09 – 6.94 (m, 2H), 4.42 (d, *J* = 48.1 Hz, 2H), 2.98 – 2.68 (m, 3H). <sup>13</sup>C NMR (101 MHz, Chloroform-*d*) δ 162.7 (d, *J*<sub>CF</sub><sup>1</sup> = 246 Hz), (131.81;131.78) (d, *J*<sub>CF</sub><sup>4</sup> = 2.6 Hz), 130.1 (d, *J*<sub>CF</sub><sup>3</sup> = 8.2 Hz), 129.2 (d, *J*<sub>CF</sub><sup>3</sup> = 8.3 Hz), (116.0;115.8, d, *J*<sub>CF</sub><sup>2</sup> = 21 Hz), (52.9;47.2), (34.1;29.5). <sup>19</sup>F NMR (377 MHz, Chloroform-*d*) δ -113.7 – -115.7 (m). **MS** (ESI, MeOH) *m/z*: 190.064 [M + Na]<sup>+</sup>. **HRMS** (MeOH): Calculated for C<sub>9</sub>H<sub>10</sub>FN ONa<sup>+</sup> [M + Na]<sup>+</sup> 190.0644, found 190.0639 (0.0005 Δ ppm)

### 1-(4-fluorophenyl)-N,N-dimethylmethanamine (4c)

To **4d** (100 mg, 0.72 mmol) in THF (5 mL) was added cooled formic acid (1.22 mmol, 50  $\mu$ L), followed by formaldehyde (2.7 mmol, 80  $\mu$ L). The solution was left to stir overnight. TLC indicated some conversion. The reaction mixture was washed with NaHCO<sub>3</sub> until gas formation ceased, and extracted with EtOAc (3x20 mL). The combined organic phases were dried over Na<sub>2</sub>SO<sub>4</sub>, and the solvent removed under reduced pressure. The crude was purified by flash column chromatography in 1:12 MeOH:DCM yielding 21% (23 mg 0.15 mmol) of **4c** as a light brown oil. <sup>1</sup>H NMR (400 MHz, Chloroform-*d*)  $\delta$  7.15 (s, 2H), 3.38 (s, 2H), 2.18 (s, 6H). See Hamid et al<sup>58</sup> for reference <sup>1</sup>H-NMR and <sup>13</sup>C-NMR. HRMS (ESI-TOF) Calculated for C<sub>9</sub>H<sub>13</sub>FNH<sup>+</sup>: 154.1032, found 154.1023 [M + H<sup>+</sup>] (0.0001  $\Delta$  ppm)<sup>59</sup>

### N-(4-iodobenzyl)-N-methylformamide (4e)

Following **typical procedure B**, the crude mixture was purified by flash column chromatography in 1:1 EtOAc:Hexanes affording **4e** in 84% as a yellow white powder. **a) 0.43 mL, 7.41 mmol of n-methylformamide b) 337 mg, 8.42 mmol NaH c) 7 mL THF d) 1.05 g, 3.37 mmol of 4-iodobenzyl bromide e) 60 °C overnight.** <sup>1</sup>H NMR (600 MHz, Chloroform-*d*)  $\delta$  8.30 – 8.10 (m, 1H), 7.75 – 7.58 (m, 2H), 7.04 – 6.88 (m, 2H), 4.39 (d, *J* = 71.1 Hz, 2H), 2.80 (dd, *J* = 46.0, 1.4 Hz, 3H). <sup>13</sup>C NMR (151 MHz, Chloroform-*d*)  $\delta$  (162.7;162.6); (138.0;137.8); (135.8;135.5);(130.2;129.3); (93.6;93.2); (53.0;47.3); (34.1;29.5). MS (ESI, MeOH) *m/z*: 297.970 [M + Na]<sup>+</sup>. HRMS (MeOH): Calculated for C<sub>9</sub>H<sub>10</sub>INO<sub>2</sub>Na<sup>+</sup> [M + Na]<sup>+</sup> 297.9708, found 297.9700 (0.0008  $\Delta$  ppm)

### N-(4-((2,2-dimethyl-4,6-dioxo-1,3-dioxan-5-ylidene)-1,3-iodanyl)benzyl)-N-methylacetamide (5a)

Following **typical procedure A**, the crude was dissolved in DCM (10 mL) and precipitated in hexanes (20 mL) yielding 29% (65 mg, 0.15 mmol) of **5a** as white solids. **a) 289 mg, 0.52 mmol of amide 5d b) 117 mg, 0.68 mmol mCPBA c) 199 mg, 3.54 mmol KOH d) 95 mg, 0.66 mmol Meldrum's acid.** <sup>1</sup>H NMR (400 MHz, DMSO-*d*<sub>6</sub>)  $\delta$  7.90 (dp, *J* = 4.2, 1.4 Hz, 1H), 7.83 – 7.71 (m, 2H), 7.28 (dd, *J* = 8.6, 2.4 Hz, 2H), 4.55 (d, *J* = 36.3 Hz, 2H), 2.84 (d, *J* = 59.4 Hz, 3H), 2.03 (d, *J* = 20.5 Hz, 3H), 1.56 (s, 6H). <sup>13</sup>C NMR (101 MHz, DMSO-*d*<sub>6</sub>)  $\delta$  (170.1;169.9), (166.1;162.8) (141.1;140.7), (133.0;132.7), (130.7;129.9)(114.6;114.4)(102.71;102.69), 58.0, (47.3;52.7)(33.5;35.7)(25.6;27.0)(21.2;21.5). MS (ESI, MeOH) *m/z*: 154.012 [M + Na]<sup>+</sup>. HRMS (MeOH): Calculated for C<sub>16</sub>H<sub>18</sub>INO<sub>5</sub>Na<sup>+</sup> [M + Na]<sup>+</sup> 454.0128, found 454.0122 (0.0006  $\Delta$  ppm)

### N-(4-fluorobenzyl)-N-methylacetamide (5b)

To a solution of 60% NaH (26 mg, 0.64 mmol) was added N-methylacetamide (46 mg, 0.64 mmol). Evolution of gas ceased and 4-fluorobenzyl bromide (108 mg, 0.57 mmol) was added dropwise and the reaction mixture were left for several hours at 60° C. TLC analysis indicated little consumption of starting material. More N-methylacetamide (255 mg, 3.49 mmol) and NaH (237 mg, 5.93 mmol) were added and the reaction was left overnight at 60 °C. TLC indicated a major conversion. The reaction mixture was diluted with H<sub>2</sub>O (10 mL), brine (5 mL) and extracted with EtOAc (3x15 mL). The combined organic phases were dried over Na<sub>2</sub>SO<sub>4</sub>, and the solvents evaporated under reduced pressure. The crude was purified using flash column chromatography with EtOAc affording **5b** in 54% (0.31 mmol, 56 mg) as brown oil. <sup>1</sup>H NMR (400 MHz, Chloroform-*d*)  $\delta$  7.24 – 7.10 (m, 2H), 7.08 – 6.95 (m, 2H), (4.53;4.48) (2H),

(2.91;2.91) (3H), 2.14 (s, 3H). See Hansen et al<sup>60</sup> for reference <sup>1</sup>H-NMR and <sup>13</sup>C-NMR. <sup>19</sup>F NMR (377 MHz, Chloroform-*d*)  $\delta$  - (114.79;115.36) (m). **MS** (ESI, MeOH) *m/z*: 204.043 [M + Na]<sup>+</sup>. **HRMS** (MeOH): Calculated for C<sub>10</sub>H<sub>12</sub>FNONa<sup>+</sup> [M + Na]<sup>+</sup> 204.0801, found 204.0431 (0.04  $\Delta$  ppm)

#### **N-(4-fluorobenzyl)-N-methylethanamine (5c)**

To a solution of **4d** (0.11 g, 0.79 mmol) dissolved in THF (5 mL) was added ethyl iodide (0.064 mL, 0.79 mmol). The solution was left to stir overnight at room temperature. TLC indicated major conversion. The solution was diluted in H<sub>2</sub>O (10 mL), NaHCO<sub>3</sub> (sat., 10 mL) and extracted in EtOAc (3x15 mL). The crude was purified using flash column chromatography (3:22 MeOH:DCM) yielding 37% of **5c** as a yellow oil (48.9 mg, 0.29 mmol). <sup>1</sup>H NMR (400 MHz, Chloroform-*d*)  $\delta$  7.33 – 7.26 (m, 2H), 7.04 – 6.95 (m, 2H), 3.47 (s, 2H), 2.46 (q, *J* = 7.2 Hz, 2H), 2.19 (s, 3H), 1.11 (t, *J* = 7.2 Hz, 3H). <sup>13</sup>C NMR (101 MHz, Chloroform-*d*)  $\delta$  162.2 (d, *J*<sub>CF</sub> = 244.5 Hz), 134.6 (br.), 130.8 (d, *J*<sub>CF</sub> = 8.0 Hz), 115.2 (d, *J*<sub>CF</sub> = 21.1 Hz), 61.2, 51.3, 41.6, 12.4. <sup>19</sup>F NMR (377 MHz, Chloroform-*d*)  $\delta$  -116.00. **MS** (ESI, MeOH) *m/z*: 168.118 [M + H]<sup>+</sup>. **HRMS** (MeOH): Calculated for C<sub>10</sub>H<sub>14</sub>FNH<sup>+</sup> [M + H]<sup>+</sup> 168.1188, found 168.1184 (0.0004  $\Delta$  ppm)

#### **N-(4-iodobenzyl)-N-methylacetamide (5d)**

To a slurry of 60% NaH (165 mg, 4.1 mmol) was added N-methylacetamide (256 mg, 3.5 mmol). Evolution of gas ceased and 4-iodobenzyl bromide (1.0 g, 3.4 mmol) was dropwise added and the reaction mixture was left to stir for several hours. TLC analysis indicated little consumption of starting material. More N-methylacetamide (262 mg, 3.6 mmol) and NaH (137 mg, 3.4 mmol) were added and the reaction was left overnight. TLC indicated a major conversion. The reaction mixture was added H<sub>2</sub>O (5 mL), washed with ammonium chloride (aq., 5 mL, 2M,) and extracted with EtOAc (3x20 mL). The combined organic phases were dried over Na<sub>2</sub>SO<sub>4</sub>, and the solvents evaporated under reduced pressure. The crude was purified using flash column chromatography with EtOAc affording **5d** in 79% (2.7 mmol, 0.78 g) as a yellow white powder. <sup>1</sup>H NMR (400 MHz, Chloroform-*d*)  $\delta$  7.72 – 7.61 (m, 2H), 7.03 – 6.89 (m, 2H), 4.49 (d, *J* = 21.1 Hz, 2H), 2.91 (d, *J* = 3.5 Hz, 3H), 2.13 (d, *J* = 7.3 Hz, 3H). <sup>13</sup>C NMR (151 MHz, Chloroform-*d*)  $\delta$  (171.0;170.9), (138.2;137.8), (137.3;136.5), (130.2;128.4), (93.0;92.9), (53.9;50.3), (35.7;33.9), (21.9;21.5). **MS** (ESI, MeOH) *m/z*: 311.986 [M + Na]<sup>+</sup>. **HRMS** (MeOH): Calculated for C<sub>10</sub>H<sub>12</sub>INONa<sup>+</sup> [M + Na]<sup>+</sup> 311.9862, found 311.9855 (0.0007  $\Delta$  ppm)

#### **N-(4-((2,2-dimethyl-4,6-dioxo-1,3-dioxan-5-ylidene)-1,3-iodanyl)benzyl)-N-methylbenzamide (6a)**

Following **typical procedure A**, the crude was dissolved in DCM (10 mL) and precipitated in hexanes (20 mL) yielding 22% (53 mg, 0.108 mmol) of **6a** as white solids. **a) 177 mg, 0.50 mmol of amide 6d b) 112 mg, 0.65 mmol mCPBA c) 211 mg, 3.75 mmol KOH d) 95 mg, 0.66 mmol Meldrum's acid.** <sup>1</sup>H NMR (400 MHz, DMSO)  $\delta$  7.80 - 7.78 (m, 2H), 7.47 - 7.39 (m, 7H), 4.70 - 4.49 (d, 2H), 2.88 - 2.84 (s, 3H), 1.57 (s, 6H). <sup>13</sup>C NMR (101 MHz, DMSO)  $\delta$  162.8, 136.1, 132.8, 130.0, 129.5, 128.4, 126.9, 108.8, 102.7, 57.9, 25.6. **MS** (ESI, MeOH) *m/z*: 539.017 [M + Na]<sup>+</sup>. **HRMS** (MeOH): Calculated for C<sub>21</sub>H<sub>20</sub>INO<sub>5</sub>Na<sup>+</sup> [M + Na]<sup>+</sup> 516.0284, found 516.0278 (0.0006  $\Delta$  ppm)

### **N-(4-fluorobenzyl)-N-methylbenzamide (6b)**

Following **typical procedure C**, the crude was purified by flash column chromatography using 1:9 MeOH:DCM yielding **6b** in 24% (40 mg, 0.18 mmol) as a white clear yellow oil.

**a) 0.10 g, 0.75 mmol of 4d) b) 4 mL THF c) 0.16 mL, 1.1 mmol triethylamine d) no DMAP e) 0.17 ml, 1.5 mmol benzoyl chloride f) left for hours at room temperature.** <sup>1</sup>H NMR (400 MHz, Chloroform-*d*) δ 7.51 – 7.27 (m, 6H), 7.18 – 6.99 (m, 3H), 4.59 (d, *J* = 96.4 Hz, 2H), 2.93 (d, *J* = 59.2 Hz, 3H). See Yin et al<sup>61</sup> for reference <sup>1</sup>H-NMR and <sup>13</sup>C-NMR. <sup>19</sup>F NMR (377 MHz, Chloroform-*d*) δ -114.86 (d, *J* = 134.8 Hz). **MS** (ESI, MeOH) *m/z*: 266.095 [M + Na]<sup>+</sup>. **HRMS** (MeOH): Calculated for C<sub>15</sub>H<sub>14</sub>FNONa<sup>+</sup> [M + Na]<sup>+</sup> 266.0957, found 266.0953 (0.0004 Δ ppm)

### **N-benzyl-1-(4-fluorophenyl)-N-methylmethanamine (6c)**

Following **typical procedure C**, the crude was purified by flash column chromatography using 10:1 hexanes:EtOAc yielding **6c** in 82% (147 mg, 0.60 mmol) as a white clear yellow oil. **a) 0.10 g, 0.73 mmol of 4d) b) 4 mL THF c) 0.2 mL, 1.4 mmol triethylamine d) no**

**DMAP e) 89 μl, 0.75 mmol benzyl bromide f) left over night at room temperature.** <sup>1</sup>H NMR (400 MHz, Chloroform-*d*) δ 7.30 – 7.22 (m, 6H), 7.20 – 7.16 (m, 1H), 6.96 – 6.88 (m, 2H), 3.44 (s, 2H), 3.40 (s, 2H), 2.09 (s, 3H). See Yan et al<sup>62</sup> for reference <sup>1</sup>H-NMR and <sup>13</sup>C-NMR. <sup>19</sup>F NMR (377 MHz, Chloroform-*d*) δ -116.22 (m). **MS** (ESI, MeOH) *m/z*: 230.134 [M + H]<sup>+</sup>. **HRMS** (MeOH): Calculated for C<sub>15</sub>H<sub>16</sub>FNH<sup>+</sup> [M + H]<sup>+</sup> 230.1345 found 230.1340 (0.0005 Δ ppm)

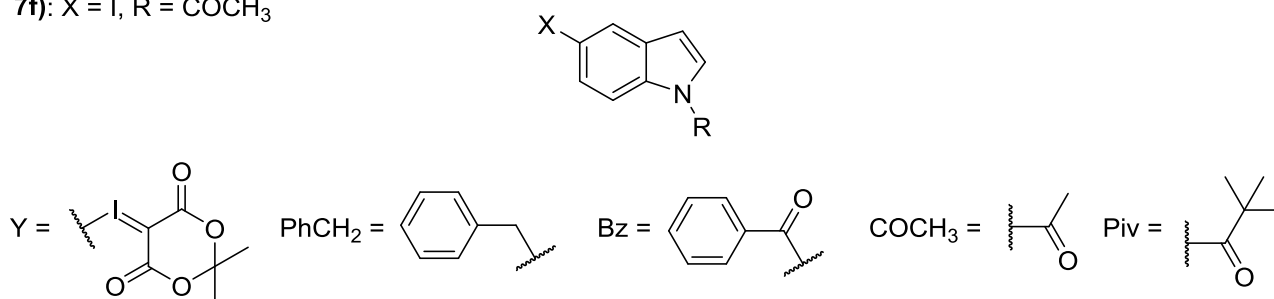
### **N-benzyl-1-(4-fluorophenyl)-N-methylmethanamine (6d)**

Following **typical procedure B**, the crude mixture was purified by flash column chromatography in 1:1 EtOAc:Hexanes affording **6d** in 74% (2.5 mmol, 0.88g) as a yellow solid. **a) 0.69 g, 5.13 mmol of n-methylbenzamide b) 349 mg, 8.72 mmol NaH c) 7 mL THF d) 1.05 g, 3.37 mmol of 4-iodobenzyl bromide e) 60 °C overnight.** <sup>1</sup>H NMR (400 MHz, CDCl<sub>3</sub>) δ 7.71 - 7.67(d, 2H), 7.46 - 7.40 (m, 5H), 7.12 - 7.11 (d, 2H), 4.69 - 4.45 (d, 2H), 3.02 - 2.86 (d, 2H). See Yin et al<sup>61</sup> for reference <sup>1</sup>H-NMR and <sup>13</sup>C-NMR. **MS** (ESI, MeOH) *m/z*: 374.001 [M + Na]<sup>+</sup>. **HRMS** (MeOH): Calculated for C<sub>15</sub>H<sub>14</sub>INONa<sup>+</sup> [M + Na]<sup>+</sup> 374.0018, found 374.0013 (0.000 Δ ppm)

**7a)**: X = Y, R = COCH<sub>3</sub>  
**7b)**: X = F, R = COCH<sub>3</sub>  
**7c)**: X = F, R = Et  
**7d)**: X = F, R = H  
**7e)**: X = I, R = H  
**7f)**: X = I, R = COCH<sub>3</sub>

**8a)**: X = Y, R = Bz  
**8b)**: X = F, R = Bz  
**8c)**: R' = F, R = PhCH<sub>2</sub>  
**8d)**: X = I, R = Bz

**9a)**: X = Y, R = Piv  
**9b)**: X = F, R = Piv  
**9c)**: X = F, R = CH<sub>2</sub>C(CH<sub>3</sub>)<sub>3</sub>  
**9d)**: X = I, R = Piv



Compounds **7d**) and **7e**) were purchased.

### 5-((1-acetyl-1H-indol-5-yl)-13-iodanylidene)-2,2-dimethyl-1,3-dioxane-4,6-dione (**7a**)

Following **typical procedure A**, the crude was dissolved in DCM (10 mL) and precipitated in hexanes (40 mL) yielding 38% (82 mg, 0.19 mmol) of **7a**) as a white solid. **a) 144 mg, 0.51 mmol of indole 7f) b) 115 mg, 0.67 mmol mCPBA c) 209 mg, 3.7 mmol KOH d) 95 mg, 0.66 mmol Meldrum's acid.** <sup>1</sup>H NMR (400 MHz, DMSO-*d*<sub>6</sub>) δ 8.36 (d, *J* = 8.8 Hz, 1H), 8.10 (d, *J* = 1.8 Hz, 1H), 7.98 (d, *J* = 3.8 Hz, 1H), 7.79 – 7.65 (m, 1H), 6.87 (dd, *J* = 3.9, 0.7 Hz, 1H), 2.67 (s, 3H), 1.54 (s, 6H). <sup>13</sup>C NMR (101 MHz, DMSO-*d*<sub>6</sub>) δ 169.8, 162.8, 135.4, 132.1, 129.2, 128.5, 126.0, 118.0, 110.2, 107.6, 102.6, 58.5, 25.6, 23.8. **MS** (ESI, MeOH) *m/z*: 449.981 [M + Na]<sup>+</sup>. Calculated for C<sub>16</sub>H<sub>14</sub>INO<sub>5</sub>Na<sup>+</sup> [M + Na]<sup>+</sup> 449.9815 found 449.9808 (0.0007 Δ ppm)

### 1-(5-fluoro-1H-indol-1-yl)ethan-1-one (**7b**)

Following **typical procedure C**, the residue was purified using 10:1 hexanes:EtOAc affording **7b**) in 63% (82 mg, 0.46 mmol) as a white solid. **a) 0.10 g, 0.74 mmol of indole 7d) b) 1.5 mL DCE c) 0.12 mL, 0.86 mmol triethylamine d) 14 mg, 0.11 mmol DMAP e) 0.1 mL, 1.1 mmol of acetic anhydride f) left overnight at 50° C.** <sup>1</sup>H NMR (400 MHz, Chloroform-*d*) δ 8.5 (q, *J* = 9.2, 4.8, 0.7 Hz, 1H), 7.8 (d, *J* = 3.8 Hz, 1H), 7.2 (dd, *J* = 8.7, 2.6 Hz, 1H), 7.1 (td, *J* = 9.2, 2.7 Hz, 1H), 6.6 (dd, *J* = 3.9, 0.7 Hz, 1H), 1.5 (s, 9H). See Zhou et al<sup>63</sup> for reference <sup>1</sup>H-NMR, <sup>13</sup>C-NMR and <sup>19</sup>F-NMR. **MS** (ESI, MeOH) *m/z*: 200.048 [M + Na]<sup>+</sup>. **HRMS** (MeOH): Calculated for C<sub>10</sub>H<sub>8</sub>FNONa<sup>+</sup> [M + Na]<sup>+</sup> 200.0488, found 200.0483 (0.0005 Δ ppm)

### 1-ethyl-5-fluoro-1H-indole (**7c**)

Following **typical procedure B**, the residue was purified by flash column chromatography using 15:1 hexanes:EtOAc affording compound **7c**) in 43% (51 mg, 0.32 mmol) as a brown oil. **a) 98 mg, 0.72 mmol of amine 7d) b) 37 mg, 0.92 mmol NaH c) 6 mL DMF d) 84 μL, 1.0 mmol e) room temperature overnight** <sup>1</sup>H NMR (400 MHz, Chloroform-*d*) δ 7.30 – 7.21 (m, 2H), 7.15 (d, *J* = 3.1 Hz, 1H), 6.95 (td, *J* = 9.1, 2.5 Hz, 1H), 6.44 (dd, *J* = 3.1, 0.9 Hz, 1H), 4.15 (q, *J* = 7.3 Hz, 2H), 1.46 (t, *J* = 7.3 Hz, 3H). See Yongcheng et al<sup>64</sup> for reference <sup>1</sup>H-NMR and <sup>13</sup>C-NMR. <sup>19</sup>F NMR (377 MHz, Chloroform-*d*) δ -125.8 (m). **MS** (APCI, MeOH) *m/z*: 164.087 [M + H]<sup>+</sup>. **HRMS** (APCI, MeOH): Calculated for C<sub>10</sub>H<sub>10</sub>FNH<sup>+</sup> [M + H]<sup>+</sup> 164.0876 found 164.0870 (0.0006 Δ ppm).

### 1-(5-iodo-1H-indol-1-yl)ethan-1-one (7f)

Following **typical procedure C**, the crude was purified by flash column chromatography using 10:1 Hexanes:EtOAc affording **7f** in 87% (0.87 g, 3.1 mmol) as a white, crystalline powder. **a) 1.0 g, 3.5 mmol of 7e) b) 8 mL DCE c) 73  $\mu$ L, 5.3 mmol triethylamine d) 0.72 mmol, 88 mg DMAP e) 0.63 ml, 6.7 mmol acetic anhydride f) left overnight at 50° C.** <sup>1</sup>H NMR (600 MHz, Chloroform-*d*)  $\delta$  8.21 (d, *J* = 8.7 Hz, 1H), 7.91 (d, *J* = 1.7 Hz, 1H), 7.62 (dd, *J* = 8.7, 1.8 Hz, 1H), 7.38 (d, *J* = 3.8 Hz, 1H), 6.56 (dd, *J* = 3.8, 0.8 Hz, 1H), 2.63 (s, 3H). <sup>13</sup>C NMR (151 MHz, Chloroform-*d*)  $\delta$  168.7, 134.9, 133.8, 132.8, 129.8, 126.1, 118.5, 108.2, 88.0, 24.0. **MS** (ESI, MeOH) *m/z*: 307.954 [M + Na]<sup>+</sup>. **HRMS** (MeOH): Calculated for C<sub>10</sub>H<sub>8</sub>NOINa<sup>+</sup> [M + Na]<sup>+</sup> 307.9548 found 307.9543 (0.0005  $\Delta$  ppm)

### 5-((1-benzoyl-1H-indol-5-yl)-13-iodanylidene)-2,2-dimethyl-1,3-dioxane-4,6-dione (8a)

Following **typical procedure A**, the crude was dissolved in DCM (10 mL) and precipitated in hexanes (40 mL) at -20° C yielding 18% (43 mg, 89  $\mu$ mol) of **8a** as a white solid. **a) 175 mg, 0.51 mmol of indole 8d) b) 114 mg, 0.66 mmol mCPBA c) 205 mg, 3.66 mmol KOH d) 94 mg, 0.65 mmol Meldrum's acid.** NMR (400 MHz, DMSO-*d*<sub>6</sub>)  $\delta$  <sup>1</sup>H NMR (400 MHz, DMSO-*d*<sub>6</sub>)  $\delta$  8.29 (d, *J* = 8.8 Hz, 1H), 8.17 (d, *J* = 1.8 Hz, 1H), 7.78 (ddd, *J* = 8.6, 4.9, 1.7 Hz, 3H), 7.74 – 7.68 (m, 1H), 7.65 – 7.58 (m, 2H), 7.53 (d, *J* = 3.8 Hz, 1H), 6.91 – 6.85 (m, 1H), 1.55 (s, 6H). <sup>13</sup>C NMR (101 MHz, DMSO-*d*<sub>6</sub>)  $\delta$  168.2, 162.8, 136.0, 133.3, 132.4, 132.3, 130.0, 129.2, 128.7, 128.6, 127.6, 126.2, 117.9, 110.7, 107.8, 102.6, 58.7, 54.9, 30.7, 25.6. **MS** (ESI, MeOH) *m/z*: 511.997 [M + Na]<sup>+</sup>. **HRMS** (MeOH): Calculated for C<sub>21</sub>H<sub>16</sub>INO<sub>5</sub>Na<sup>+</sup> [M + Na]<sup>+</sup> 511.9971 found 511.9965 (0.0006  $\Delta$  ppm)

### (5-fluoro-1H-indol-1-yl)(phenyl)methanone (8b)

Following **typical procedure C**, the crude was purified by flash column chromatography using 3:1 hexanes:DCM yielding **8b** in 59% (72 mg, 0.33 mmol) as a white clear yellow oil. **a) 0.10 g, 0.56 mmol of 7d) b) 4 mL DCM c) 0.12 mL, 0.86 mmol triethylamine d) 14 mg, 0.11 mmol DMAP e) 0.16 ml, 1.4 mmol benzoyl chloride f) left for hours at room temperature.** <sup>1</sup>H NMR (400 MHz, Chloroform-*d*)  $\delta$  8.36 (dd, *J* = 9.0, 4.7 Hz, 1H), 7.77 – 7.64 (m, 2H), 7.63 – 7.44 (m, 3H), 7.30 (s, 1H), 7.27 – 7.17 (d, 1H), 7.08 (td, *J* = 9.1, 2.6 Hz, 1H), 6.54 (dd, *J* = 3.8, 0.8 Hz, 1H). See Qingshuai et al<sup>65</sup> for reference <sup>1</sup>H-NMR and <sup>13</sup>C-NMR. <sup>19</sup>F NMR (377 MHz, Chloroform-*d*)  $\delta$  -118.9 (m). **MS** (ESI, MeOH) *m/z*: 262.064 [M + Na]<sup>+</sup>. **HRMS** (MeOH): Calculated for C<sub>15</sub>H<sub>10</sub>FNONa<sup>+</sup> [M + Na]<sup>+</sup> 262.0644 found 262.0639 (0.0005  $\Delta$  ppm)

### 1-benzyl-5-fluoro-1H-indole (8c)

Following **typical procedure B**, the crude was purified by flash column chromatography using 1:15 EtOAc:Hexanes yielding **8c** in 61% (102 mg, 0.45 mmol) as a clear yellow oil. **a) 101 mg, 0.74 mmol of indole 7d) b) 32 mg, 0.81 mmol NaH c) 5 mL THF d) 0.11 mL, 0.89 mmol benzyl bromide e) room temperature for several days** <sup>1</sup>H NMR (400 MHz, Chloroform-*d*)  $\delta$  7.32 – 7.21 (m, 4H), 7.17 – 7.10 (m, 2H), 7.09 – 7.00 (m, 2H), 6.89 (td, *J* = 9.1, 2.5 Hz, 1H), 6.49 (dd, *J* = 3.1, 0.9 Hz, 1H), 5.26 (s, 2H). See Choy et al<sup>66</sup> for reference <sup>1</sup>H-NMR and <sup>13</sup>C-NMR. <sup>19</sup>F NMR (377 MHz, Chloroform-*d*)  $\delta$  -125.20 – -125.31 (m). **MS** (ESI, MeOH) *m/z*: 226.103 [M + H]<sup>+</sup>. **HRMS** (MeOH): Calculated for C<sub>15</sub>H<sub>12</sub>FNH<sup>+</sup> [M + H]<sup>+</sup> 225.0954 found 226.1029 (0.0003  $\Delta$  ppm).



### **(5-iodo-1H-indol-1-yl)(phenyl)methanone (8d)**

Following **typical procedure C**, the residue was purified by flash column chromatography using 3:1 hexanes:DCM yielding 74% (1.05g, 3.02 mmol) of **8d** as a white, fluffy powder. **a) 0.99 g, 4.1 mmol of 7e) b) 8 mL dry DCM c) 2.2 mL, 15.8 mmol triethylamine d) 100 mg, 0.82 mmol DMAP e) 0.85 mL, 7.3 mmol benzoyl chloride f) left for hours at room temperature.** <sup>1</sup>H NMR (400 MHz, Chloroform-*d*) δ 8.16 (dt, *J* = 8.8, 0.7 Hz, 1H), 7.96 (d, *J* = 1.7 Hz, 1H), 7.78 – 7.69 (m, 2H), 7.69 – 7.58 (m, 2H), 7.54 (ddt, *J* = 8.4, 6.7, 1.2 Hz, 2H), 7.28 (d, *J* = 3.8 Hz, 1H), 6.54 (dd, *J* = 3.8, 0.8 Hz, 1H). <sup>13</sup>C NMR (101 MHz, Chloroform-*d*) δ 168.7, 135.5, 134.3, 133.6, 133.2, 132.3, 129.9, 129.3, 128.8, 128.5, 118.3, 107.6, 88.2. **MS** (ESI, MeOH) *m/z*: 369.970 [M + Na]<sup>+</sup>. **HRMS** (MeOH): Calculated for C<sub>15</sub>H<sub>10</sub>NOINa<sup>+</sup> [M + Na]<sup>+</sup> 369.9705, found 369.9699 (0.0006 Δ ppm)

### **2,2-dimethyl-5-((1-pivaloyl-1H-indol-5-yl)-I3-iodanylidene)-1,3-dioxane-4,6-dione (9a)**

Following **typical procedure A**, the crude was dissolved in DCM (10 mL) and precipitated in hexanes (80 mL) at -20° C affording **9a** in 34% (79 mg, 0.17 mmol) as a yellow white solid. **a) 164 mg, 0.50 mmol of indole 9d) b) 112 mg, 0.65 mmol mCPBA c) 220 mg, 3.92 mmol KOH d) 92 mg, 0.64 mmol Meldrum's acid.** <sup>1</sup>H NMR (400 MHz, DMSO-*d*<sub>6</sub>) δ 8.37 (d, *J* = 8.9 Hz, 1H), 8.22 (d, *J* = 3.9 Hz, 1H), 8.10 (d, *J* = 1.8 Hz, 1H), 7.72 (dd, *J* = 8.9, 1.9 Hz, 1H), 6.87 (dd, *J* = 3.8, 0.7 Hz, 1H), 1.54 (s, 6H), 1.45 (s, 9H). <sup>13</sup>C NMR (101 MHz, DMSO-*d*<sub>6</sub>) δ 177.1, 162.8, 136.7, 131.1, 128.8, 128.6, 125.7, 118.7, 110.3, 107.5, 102.6, 58.6, 41.0, 27.8, 25.5. **MS** (ESI, MeOH) *m/z*: 492.028 [M + Na]<sup>+</sup>. **HRMS** (MeOH): Calculated for C<sub>21</sub>H<sub>16</sub>INO<sub>5</sub>Na<sup>+</sup> [M + Na]<sup>+</sup> 492.0284 found 492.0280 (0.0004 Δ ppm)

### **1-(5-fluoro-1H-indol-1-yl)-2,2-dimethylpropan-1-one (9b)**

Following **typical procedure B**, the crude was purified by flash column chromatography using 1:15 EtOAc:Hexanes yielding **9b** in 55% (89 mg, 0.41 mmol) as a clear yellow oil. **a) 94 mg, 0.43 mmol of indole 7d) b) 40 mg, 1 mmol NaH c) 5 mL THF d) 0.11 mL, 0.89 mmol pivaloyl chloride e) room temperature for several days.** <sup>1</sup>H NMR (400 MHz, Chloroform-*d*) δ 8.48 (ddt, *J* = 9.2, 4.8, 0.7 Hz, 1H), 7.77 (d, *J* = 3.8 Hz, 1H), 7.20 (dd, *J* = 8.7, 2.6 Hz, 1H), 7.06 (td, *J* = 9.2, 2.7 Hz, 1H), 6.57 (dd, *J* = 3.9, 0.7 Hz, 1H), 1.52 (s, 9H). <sup>13</sup>C NMR (101 MHz, Chloroform-*d*) δ (177.0;174.1), 159.7 (d, *J*<sub>CF</sub> = 240.0 Hz), 133.3 (Br.), (130.5, d *J*<sub>CF</sub> = 10 Hz), 127.2, 118.5 (d, *J*<sub>CF</sub> = 8.9 Hz), 112.8 (d, *J*<sub>CF</sub> = 24.4 Hz), 108.0 (d, *J*<sub>CF</sub> = 4.0 Hz), 106.1 (d, *J*<sub>CF</sub> = 23.7 Hz), (41.3;40.3), (28.8;26.6). <sup>19</sup>F NMR (377 MHz, Chloroform-*d*) δ -119.8 (td, *J* = 8.9, 4.8 Hz). **MS** (ESI, MeOH) *m/z*: 242.096 [M + Na]<sup>+</sup>. **HRMS** (MeOH): Calculated for C<sub>13</sub>H<sub>14</sub>FNONa<sup>+</sup> [M + Na]<sup>+</sup> 242.0952 found 242.0952 (0.0005 Δ ppm)

### **5-fluoro-1-neopentyl-1H-indole (9c)**

To a solution of **9b** (67 mg, 0.30 mmol) in THF was added BH<sub>3</sub> • SMe<sub>2</sub> (1.2 mL, 2 M). The solution was left to stir over the weekend. The mixture was diluted in water (10 mL), NaHCO<sub>3</sub> (10 mL, sat.) and extracted using EtOAc (3x10 mL). The crude was purified using flash column chromatography (1:20 EtOAc:Hexanes) yielding **9c** in 50% (31 mg, 0.15 mmol) as a white solid. <sup>1</sup>H NMR (400 MHz, Chloroform-*d*) δ 7.25 – 7.20 (m, 2H), 7.10 (d, *J* = 3.1 Hz, 1H), 6.92 (td, *J* = 9.1, 2.5 Hz, 1H), 6.44 (dd, *J* = 3.1, 0.8 Hz, 1H), 3.88 (s, 2H), 0.99 (s, 9H). <sup>13</sup>C NMR (101 MHz, Chloroform-*d*) δ 157.7 (d, *J*<sub>C</sub> = 233.5 Hz), 134.2, 131.2, 128.4 (d, *J*<sub>C</sub> = 10.1 Hz), 110.9 (d, *J*<sub>C</sub> = 9.8 Hz), 109.8 (d, *J*<sub>C</sub> = 26.4 Hz), 105.4 (d, *J*<sub>C</sub> = 23.2 Hz), 100.9 (d, *J*<sub>C</sub> = 4.6 Hz), 58.3, 34.5, 28.3. <sup>19</sup>F NMR (377 MHz, Chloroform-*d*) δ -126.22 (td, *J* = 9.4, 4.3 Hz). **MS** (ESI, MeOH) *m/z*: 206.134 [M + H]<sup>+</sup>. **HRMS** (MeOH): Calculated for C<sub>13</sub>H<sub>16</sub>FNH<sup>+</sup> [M + H]<sup>+</sup> 205.1267 found 206.1339 (0.0006 Δ ppm)

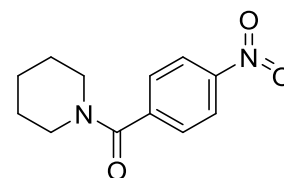
### 1-(5-iodo-1H-indol-1-yl)-2,2-dimethylpropan-1-one (9d)

Following **typical procedure B**, the residue was purified by flash column chromatography using hexanes yielding affording **9d** in 26% (352 mg, 1.08 mmol) as yellow-grey crystals.

**a) 1.0 g, 4.1 mmol of indole 7e b) 209 mg, 5.23 mmol NaH c) 5 mL THF d) 0.66 mL, 5.4 mmol pivaloyl chloride e) room temperature overnight.**  $^1\text{H NMR}$  (400 MHz, Chloroform-*d*)  $\delta$  8.27 (dt,  $J = 8.8, 0.7$  Hz, 1H), 7.89 (d,  $J = 1.7$  Hz, 1H), 7.70 (d,  $J = 3.8$  Hz, 1H), 7.61 (dd,  $J = 8.8, 1.8$  Hz, 1H), 6.54 (dd,  $J = 3.9, 0.8$  Hz, 1H), 1.54 – 1.47 (m, 9H).  $^{13}\text{C NMR}$  (101 MHz, Chloroform-*d*)  $\delta$  177.1, 136.2, 133.7, 131.8, 129.5, 126.5, 119.3, 107.3, 87.7, 41.5, 28.8. **MS** (ESI, MeOH)  $m/z$ : 350.001  $[\text{M} + \text{Na}]^+$ . **HRMS** (MeOH): Calculated for  $\text{C}_{13}\text{H}_{14}\text{INONa}^+$   $[\text{M} + \text{Na}]^+$  350.0018 found 350.0012 (0.0006  $\Delta$  ppm)

### 4-(dihydroxyamino)phenyl(piperidin-1-yl)methanone (43)

To a stirred solution of triethylamine (0.94 mL, 6.8 mmol) and piperidine (0.59 mL, 5.9 mmol) was added to 4-nitrobenzoyl chloride (1.0 g, 5.5 mmol) in DCM (10 mL). The reaction mixture was left at room temperature overnight. TLC showed major conversion. The



mixture was added  $\text{H}_2\text{O}$  (10 mL),  $\text{NaHCO}_3$  (10 mL) and extracted using EtOAc (3x15 mL). The combined organic phases were dried over  $\text{Na}_2\text{SO}_4$ , and solvents removed under reduced pressure. The residue was recrystallized from MeOH affording **43** in 74% (945 mg, 4.03 mmol) as a yellow brown crystals.  $^1\text{H NMR}$  (400 MHz, Chloroform-*d*)  $\delta$  8.30 – 8.22 (m, 2H), 7.58 – 7.50 (m, 2H), 3.82 – 3.60 (m, 2H), 3.38 – 3.17 (m, 2H), 1.69 (q,  $J = 4.3, 3.6$  Hz, 4H).  $^{13}\text{C NMR}$  (101 MHz, Chloroform-*d*)  $\delta$  168.0, 148.3, 142.8, 127.9, 124.0, 48.8, 43.3, 26.6, 25.6, 24.5. **MS** (ESI, MeOH)  $m/z$ : 257.090  $[\text{M} + \text{Na}]^+$ . **HRMS** (MeOH): Calculated for  $\text{C}_{12}\text{H}_{14}\text{N}_2\text{O}_3\text{Na}^+$   $[\text{M} + \text{Na}]^+$  257.0902, found 257.0897 (0.0005  $\Delta$  ppm)

## 5 Conclusions and outlook

In this study the design, synthesis and characterization of 4-substituted N-(4-fluorophenyl)-N-methylamides, 4-substituted N-(4-fluorobenzyl)-N-methylamide and 5-, 1- substituted indoles as drug scaffolds are presented. A fast, high-yielding method for  $^{18}\text{F}$ -labeling and trapping amides followed by a functional group reduction with amine purification was developed.

The designed library compounds for starting compound, intermediate and final products were synthesized by a series of iodo- or fluoro-substituted precursors. Iodonium ylides were synthesized using a two-step, one pot procedure published by Cardinale & Ermert<sup>40</sup> from an iodo-precursor and Meldrum's acid in moderate yields, similar to those reported in literature. The iodonium ylide of N-methyl-N-phenyl-formamide went on for designing a route for amide/amine functional group interconversion after the  $^{18}\text{F}$ -incorporation.

Among the different conditions screened a method with high radiofluorine incorporation and high yielding reduction was designed with a total reaction time of 90 minutes, including purification. This resulted in a total of 36% of the initial starting activity in the final product. Despite optimization the method required higher temperatures, more time and reducing equivalents to be translatable for a wide variety of compound. Increasing the reducing agent equivalents and temperature resulted maintaining a high yield for structurally similar and simple compounds. Applying the method to subspecies of indoles gave no  $^{18}\text{F}$ -incorporation, leaving no intermediate to be reduced. Investigation into  $^{18}\text{F}$ -introduction by iodonium ylides in the presence of the non-protected indole carbon skeleton proved to be detrimental to the yield. An NMR study indicated the indole ylide produced a new product, but the study was unable to determine which product was being formed.

# Bibliography

1. Maus, J., Schema of a PET acquisition process. PET-schema.png, Ed. Public domain: Wikipedia.org, 2003.
2. Letho, J. a. H., Xiaolin, *Chemistry and analysis of radionuclides*. Wiley-VCH: Germany, 2011.
3. Saha, G. B., *Physics and Radiobiology in Nuclear Medicine*. Second Edition ed.; Springer: Ann Arbor, MI, USA.
4. Miller, P. W.; Long, N. J.; Vilar, R.; Gee, A. D., Synthesis of <sup>11</sup>C, <sup>18</sup>F, <sup>15</sup>O, and <sup>13</sup>N Radiolabels for Positron Emission Tomography. *Angewandte Chemie International Edition* **2008**, *47* (47), 8998-9033.
5. Hatcher, R. A.; Eggleston, C., THE FATE OF STRYCHNIN IN THE BODY. *Journal of Pharmacology and Experimental Therapeutics* **1917**, *10* (4), 281.
6. Siegel, J. A.; Pennington, C. W.; Sacks, B., Subjecting Radiologic Imaging to the Linear No-Threshold Hypothesis: A Non Sequitur of Non-Trivial Proportion. *Journal of Nuclear Medicine* **2017**, *58* (1), 1-6.
7. Sacks, B.; Meyerson, G.; Siegel, J. A., Epidemiology Without Biology: False Paradigms, Unfounded Assumptions, and Specious Statistics in Radiation Science (with Commentaries by Inge Schmitz-Feuerhake and Christopher Busby and a Reply by the Authors). *Biological Theory* **2016**, *11*, 69-101.
8. Brooks, A. F.; Topczewski, J. J.; Ichiishi, N.; Sanford, M. S.; Scott, P. J. H., Late-stage [<sup>18</sup>F]fluorination: new solutions to old problems. *Chemical Science* **2014**, *5* (12), 4545-4553.
9. Hjelstuen, O. K.; Svadberg, A.; Olberg, D. E.; Rosser, M., Standardization of fluorine-18 manufacturing processes: New scientific challenges for PET. *European Journal of Pharmaceutics and Biopharmaceutics* **2011**, *78* (3), 307-313.
10. Lee, C.-M.; Farde, L., Using positron emission tomography to facilitate CNS drug development. *Trends in Pharmacological Sciences* **2006**, *27* (6), 310-316.
11. Pike, V. W., PET Radiotracers: crossing the blood-brain barrier and surviving metabolism. *Trends in pharmacological sciences* **2009**, *30* (8), 431-440.
12. Hill, D. E.; Holland, J. P., Computational studies on hypervalent iodonium(III) compounds as activated precursors for <sup>18</sup>F radiofluorination of electron-rich arenes. *Computational and Theoretical Chemistry* **2015**, *1066*, 34-46.
13. Neumann, C. N.; Ritter, T., Late-Stage Fluorination: Fancy Novelty or Useful Tool? *Angewandte Chemie International Edition* **2015**, *54* (11), 3216-3221.
14. Agency, I. A. E. *Cyclotron produced radionuclides: Principle and practice*; IAEA: Vienna, 2008.
15. agency, I. a. e., Cyclotron produced radionuclides: Operation and maintenance of gas and liquid targets. *IAEA Radioisotope and radiopharmaceuticals series* **2012**, *Volume 4*.
16. Satyamurthy, N.; Barrio, J. R., No-carrier-added nucleophilic [<sup>18</sup>F] fluorination of aromatic compounds. Google Patents: 2010.
17. Preshlock, S.; Tredwell, M.; Gouverneur, V., F-18-Labeling of Arenes and Heteroarenes for Applications in Positron Emission Tomography. *Chemical Reviews* **2016**, *116* (2), 719-766.
18. Jacobson, O.; Kiesewetter, D. O.; Chen, X., Fluorine-18 Radiochemistry, Labeling Strategies and Synthetic Routes. *Bioconjugate Chemistry* **2015**, *26* (1), 1-18.
19. Yusubov, M.; Svitich, D.; Larkina, M. and Zhdankin, V., Applications of iodonium salts and iodonium ylides as precursors for nucleophilic fluorination in positron emission tomography. *Arkivoc* **2013**, 364-395.

20. Ermert, J., 18F-Labelled Intermediates for Radiosynthesis by Modular Build-Up Reactions: Newer Developments. *BioMed Research International* **2014**, *2014*, 15.
21. Tredwell, M.; Gouverneur, V., 18F Labeling of Arenes. *Angew. Chem., Int. Ed.* **2012**, *51* (46), 11426-11437.
22. Tressaud, A. H., Günter, *Fluorine and Health - Molecular imaging, Biomedical Materials and Pharmaceuticals*. Elsevier: 2008.
23. Pike, V. W.; Aigbirhio, F. I., Reactions of Cyclotron-Produced [F-18] Fluoride with Diaryliodonium-Salts - a Novel Single-Step Route to No-Carrier-Added [(18)]Fluoroarenes. *Journal of the Chemical Society-Chemical Communications* **1995**, (21), 2215-2216.
24. Sanford, M. S.; Scott, P. J. H., Moving Metal-Mediated 18F-Fluorination from Concept to Clinic. *ACS Cent. Sci.* **2016**, *2* (3), 128-130.
25. Chun, J.-H.; Morse, C. L.; Chin, F. T.; Pike, V. W., No-carrier-added [18F]fluoroarenes from the radiofluorination of diaryl sulfoxides. *Chemical Communications* **2013**, *49* (21), 2151-2153.
26. Stang, P. J., Polyvalent Iodine in Organic Chemistry. *J. Org. Chem.* **2003**, *68* (8), 2997-3008.
27. Yoshimura, A.; Zhdankin, V. V., Advances in Synthetic Applications of Hypervalent Iodine Compounds. *Chemical Reviews* **2016**, *116* (5), 3328-3435.
28. Gillespie, R. J.; Silvi, B., The octet rule and hypervalence: two misunderstood concepts. *Coordination Chemistry Reviews* **2002**, *233-234*, 53-62.
29. Der Puy, M. V., Conversion of diaryliodonium salts to aryl fluorides. *Journal of Fluorine Chemistry* **1982**, *21* (3), 385-392.
30. Stang, P. J.; Zhdankin, V. V., Organic Polyvalent Iodine Compounds. *Chemical Reviews* **1996**, *96* (3), 1123-1178.
31. Yusubov, M. S.; Svitich, D. Y.; Larkina, M. S.; Zhdankin, V. V., Applications of iodonium salts and iodonium ylides as precursors for nucleophilic fluorination in Positron Emission Tomography. *Arkivoc* **2013**, 364-395.
32. Zhdankin, V. V., Hypervalent iodine(III) reagent in organic synthesis. *Arkivoc* **2009**, 1-62.
33. Kohlhepp, S. V.; Gulder, T., Hypervalent iodine(III) fluorinations of alkenes and diazo compounds: new opportunities in fluorination chemistry. *Chem. Soc. Rev.* **2016**, *45* (22), 6270-6288.
34. Kirmse, W., Carbene Complexes of Nonmetals. *European Journal of Organic Chemistry* **2005**, *2005* (2), 237-260.
35. Cardinale, J.; Ermert, J.; Humpert, S.; Coenen, H. H., Iodonium ylides for one-step, no-carrier-added radiofluorination of electron rich arenes, exemplified with 4-([(18F]fluorophenoxy)-phenylmethyl)piperidine NET and SERT ligands. *RSC Advances* **2014**, *4* (33), 17293-17299.
36. Rotstein, B. H.; Wang, L.; Liu, R. Y.; Patteson, J.; Kwan, E. E.; Vasdev, N.; Liang, S. H., Mechanistic studies and radiofluorination of structurally diverse pharmaceuticals with spirocyclic iodonium(iii) ylides. *Chemical Science* **2016**, *7* (7), 4407-4417.
37. Zhdankin, V. V.; Stang, P. J., Chemistry of Polyvalent Iodine. *Chemical Reviews* **2008**, *108* (12), 5299-5358.
38. Chun, J.-H.; Lu, S.; Lee, Y.-S.; Pike, V. W., Fast and High-Yield Microreactor Syntheses of ortho-Substituted [18F]Fluoroarenes from Reactions of [18F]Fluoride Ion with Diaryliodonium Salts. *J. Org. Chem.* **2010**, *75* (10), 3332-3338.
39. Chun, J.-H.; Pike, V. W., Single-step syntheses of no-carrier-added functionalized [18F]fluoroarenes as labeling synthons from diaryliodonium salts. *Org. Biomol. Chem.* **2013**, *11* (37), 6300-6306.

40. Cardinale, J.; Ermert, J., Simplified synthesis of arylodonium ylides by a one-pot procedure. *Tetrahedron Letters* **2013**, *54* (16), 2067-2069.
41. Cardinale, J.; Ermert, J.; Humpert, S.; Coenen, H. H., Iodonium ylides for one-step, no-carrier-added radiofluorination of electron rich arenes, exemplified with 4-([F-18] fluorophenoxy)-phenylmethyl) piperidine NET and SERT ligands. *Rsc Advances* **2014**, *4* (33), 17293-17299.
42. Meldrum, A. N., LIV.-A [small beta]-lactonic acid from acetone and malonic acid. *Journal of the Chemical Society, Transactions* **1908**, *93* (0), 598-601.
43. Davidson, D.; Bernhard, S. A., The Structure of Meldrum's Supposed  $\beta$ -Lactonic Acid. *Journal of the American Chemical Society* **1948**, *70* (10), 3426-3428.
44. Dumas, A. M.; Fillion, E., Meldrum's Acids and 5-Alkylidene Meldrum's Acids in Catalytic Carbon-Carbon Bond-Forming Processes. *Accounts of Chemical Research* **2010**, *43* (3), 440-454.
45. Nakamura Satoshi, H. H. a. T. O., Rationale for the Acidity of Meldrum's Acid. Consistent Relation of C-H Acidities to the Properties of Localized Reactive Orbital. *Journal of organic chemistry* **2004**, *69* (13), 4309-4316.
46. Petersen, I. N.; Villadsen, J.; Hansen, H. D.; Madsen, J.; Jensen, A. A.; Gillings, N.; Lehel, S.; Herth, M. M.; Knudsen, G. M.; Kristensen, J. L., 18F-Labeling of electron rich iodonium ylides: application to the radiosynthesis of potential 5-HT<sub>2A</sub> receptor PET ligands. *Organic & Biomolecular Chemistry* **2017**.
47. Patrick, G. L., *An Introduction to Medicinal chemistry*. 4th ed.; Oxford University Press, 2009.
48. Clayden, G., Warren and Wothers, *Organic Chemistry*. Oxford University Press: United States, New York, 2008.
49. Smith, M. B., Chapter 4 - Reduction. In *Organic Synthesis (Third Edition)*, Academic Press: Oxford, 2010; pp 347-490.
50. Blondiaux, E.; Pouessel, J.; Cantat, T., Carbon Dioxide Reduction to Methylamines under Metal-Free Conditions. *Angewandte Chemie International Edition* **2014**, *53* (45), 12186-12190.
51. Yang, C.; Cheng, G.; Huang, B.; Xue, F.; Jiang, C., Metal-free regioselective construction of indolin-3-ones via hypervalent iodine oxidation of N-substituted indoles. *RSC Advances* **2016**, *6* (90), 87134-87141.
52. Wang, L.; Qu, X.; Fang, L.; Li, Z.; Hu, S.; Wang, F., Synthesis of 3-Acetoxyoxindole Derivatives by Metal-Free PhI(OAc)<sub>2</sub>-Mediated Oxidation of 3-Substituted Indoles. *Eur. J. Org. Chem.* **2016**, *2016* (33), 5494-5501.
53. Dong, B.; Wang, L.; Zhao, S.; Ge, R.; Song, X.; Wang, Y.; Gao, Y., Immobilization of ionic liquids to covalent organic frameworks for catalyzing the formylation of amines with CO<sub>2</sub> and phenylsilane. *Chemical Communications* **2016**, *52* (44), 7082-7085.
54. Linstad, E. J.; Vavere, A. L.; Hu, B.; Kempinger, J. J.; Snyder, S. E.; DiMugno, S. G., Thermolysis and radiofluorination of diaryliodonium salts derived from anilines. *Organic & Biomolecular Chemistry* **2017**, *15* (10), 2246-2252.
55. Knauber, T.; Arikian, F.; Roeschenthaler, G.-V.; Goossen, L. J., Copper-catalyzed trifluoromethylation of aryl iodides with potassium (trifluoromethyl)trimethoxyborate. *Chem. - Eur. J.* **2011**, *17* (9), 2689-2697, S2689/1-S2689/83.
56. Wang, S.; Wang, J.; Guo, R.; Wang, G.; Chen, S.-Y.; Yu, X.-Q., nBu<sub>4</sub>NI-catalyzed oxidative amidation of aldehydes with tertiary amines. *Tetrahedron Lett.* **2013**, *54* (46), 6233-6236.
57. Kato, H.; Shibata, I.; Yasaka, Y.; Tsunoi, S.; Yasuda, M.; Baba, A., The reductive amination of aldehydes and ketones by catalytic use of dibutylchlorotin hydride complex. *Chem. Commun. (Cambridge, U. K.)* **2006**, (40), 4189-4191.

58. Xu, X.-L.; Xu, W.-T.; Wu, J.-W.; He, J.-B.; Xu, H.-J., Silver-promoted decarboxylative amidation of  $\alpha$ -keto acids with amines. *Org. Biomol. Chem.* **2016**, *14* (42), 9970-9973.
59. Hamid, M. H. S. A.; Allen, C. L.; Lamb, G. W.; Maxwell, A. C.; Maytum, H. C.; Watson, A. J. A.; Williams, J. M. J., Ruthenium-Catalyzed N-Alkylation of Amines and Sulfonamides Using Borrowing Hydrogen Methodology. *Journal of the American Chemical Society* **2009**, *131* (5), 1766-1774.
60. Hansen, M. M.; Borders, S. S. K.; Clayton, M. T.; Heath, P. C.; Kolis, S. P.; Larsen, S. D.; Linder, R. J.; Reutzler-Edens, S. M.; Smith, J. C.; Tameze, S. L.; Ward, J. A.; Weigel, L. O., Development of a Practical Synthesis of an Aminoindanol-Derived M1 Agonist. *Organic Process Research & Development* **2009**, *13* (2), 198-208.
61. Yin, Z.; Wang, Z.; Li, W.; Wu, X.-F., Copper-Catalyzed Carbonylative Cross-Coupling of Arylboronic Acids with N-Chloroamines for the Synthesis of Aryl Amides. *European Journal of Organic Chemistry* **2017**, *2017* (13), 1769-1772.
62. Yan, T.; Feringa, B. L.; Barta, K., Benzylamines via Iron-Catalyzed Direct Amination of Benzyl Alcohols. *ACS Catalysis* **2016**, *6* (1), 381-388.
63. Zhou, J.; Hu, P.; Zhang, M.; Huang, S.; Wang, M.; Su, W., A Versatile Catalyst for Intermolecular Direct Arylation of Indoles with Benzoic Acids as Arylating Reagents. *Chemistry – A European Journal* **2010**, *16* (20), 5876-5881.
64. Wu, Y.; Peng, X.; Luo, B.; Wu, F.; Liu, B.; Song, F.; Huang, P.; Wen, S., Palladium catalyzed dual C-H functionalization of indoles with cyclic diaryliodoniums, an approach to ring fused carbazole derivatives. *Organic & Biomolecular Chemistry* **2014**, *12* (48), 9777-9780.
65. Han, Q.; Fu, S.; Zhang, X.; Lin, S.; Huang, Q., Facile approaches toward the synthesis of 6H-isoindolo[2,1- $\alpha$ ]indol-6-ones via palladium-catalyzed carbonylation with carbon monoxide. *Tetrahedron Lett.* **2016**, *57* (37), 4165-4169.
66. Choy, P. Y.; Lau, C. P.; Kwong, F. Y., Palladium-Catalyzed Direct and Regioselective C-H Bond Functionalization/Oxidative Acetoxylation of Indoles. *J. Org. Chem.* **2011**, *76* (1), 80-84.





# Appendix

## $^1\text{H-NMR}$ , $^{13}\text{C-NMR}$ and $^{19}\text{F-NMR}$ spectras

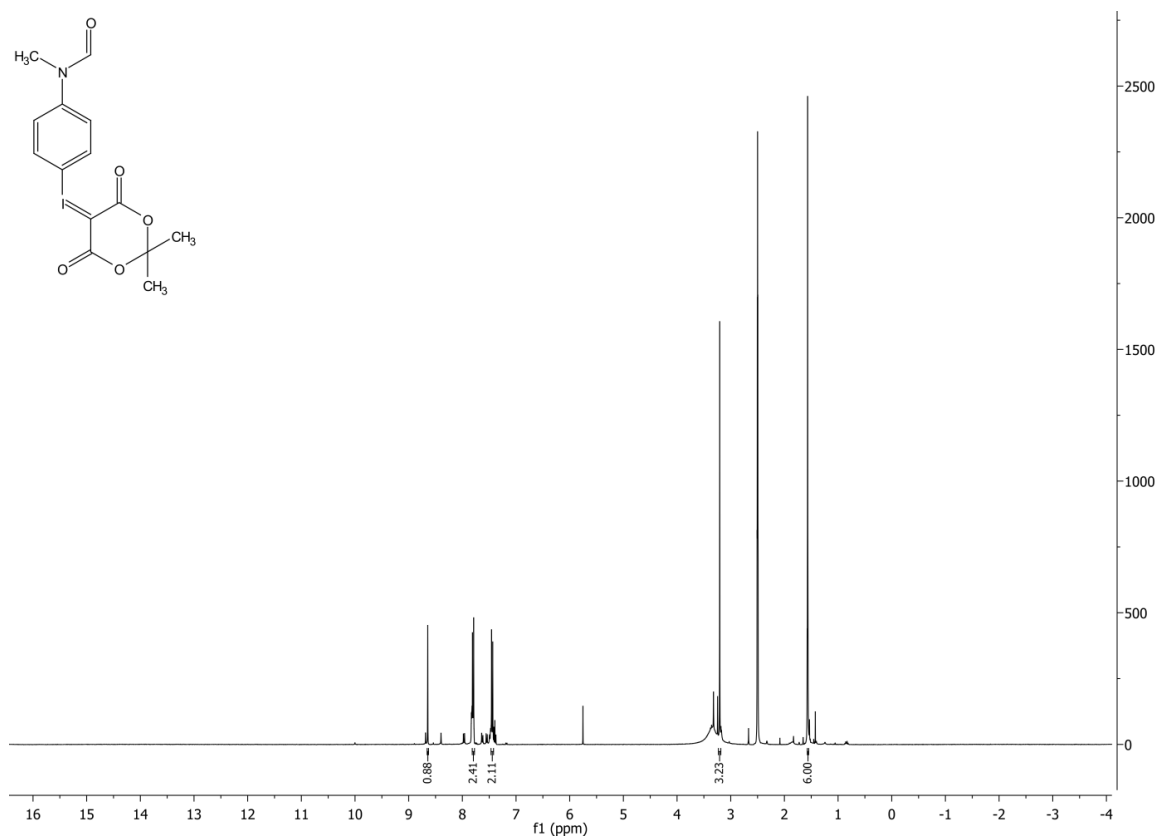


Figure V  $^1\text{H-NMR}$  of compound 1a)

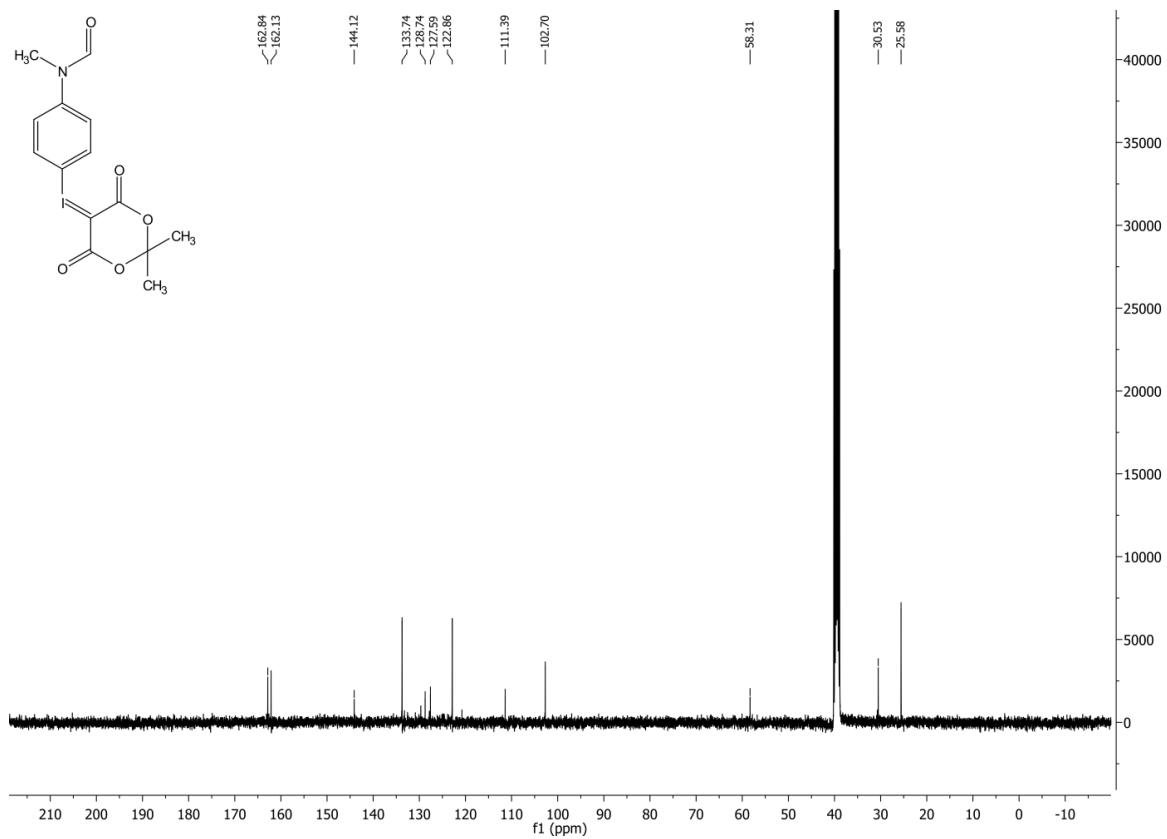


Figure VI  $^{13}\text{C-NMR}$  of compound 1a)

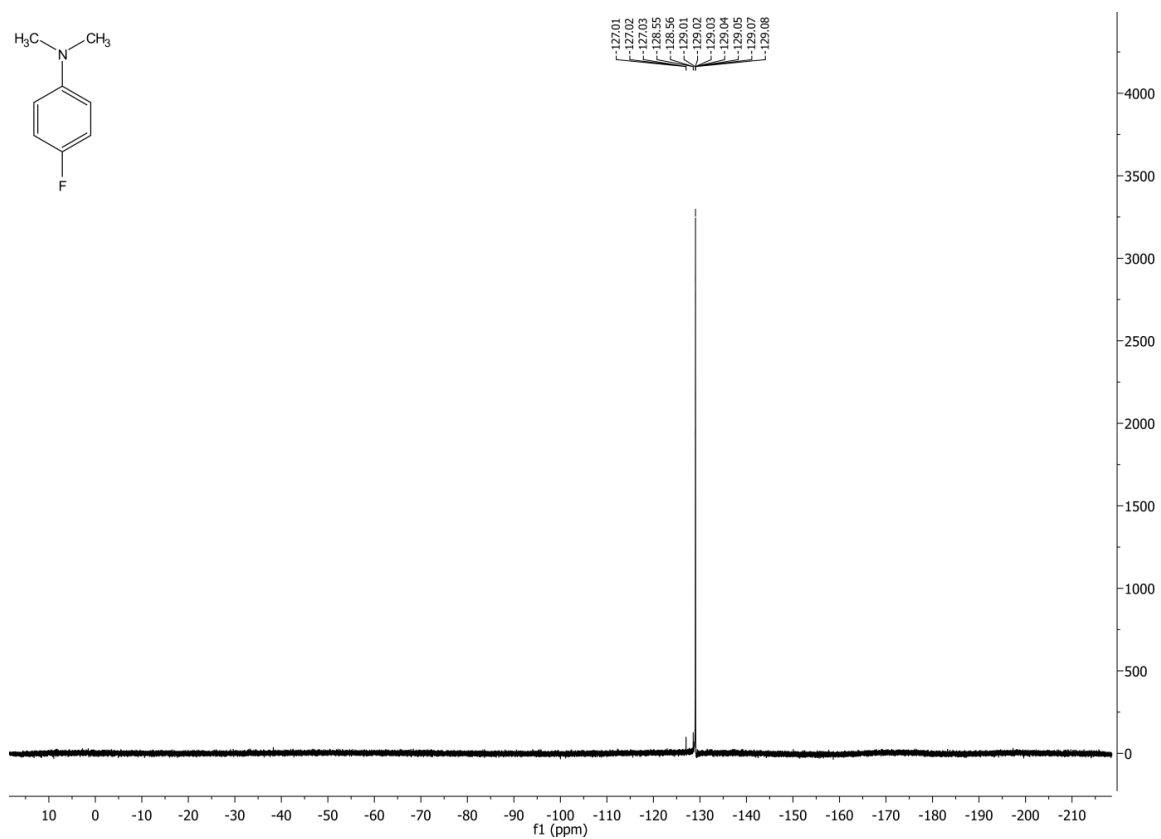


Figure VII  $^{19}\text{F-NMR}$  of compound 1c)

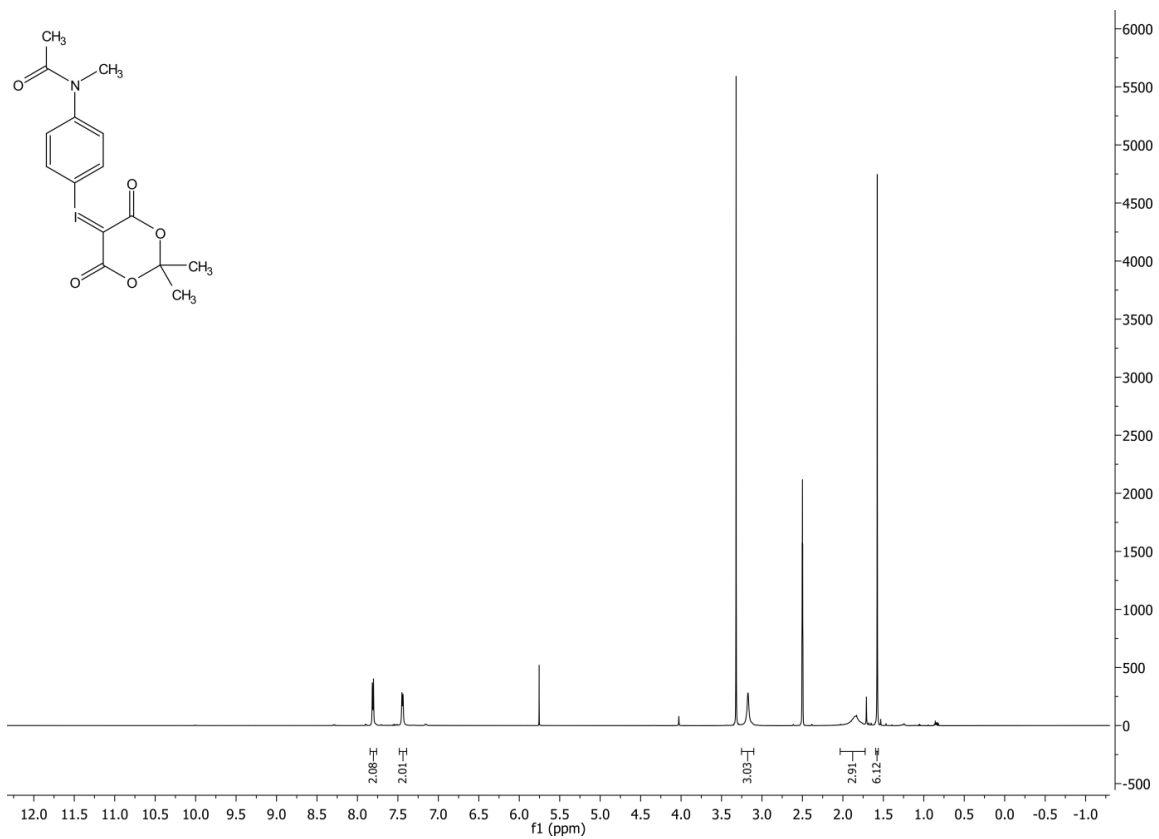


Figure VIII <sup>1</sup>H-NMR of compound 2a)

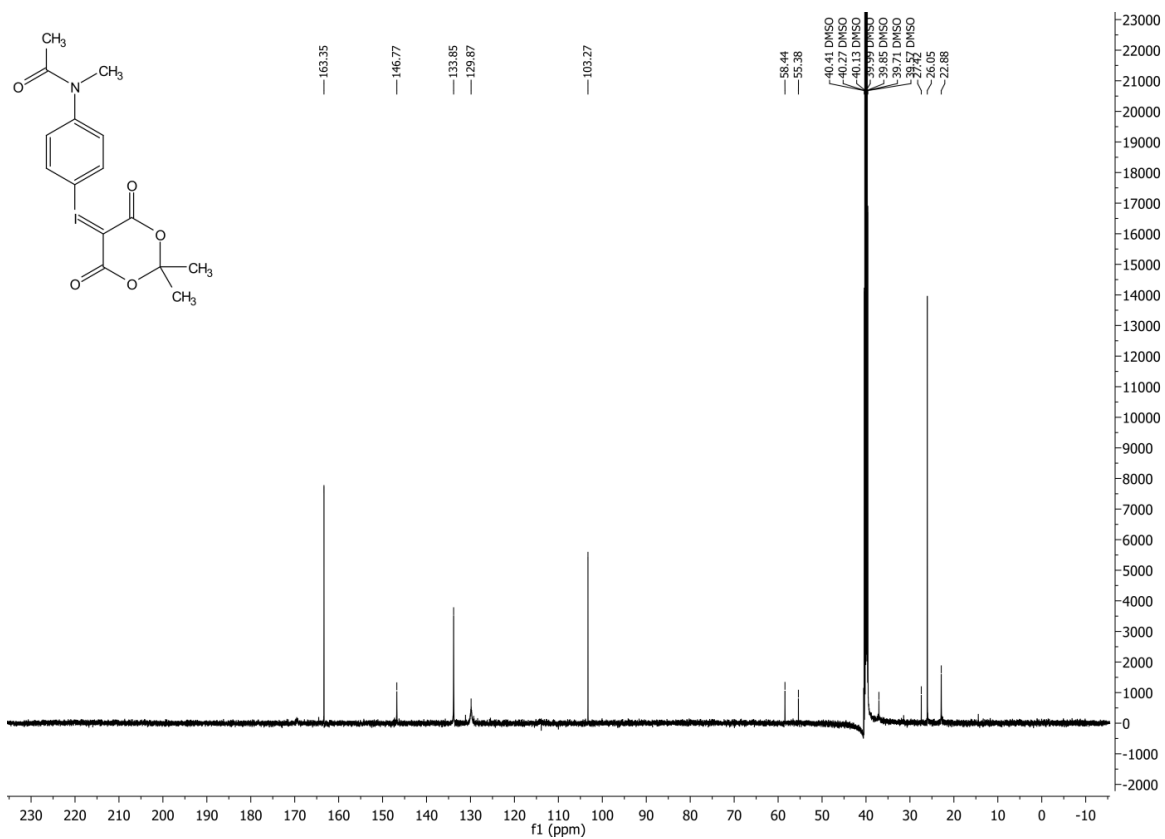


Figure IX <sup>13</sup>C-NMR of compound 2a)

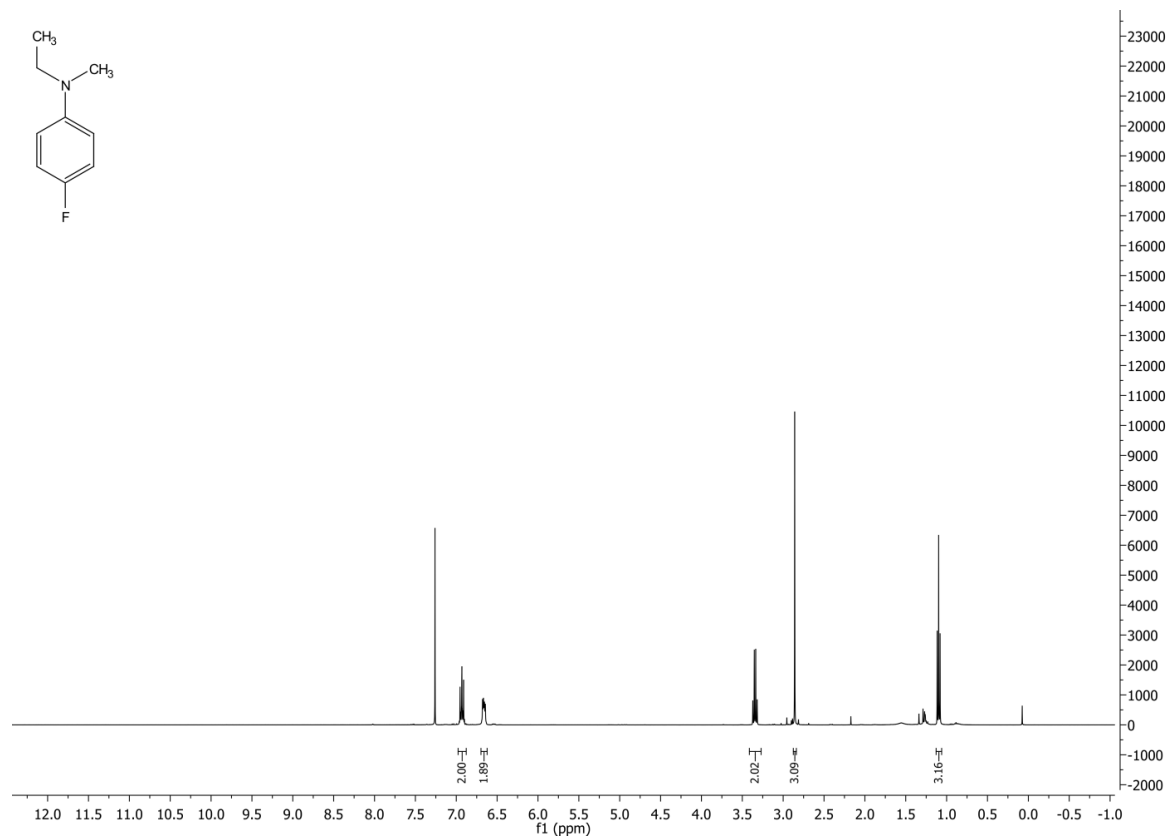


Figure X <sup>1</sup>H-NMR of compound 2c)

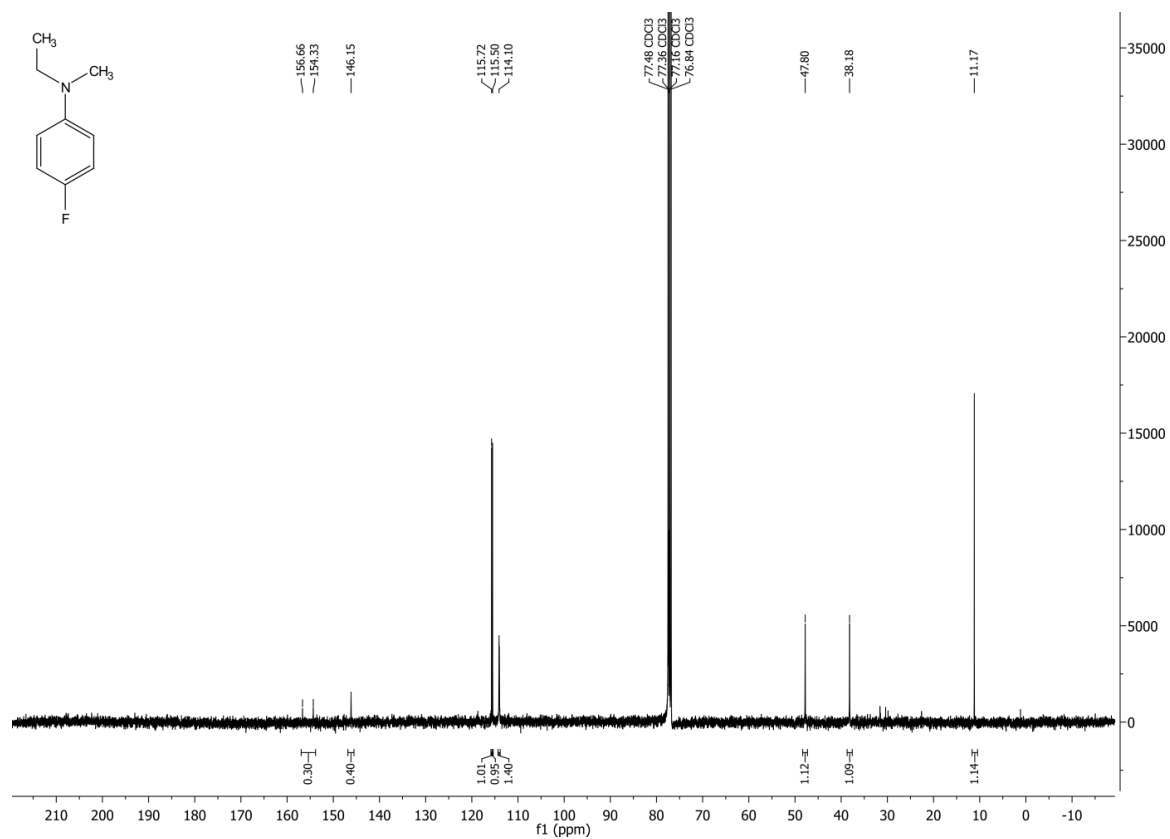


Figure XI <sup>13</sup>C-NMR of compound 2c)

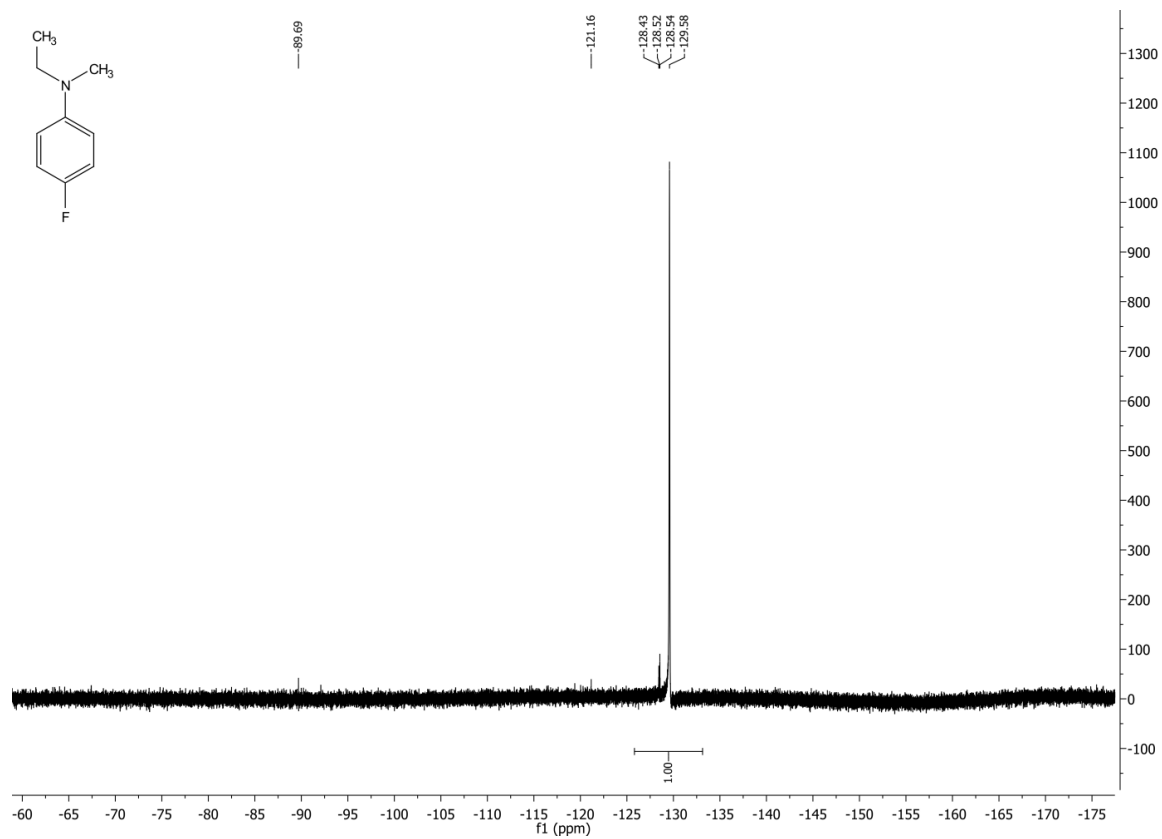


Figure XII  $^{19}\text{F}$ -NMR of compound 2c)

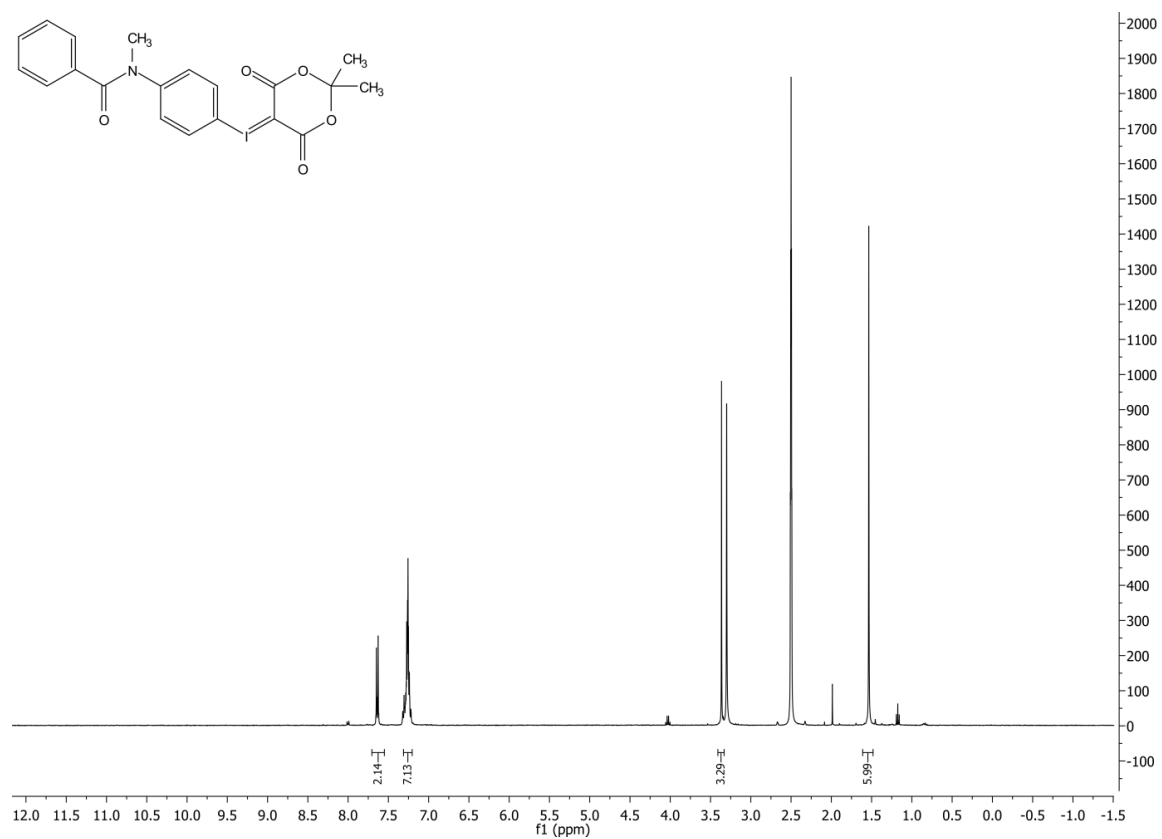


Figure XIII  $^1\text{H}$ -NMR of compound 3a)

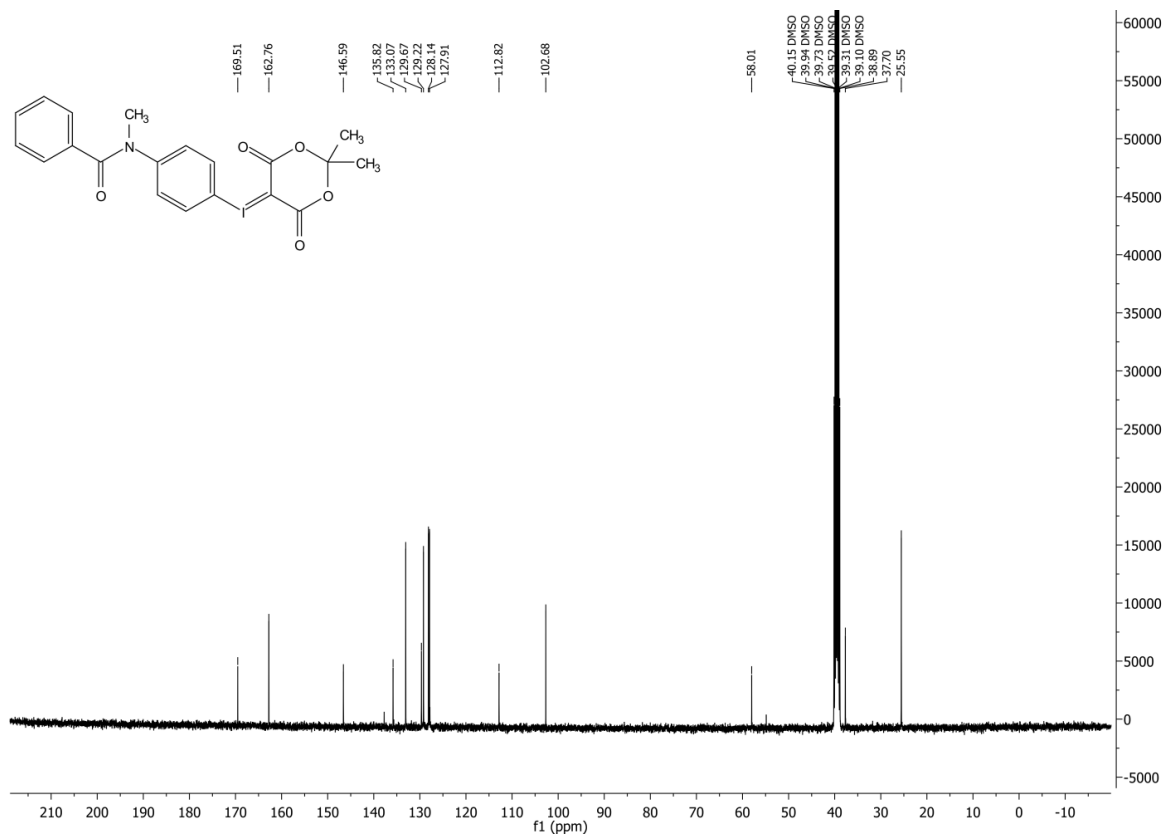


Figure XIV  $^{13}\text{C-NMR}$  of compound 3a)

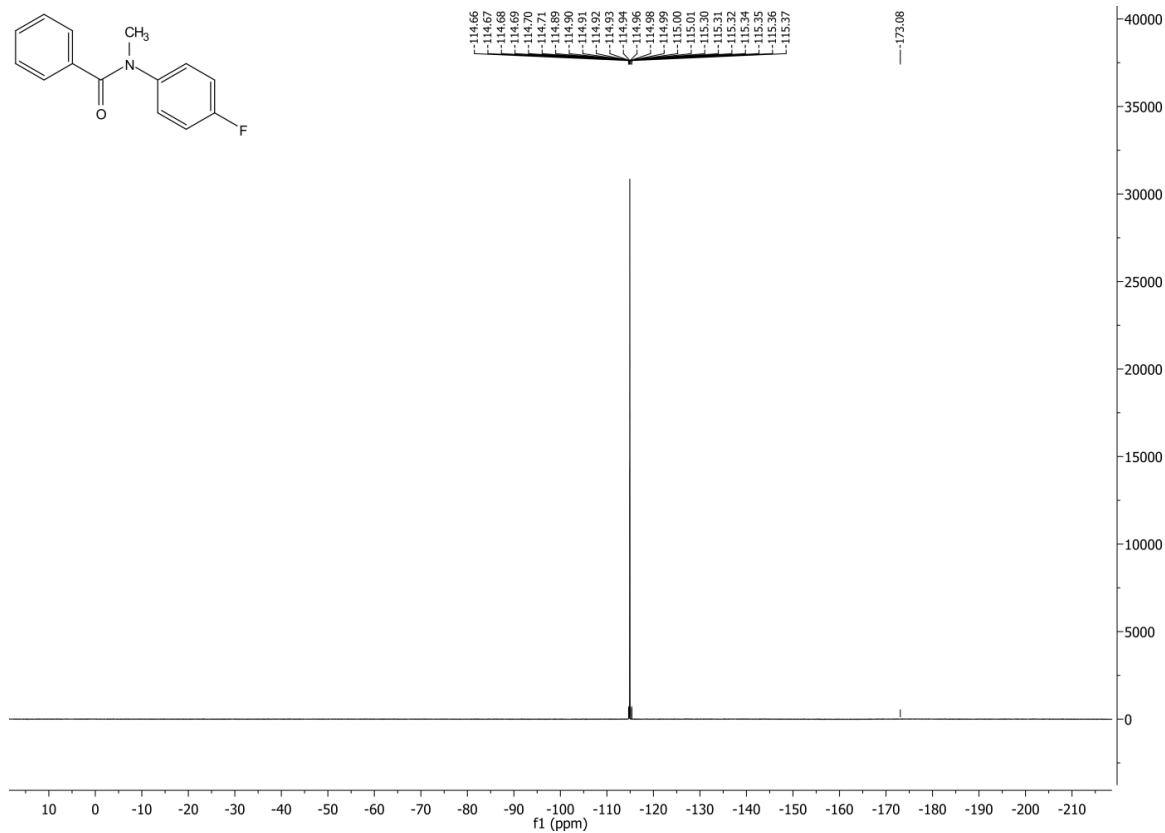


Figure XV  $^{13}\text{C-NMR}$  of compound 3b)

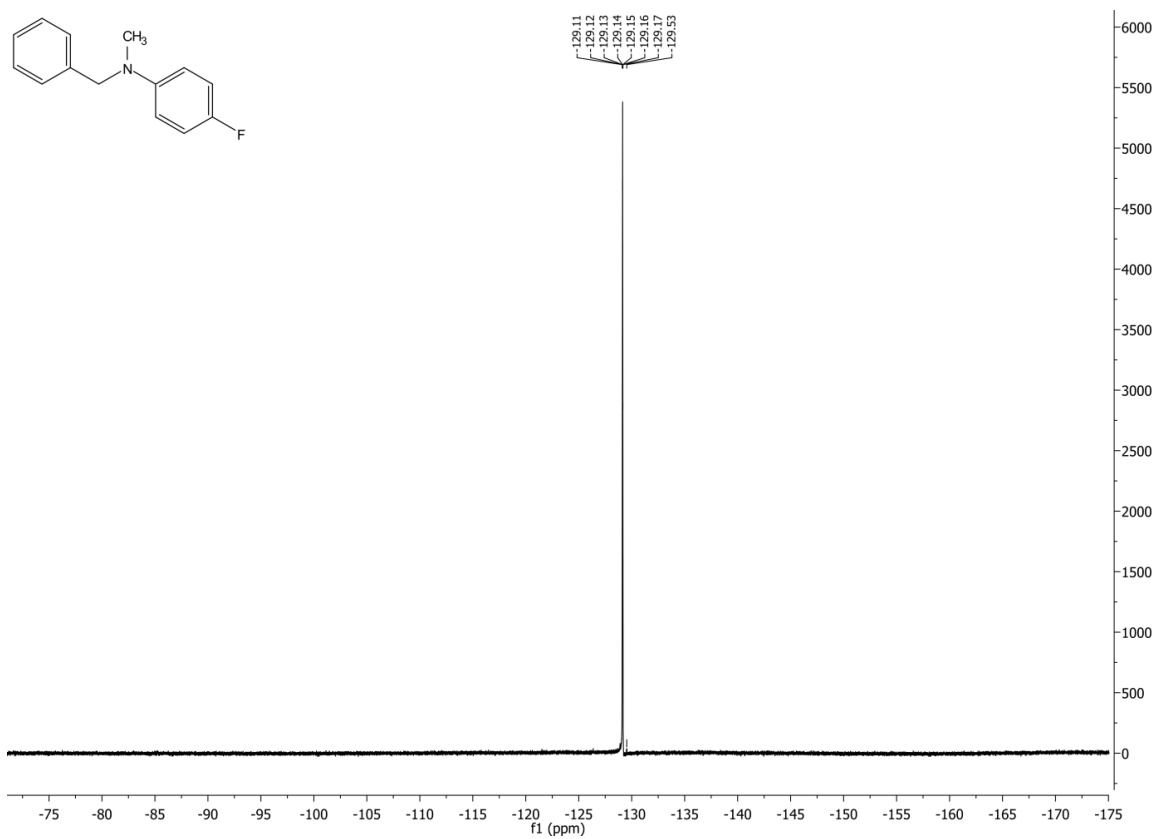


Figure XVI  $^{19}\text{F}$ -NMR of compound 3c)

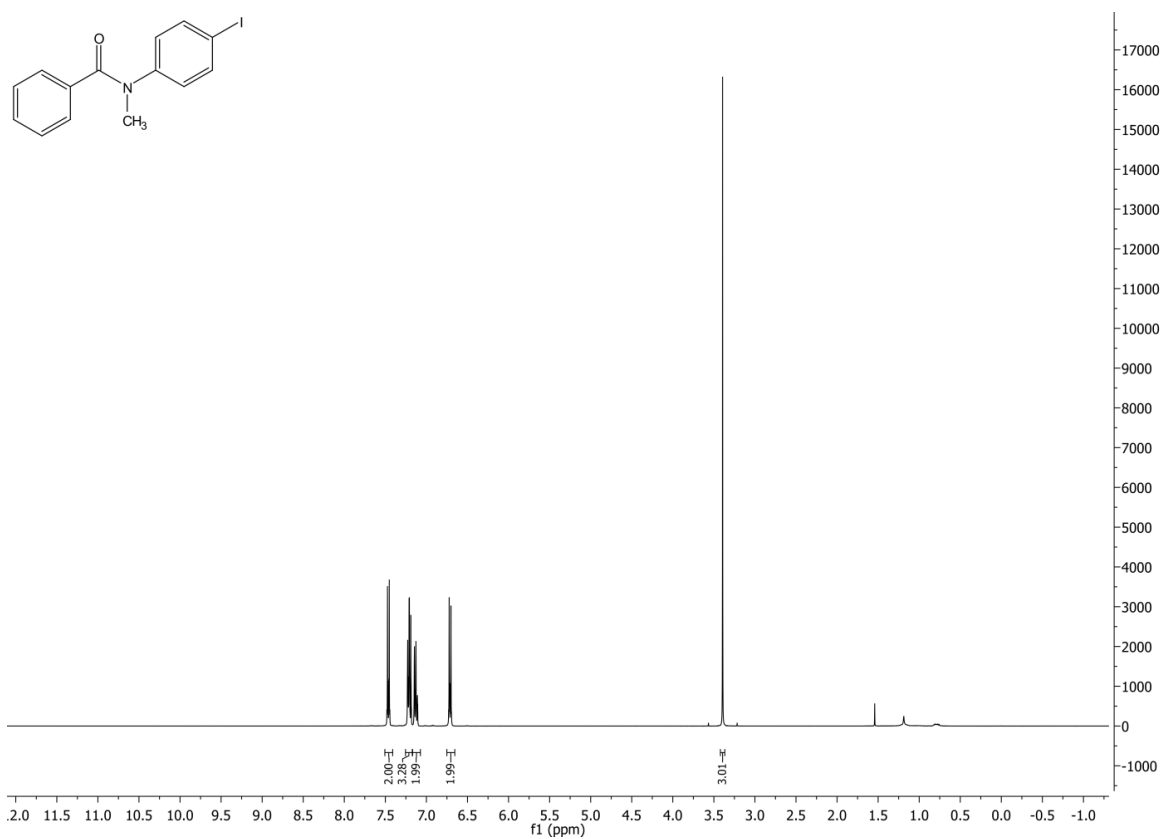


Figure XVII  $^1\text{H}$ -NMR of compound 3e)

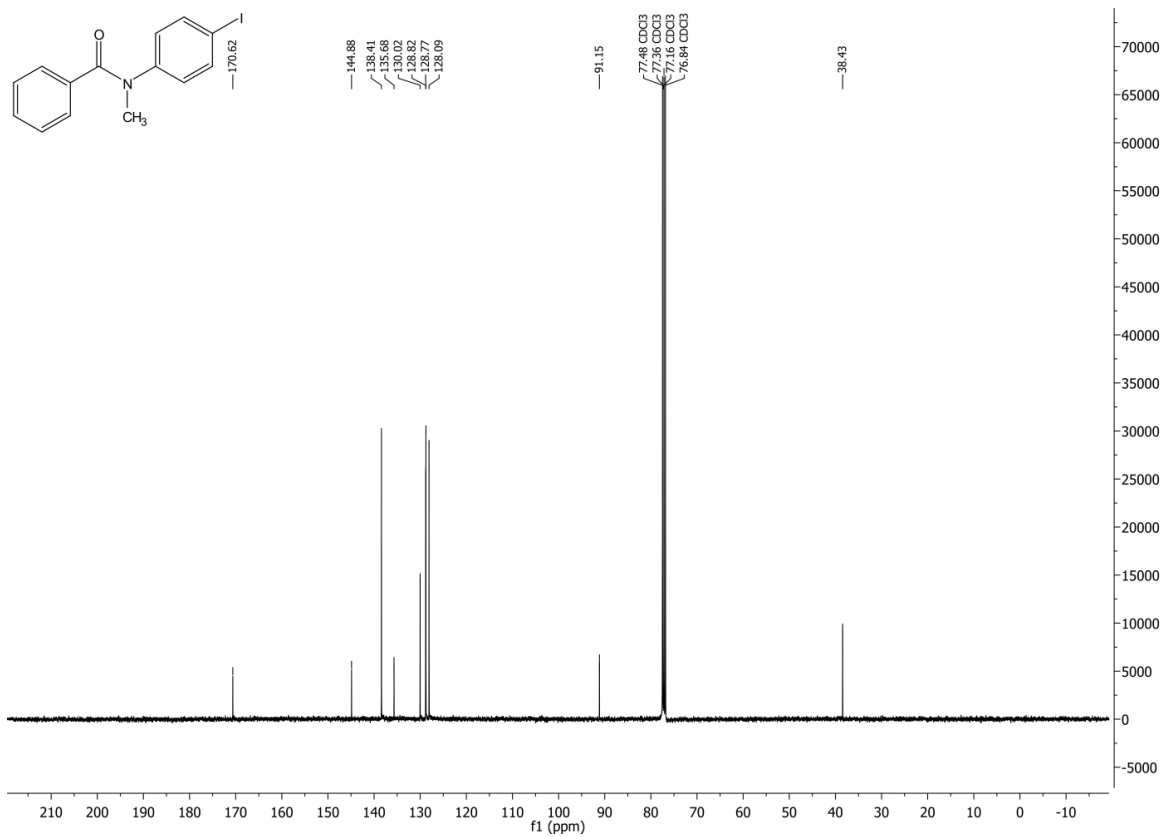


Figure XVIII <sup>13</sup>C-NMR of compound 3e)

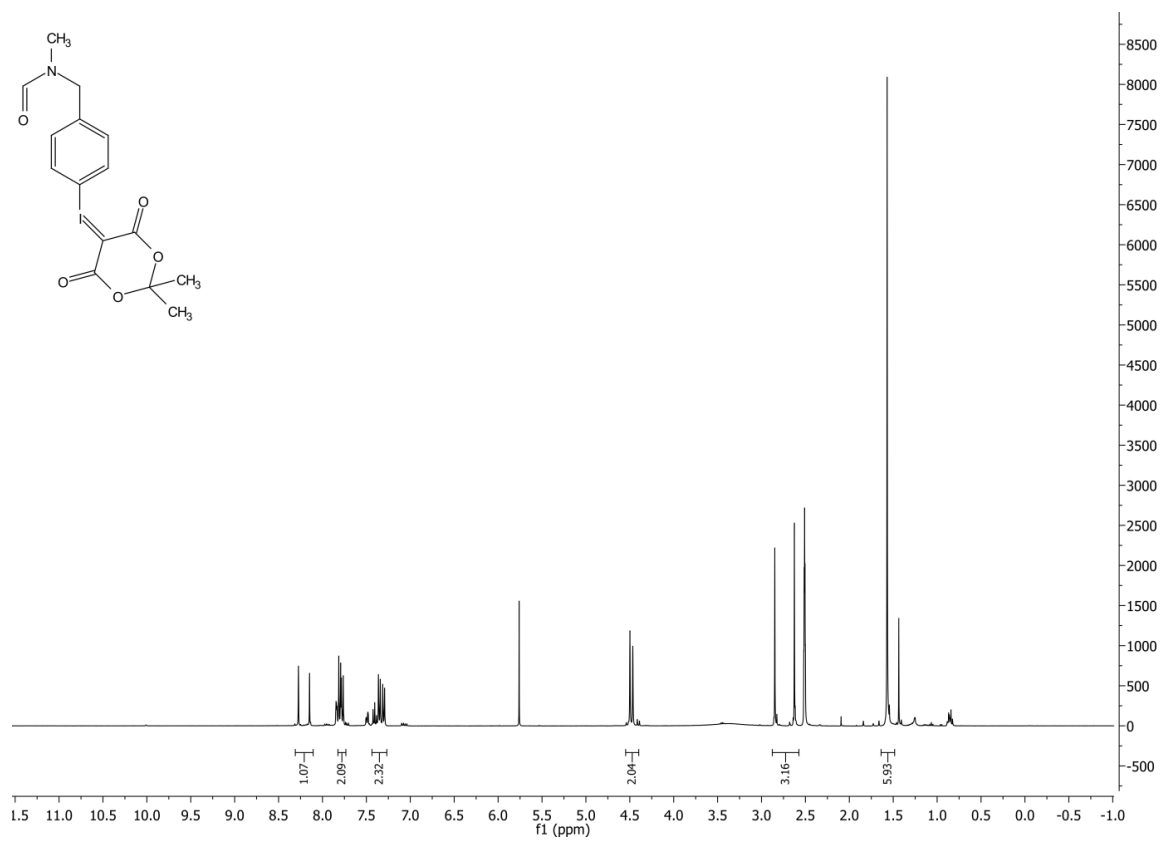


Figure XIX <sup>1</sup>H-NMR of compound 4a)



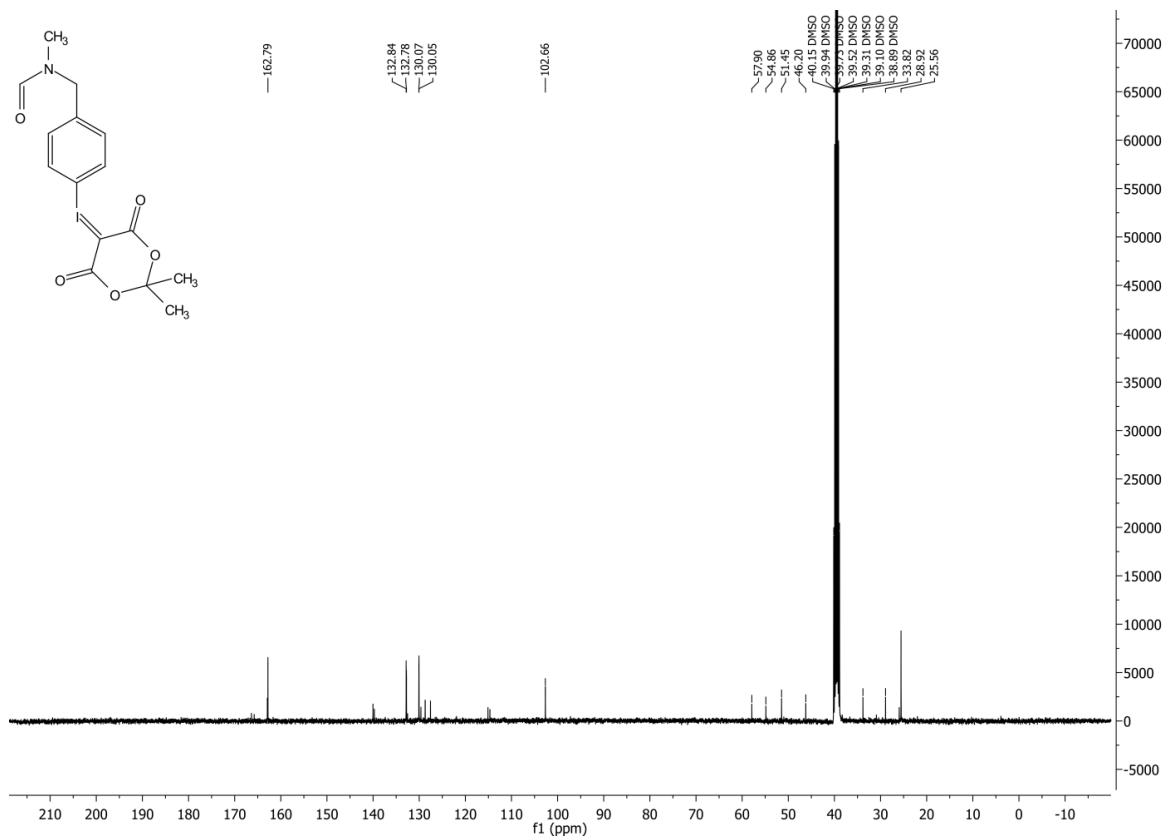


Figure XX  $^{13}\text{C-NMR}$  of compound 4a)

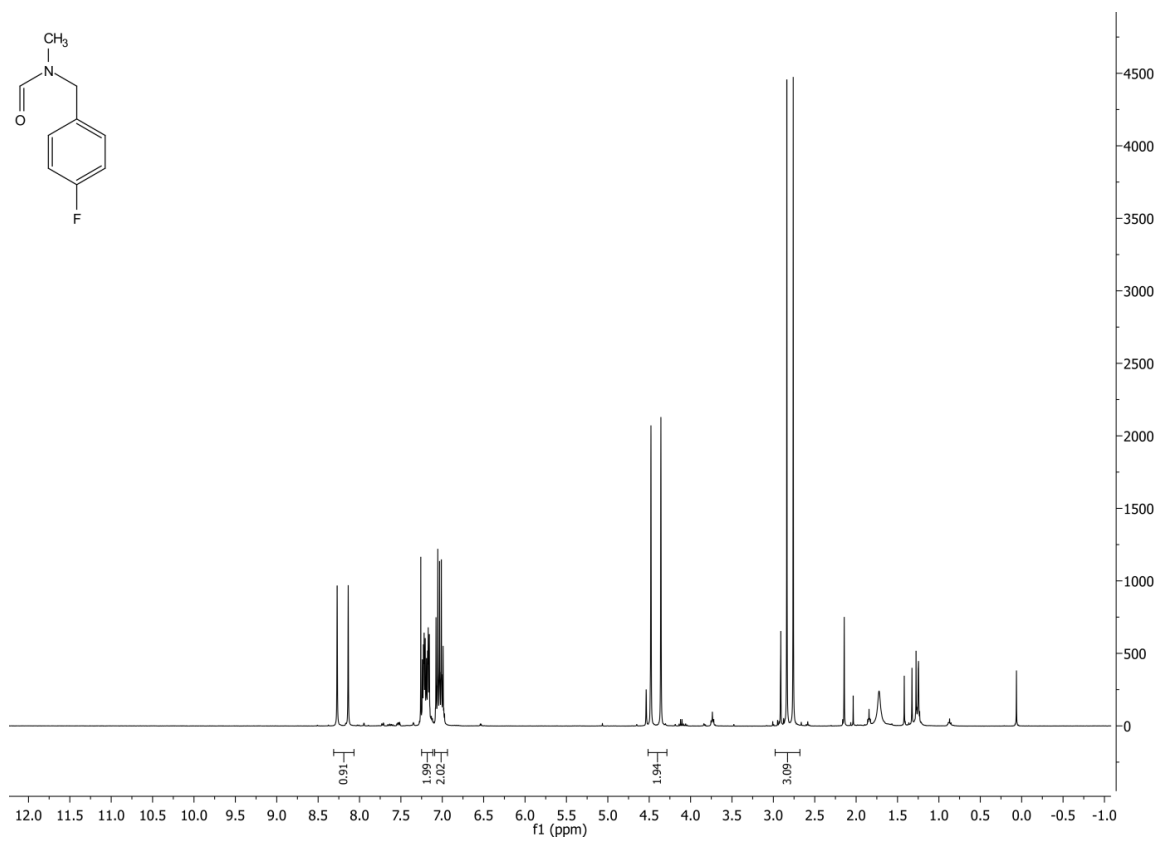


Figure XXI  $^1\text{H-NMR}$  of compound 4b)

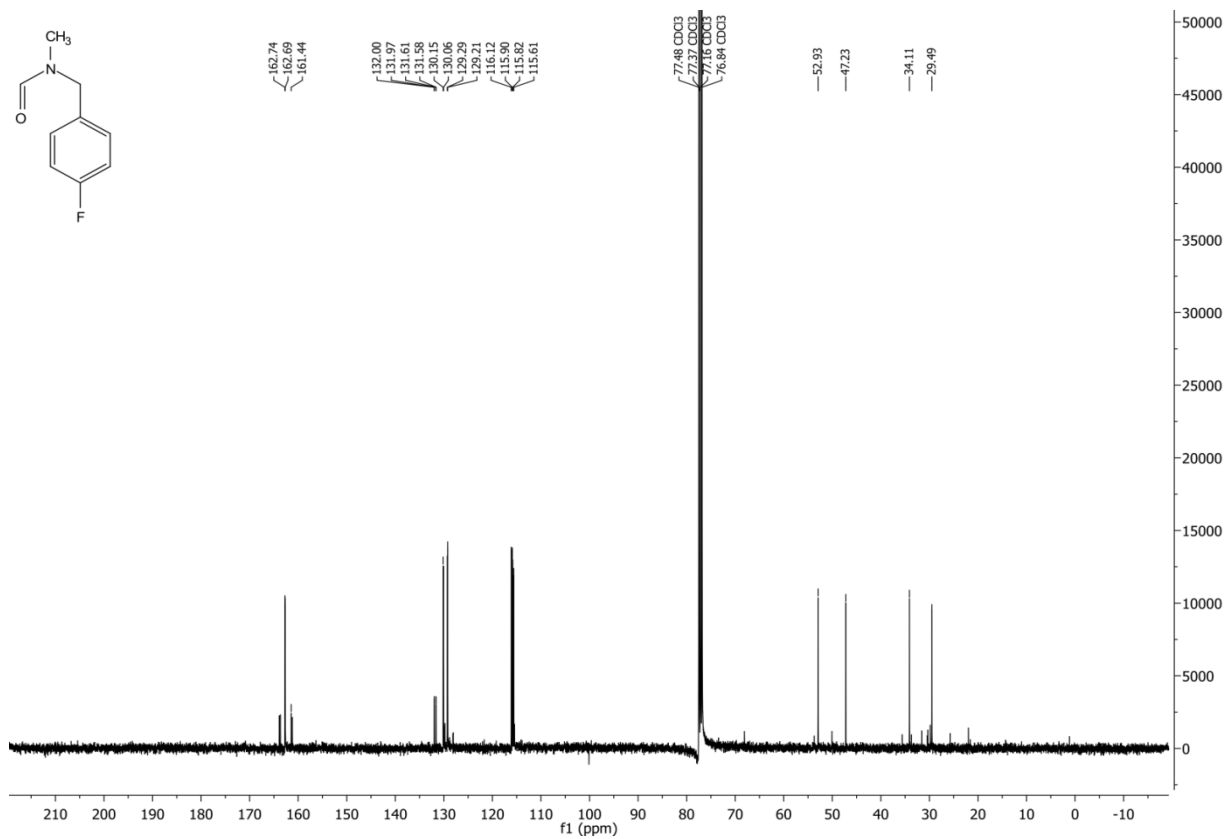


Figure XXII  $^{13}\text{C-NMR}$  of compound 4b)

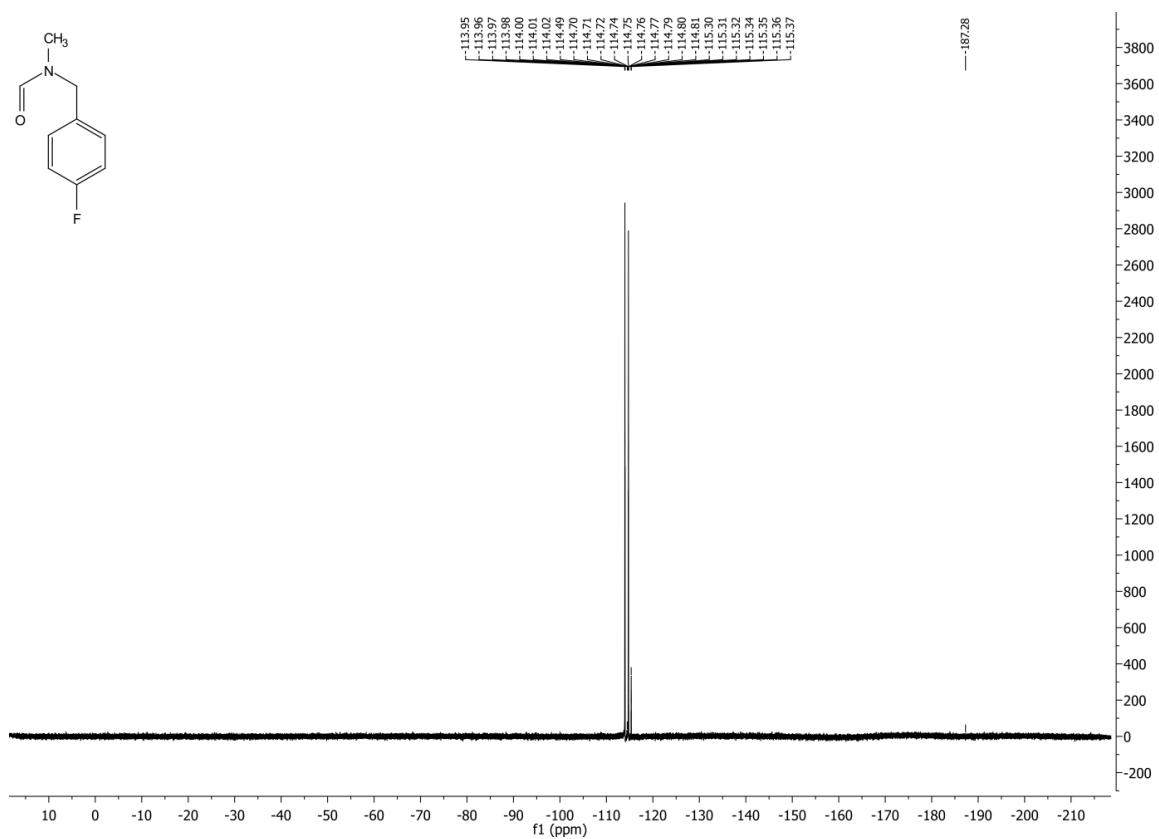
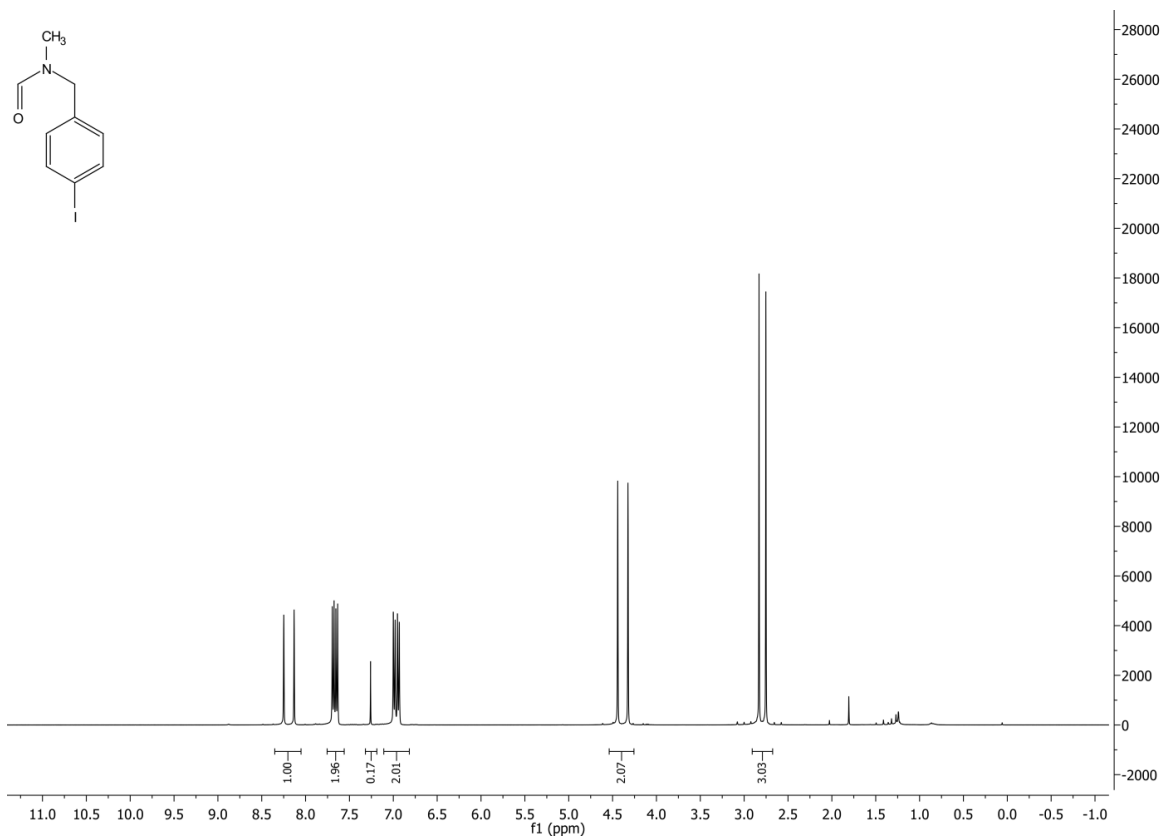
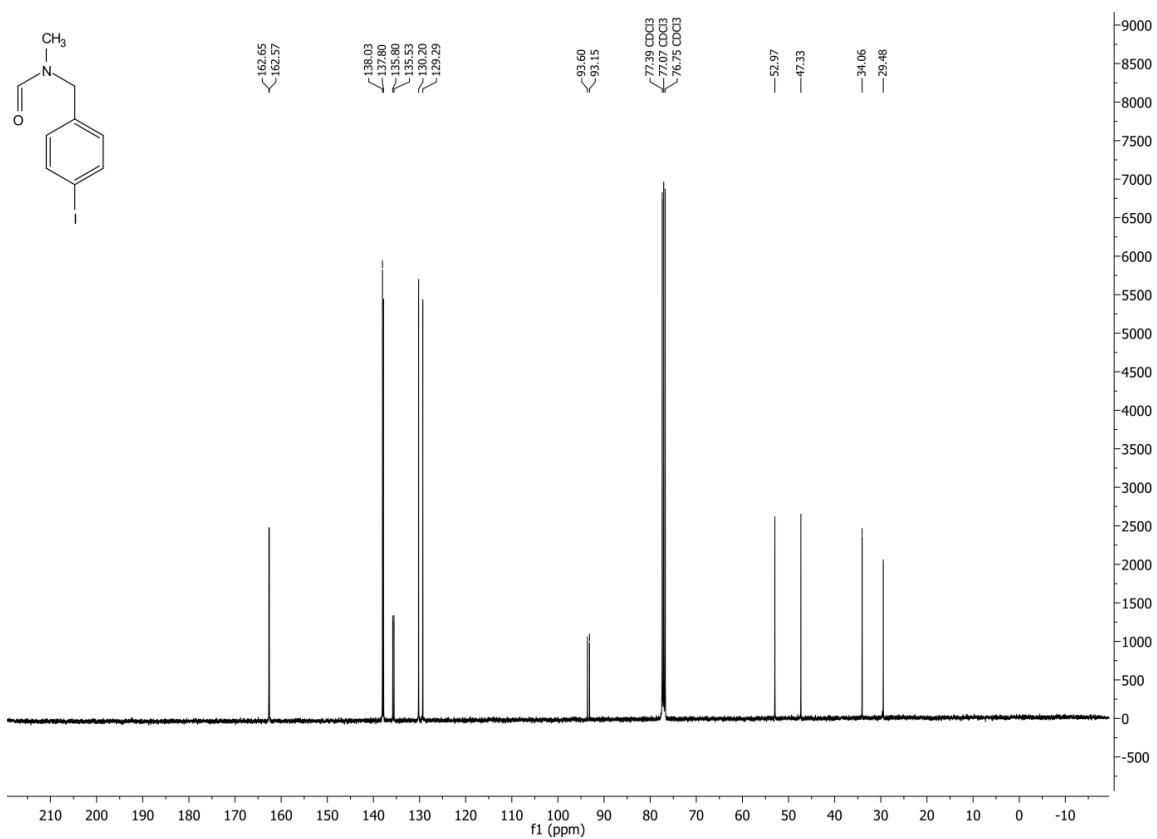


Figure XXIII  $^{19}\text{F-NMR}$  of compound 4b)



**Figure XXIV  $^1\text{H-NMR}$  of compound 4e)**



**Figure XXV  $^{13}\text{C-NMR}$  of compound 4e)**

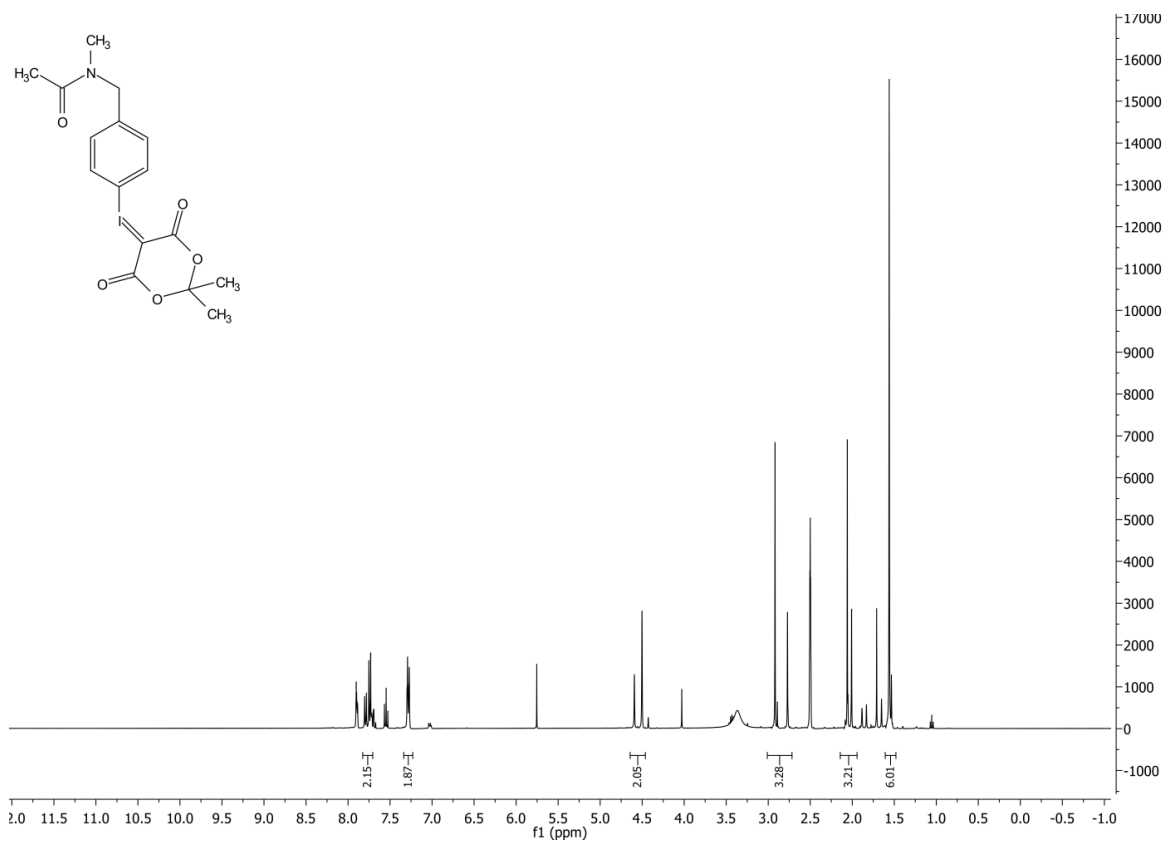


Figure XXVI <sup>1</sup>H-NMR of compound 5a)

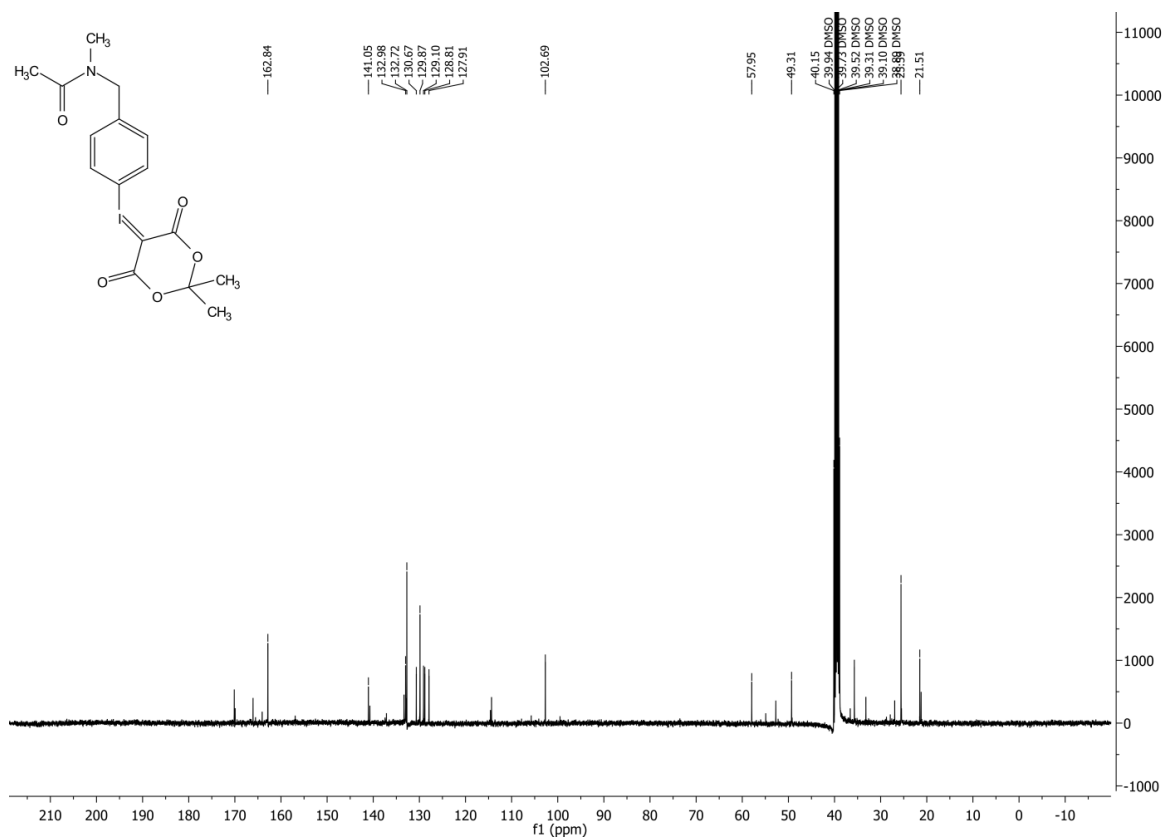


Figure XXVII <sup>13</sup>C-NMR of compound 5a)

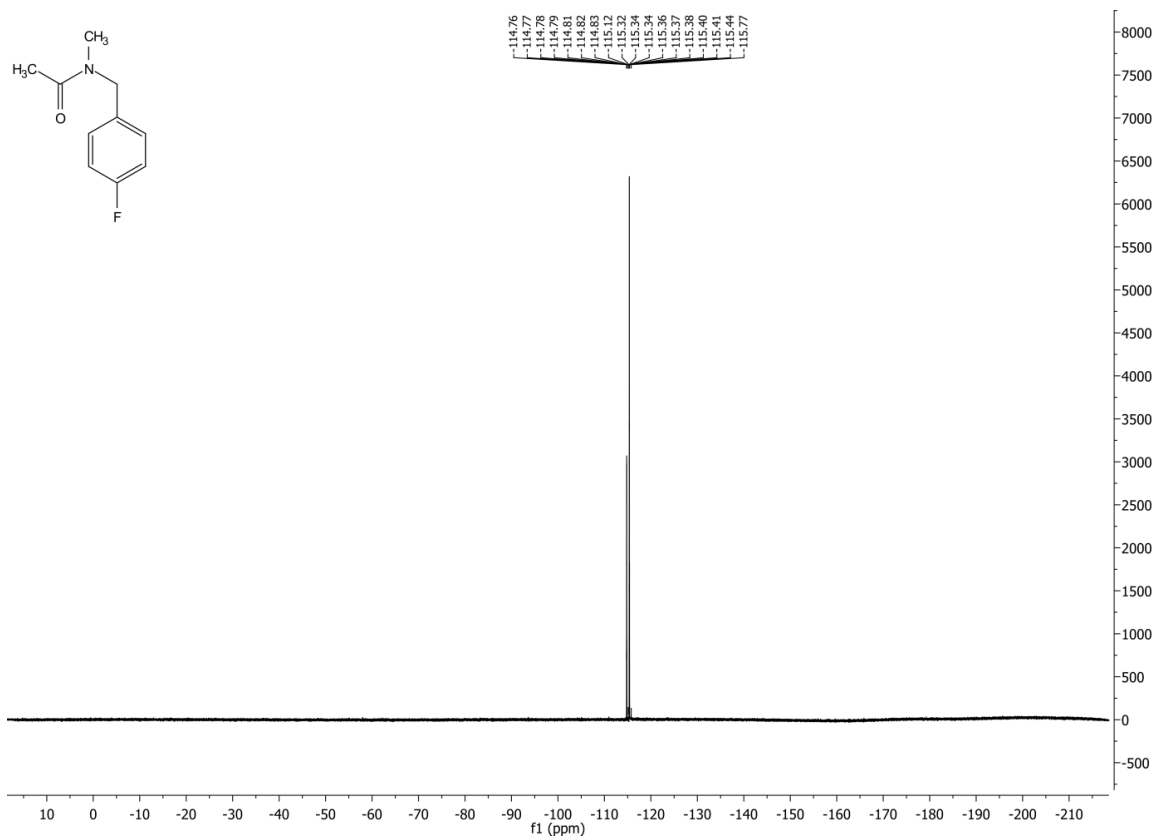


Figure XXVIII  $^{19}\text{F}$ -NMR of compound 5b)

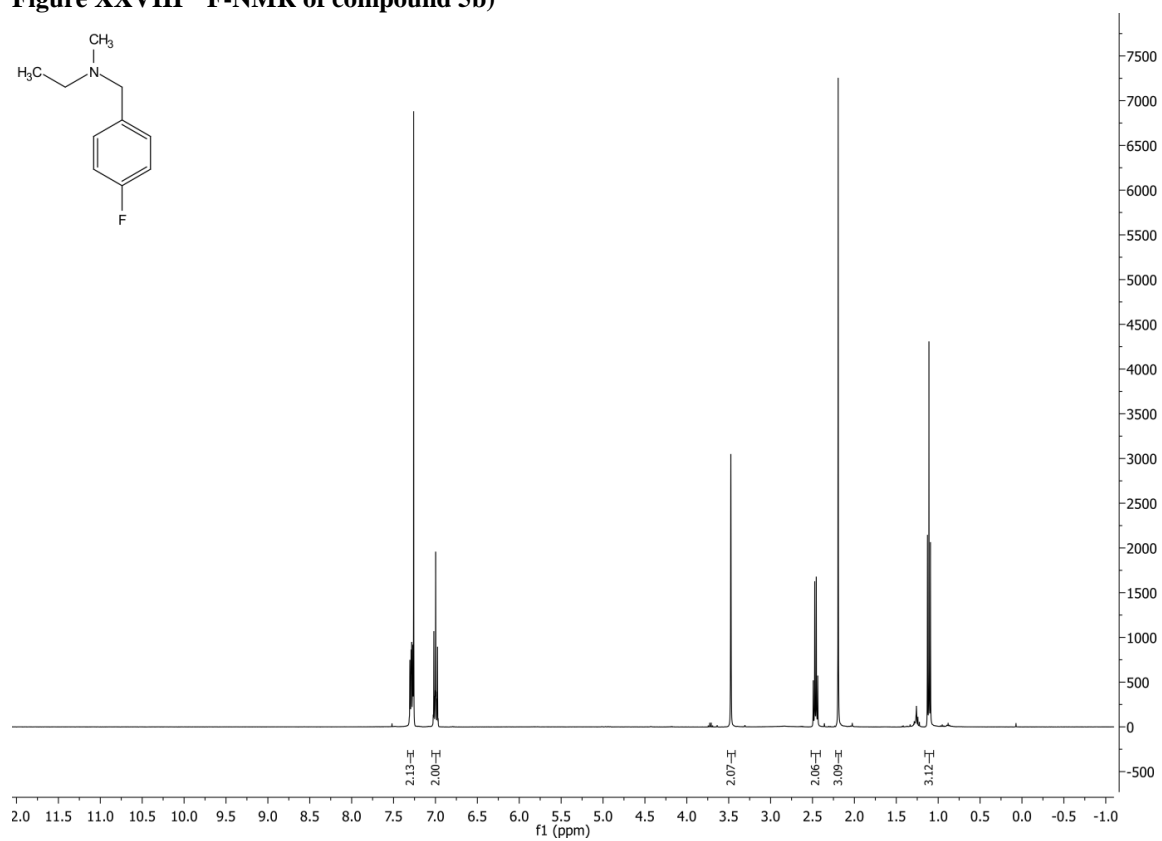


Figure XXIX  $^1\text{H}$ -NMR of compound 5c)

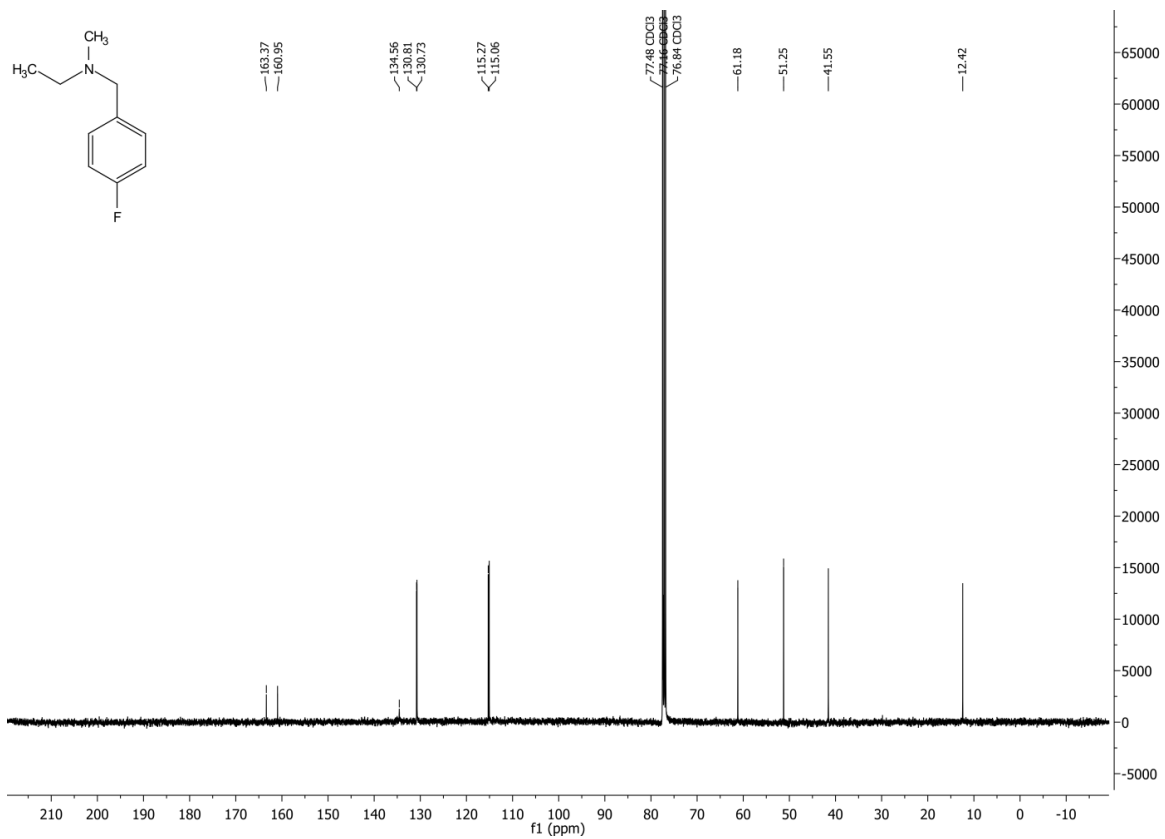


Figure XXX <sup>13</sup>C-NMR of compound 5c)

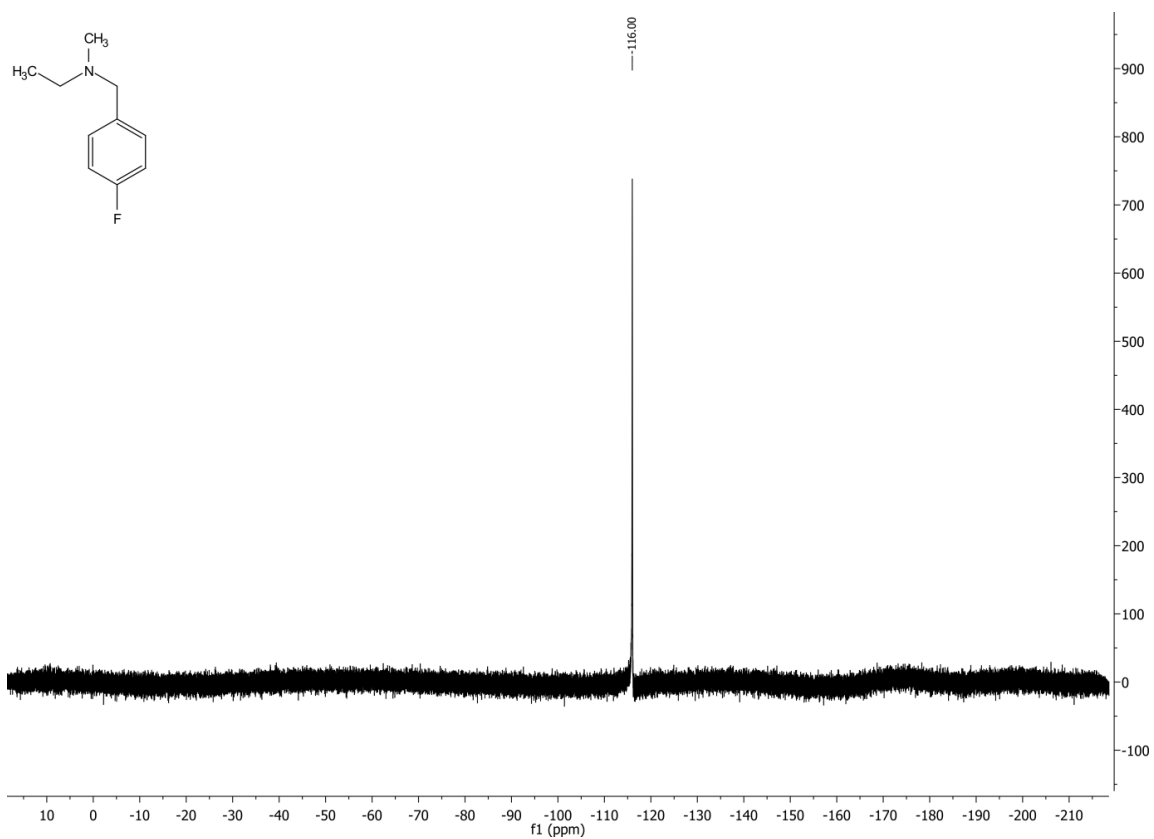


Figure XXXI <sup>19</sup>F-NMR of compound 5c)

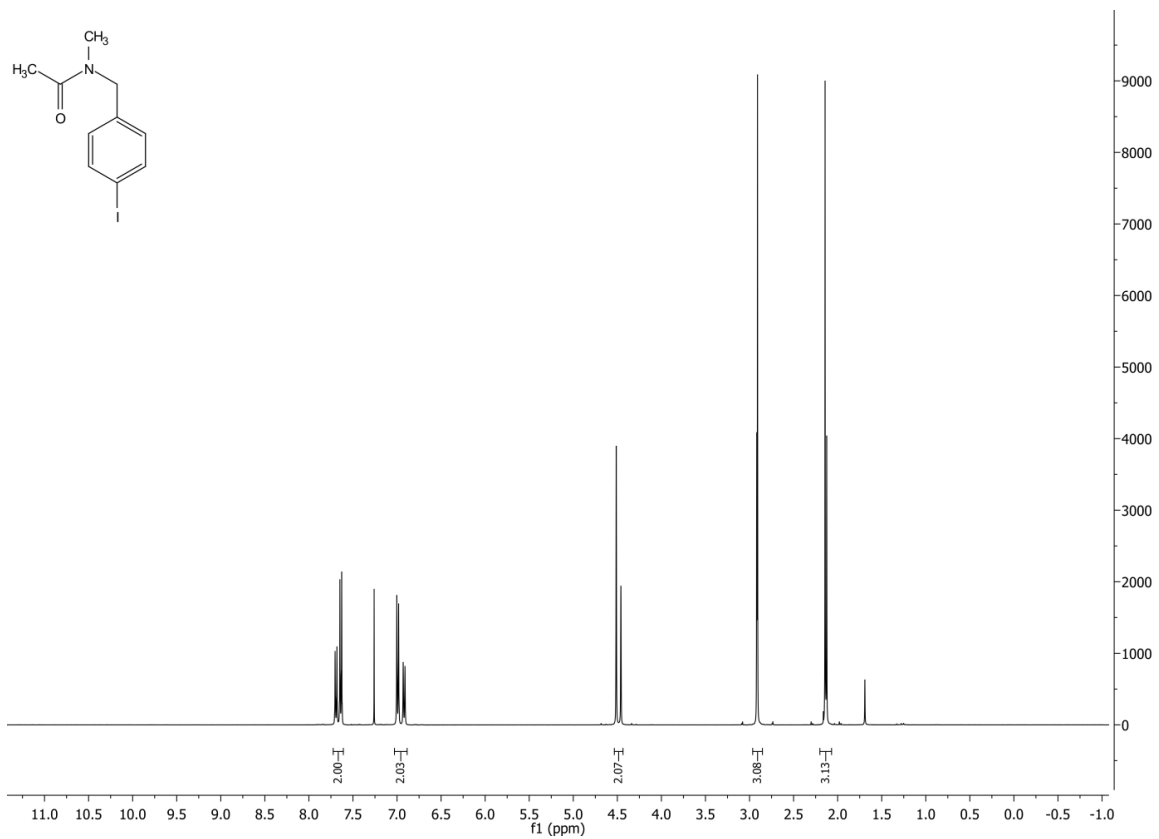


Figure XXXII <sup>1</sup>H-NMR of compound 5d)

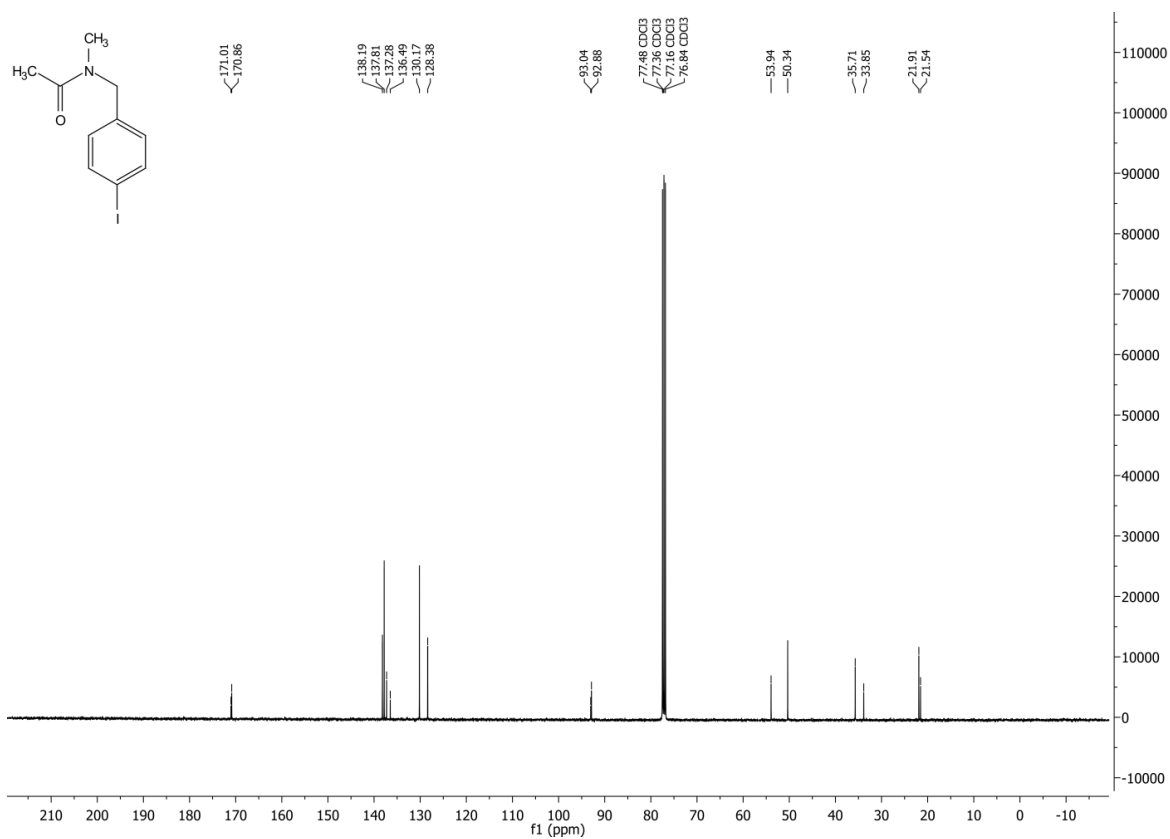


Figure XXXIII <sup>13</sup>C-NMR of compound 5d)

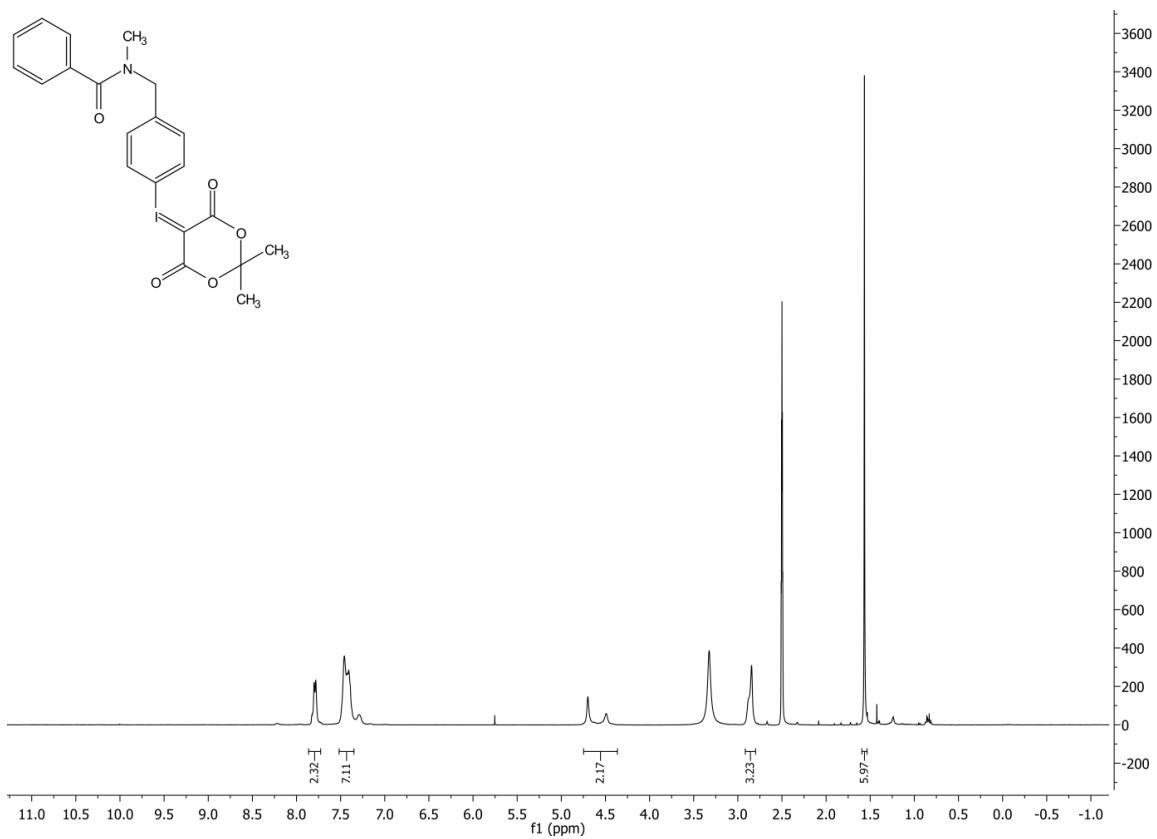


Figure XXXIV <sup>1</sup>H-NMR of compound 6a)

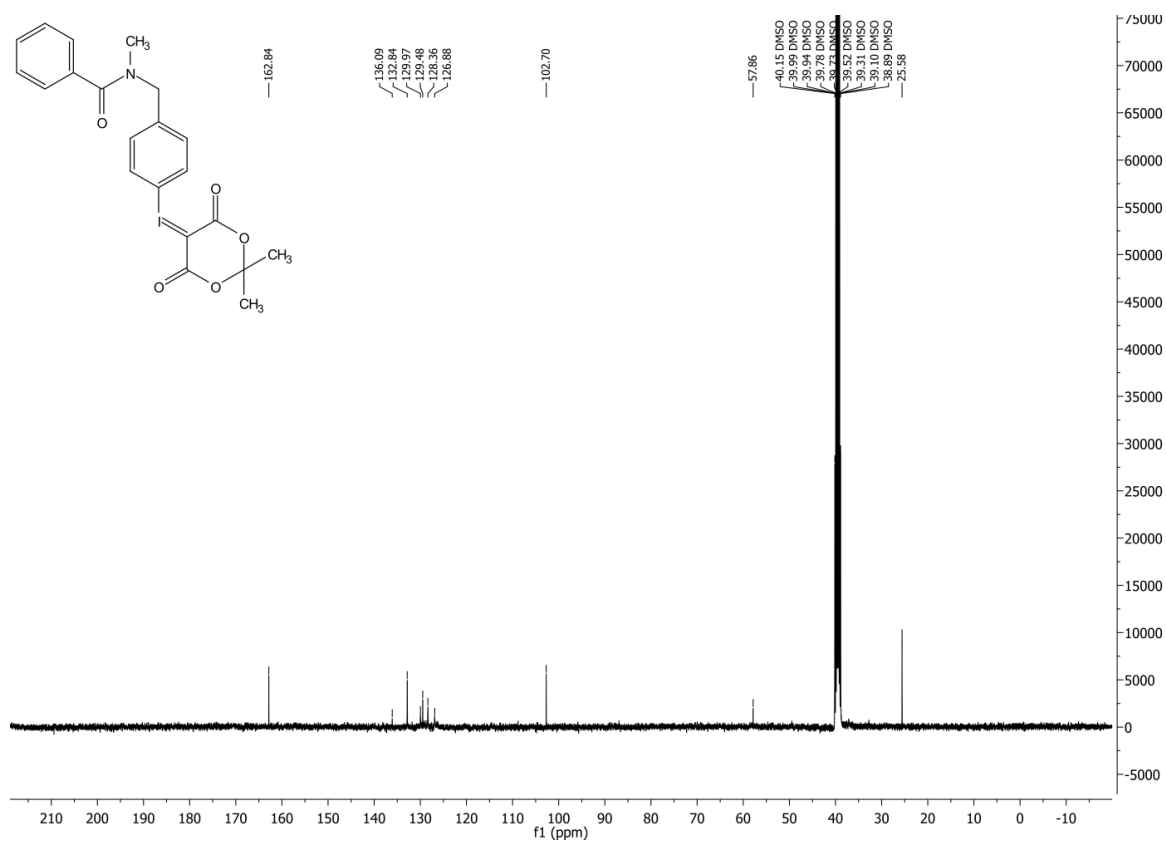


Figure XXXV <sup>13</sup>C-NMR of compound 6a)



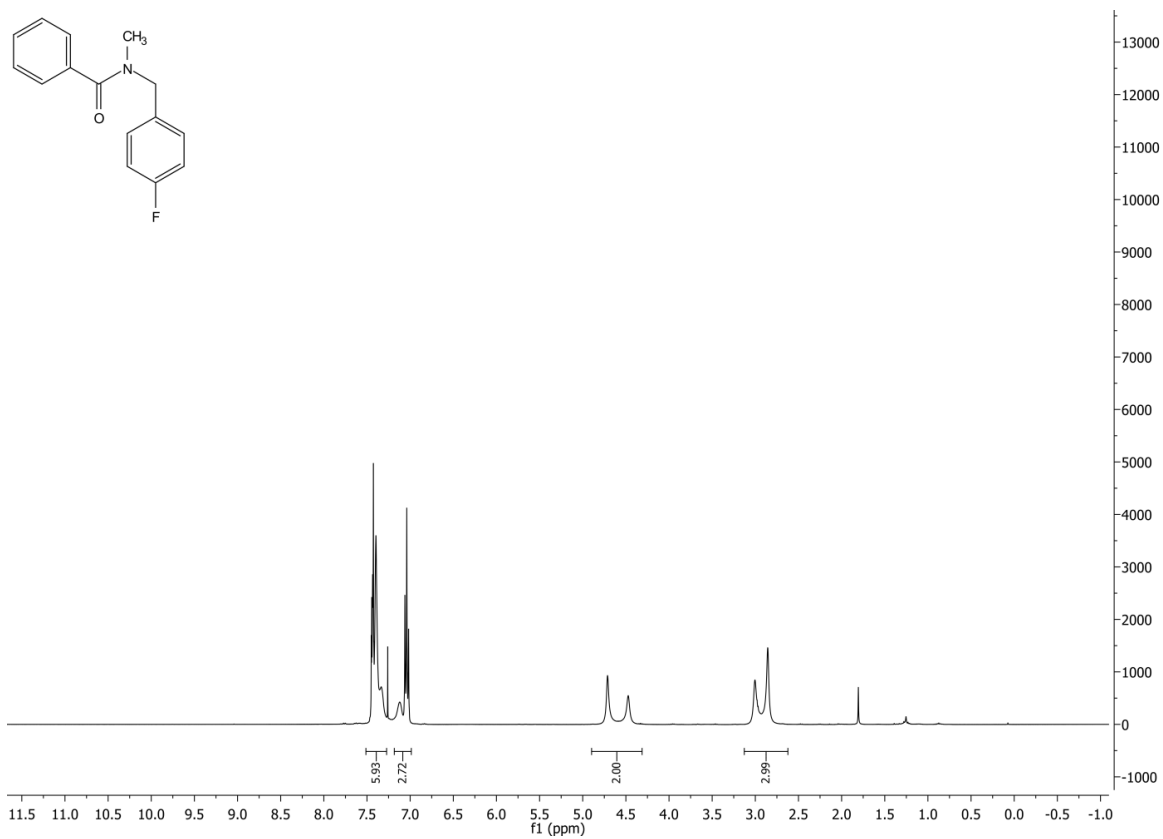


Figure XXXVI  $^1\text{H-NMR}$  of compound 6b)

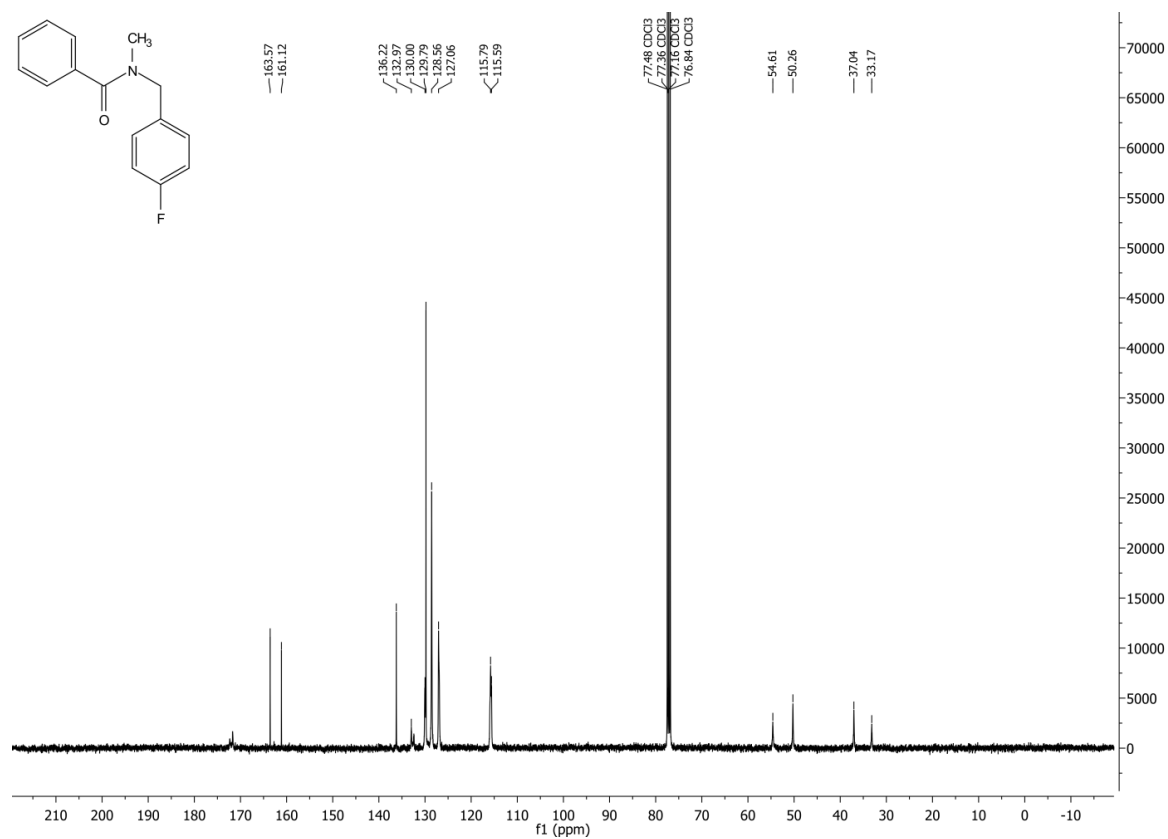


Figure XXXVII  $^{13}\text{C-NMR}$  of compound 6b)

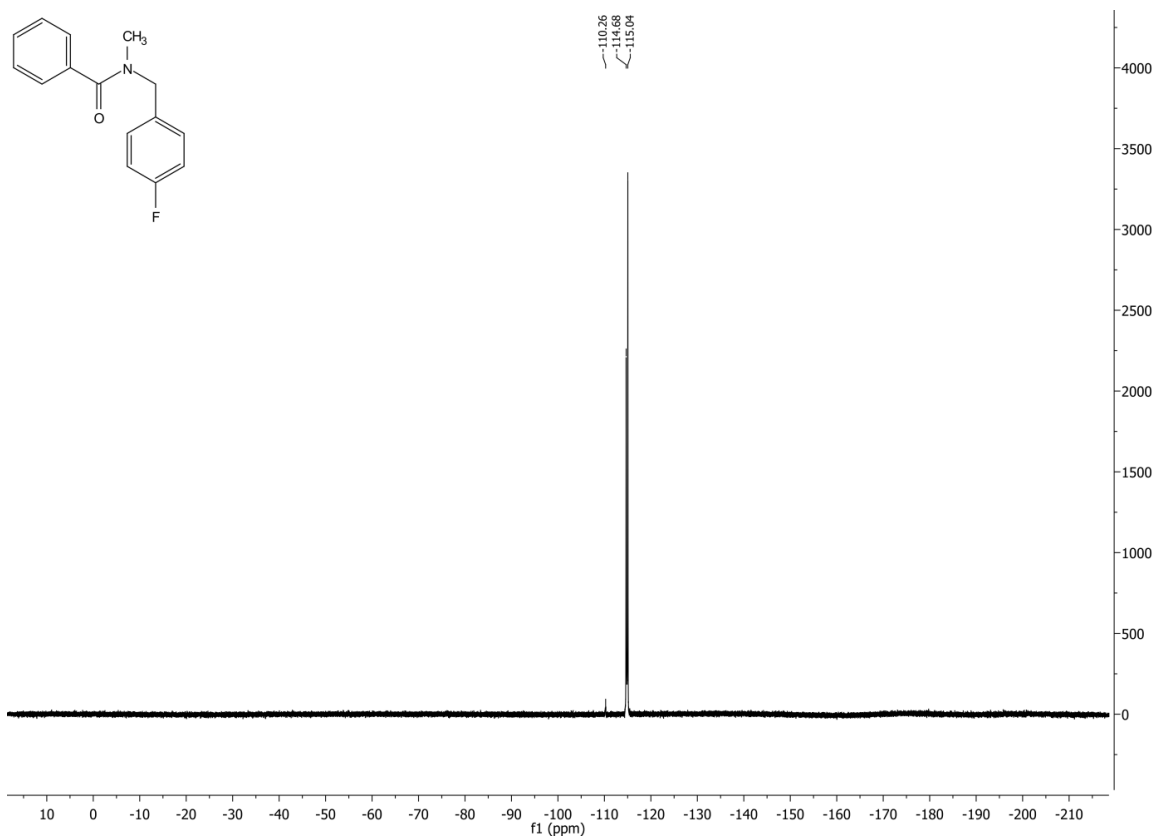


Figure XXXVIII  $^{19}\text{F}$ -NMR of compound 6b)

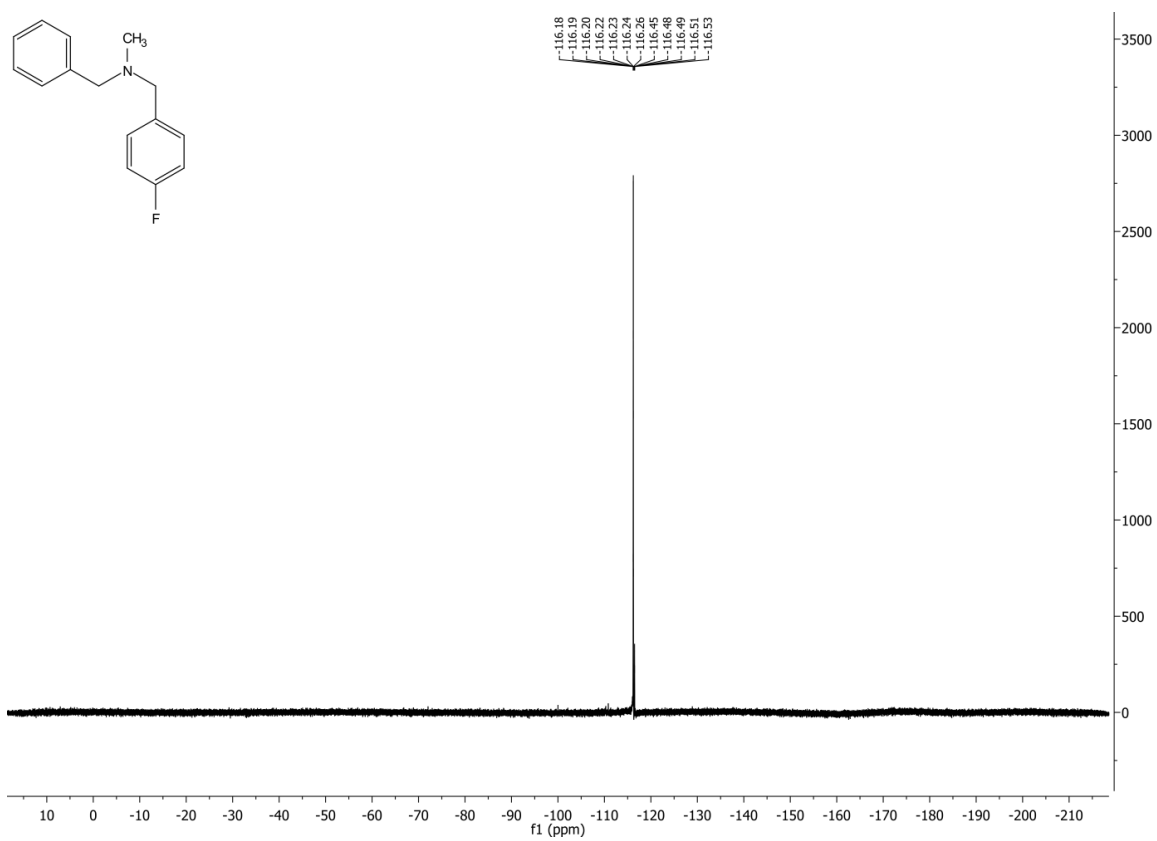
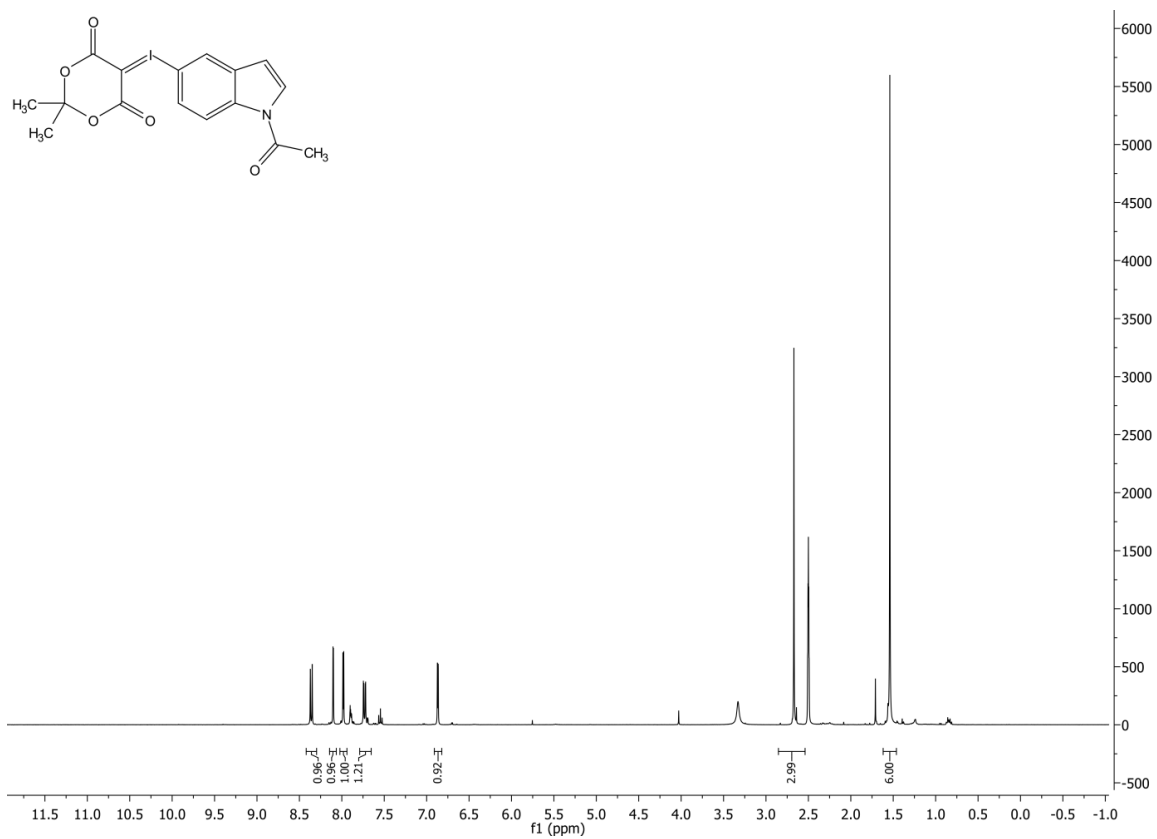
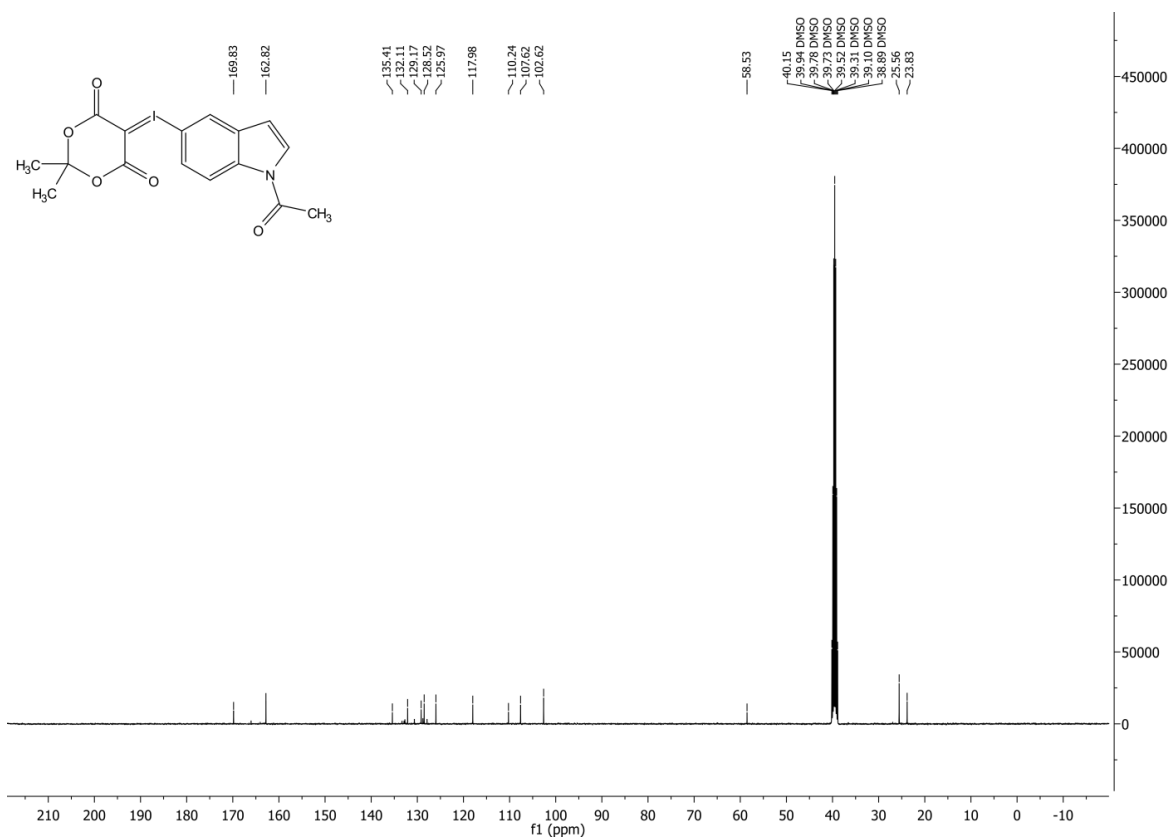


Figure XXXIX  $^{19}\text{F}$ -NMR of compound 6c)



**Figure XL  $^1\text{H-NMR}$  of compound 7a)**



**Figure XLI  $^{13}\text{C-NMR}$  of compound 7a)**

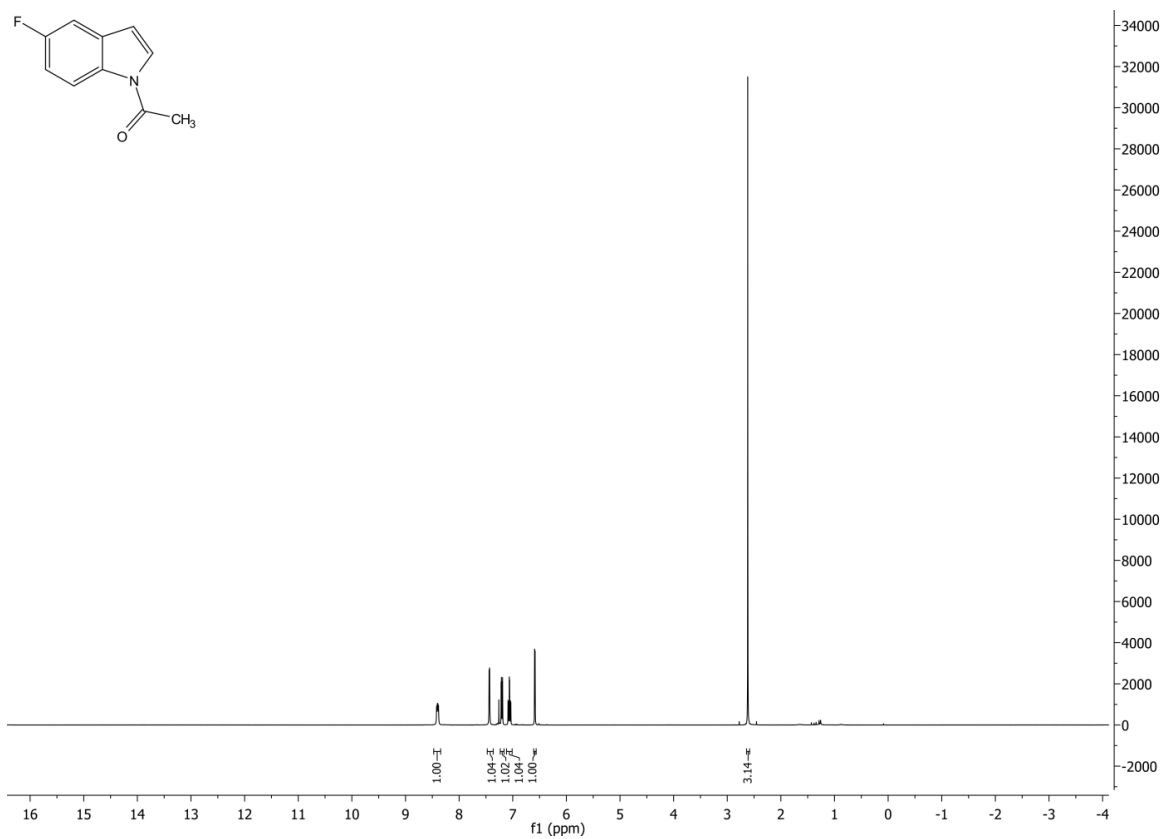


Figure XLII <sup>1</sup>H-NMR of compound 7b)

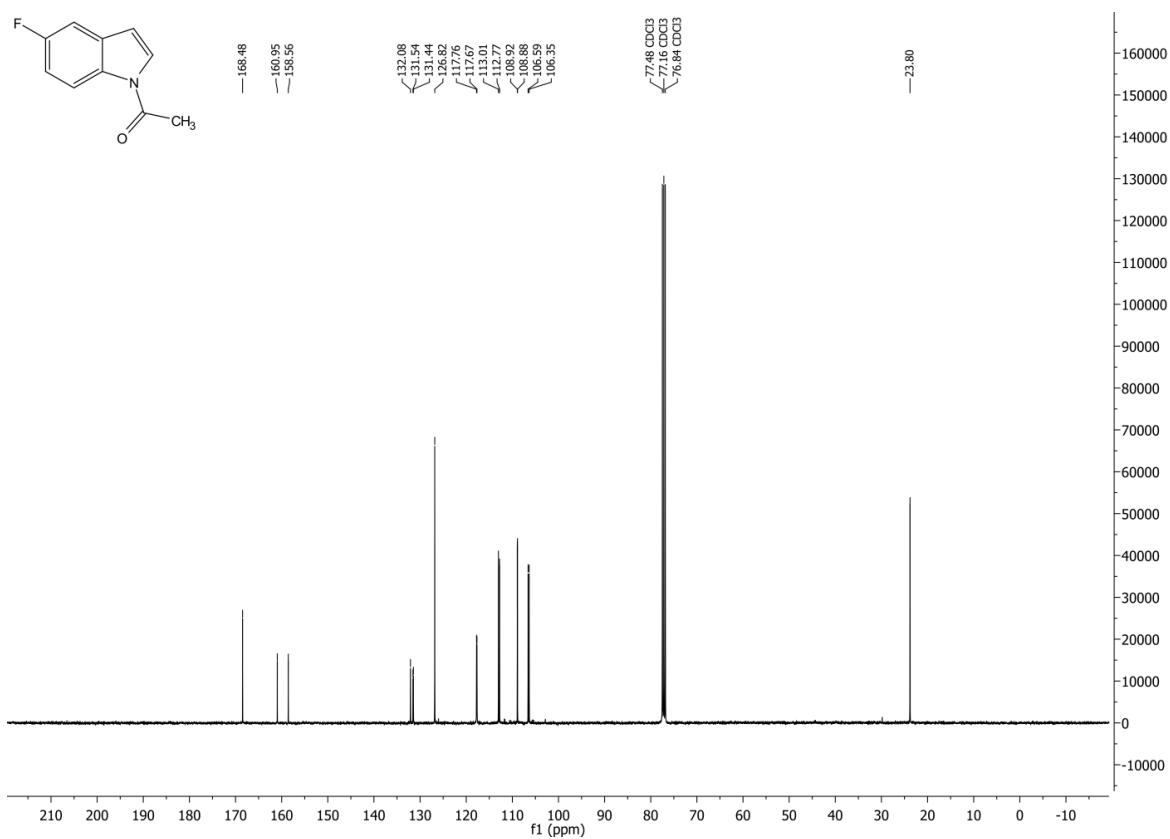


Figure XLIII <sup>13</sup>C-NMR of compound 7b)

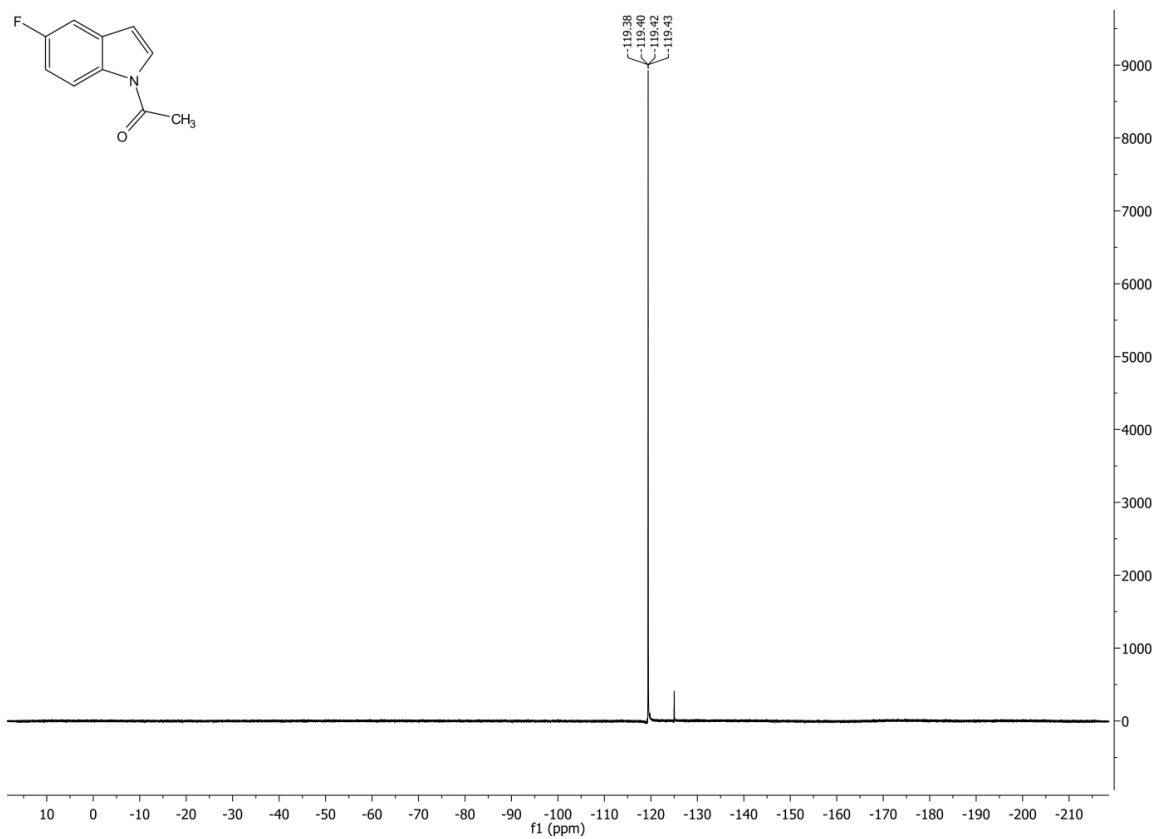


Figure XLIV  $^{19}\text{F}$ -NMR of compound 7b)

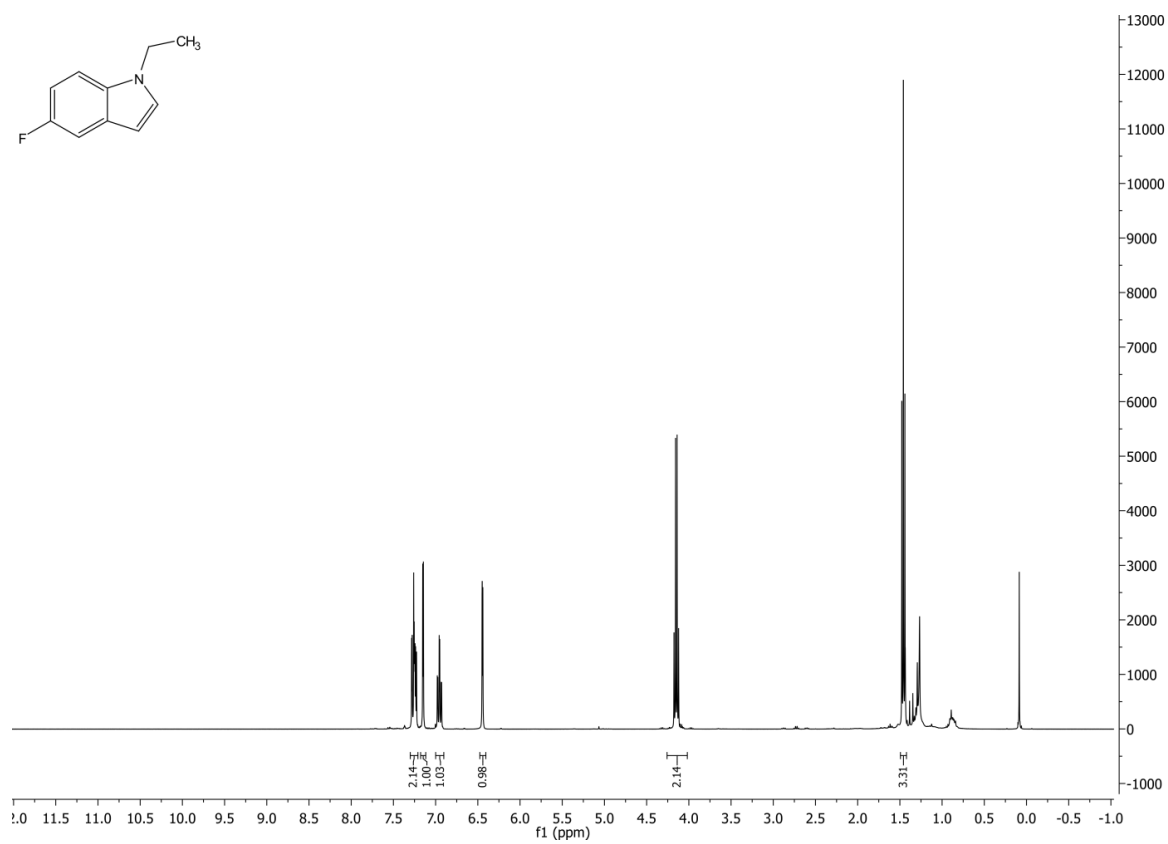


Figure XLV  $^1\text{H}$ -NMR of compound 7c)

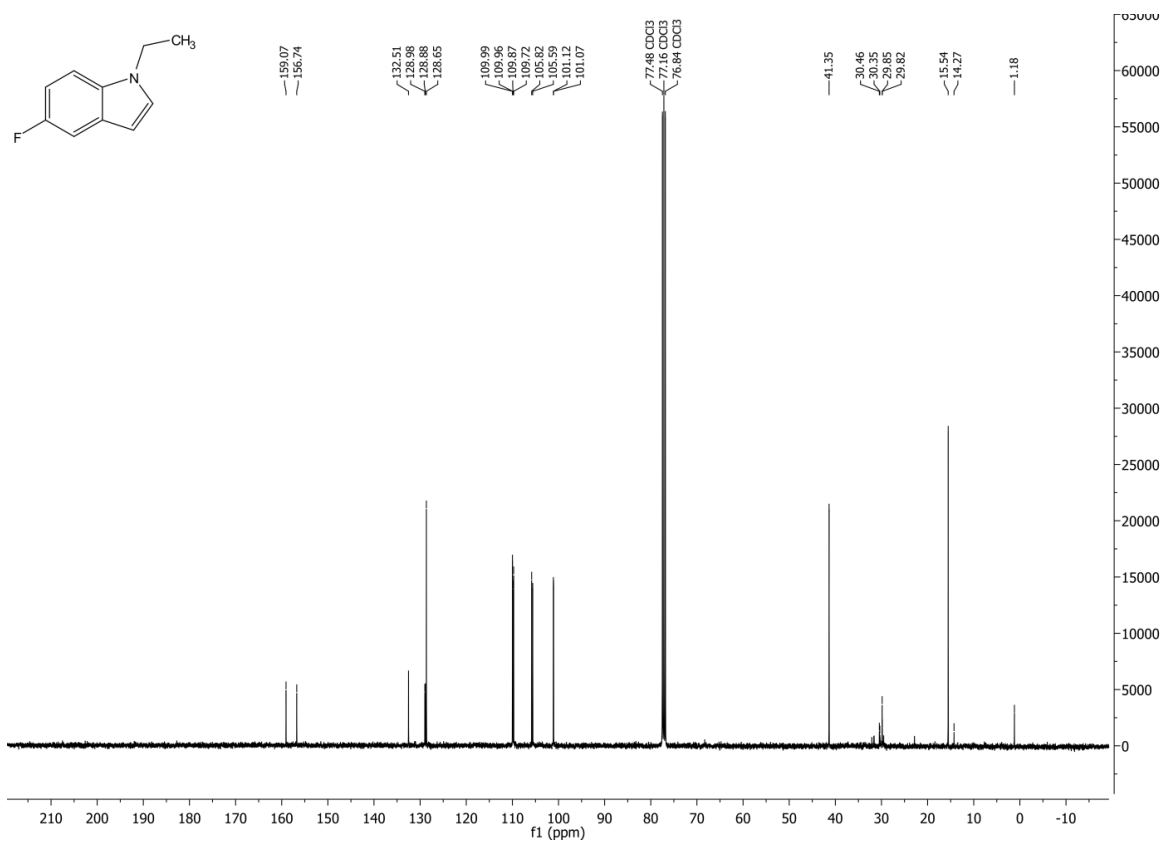


Figure XLVI <sup>13</sup>C-NMR of compound 7c)

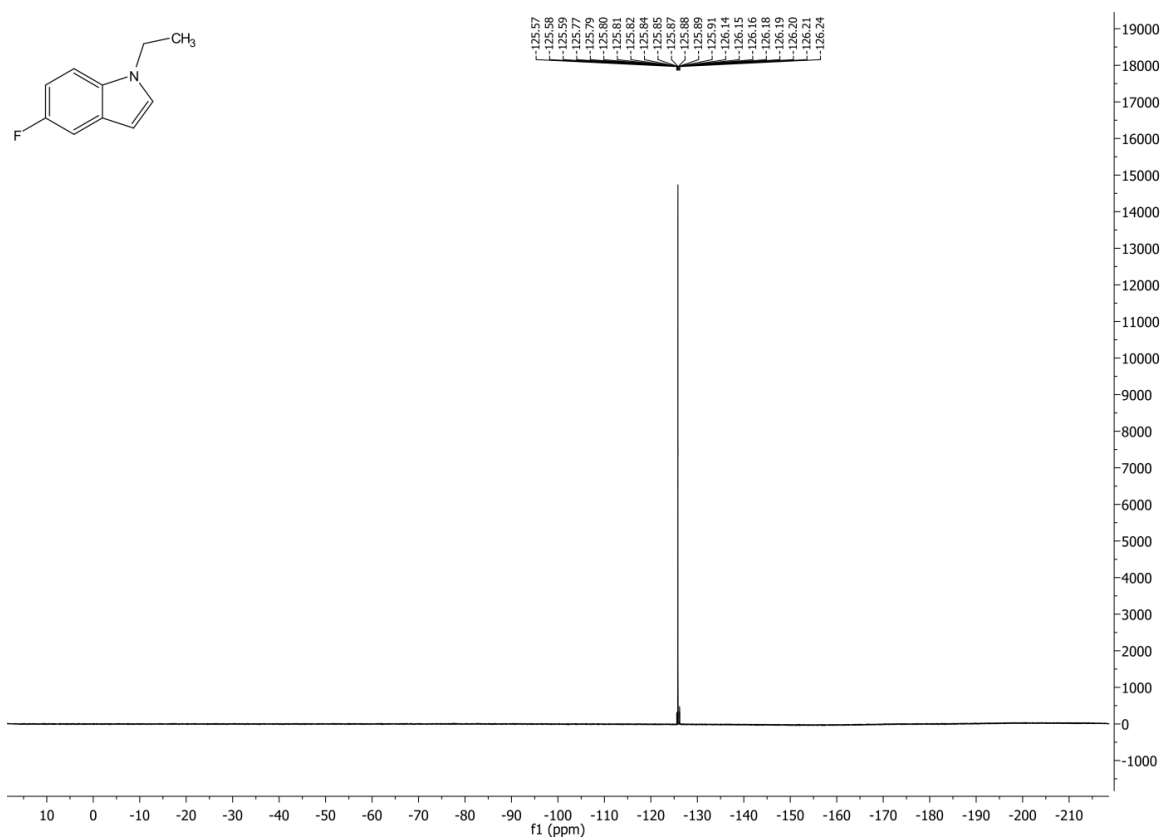


Figure XLVII <sup>19</sup>F-NMR of compound 7c)

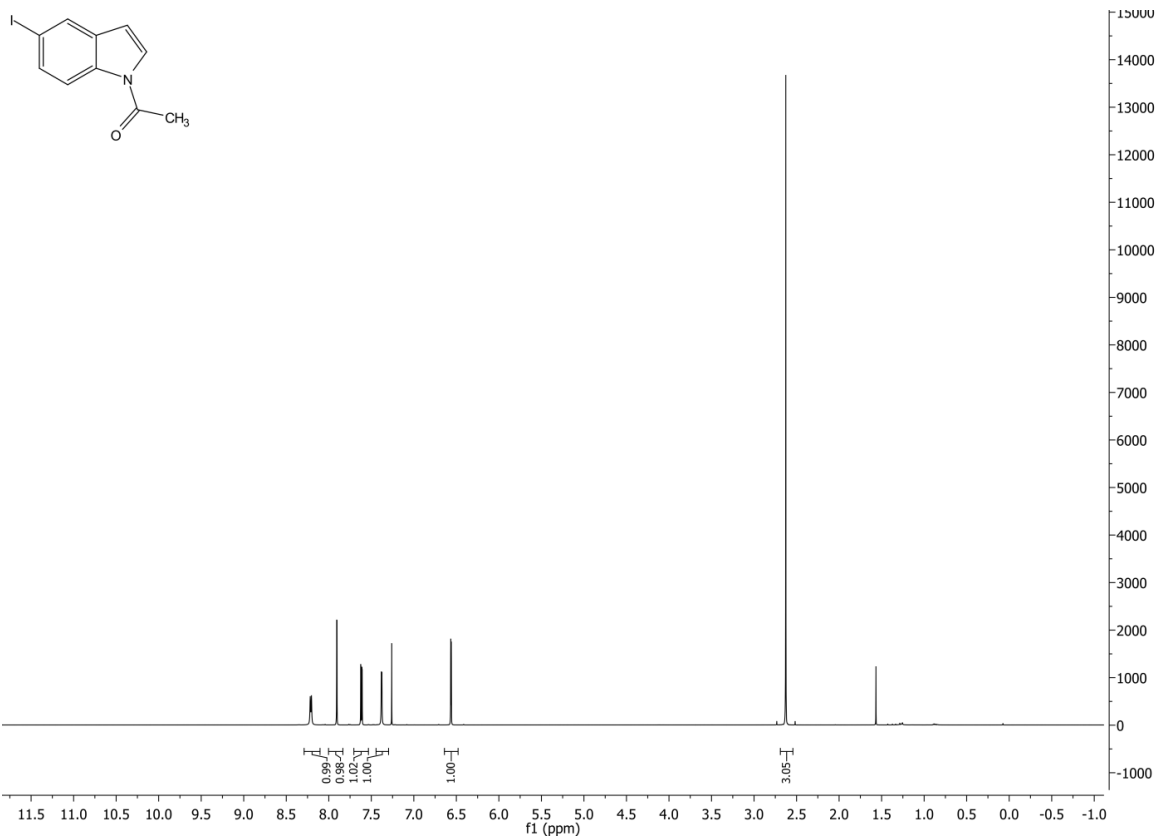


Figure XLVIII <sup>1</sup>H-NMR of compound 7f)

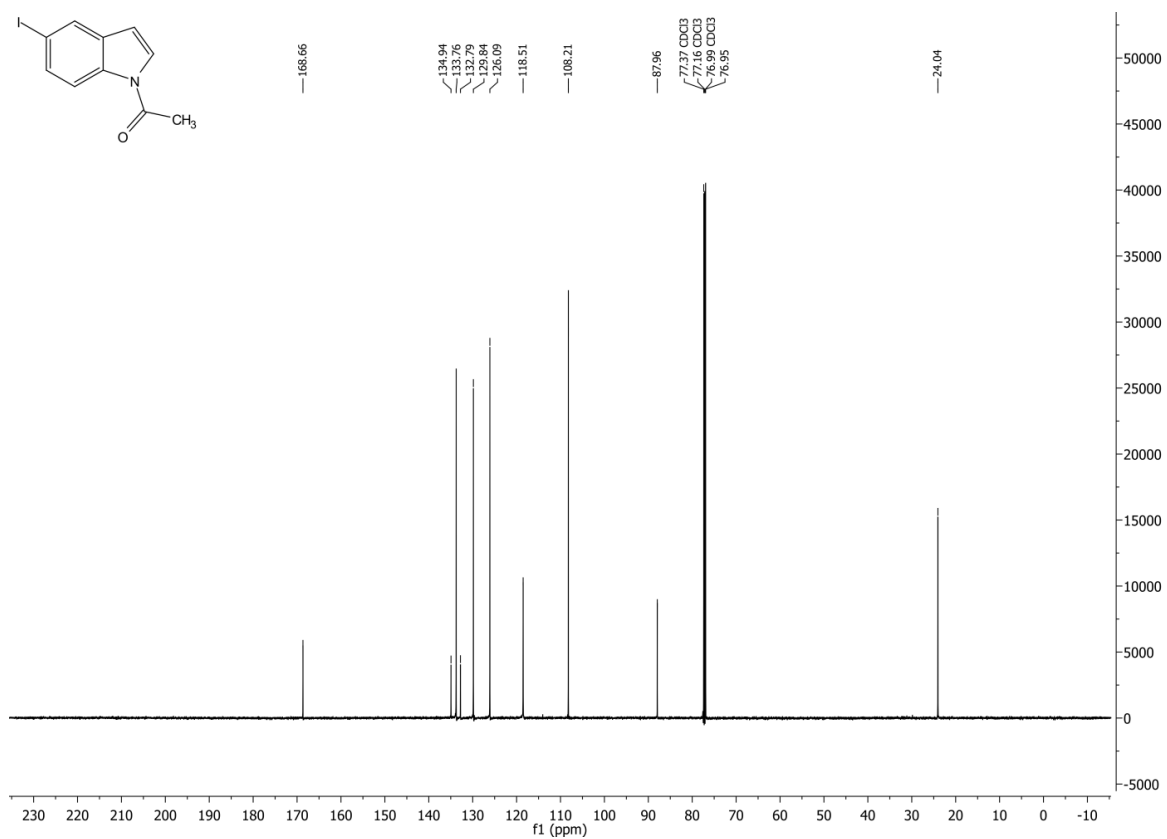


Figure XLIX <sup>13</sup>C-NMR of compound 7f)

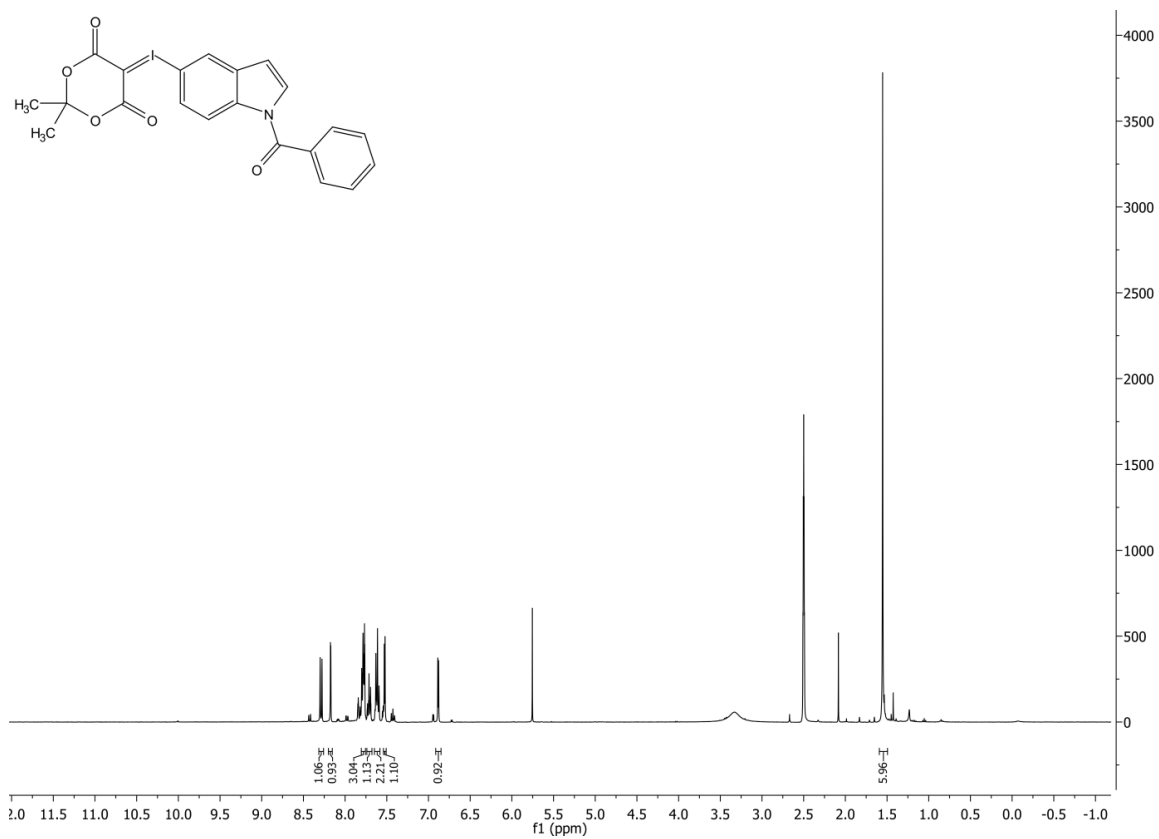


Figure L <sup>1</sup>H-NMR of compound 8a)

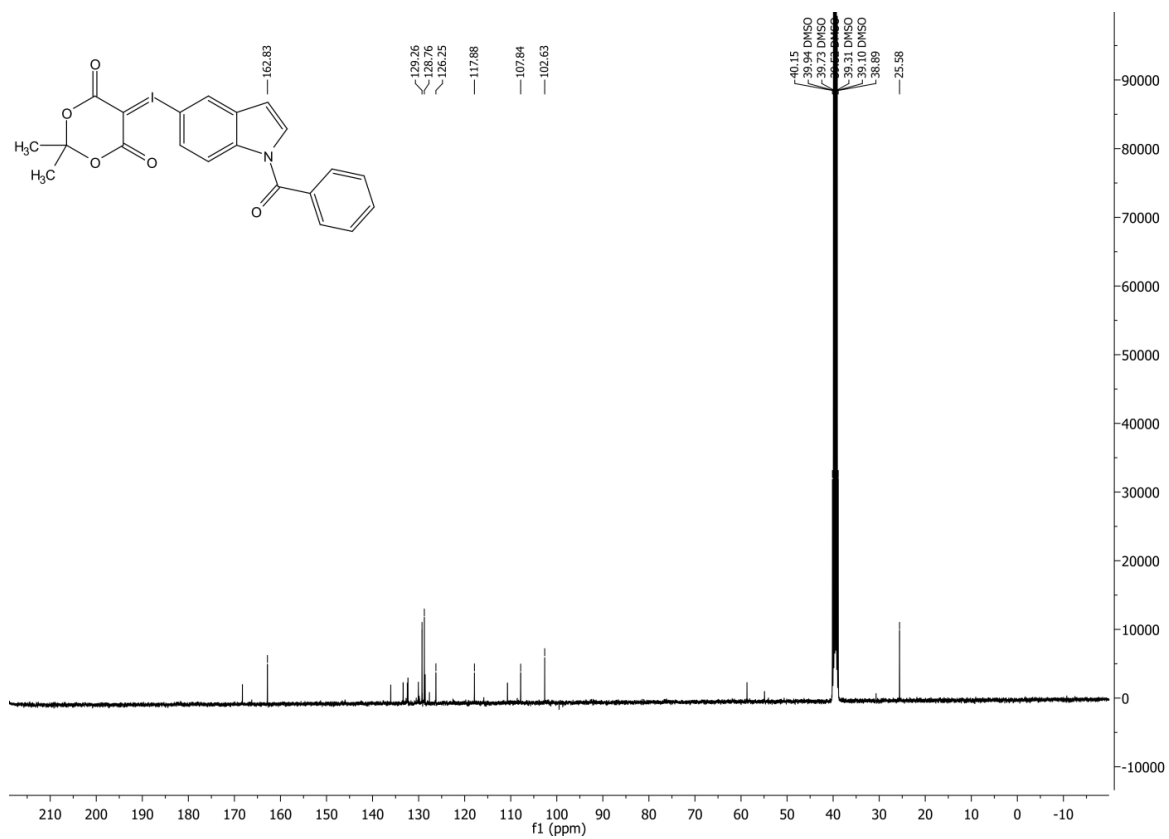


Figure LI <sup>13</sup>C-NMR of compound 8a)



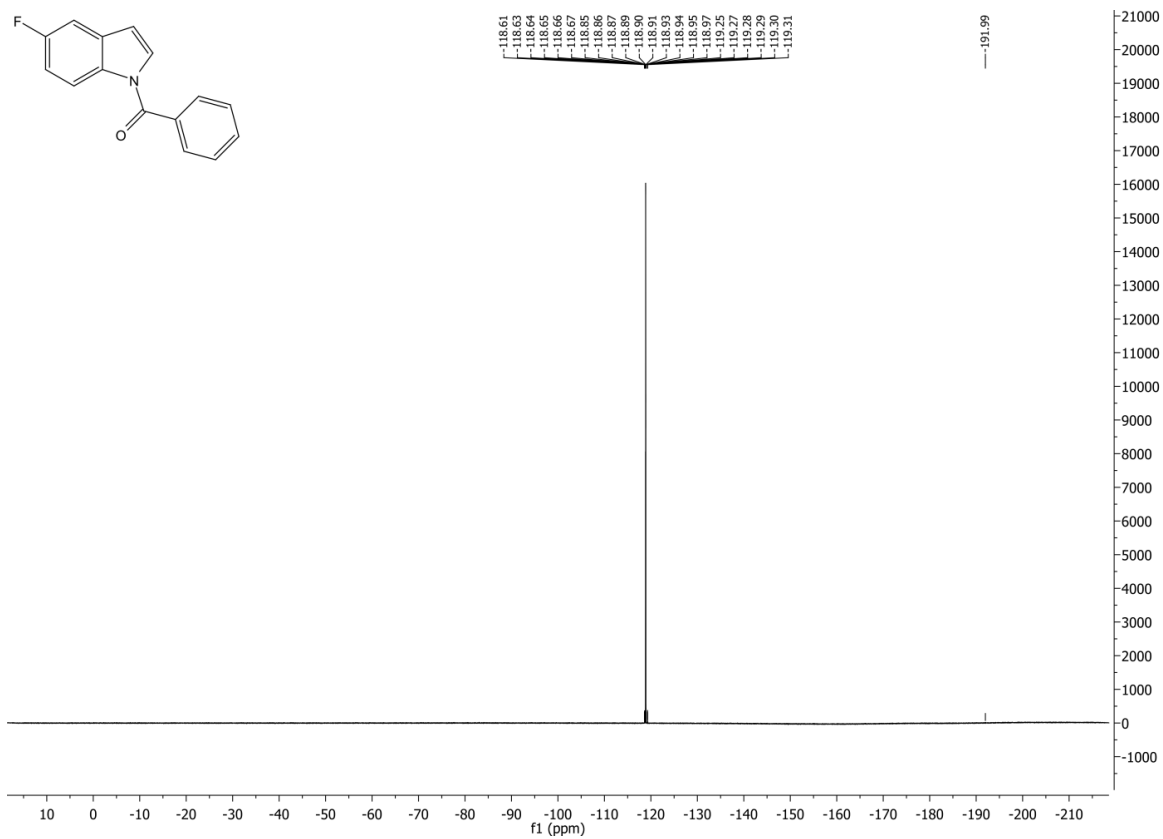


Figure LII  $^{19}\text{F}$ -NMR of compound 8b)

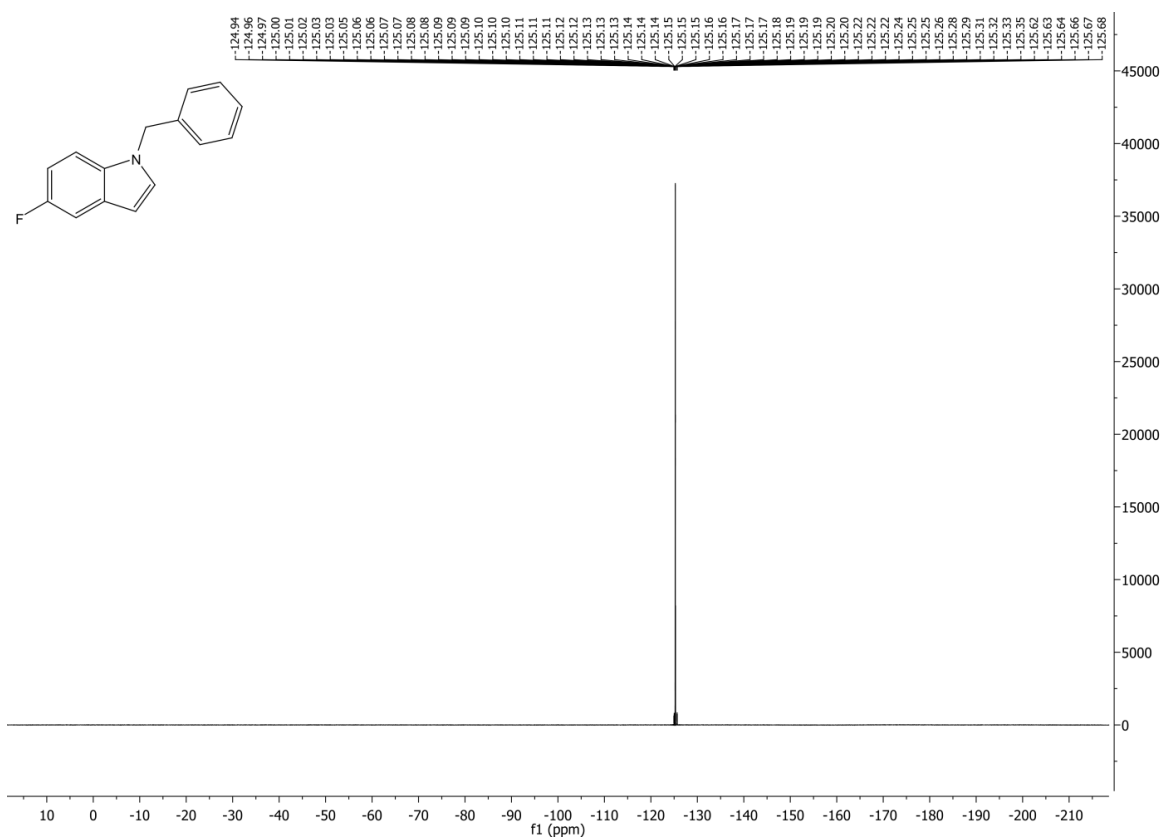


Figure LIII  $^{19}\text{F}$ -NMR of compound 8c)

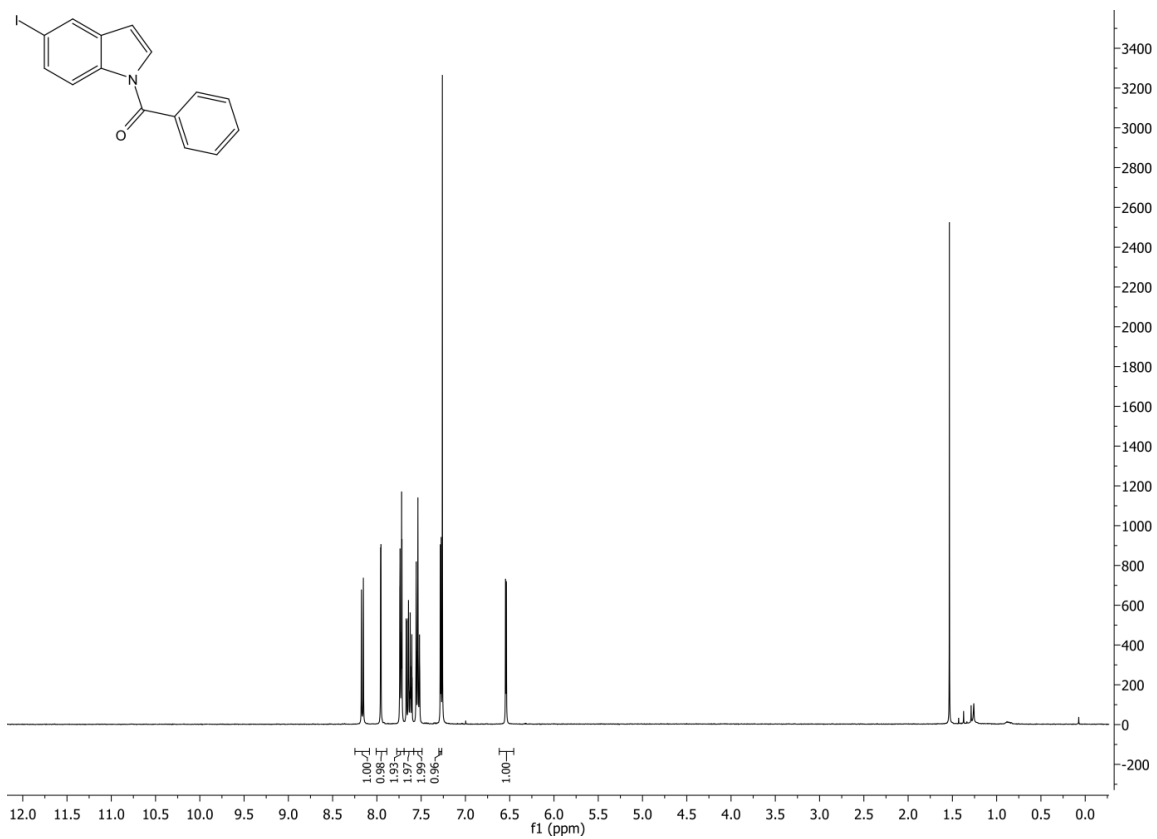


Figure LIV <sup>1</sup>H-NMR of compound 8d)

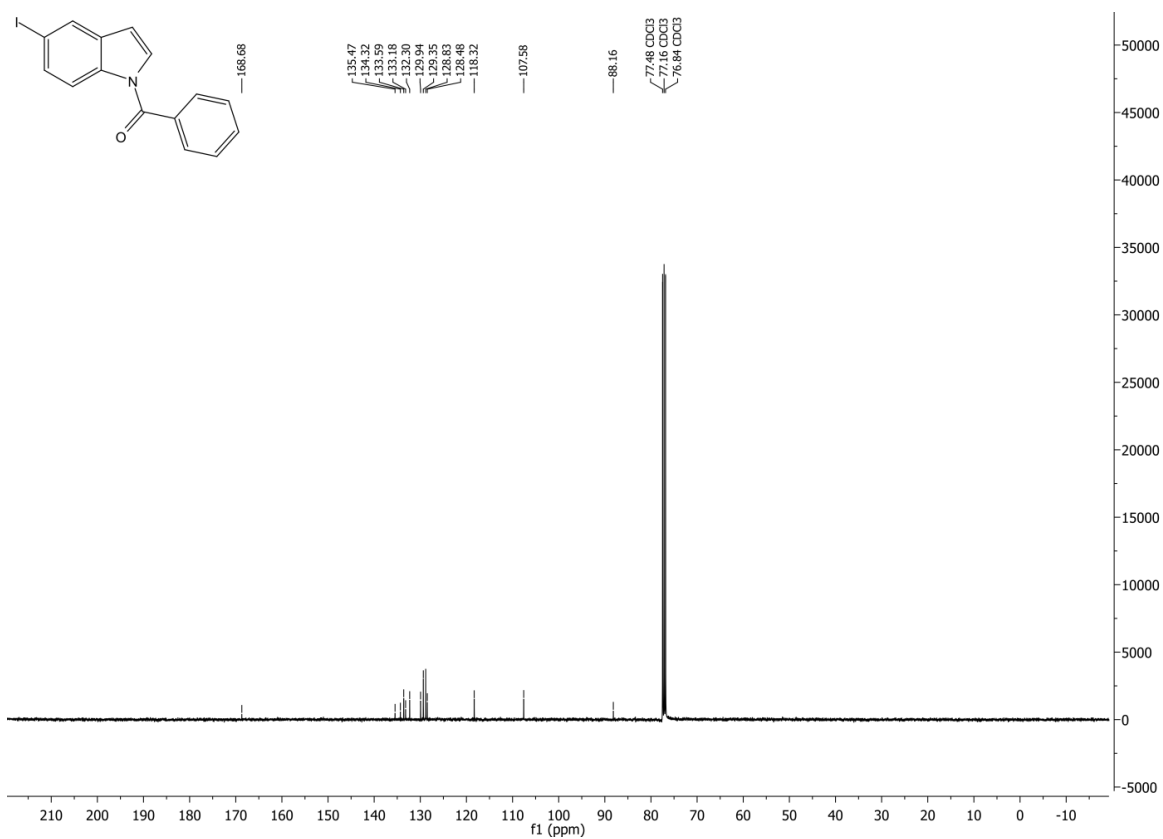
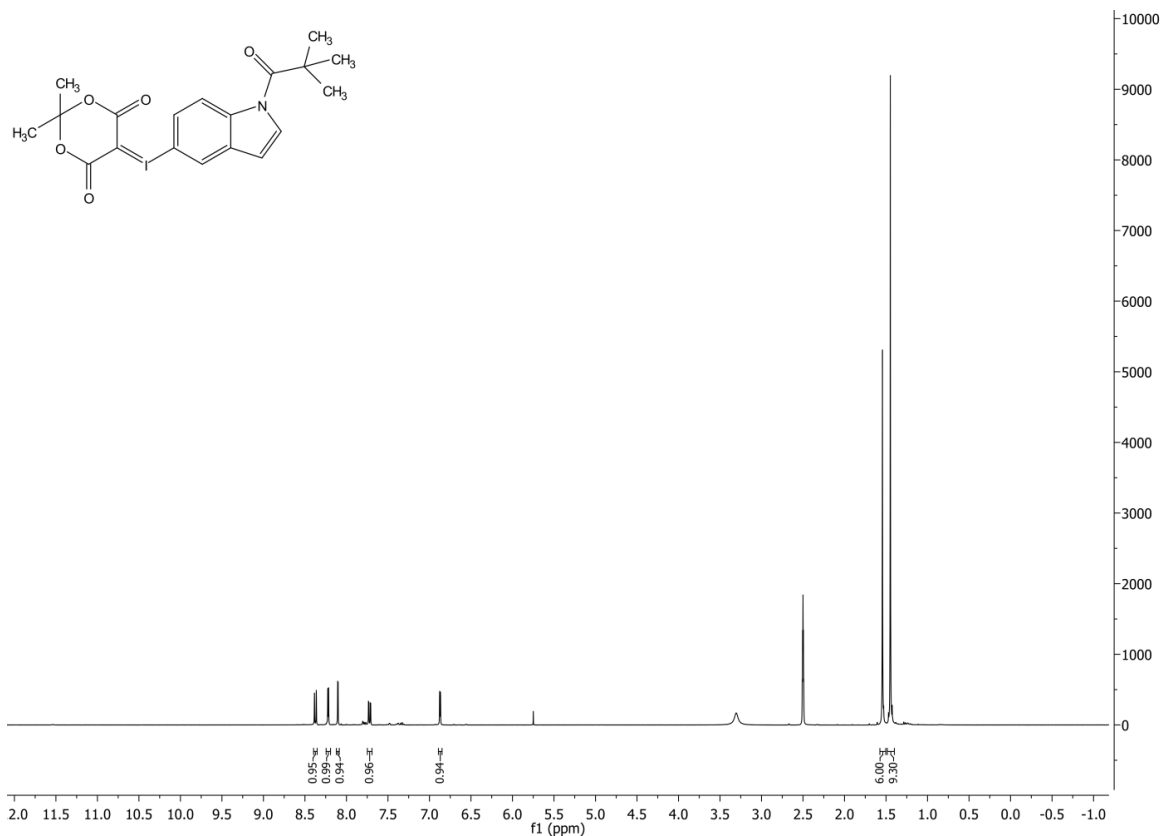
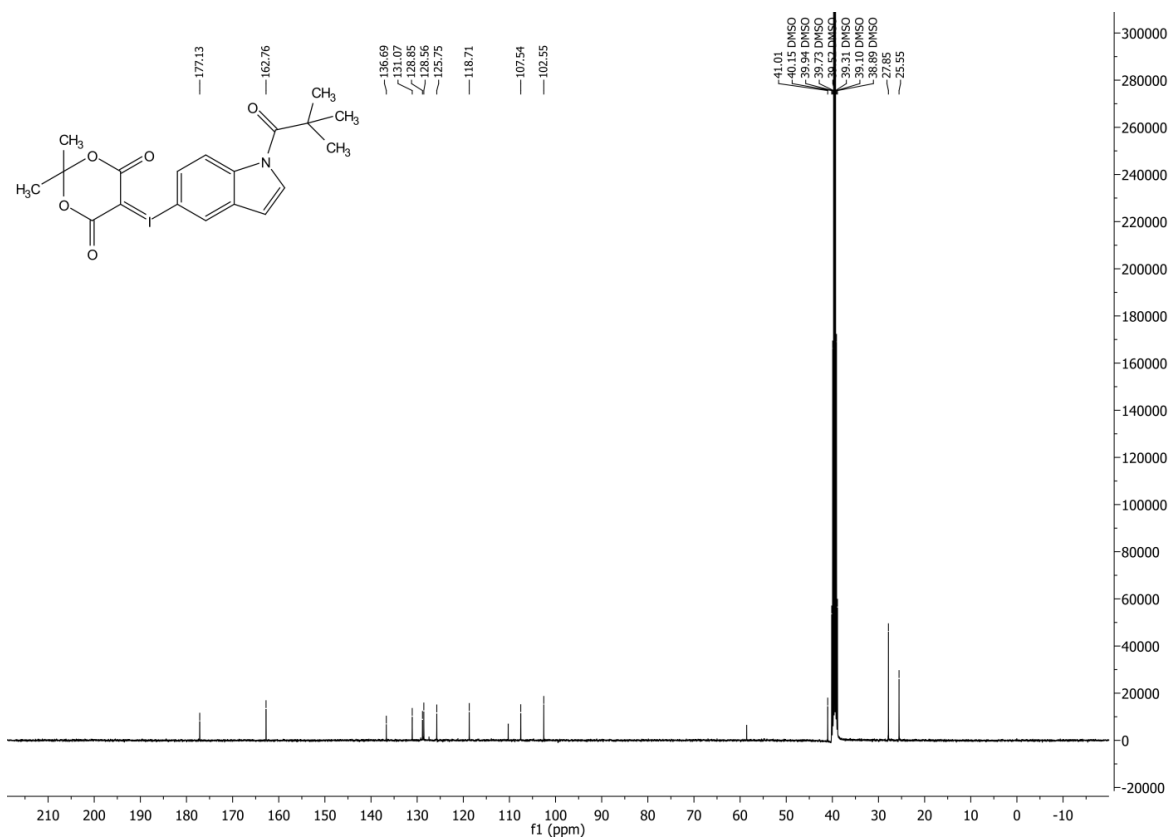


Figure LV <sup>13</sup>C-NMR of compound 8d)



**Figure LVI  $^1\text{H-NMR}$  of compound 9a)**



**Figure LVII  $^{13}\text{C-NMR}$  of compound 9a)**

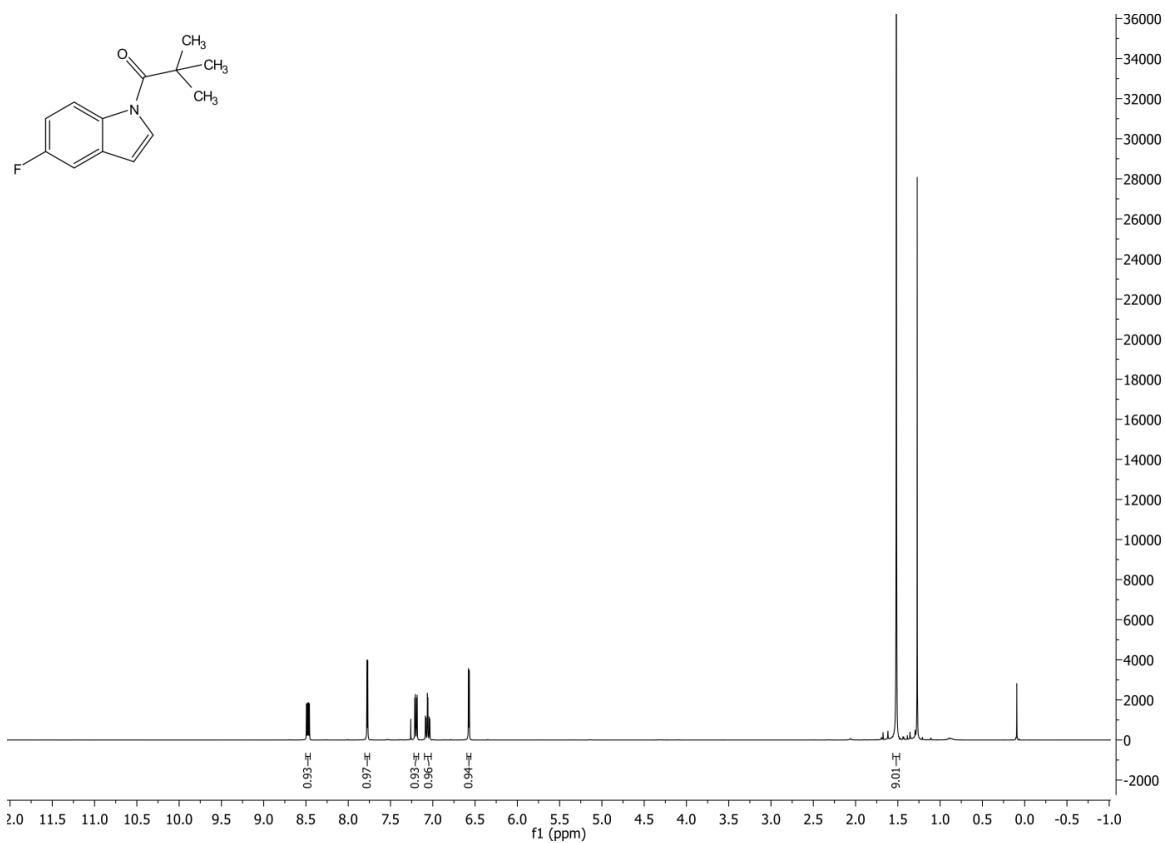


Figure LVIII  $^1\text{H-NMR}$  of compound 9b)

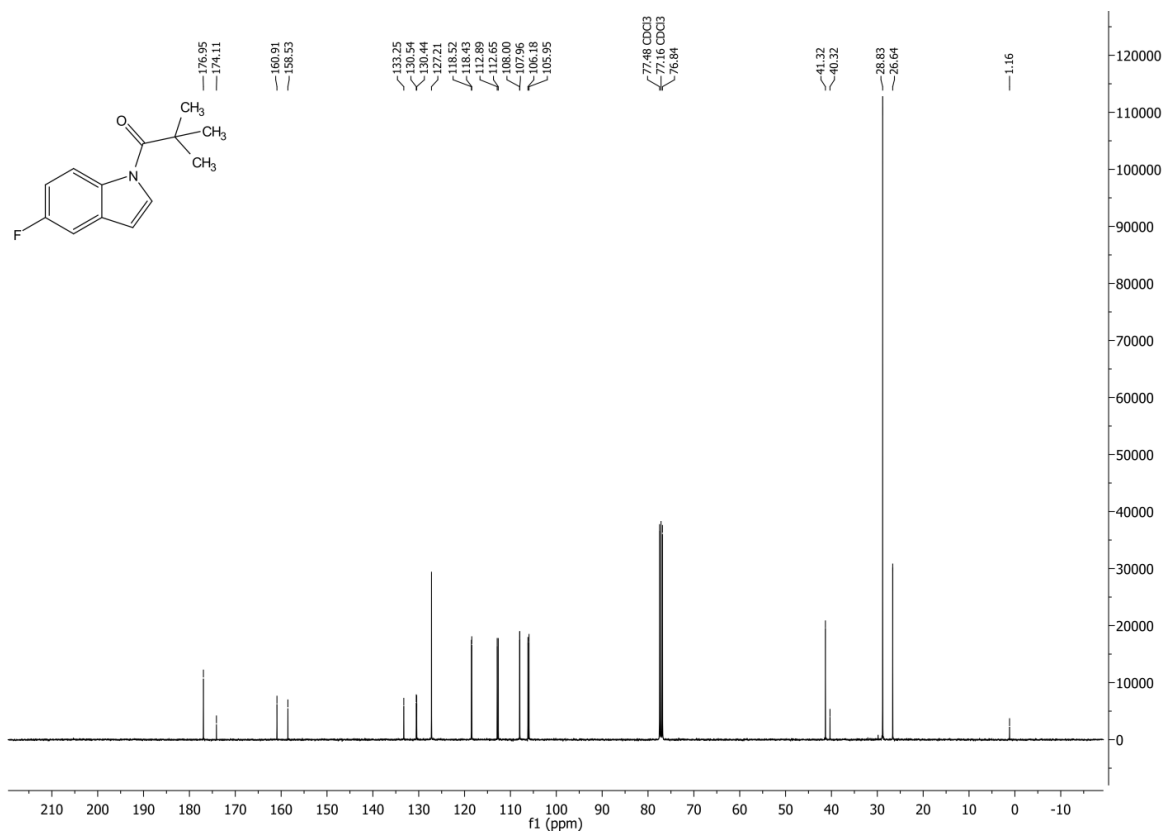


Figure LIX  $^{13}\text{C-NMR}$  of compound 9b)

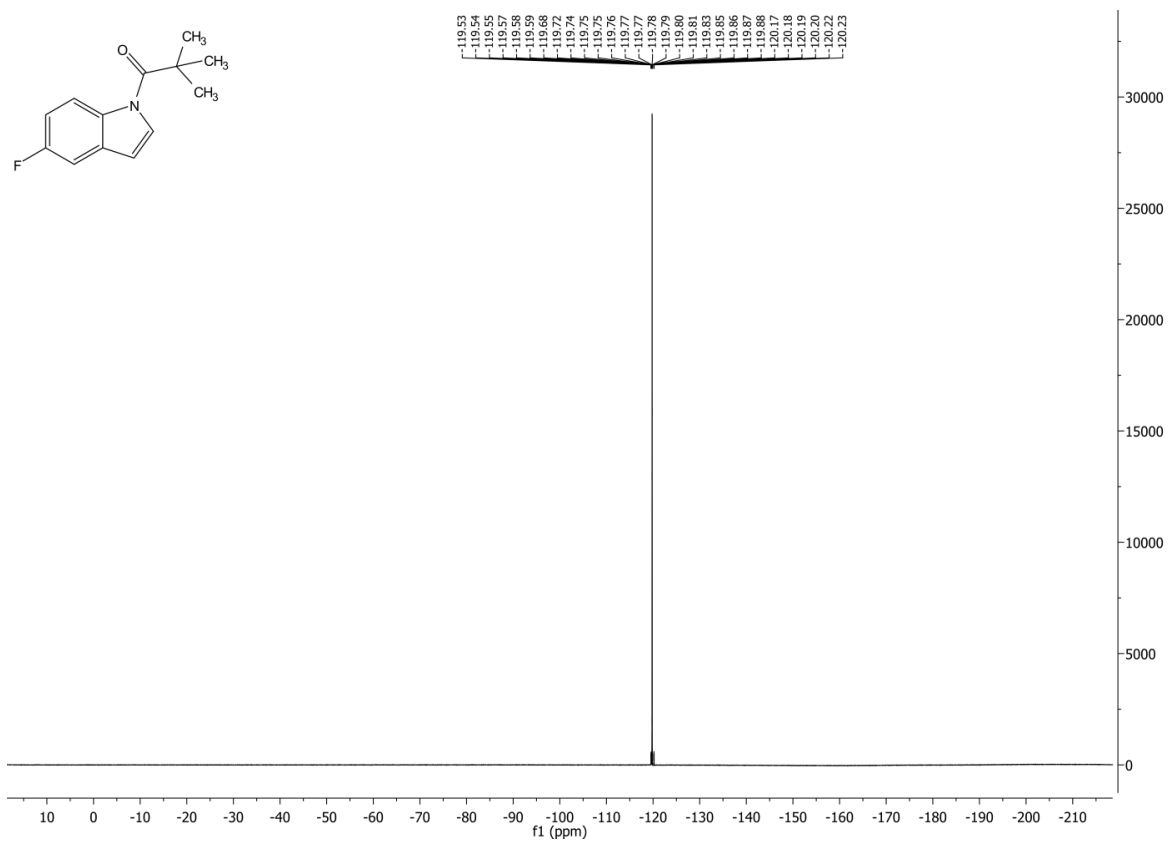


Figure LX  $^{19}\text{F}$ -NMR of compound 9b)

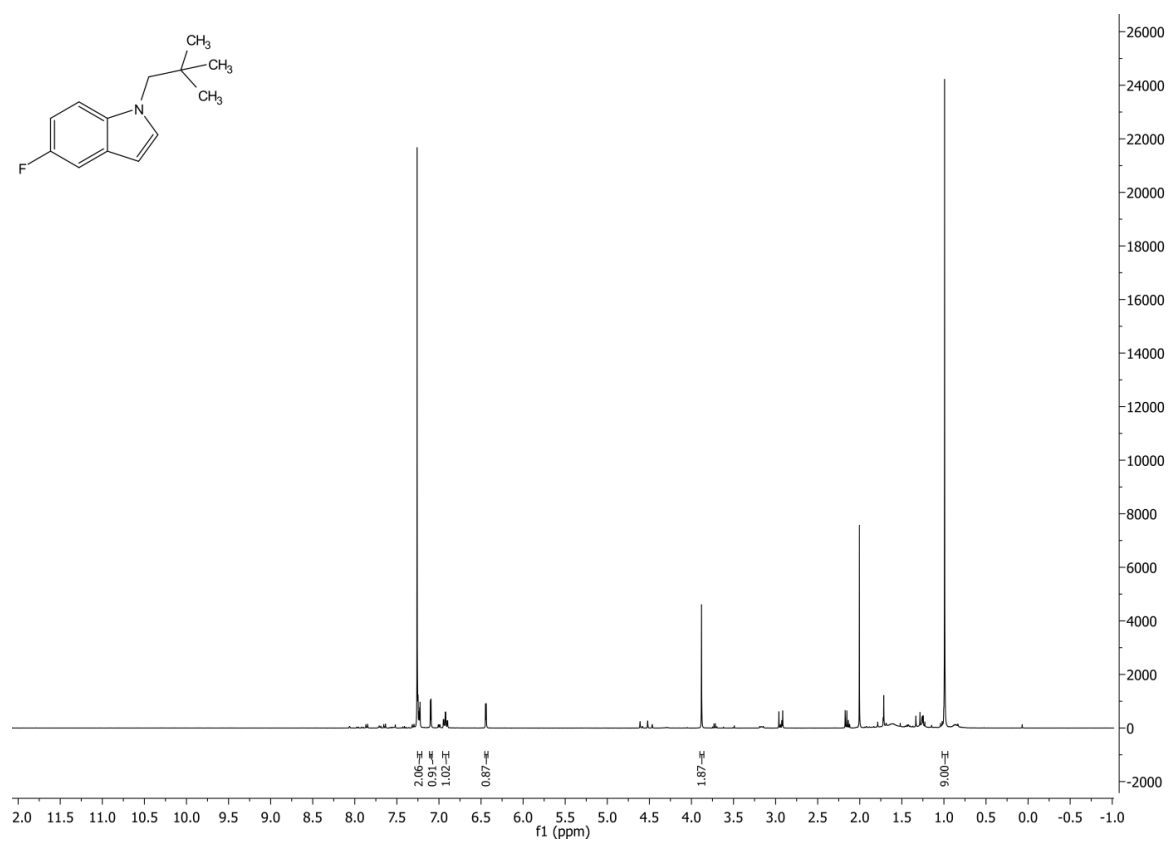


Figure LXI  $^1\text{H}$ -NMR of compound 9c)

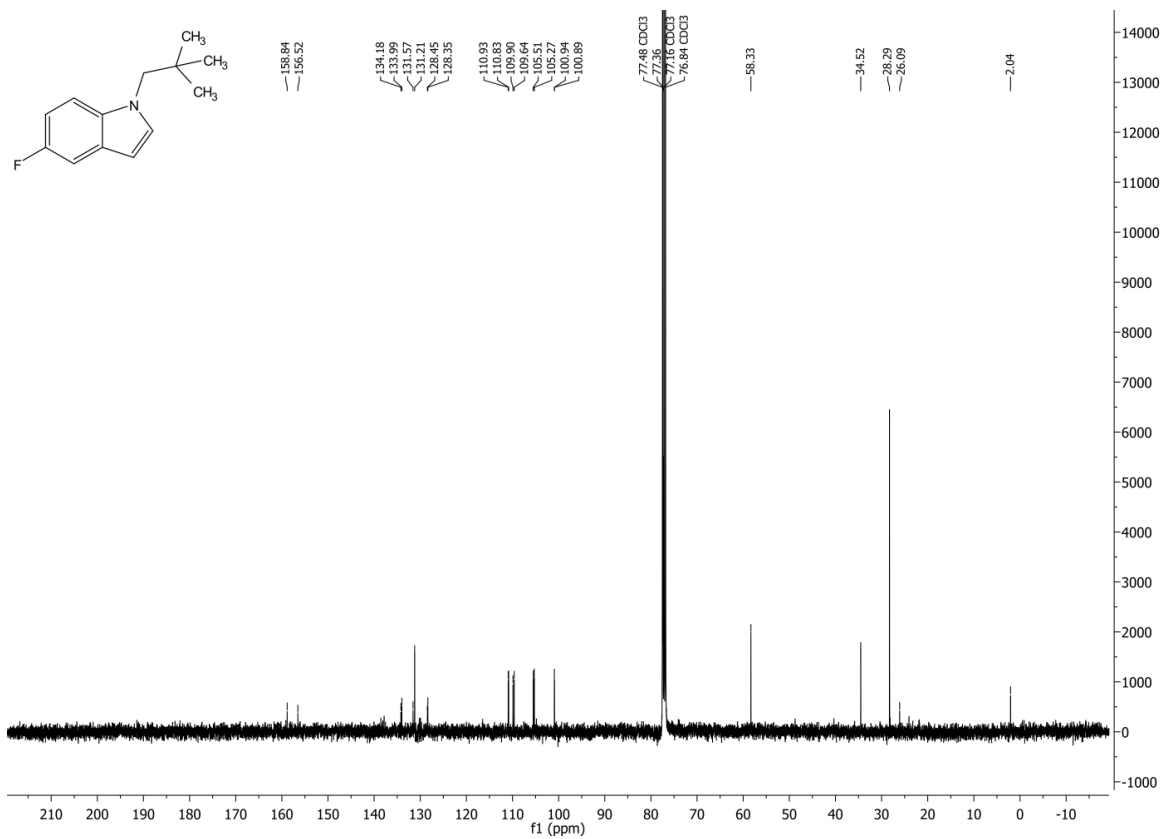


Figure LXII <sup>13</sup>C-NMR of compound 9c)

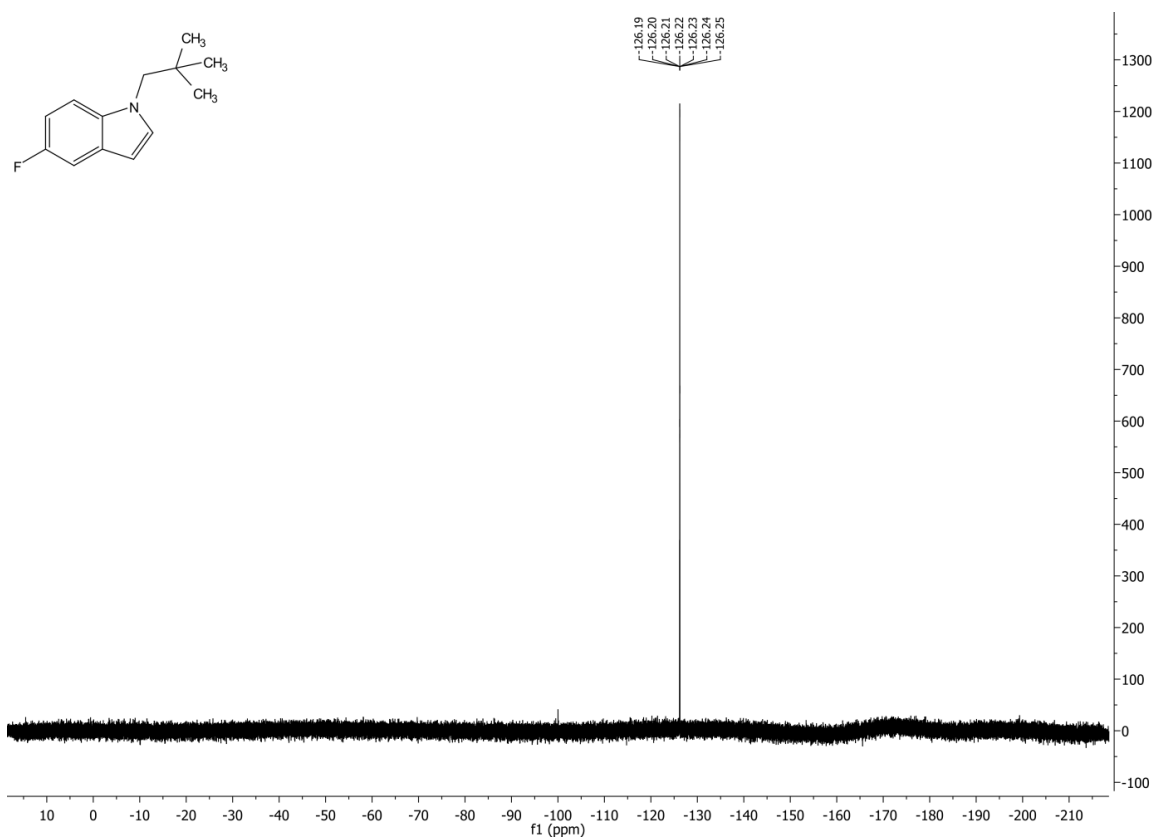


Figure LXIII <sup>19</sup>F-NMR of compound 9c)

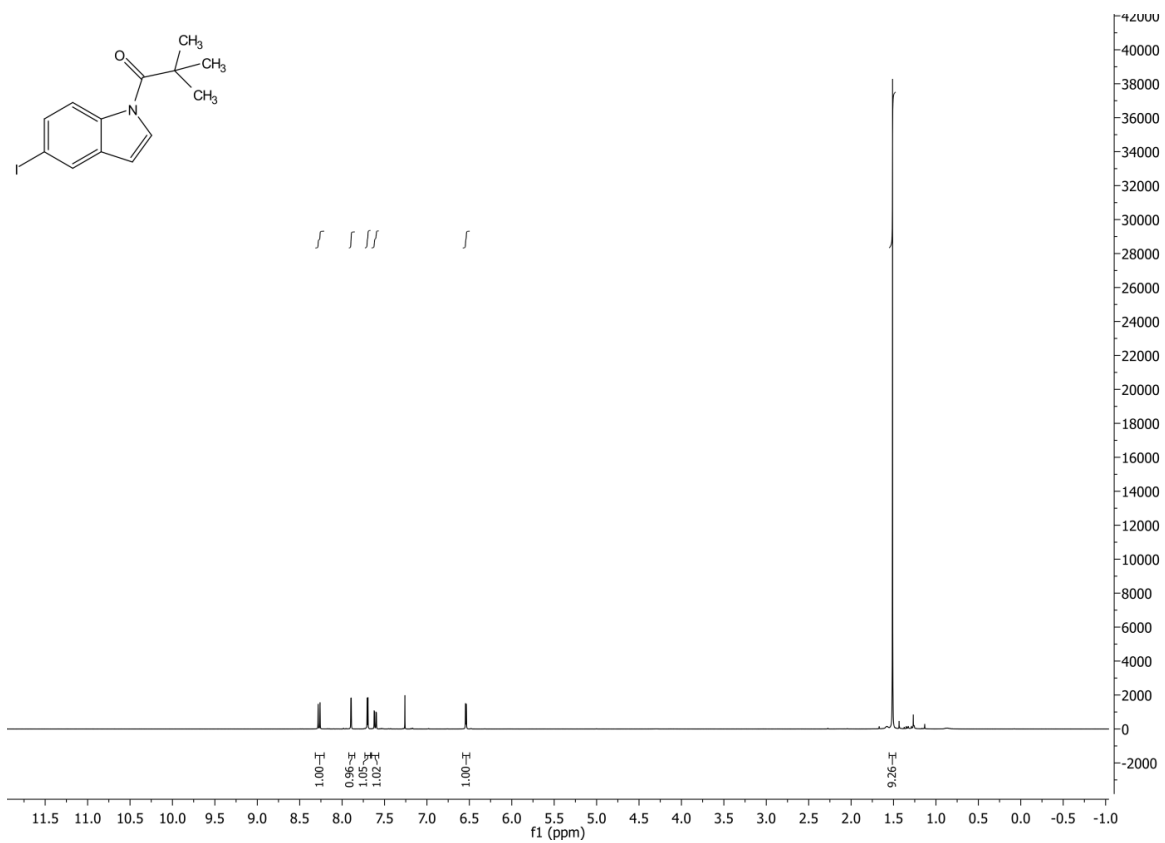


Figure LXIV <sup>1</sup>H-NMR of compound 9d)

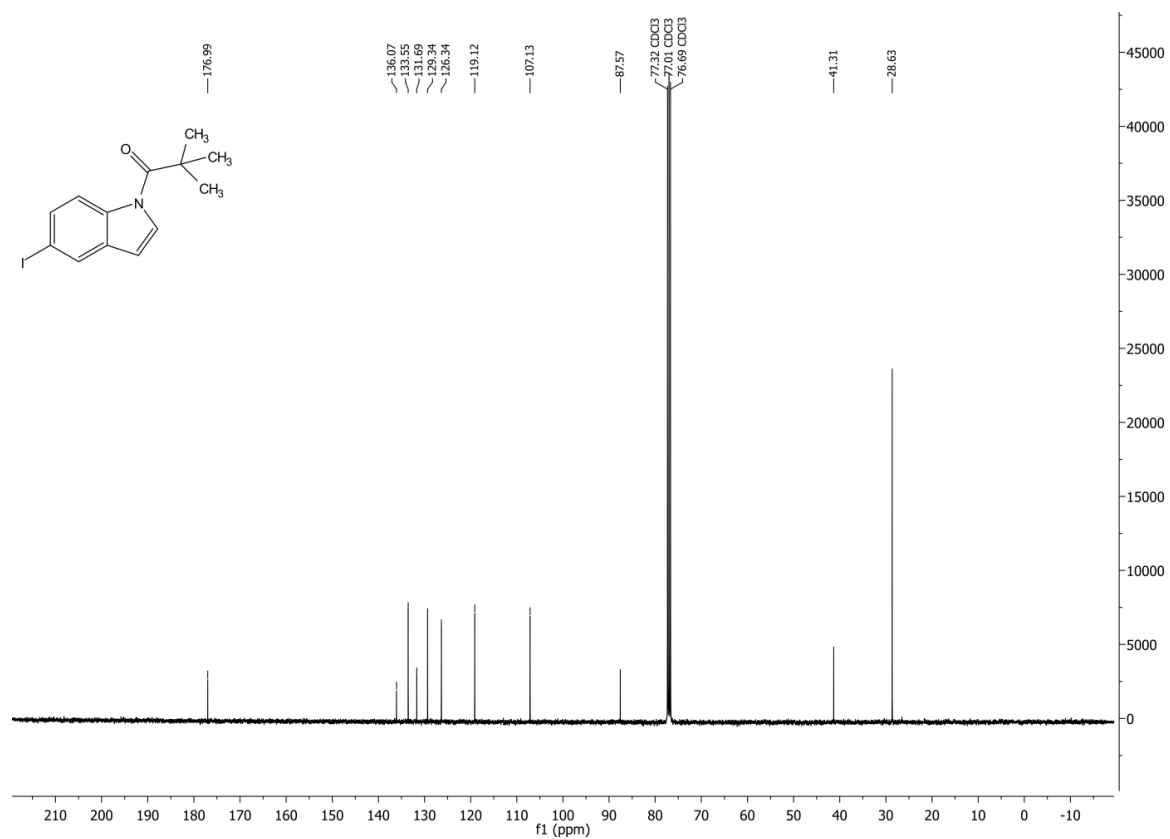


Figure LXV <sup>13</sup>C-NMR of compound 9d)

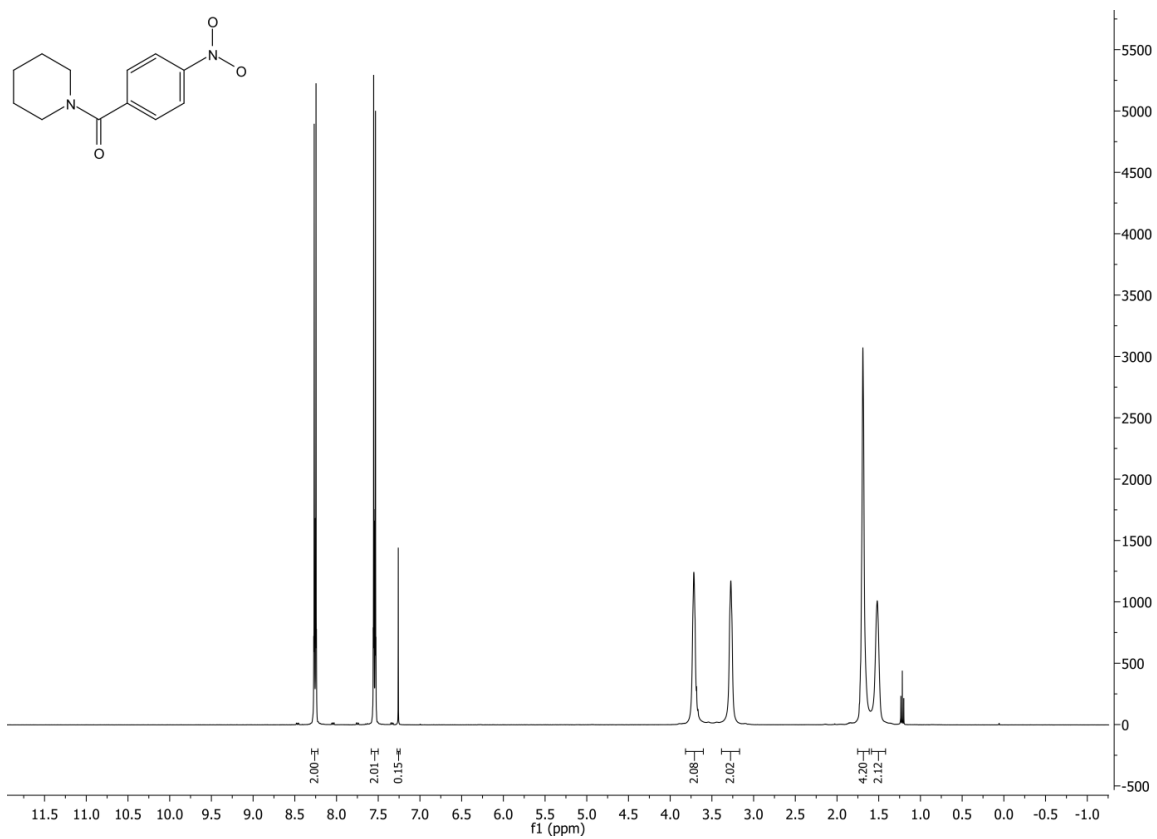


Figure LXVI <sup>1</sup>H-NMR of compound 43)

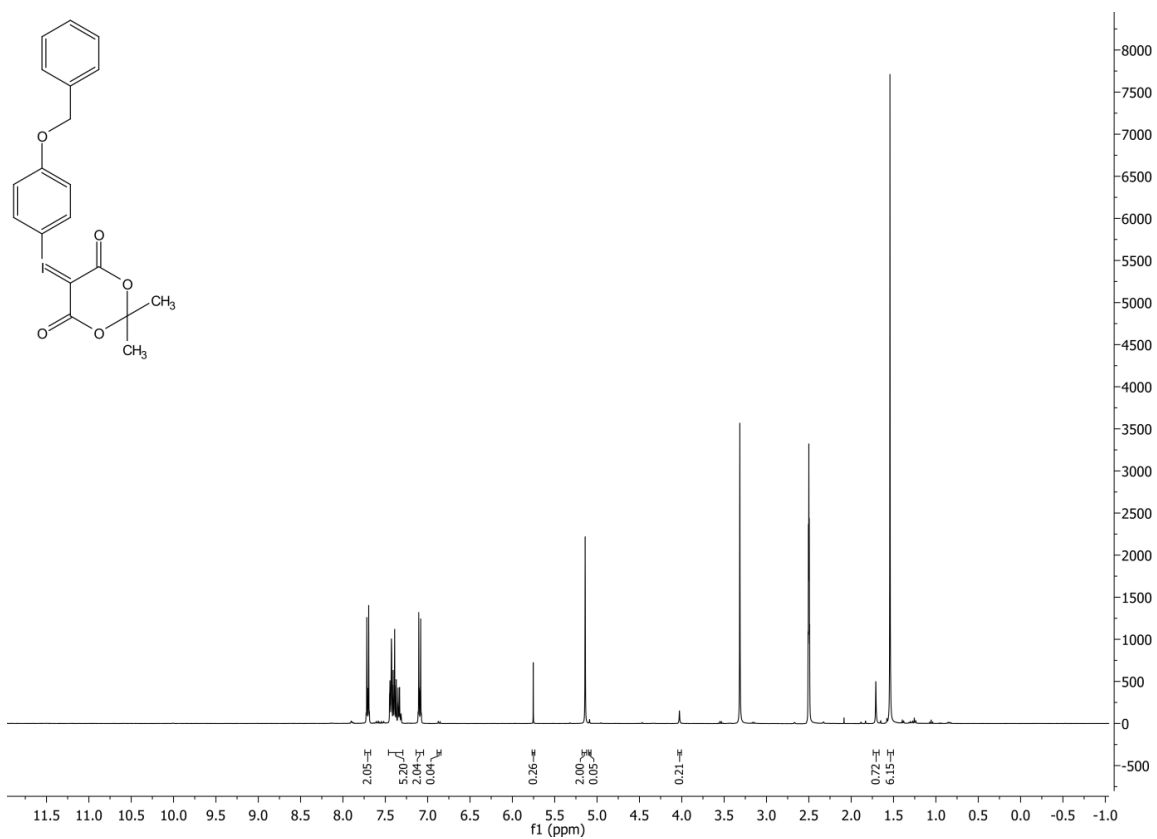


Figure LXVII <sup>1</sup>H-NMR of compound 38), freshly synthesized



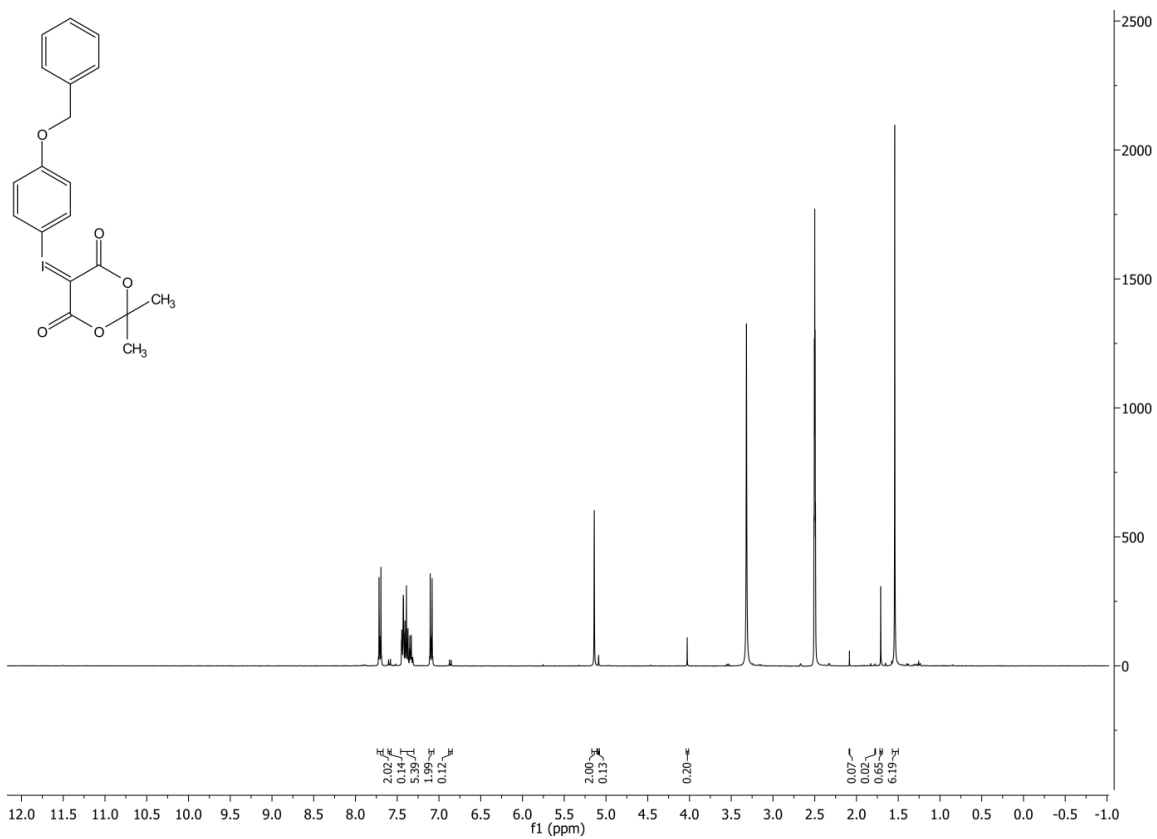


Figure LXVIII <sup>1</sup>H-NMR of compound 38), exposed to air, 1 week

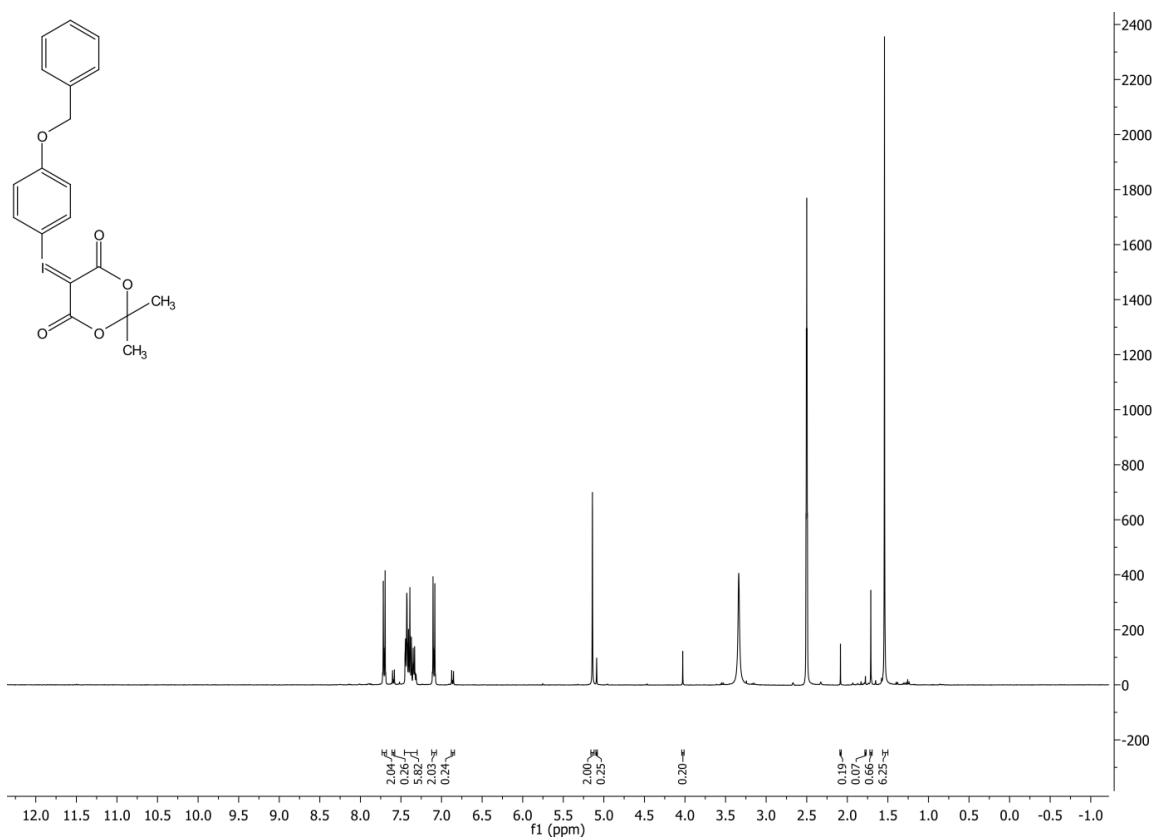


Figure LXIX <sup>1</sup>H-NMR of compound 38), exposed to air, 2 weeks

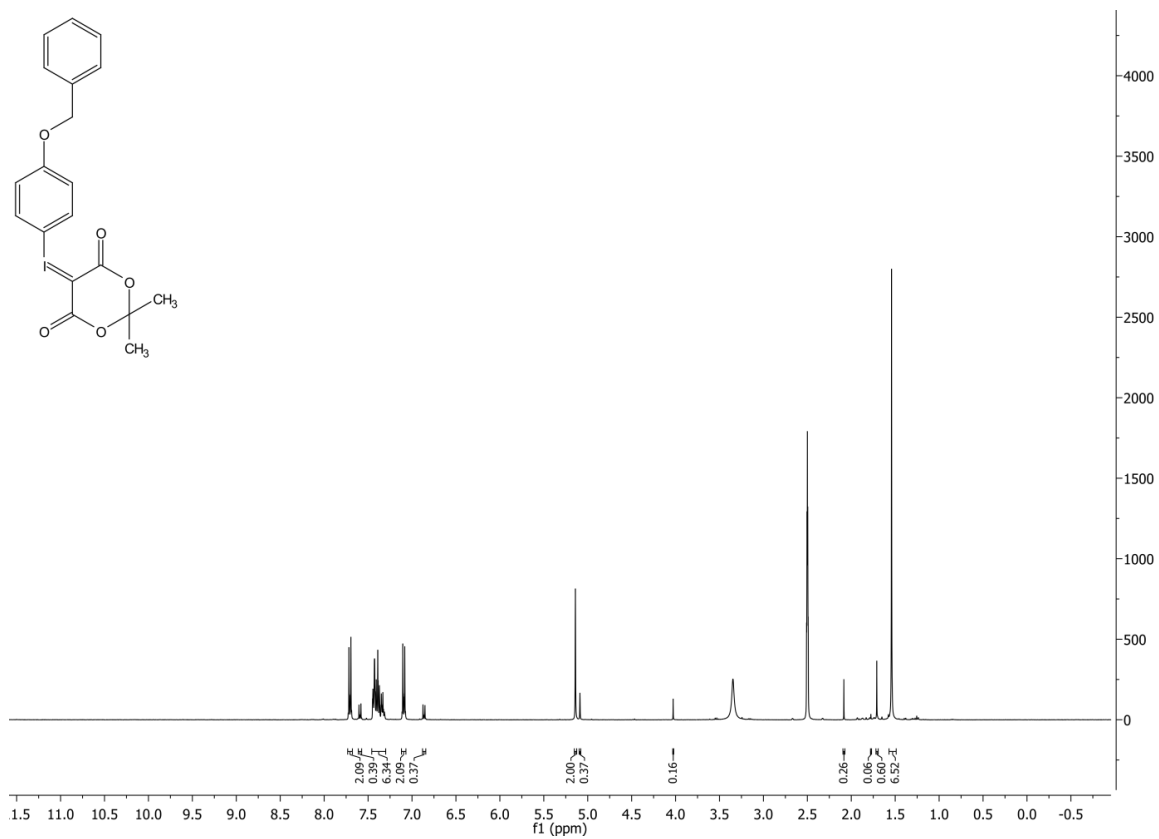


Figure LXX <sup>1</sup>H-NMR of compound 38), exposed to air, 4 weeks

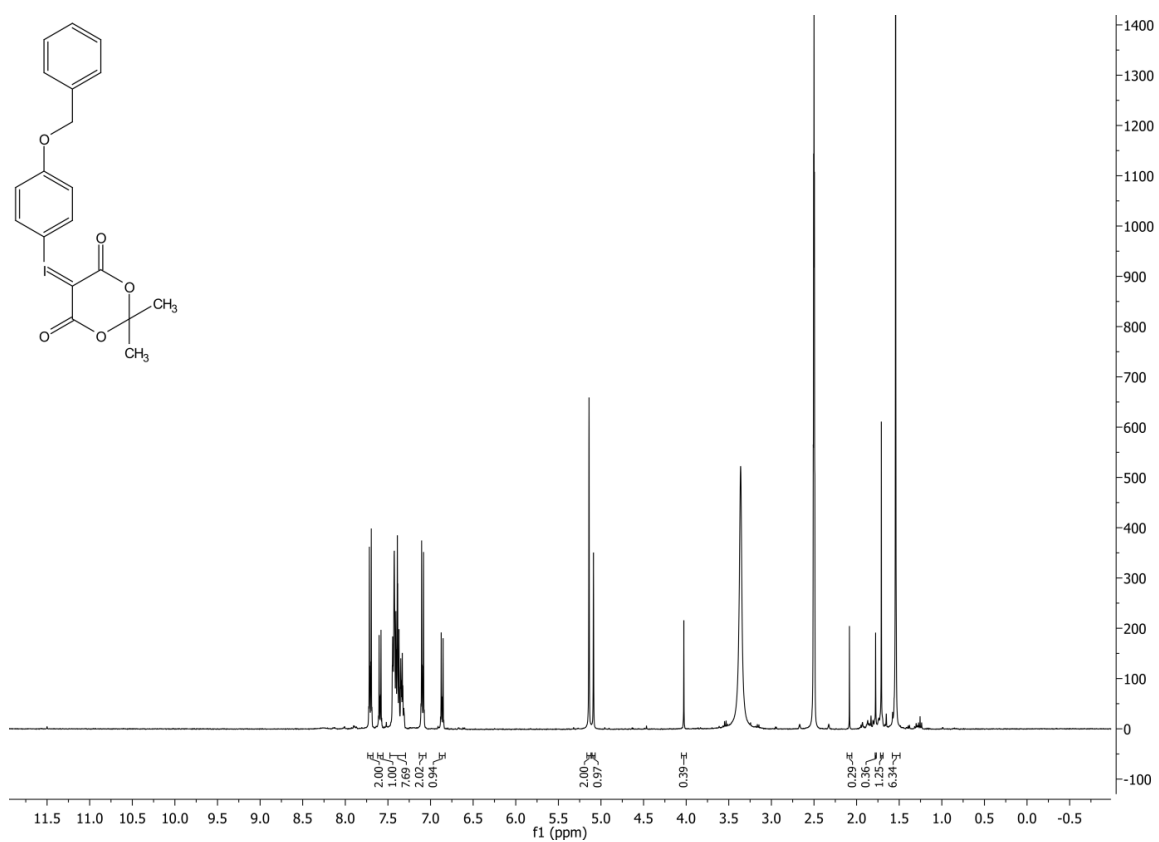


Figure LXXI <sup>1</sup>H-NMR of compound 38), exposed to air and light, 1 week

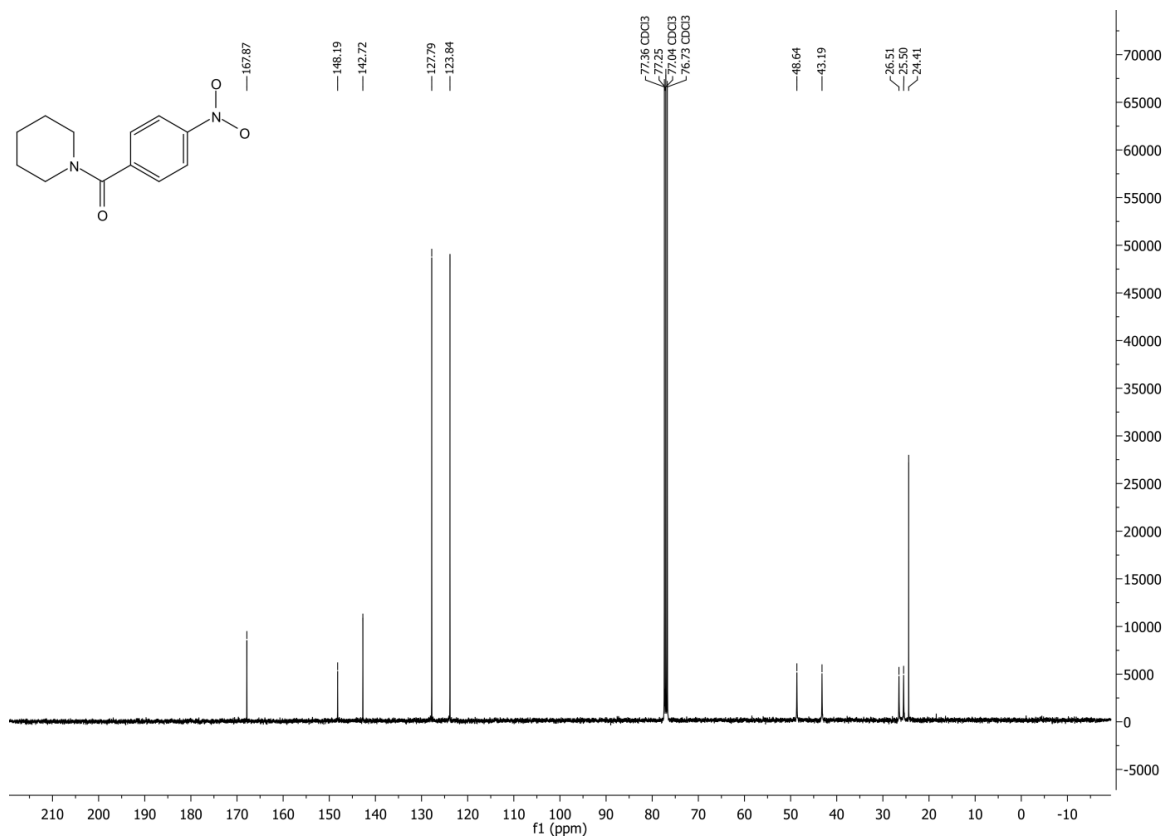


Figure LXXII <sup>1</sup>H-NMR of compound 43)

# Characterization of $^{18}\text{F}$ -arenes and -heteroarenes

Stationary phase: Bondapak C18 300x4 mm

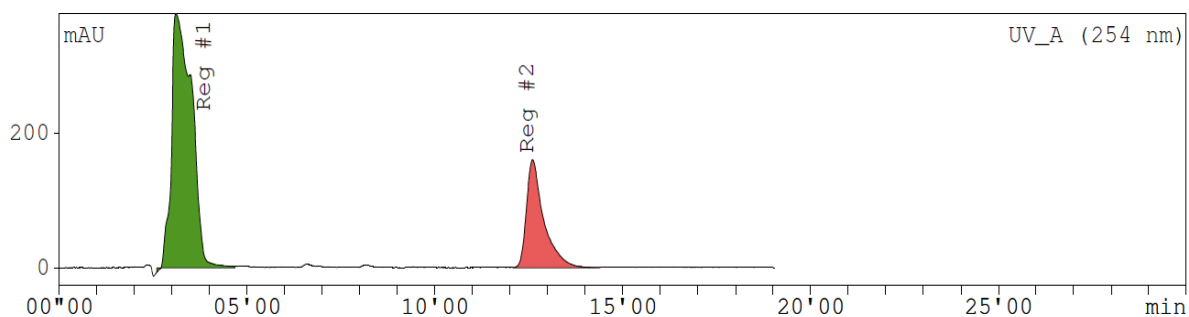
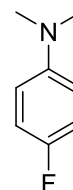
Radio detector: Raytest Gabi star

UV-monitor: Agilent 1100/1200 DAD

## 4-(fluoro)-N,N-dimethylaniline

*HPLC chromatography, UV monitor*

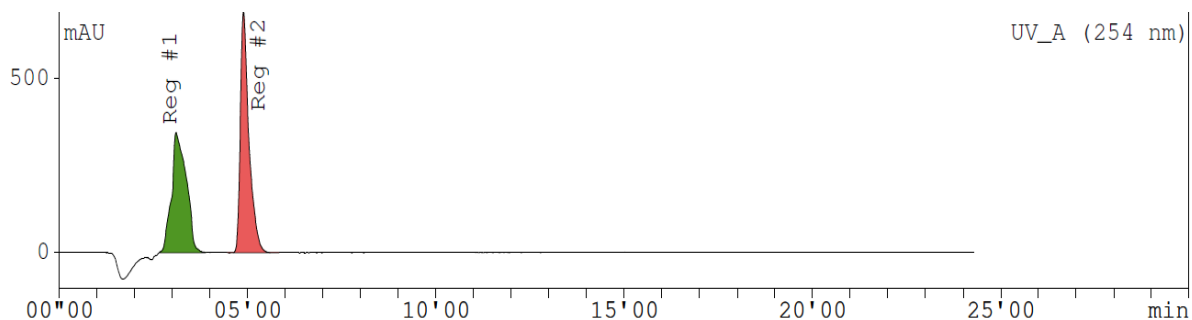
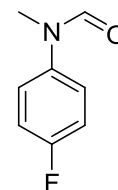
Mobile phase: 45% AcN, 55% 50 mM 3-morpholinopropane-1-sulfonic acid (MOPS), 1mL/min



## N-(4-fluorophenyl)-N-methylformamide

*HPLC chromatography, UV Monitor*

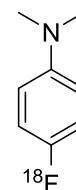
Mobile phase: 45% AcN, 55% 50 mM 3-morpholinopropane-1-sulfonic acid (MOPS), 1mL/min



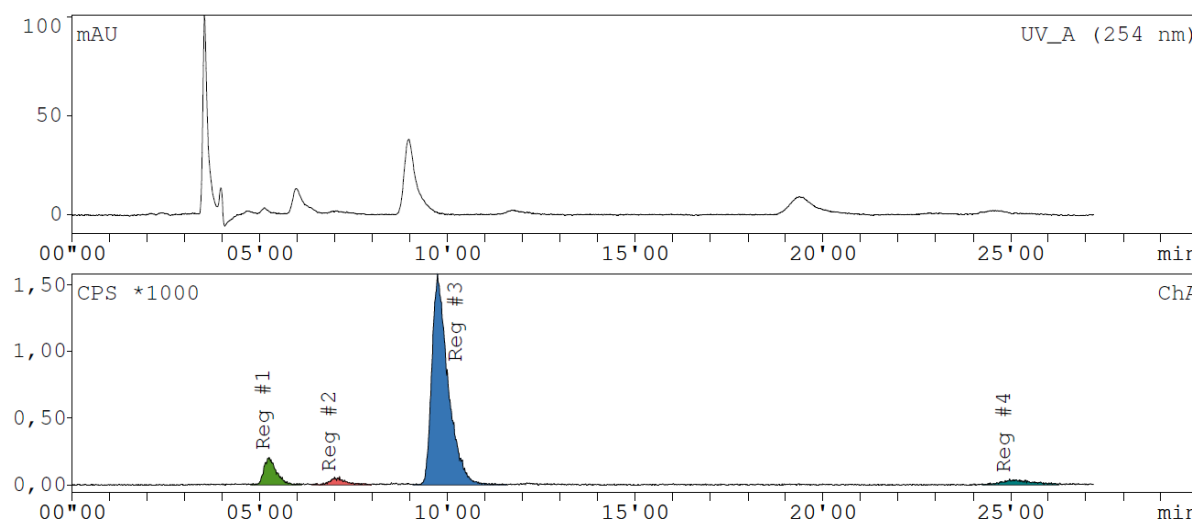
### 4-(<sup>18</sup>F-fluoro)-N,N-dimethylaniline

#### RadioHPLC chromatography

Mobile phase: 45% AcN, 55% 50 mM 3-morpholinopropane-1-sulfonic acid (MOPS), 1mL/min



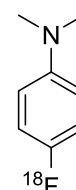
Reaction conditions: 5 mol% NHC, THF, 5 Eq. 9 BBN 90 °C, 10 min



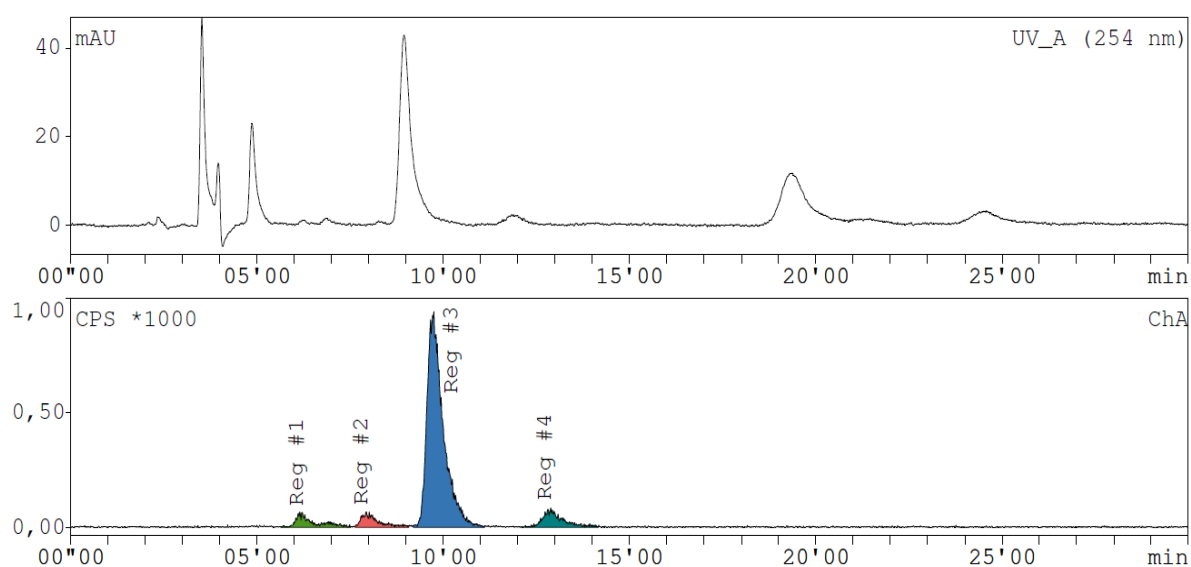
### 4-(<sup>18</sup>F-fluoro)-N,N-dimethylaniline

#### RadioHPLC chromatography

Mobile phase: 45% AcN, 55% 50 mM 3-morpholinopropane-1-sulfonic acid (MOPS), 1mL/min



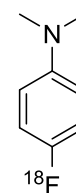
Reaction conditions: 5 mol% NHC, THF, 5 Eq. BH<sub>3</sub> • SMe<sub>2</sub> 90 °C, 10 min



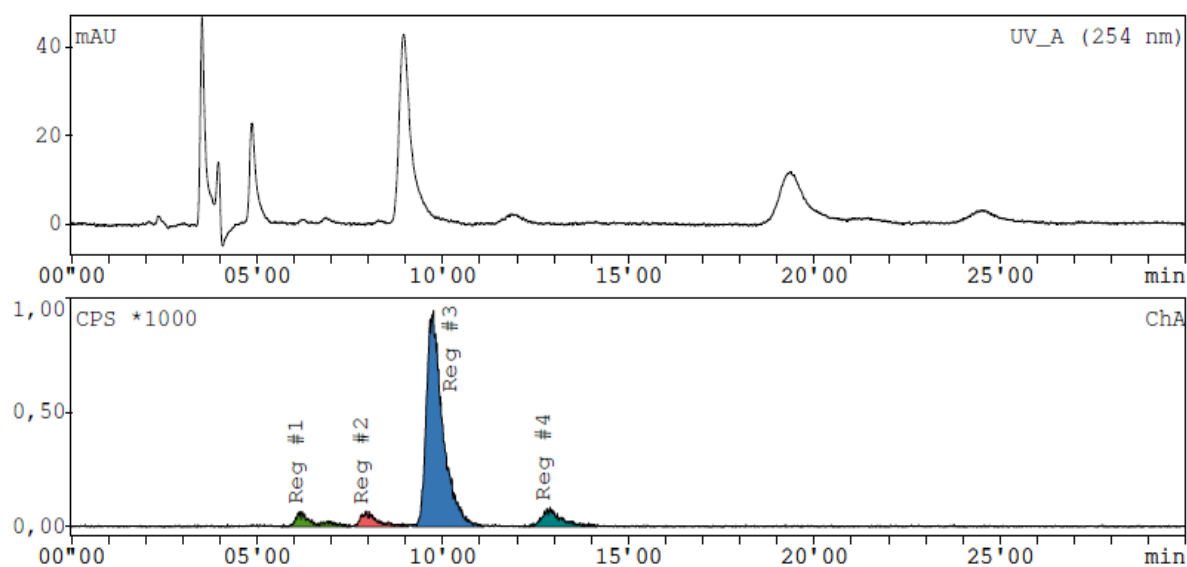
## 4-(<sup>18</sup>F-fluoro)-N,N-dimethylaniline

### RadioHPLC chromatography

Mobile phase: 45% AcN, 55% 50 mM 3-morpholinopropane-1-sulfonic acid (MOPS), 1mL/min



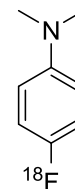
Reaction conditions: 5 mol% PPh<sub>3</sub>, THF, 5 Eq. 9 BBN, 90 °C, 10 min



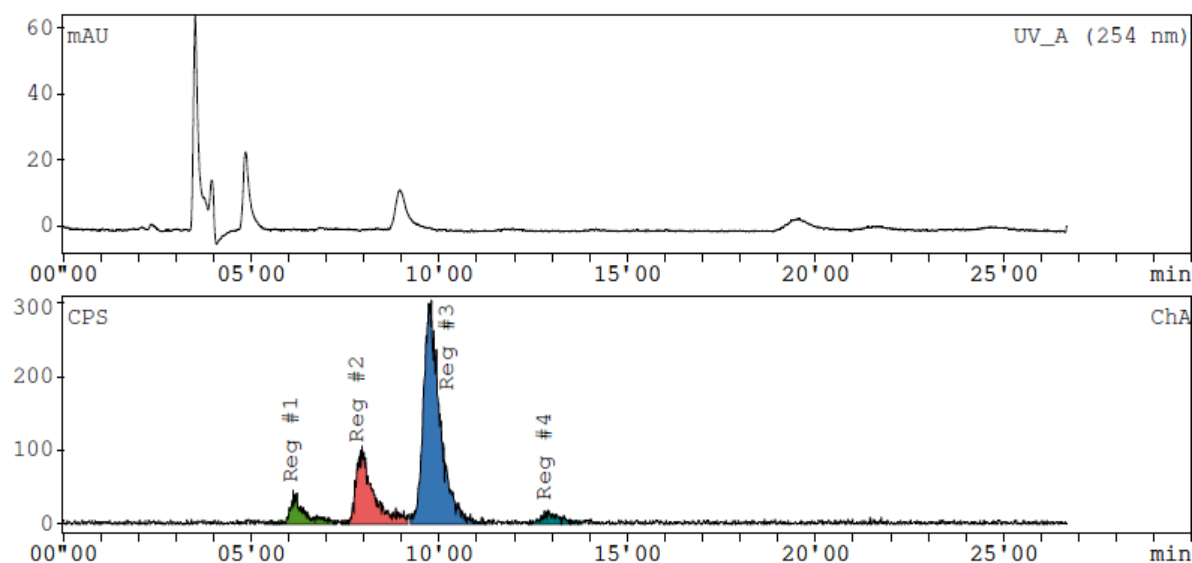
## 4-(<sup>18</sup>F-fluoro)-N,N-dimethylaniline

### RadioHPLC chromatography

Mobile phase: 45% AcN, 55% 50 mM 3-morpholinopropane-1-sulfonic acid (MOPS), 1mL/min



Reaction conditions: 5 mol% P(NMe<sub>2</sub>)<sub>3</sub>, THF, 5 Eq. 9 BBN, 90 °C, 10 min

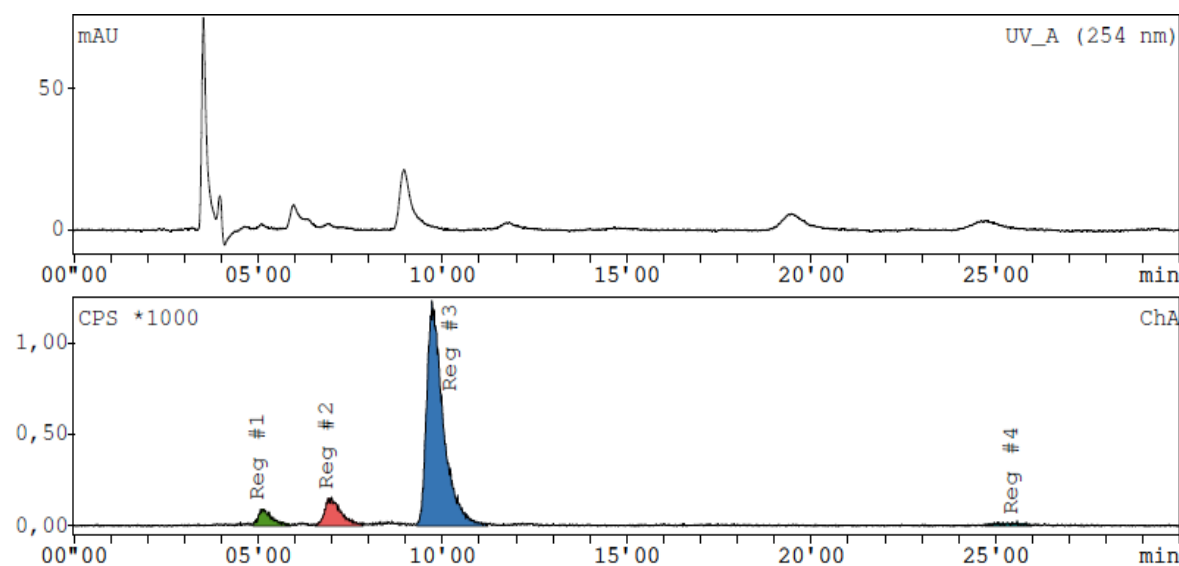
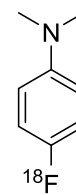


#### 4-(<sup>18</sup>F-fluoro)-N,N-dimethylaniline

##### RadioHPLC chromatography

Mobile phase: 45% AcN, 55% 50 mM 3-morpholinopropane-1-sulfonic acid (MOPS), 1mL/min

Reaction conditions: 5 mol% VB<sup>iPr</sup>, THF, 5 Eq. 9 BBN, 90 °C, 10 min

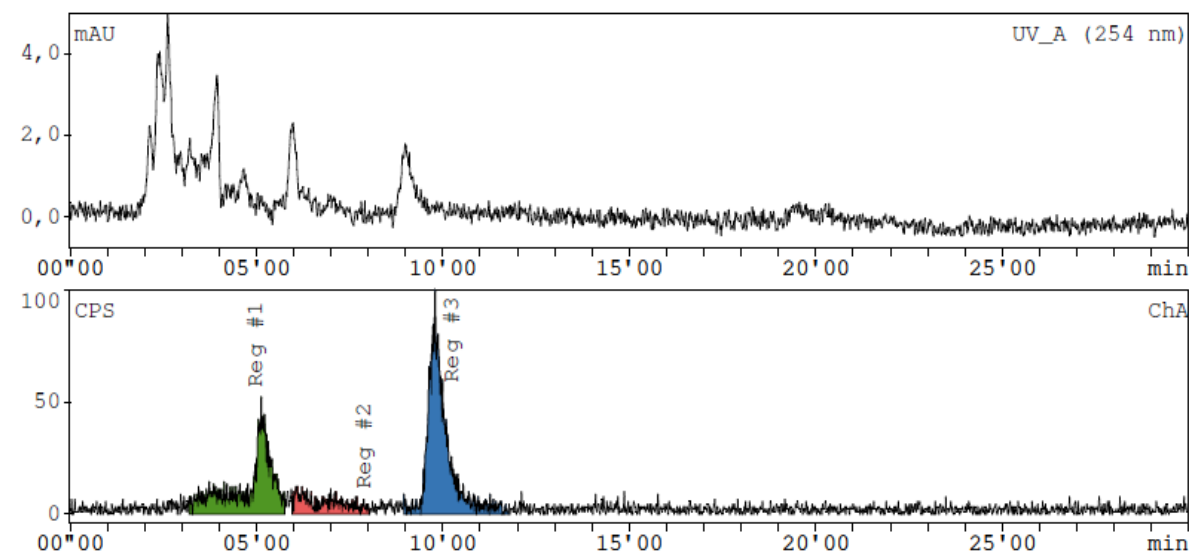
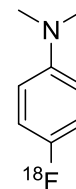


#### 4-(<sup>18</sup>F-fluoro)-N,N-dimethylaniline

##### RadioHPLC chromatography

Mobile phase: 45% AcN, 55% 50 mM 3-morpholinopropane-1-sulfonic acid (MOPS), 1mL/min

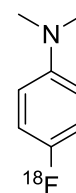
Reaction conditions: DCE, 5 Eq. 9 BBN, 90 °C, 10 min



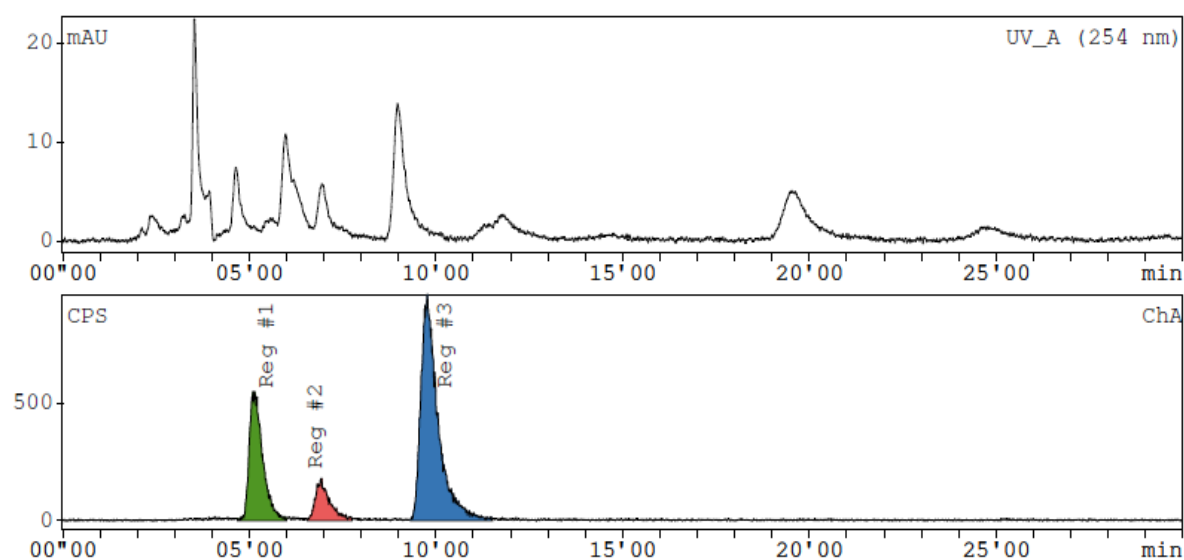
#### 4-(<sup>18</sup>F-fluoro)-N,N-dimethylaniline

##### RadioHPLC chromatography

Mobile phase: 45% AcN, 55% 50 mM 3-morpholinopropane-1-sulfonic acid (MOPS), 1mL/min



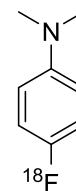
Reaction conditions: AcN, 5 Eq. 9 BBN, 90 °C, 10 min



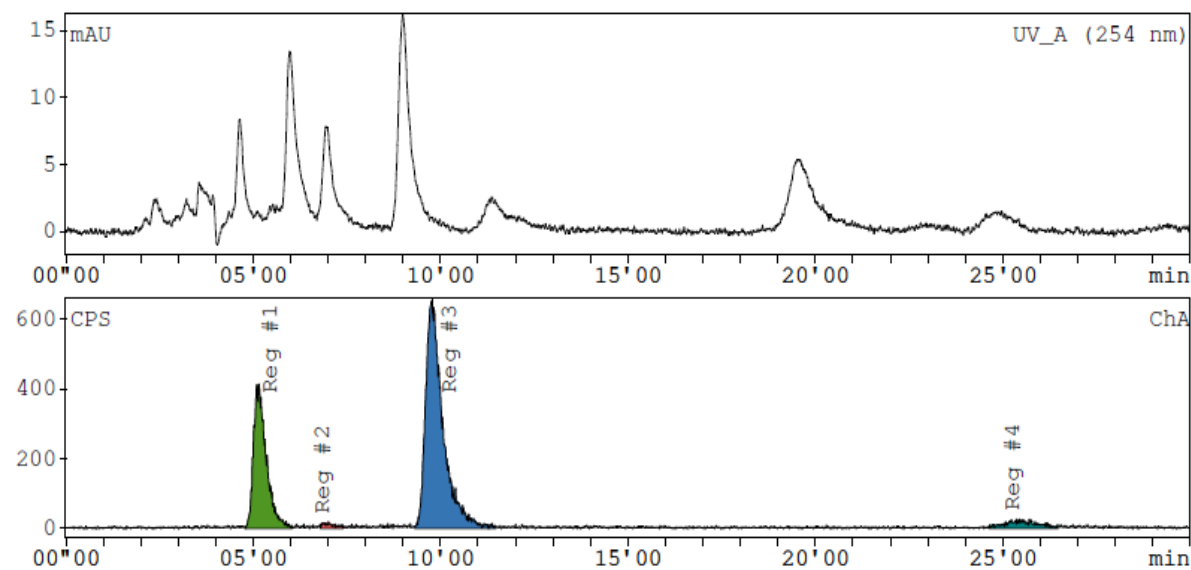
#### 4-(<sup>18</sup>F-fluoro)-N,N-dimethylaniline

##### RadioHPLC chromatography

Mobile phase: 45% AcN, 55% 50 mM 3-morpholinopropane-1-sulfonic acid (MOPS), 1mL/min



Reaction conditions: DME, 5 Eq. 9 BBN, 90 °C, 10 min



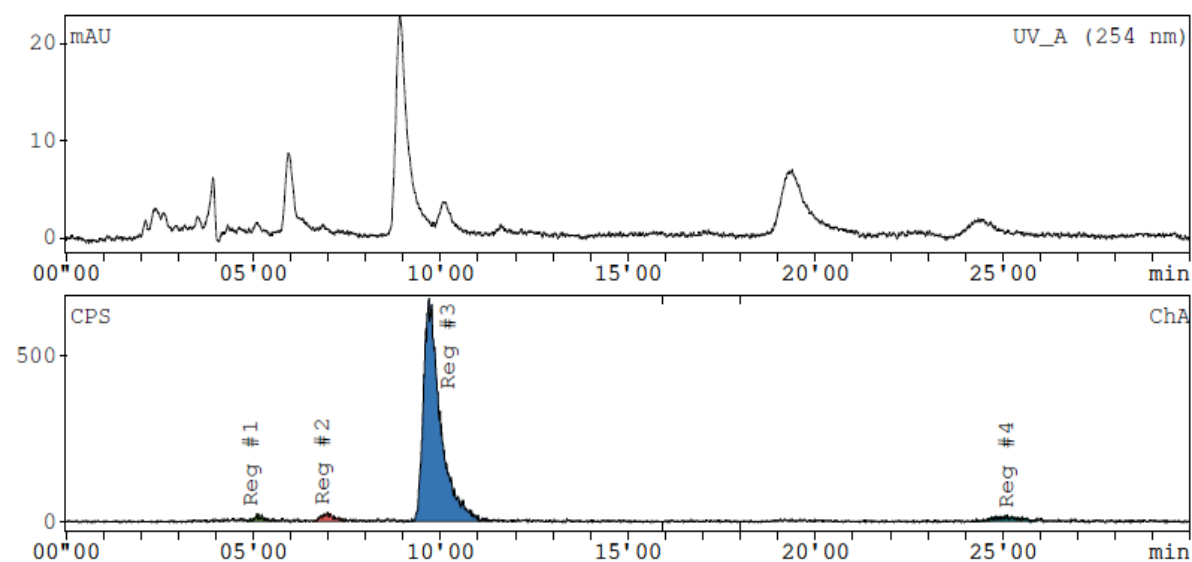
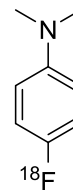


#### 4-(<sup>18</sup>F-fluoro)-N,N-dimethylaniline

##### RadioHPLC chromatography

Mobile phase: 45% AcN, 55% 50 mM 3-morpholinopropane-1-sulfonic acid (MOPS), 1mL/min

Reaction conditions: iPr<sub>2</sub>O, 5 Eq. 9 BBN, 90 °C, 10 min

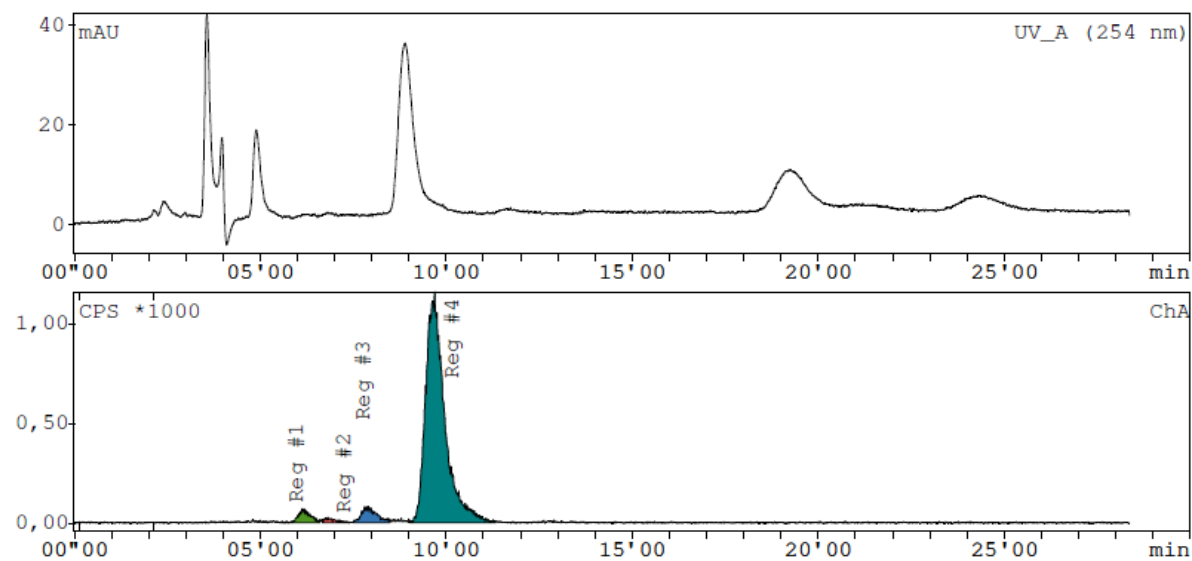
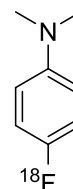


#### 4-(<sup>18</sup>F-fluoro)-N,N-dimethylaniline

##### RadioHPLC chromatography

Mobile phase: 45% AcN, 55% 50 mM 3-morpholinopropane-1-sulfonic acid (MOPS), 1mL/min

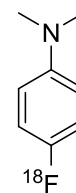
Reaction conditions: THF, 5 Eq. BH<sub>3</sub> • SMe<sub>2</sub>, 90 °C, 10 min



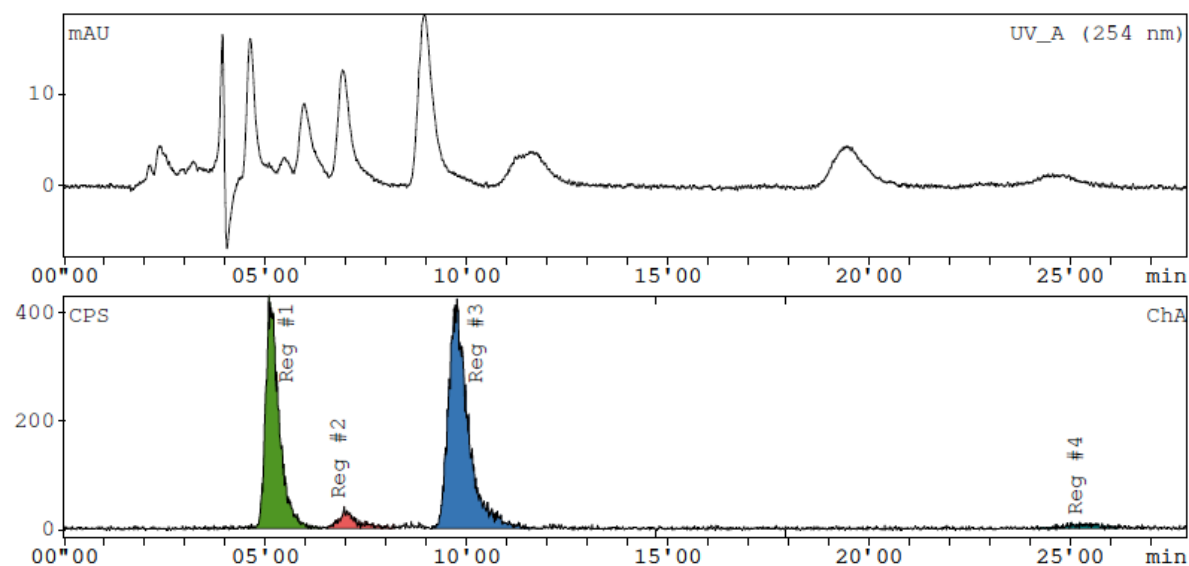
#### 4-(<sup>18</sup>F-fluoro)-N,N-dimethylaniline

##### RadioHPLC chromatography

Mobile phase: 45% AcN, 55% 50 mM 3-morpholinopropane-1-sulfonic acid (MOPS), 1mL/min



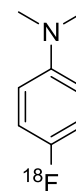
Reaction conditions: THF, 3 Eq. 9 BBN, 90 °C, 10 min



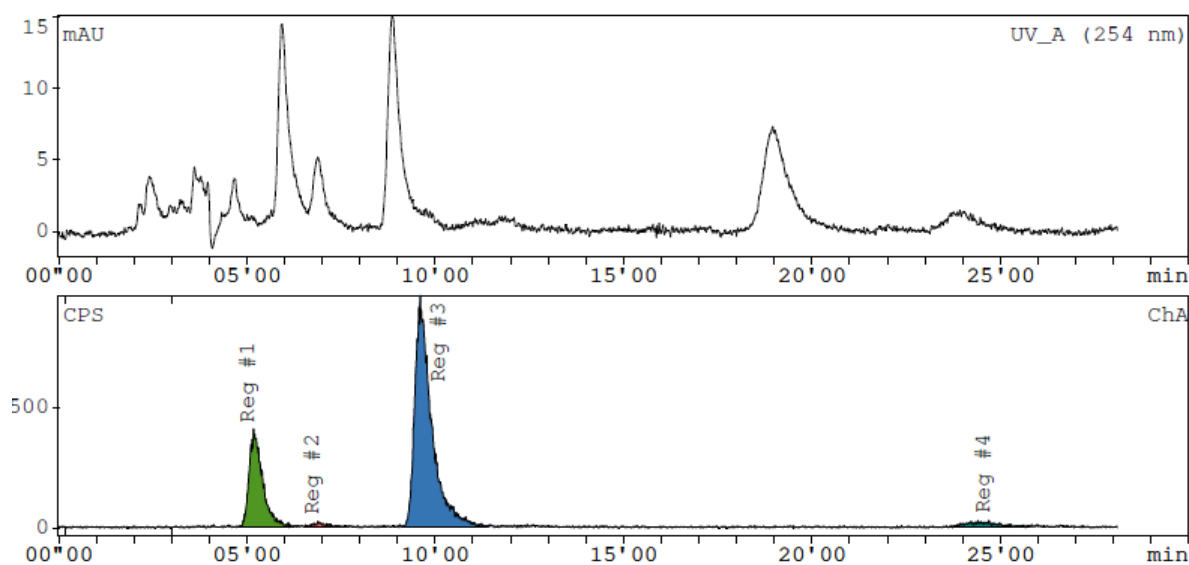
#### 4-(<sup>18</sup>F-fluoro)-N,N-dimethylaniline

##### RadioHPLC chromatography

Mobile phase: 45% AcN, 55% 50 mM 3-morpholinopropane-1-sulfonic acid (MOPS), 1mL/min



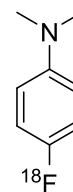
Reaction conditions: DME, 5 Eq. 9 BBN, 75 °C, 10 min



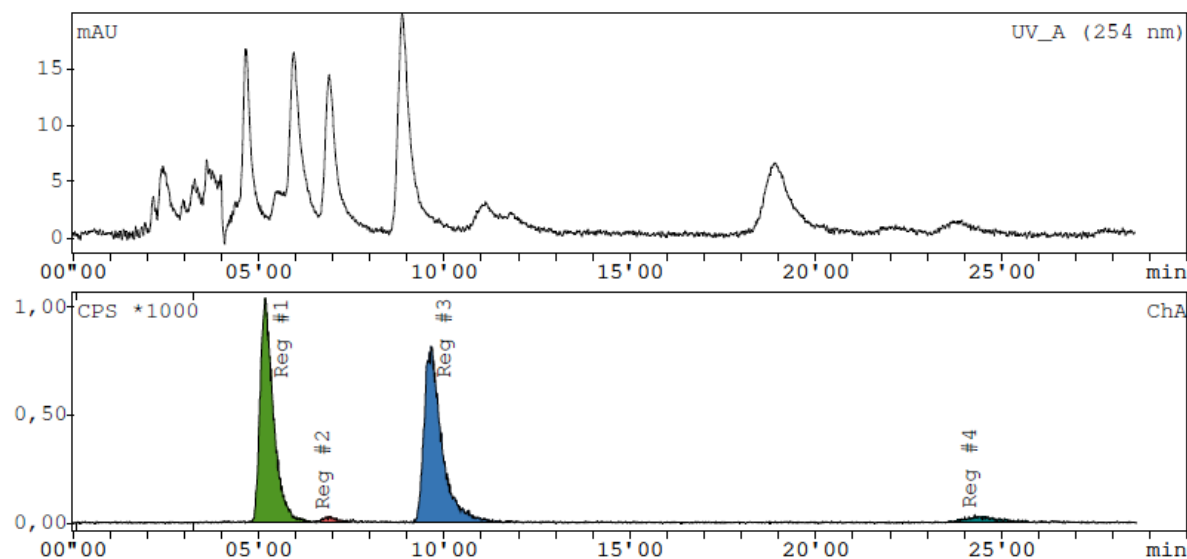
### 4-(<sup>18</sup>F-fluoro)-N,N-dimethylaniline

#### RadioHPLC chromatography

Mobile phase: 45% AcN, 55% 50 mM 3-morpholinopropane-1-sulfonic acid (MOPS), 1mL/min



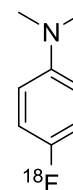
Reaction conditions: DME, 5 Eq. 9 BBN, 60 °C, 10 min



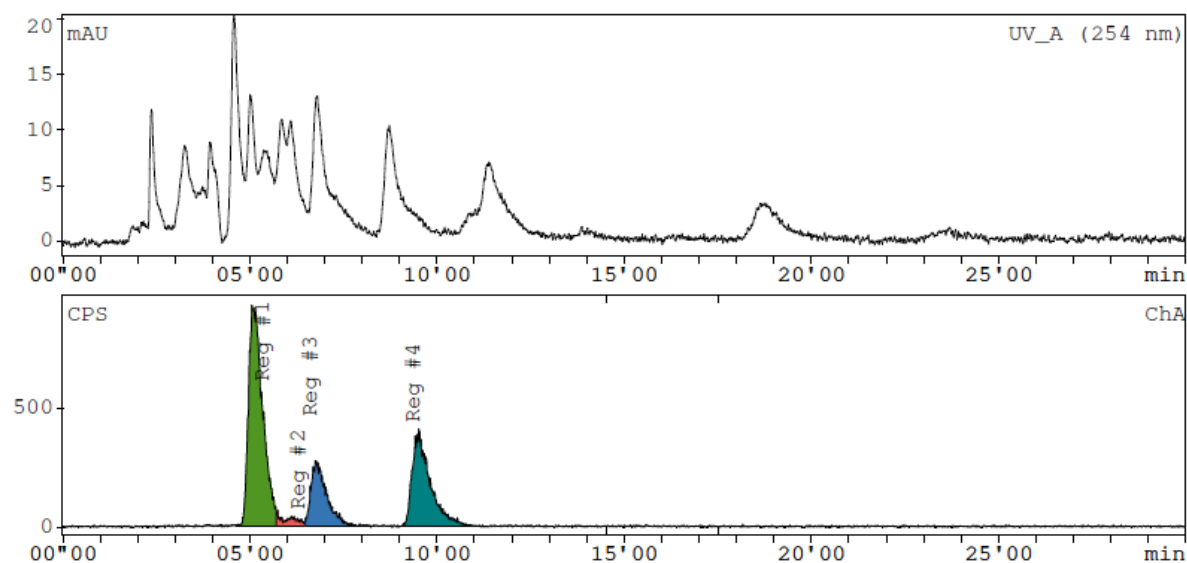
### 4-(<sup>18</sup>F-fluoro)-N,N-dimethylaniline

#### RadioHPLC chromatography

Mobile phase: 45% AcN, 55% 50 mM 3-morpholinopropane-1-sulfonic acid (MOPS), 1mL/min



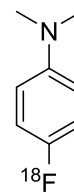
Reaction conditions: THF, 5 Eq. 9 BBN, 10 Eq. TMEDA, 90 °C, 10 min



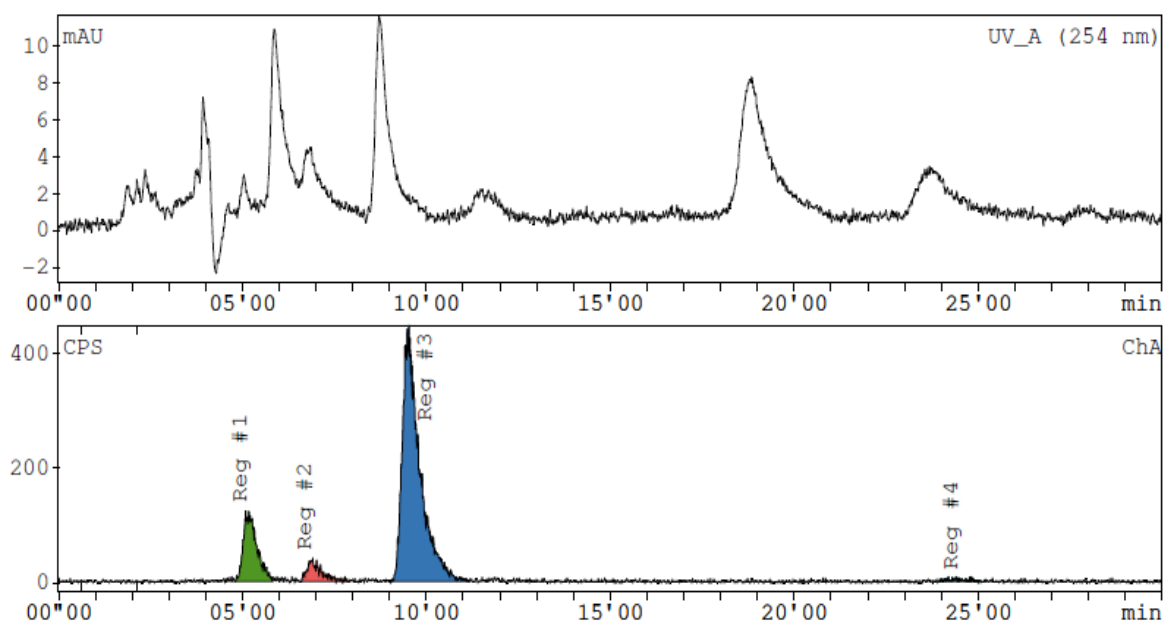
### 4-(<sup>18</sup>F-fluoro)-N,N-dimethylaniline

#### RadioHPLC chromatography

Mobile phase: 45% AcN, 55% 50 mM 3-morpholinopropane-1-sulfonic acid (MOPS), 1mL/min



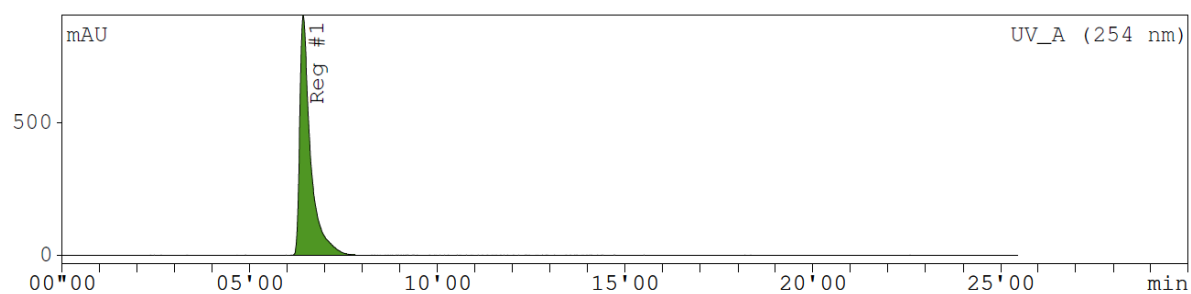
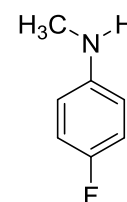
Reaction conditions: THF, 5 Eq. 9 BBN, 10 Eq. DME, 90 °C, 10 min



### 4-fluoro-N-methylaniline

#### HPLC chromatography, UV monitor

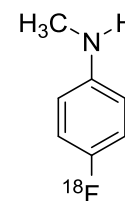
Mobile phase: 45% AcN, 55% 50 mM 3-morpholinopropane-1-sulfonic acid (MOPS), 1mL/min



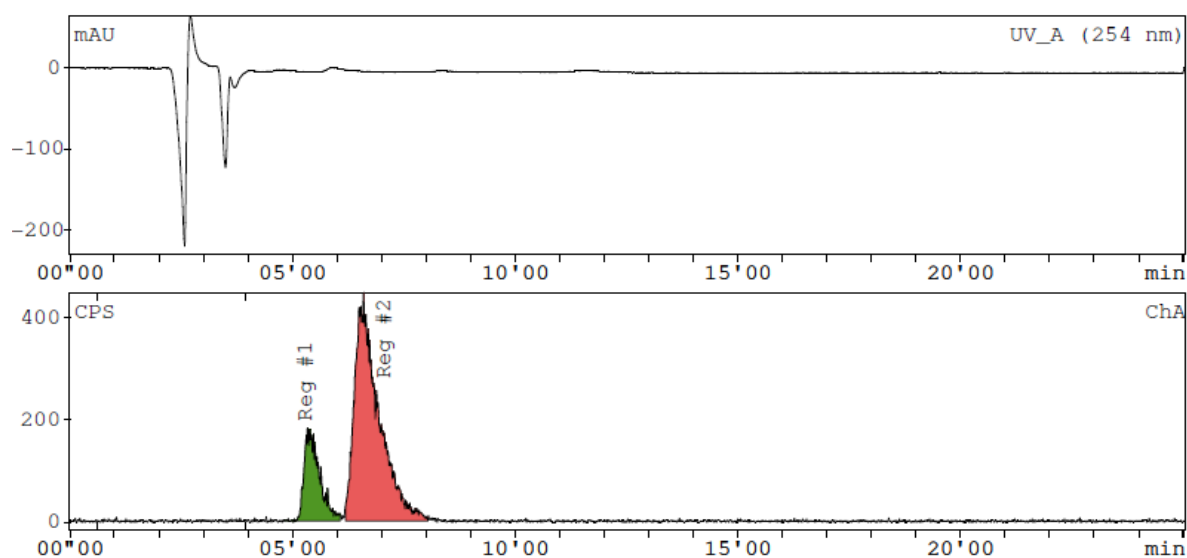
#### 4-(<sup>18</sup>F-fluoro)-N,N-dimethylaniline

##### RadioHPLC chromatography

Mobile phase: 45% AcN, 55% 50 mM 3-morpholinopropane-1-sulfonic acid (MOPS), 1mL/min



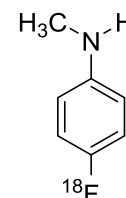
Reaction conditions: dioxane/H<sub>2</sub>O 3 mL, 10% HCl, 100 °C, 10 min



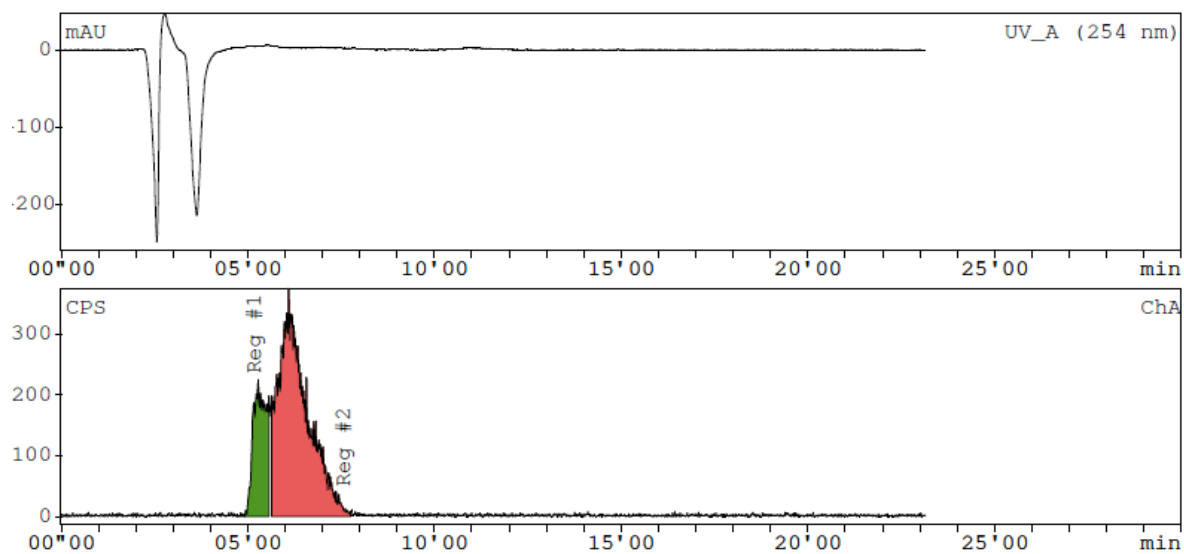
#### 4-(<sup>18</sup>F-fluoro)-N,N-dimethylaniline

##### RadioHPLC chromatography

Mobile phase: 45% AcN, 55% 50 mM 3-morpholinopropane-1-sulfonic acid (MOPS), 1mL/min



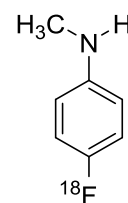
Reaction conditions: dioxane/H<sub>2</sub>O 3 mL, 10% HCl, 100 °C, 25 min



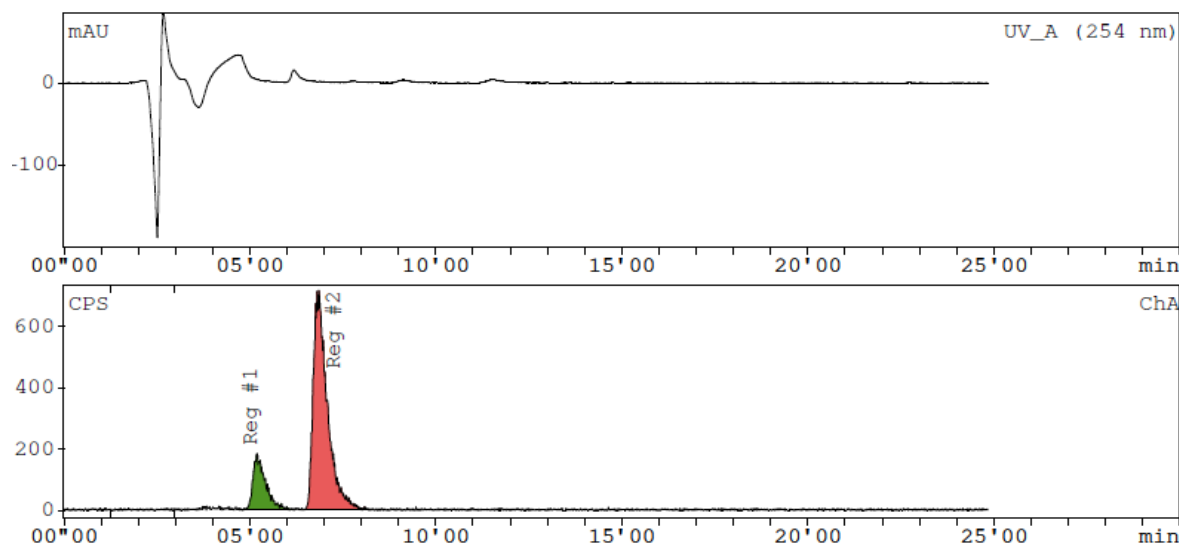
#### 4-(<sup>18</sup>F-fluoro)-N,N-dimethylaniline

##### RadioHPLC chromatography

Mobile phase: 45% AcN, 55% 50 mM 3-morpholinopropane-1-sulfonic acid (MOPS), 1mL/min



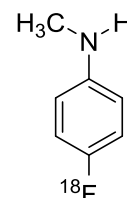
Reaction conditions: dioxane/H<sub>2</sub>O 3 mL, 18.5% HCl, 100 °C, 10 min



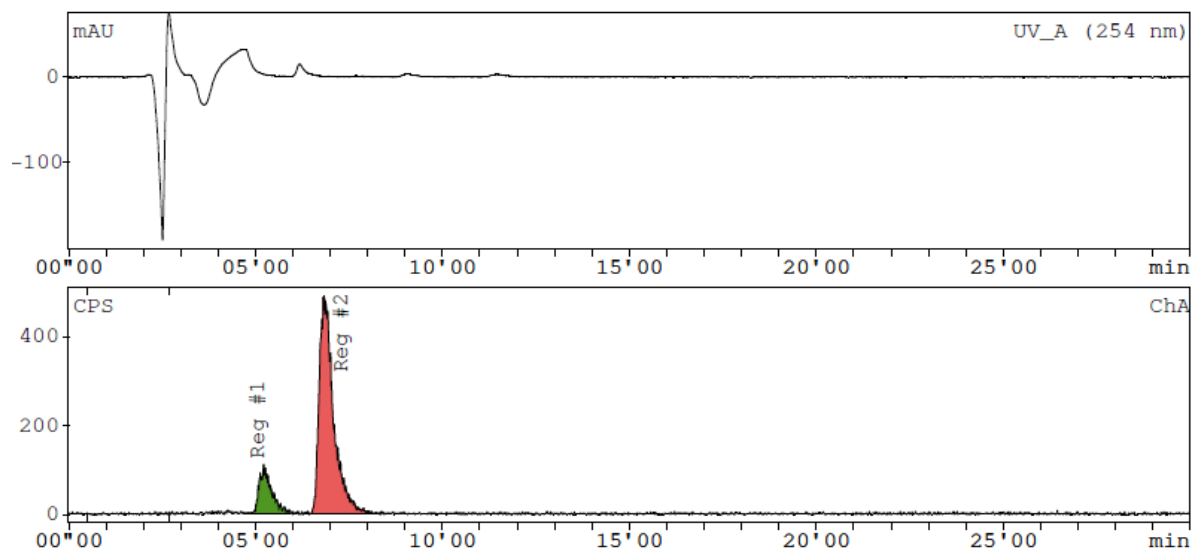
#### 4-(<sup>18</sup>F-fluoro)-N,N-dimethylaniline

##### RadioHPLC chromatography

Mobile phase: 45% AcN, 55% 50 mM 3-morpholinopropane-1-sulfonic acid (MOPS), 1mL/min



Reaction conditions: dioxane/H<sub>2</sub>O 3 mL, 18.5% HCl, 100 °C, 25 min

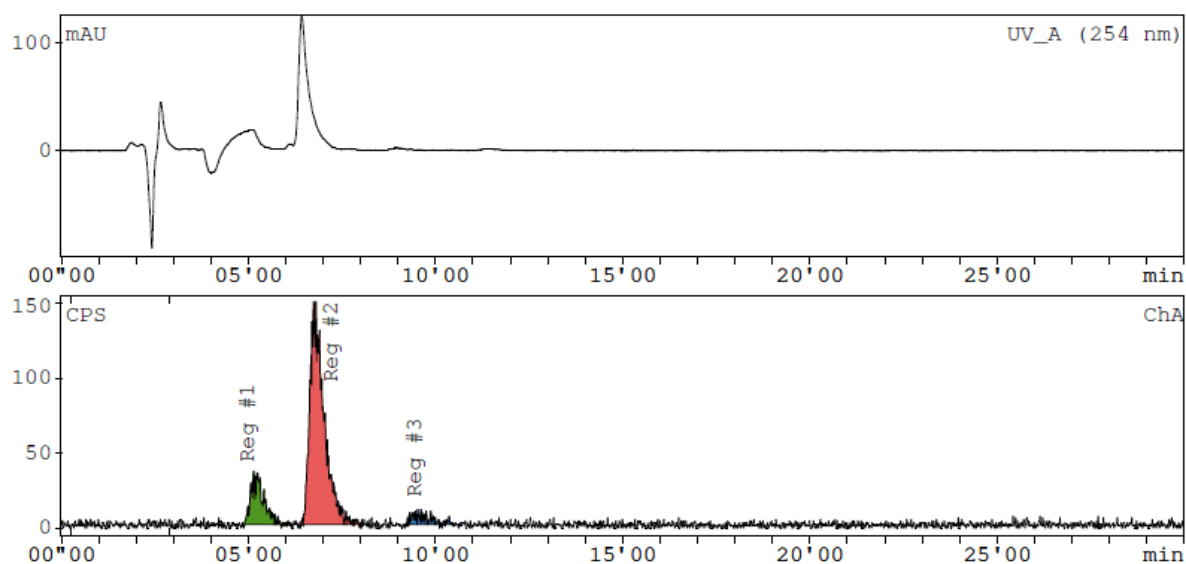
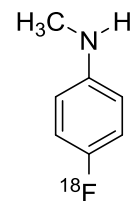


### 4-(<sup>18</sup>F-fluoro)-N,N-dimethylaniline

#### RadioHPLC chromatography

Mobile phase: 45% AcN, 55% 50 mM 3-morpholinopropane-1-sulfonic acid (MOPS), 1mL/min

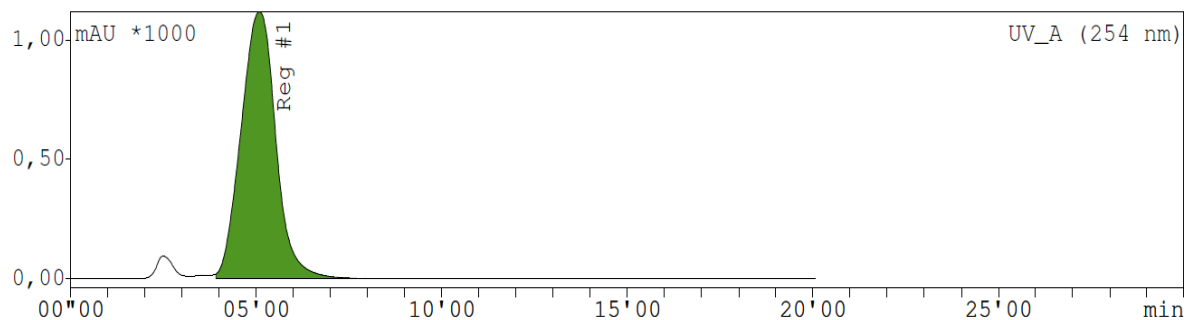
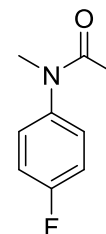
Reaction conditions: dioxane/H<sub>2</sub>O 3 mL, 10% HCl, 5 Eq. Cold product 100 °C, 10 min



### N-(4-fluorophenyl)-N-methylacetamide

#### HPLC chromatography, UV monitor

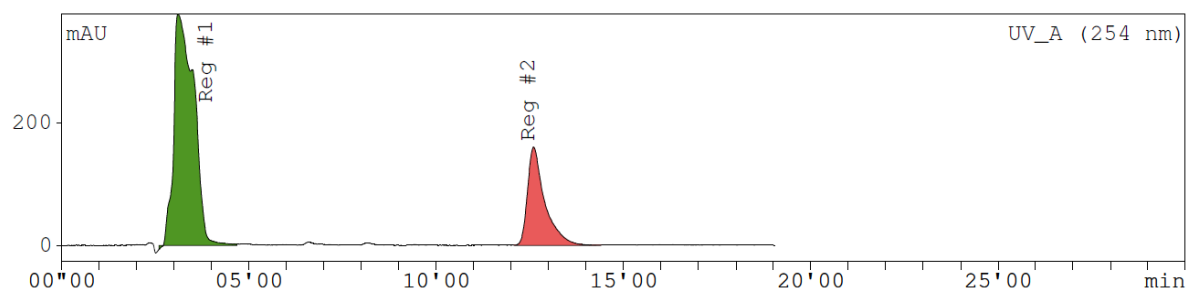
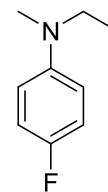
Mobile phase: 45% AcN, 55% 50 mM 3-morpholinopropane-1-sulfonic acid (MOPS), 1mL/min



### N-ethyl-4-fluoro-N-methylaniline

HPLC chromatography, UV monitor

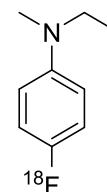
Mobile phase: 45% AcN, 55% 50 mM 3-morpholinopropane-1-sulfonic acid (MOPS), 1mL/min



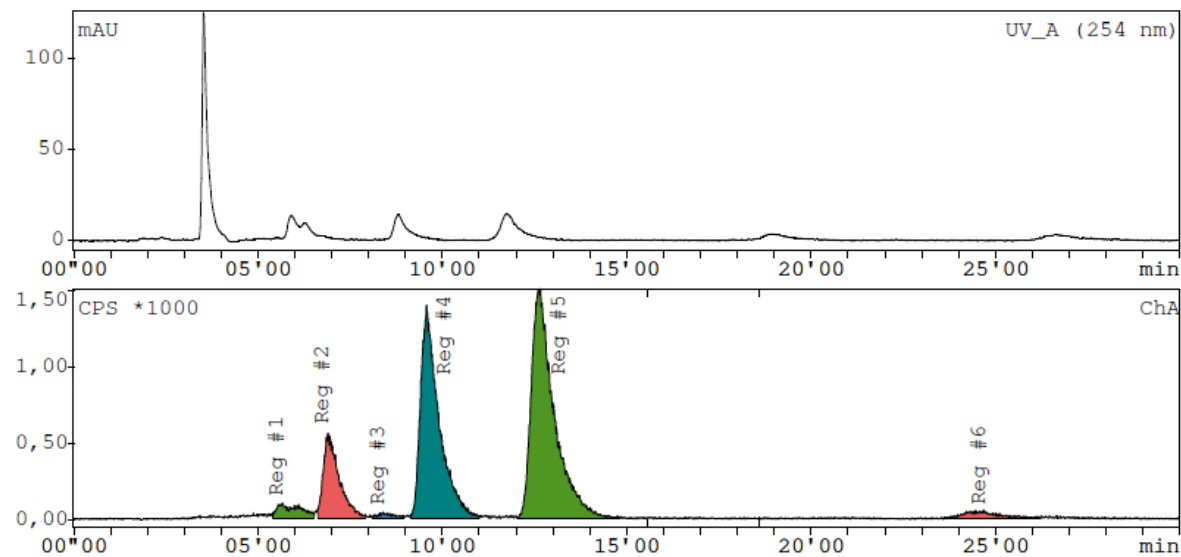
### N-Ethyl-4-(<sup>18</sup>F-fluoro)-N-methylaniline

RadioHPLC chromatography

Mobile phase: 45% AcN, 55% 50 mM 3-morpholinopropane-1-sulfonic acid (MOPS), 1mL/min



Reaction conditions: 38% THF in DME, 10 Eq. 9 BBN, 120 °C, 20 min

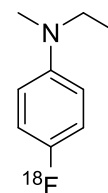




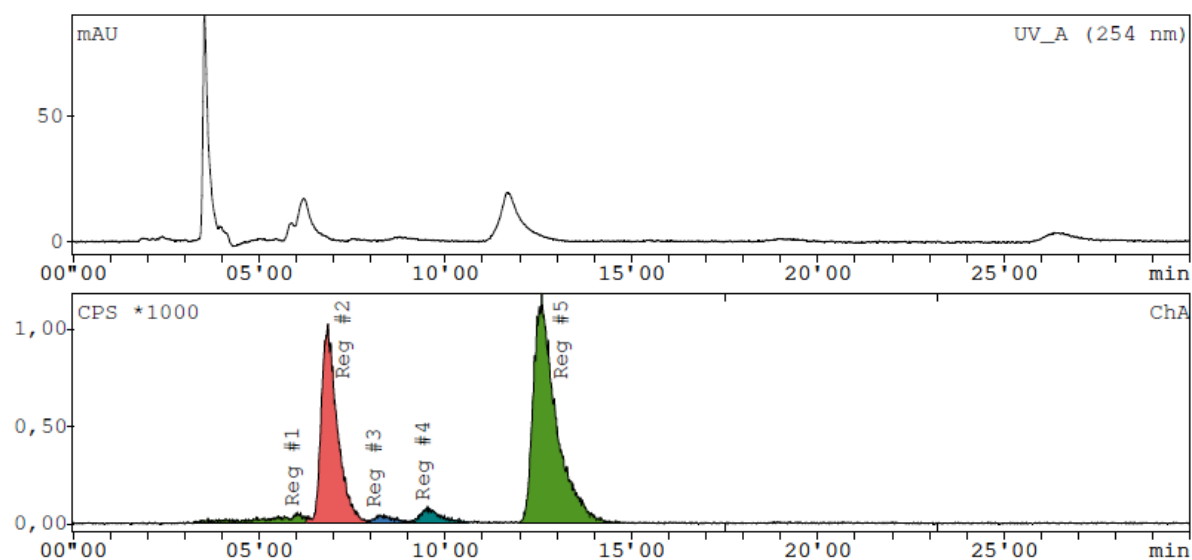
## N-Ethyl-4-(<sup>18</sup>F-fluoro)-N-methylaniline

### RadioHPLC chromatography

Mobile phase: 45% AcN, 55% 50 mM 3-morpholinopropane-1-sulfonic acid (MOPS), 1mL/min



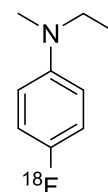
Reaction conditions: THF, 26 Eq. 9 BBN, 120 °C, 20 min



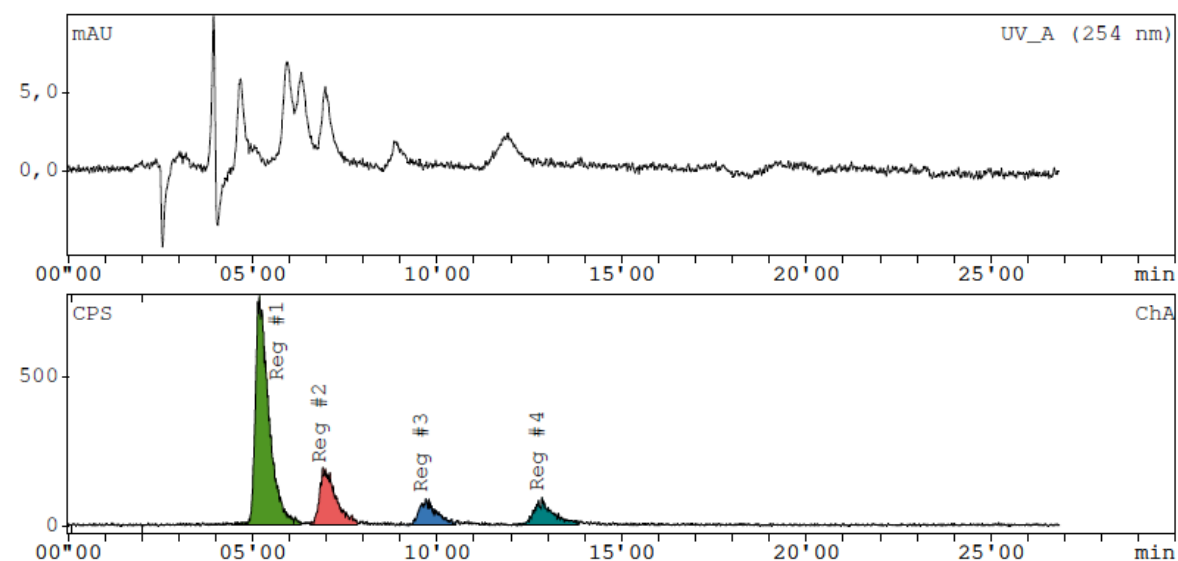
## N-Ethyl-4-(<sup>18</sup>F-fluoro)-N-methylaniline

### RadioHPLC chromatography

Mobile phase: 45% AcN, 55% 50 mM 3-morpholinopropane-1-sulfonic acid (MOPS), 1mL/min



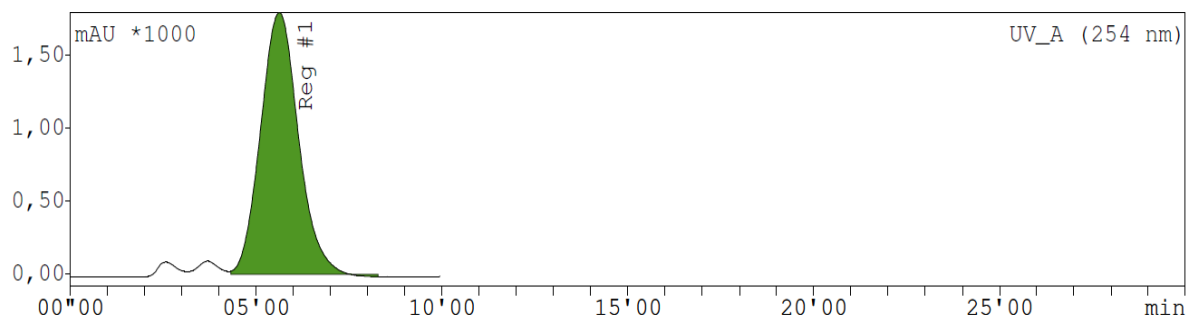
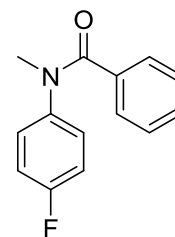
Reaction conditions: THF, 5 Eq. 9 BBN, 90 °C, 10 min



### N-(4-fluorophenyl)-N-methylbenzamide

HPLC chromatography, UV monitor

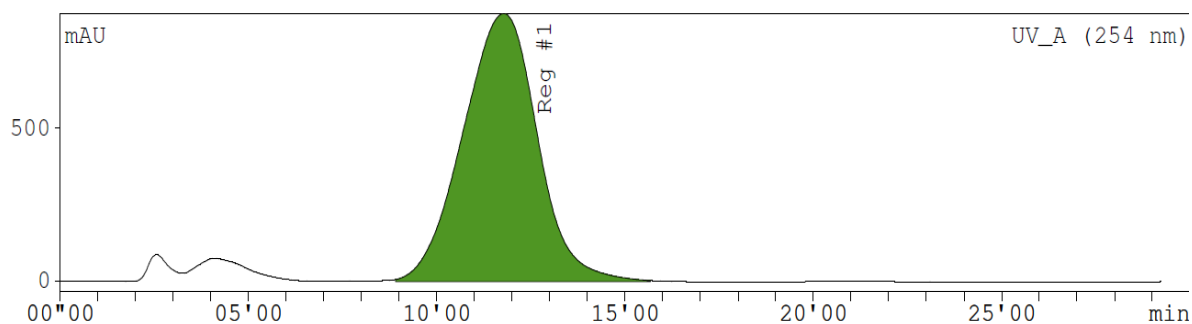
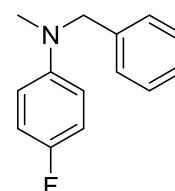
Mobile phase: 55% AcN, 45% 50 mM 3-morpholinopropane-1-sulfonic acid (MOPS), 1mL/min



### N-benzyl-4-fluoro-N-methylaniline

HPLC chromatography, UV monitor

Mobile phase: 55% AcN, 45% 50 mM 3-morpholinopropane-1-sulfonic acid (MOPS), 1mL/min

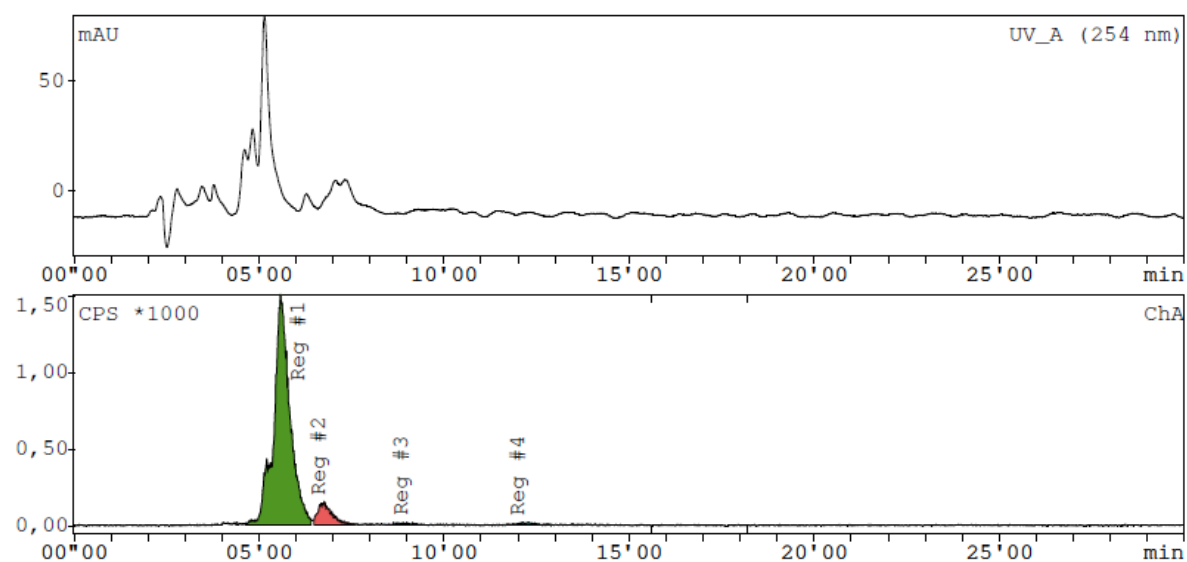
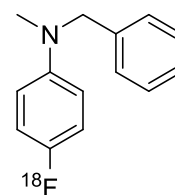


## N-benzyl-4-(<sup>18</sup>F-fluoro)-N-methylaniline

### RadioHPLC chromatography

Mobile phase: 55% AcN, 45% 50 mM 3-morpholinopropane-1-sulfonic acid (MOPS), 1mL/min

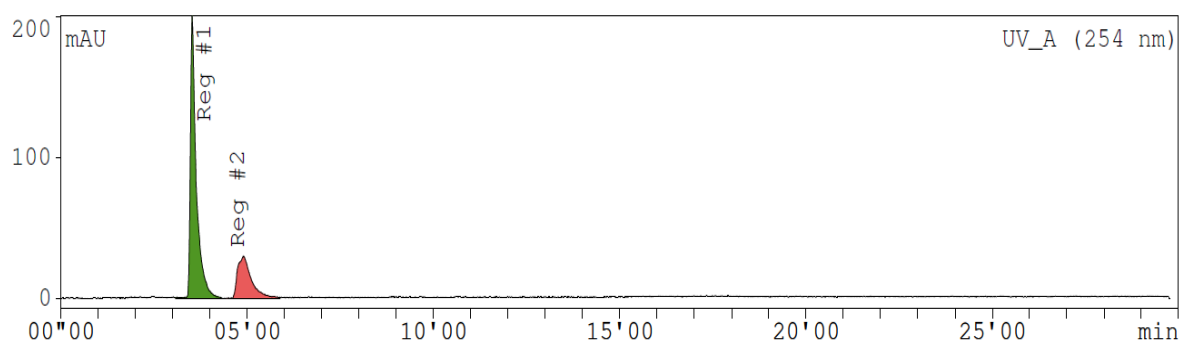
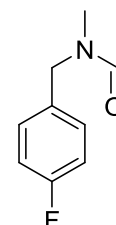
Reaction conditions: THF, 5 Eq. 9 BBN, 90 °C, 10 min



## N-(4-fluorobenzyl)-N-methylformamide

### HPLC chromatography, UV monitor

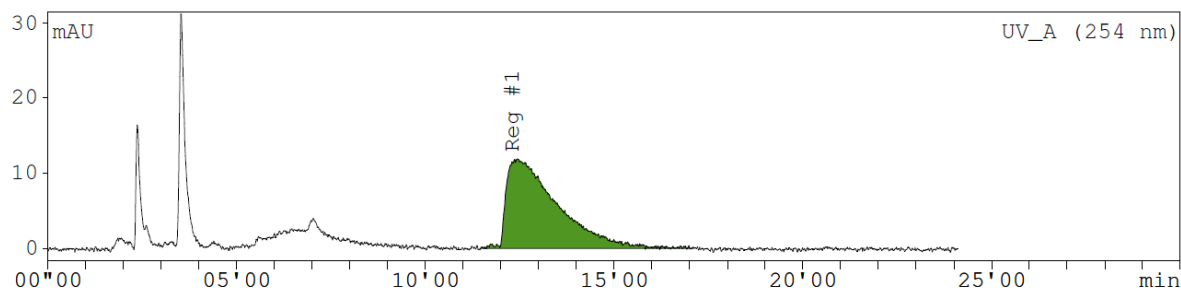
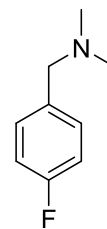
Mobile phase: 45% AcN, 55% 50 mM 3-morpholinopropane-1-sulfonic acid (MOPS), 1mL/min



## N-(4-fluorophenyl)-N,N-dimethylmethanamine

*HPLC chromatography, UV monitor*

Mobile phase: 45% AcN, 55% 50 mM 3-morpholinopropane-1-sulfonic acid (MOPS),  
1mL/min

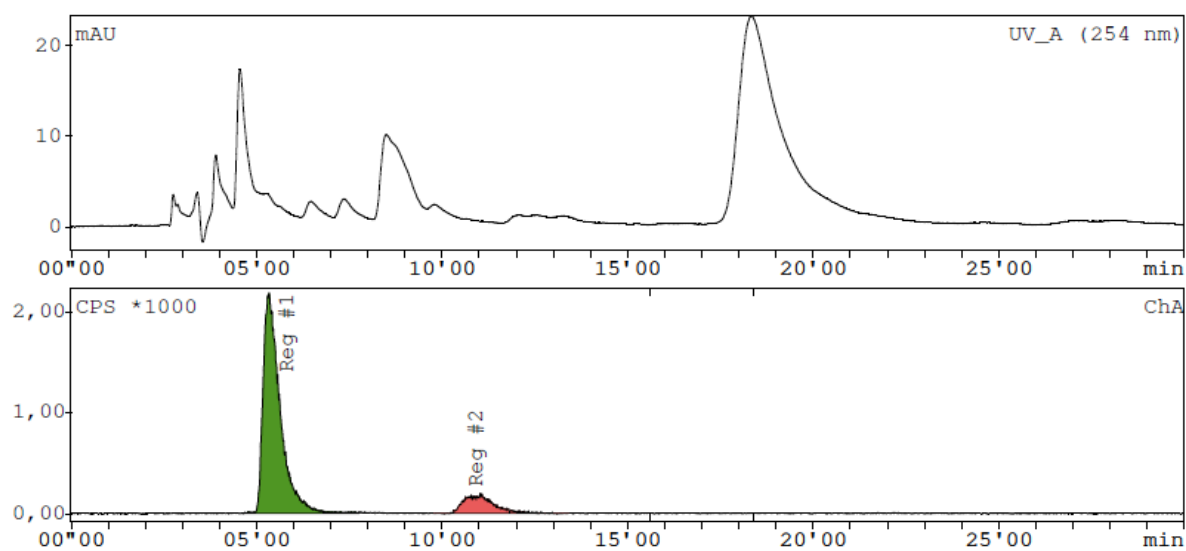
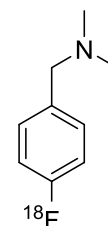


## 1-(4-(<sup>18</sup>F-fluoro)phenyl)-N,N-dimethylmethanamine

*RadioHPLC chromatography*

Mobile phase: 55% AcN, 45% 50 mM 3-morpholinopropane-1-sulfonic acid (MOPS), 1mL/min

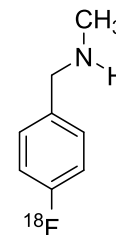
Reaction conditions: DME, 5 Eq. 9 BBN, 90 °C, 10 min



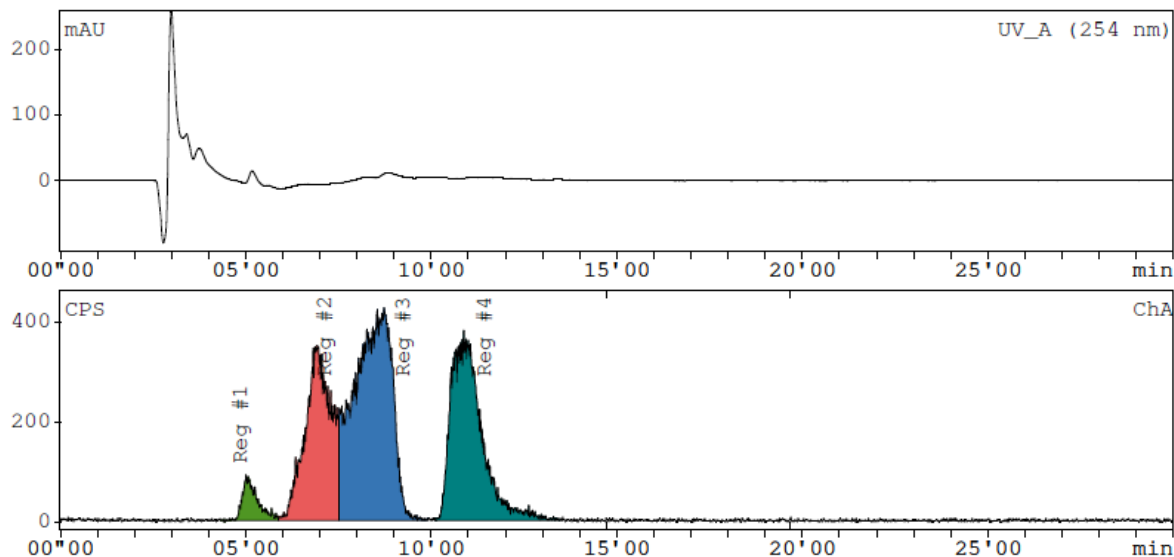
## 1-(4-<sup>18</sup>F-fluoro)phenyl)-N-methylmethanamine

### RadioHPLC chromatography

Mobile phase: 55% AcN, 45% 50 mM 3-morpholinopropane-1-sulfonic acid (MOPS), 1mL/min



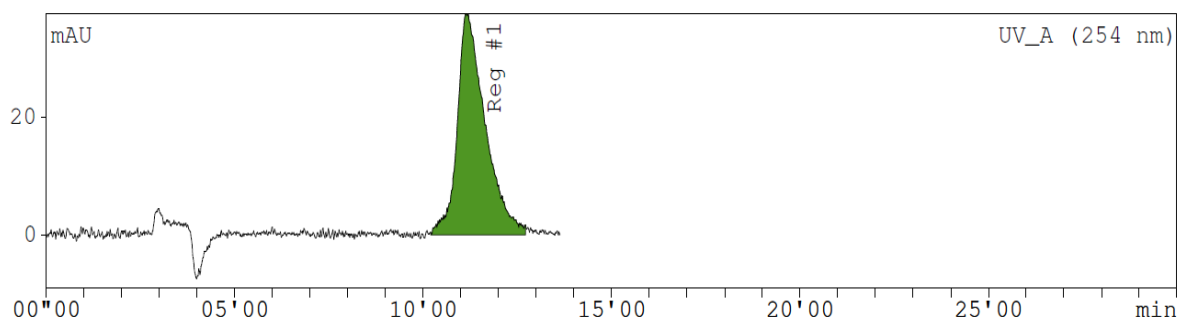
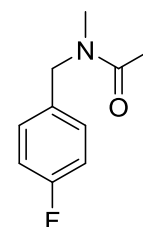
Reaction conditions: dioxane/H<sub>2</sub>O 3 mL, 10 % HCl, 100 °C, 10 min



## N-(4-fluorobenzyl)-N-methylacetamide

### HPLC chromatography, UV monitor

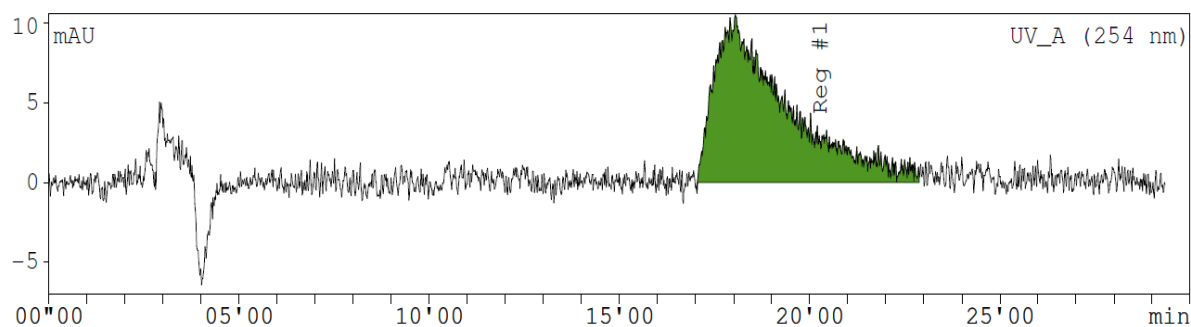
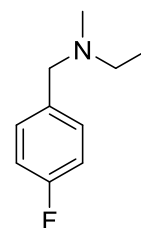
Mobile phase: 25% AcN, 75% 50 mM 3-morpholinopropane-1-sulfonic acid (MOPS), 1mL/min



## N-(4-fluorobenzyl)-N-methylethanamine

*HPLC chromatography, UV Monitor*

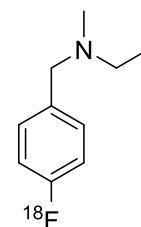
Mobile phase: 25% AcN, 75% 50 mM 3-morpholinopropane-1-sulfonic acid (MOPS), 1mL/min



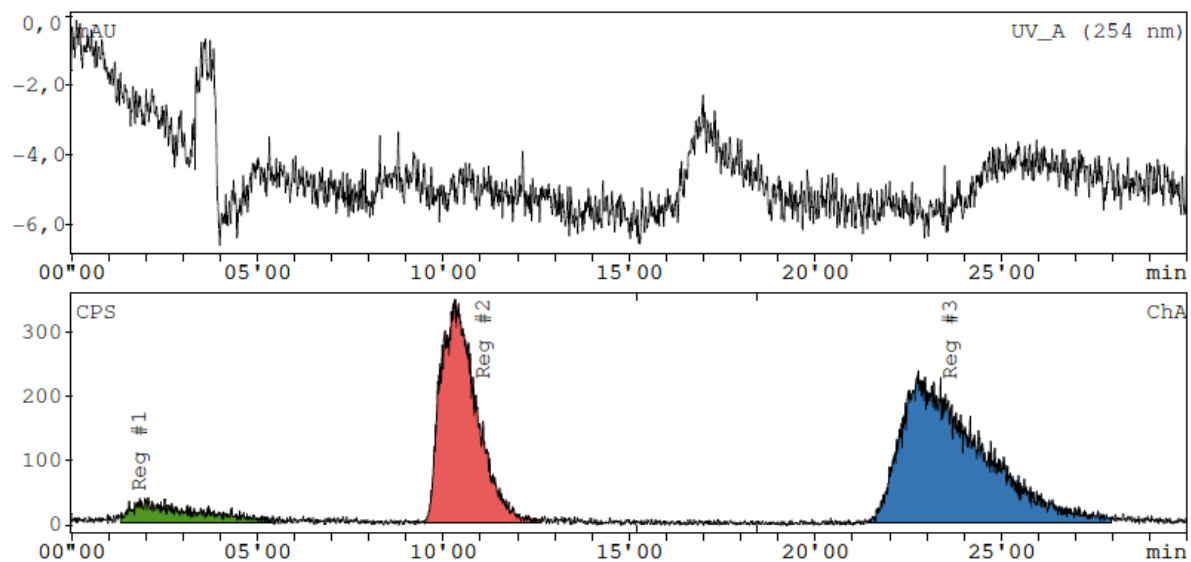
## N-(4-(<sup>18</sup>F-fluoro)benzyl)-N-methylethanamine

*RadioHPLC chromatography*

Mobile phase: 25% AcN, 75% 50 mM 3-morpholinopropane-1-sulfonic acid (MOPS), 1mL/min



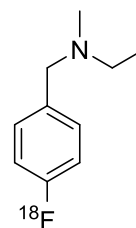
Reaction conditions: THF, 5 Eq. 9 BBN, 90 °C, 10 min



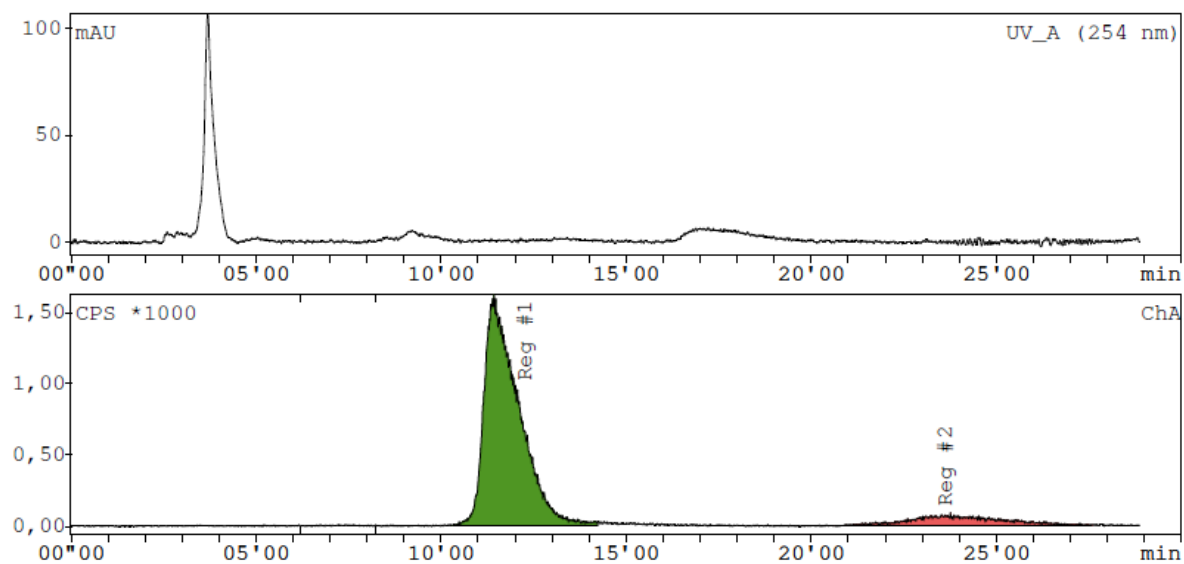
## N-(4-(<sup>18</sup>F-fluoro)benzyl)-N-methylethanamine

### RadioHPLC chromatography

Mobile phase: 25% AcN, 75% 50 mM 3-morpholinopropane-1-sulfonic acid (MOPS), 1mL/min



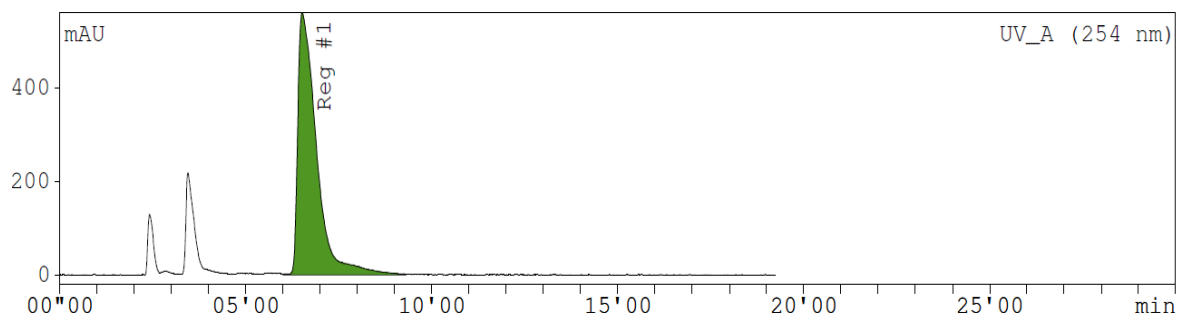
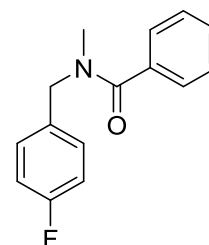
Reaction conditions: THF, 25 Eq. 9 BBN, 120 °C, 20 min



## N-(4-fluorobenzyl)-N-methylbenzamide

### HPLC chromatography, UV monitor

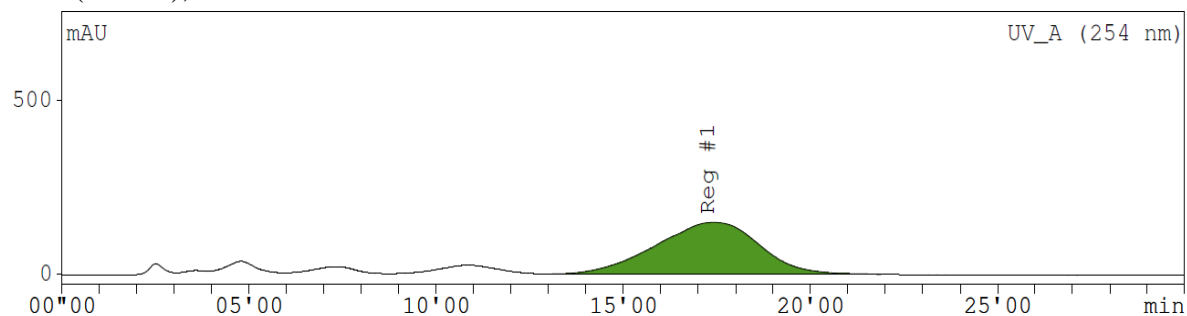
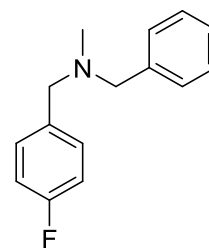
Mobile phase: 45% AcN, 55% 50 mM 3-morpholinopropane-1-sulfonic acid (MOPS), 1mL/min



### N-benzyl-1-(4-fluorophenyl)-N-methylmethanamine

HPLC chromatography, UV monitor

Mobile phase: 50% AcN, 50% 50 mM 3-morpholinopropane-1-sulfonic acid (MOPS), 1mL/min

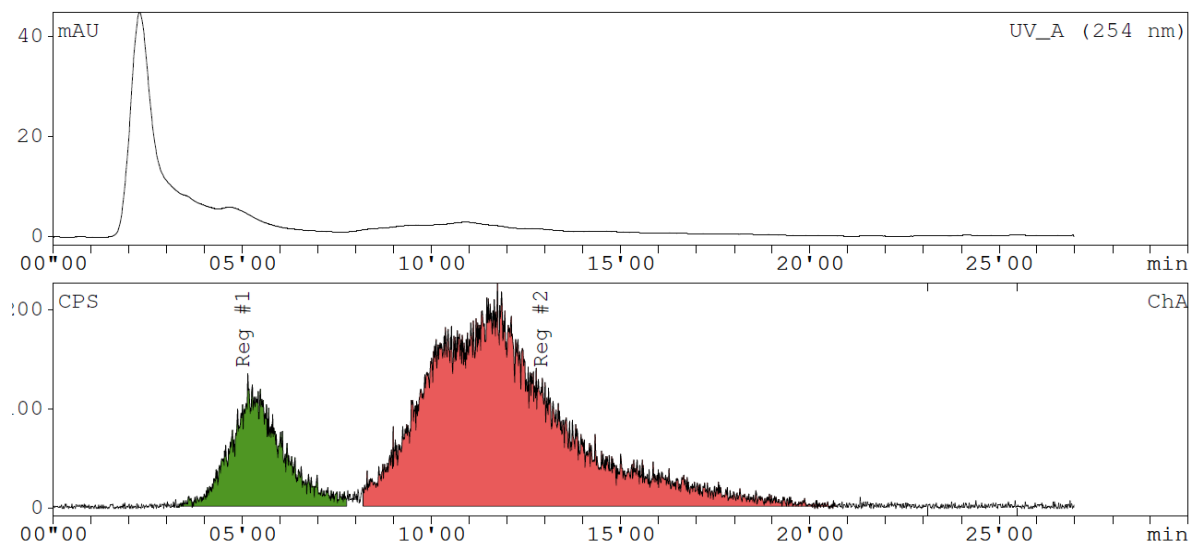
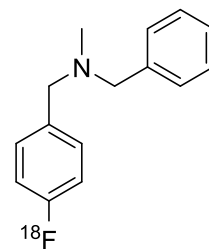


### N-benzyl-1-(4-<sup>18</sup>F-fluoro)phenyl-N-methylmethanamine

RadioHPLC chromatography

Mobile phase: 55% AcN, 45% 50 mM 3-morpholinopropane-1-sulfonic acid (MOPS), 1mL/min

Reaction conditions: THF, 25 Eq. 9 BBN, 120 °C, 20 min

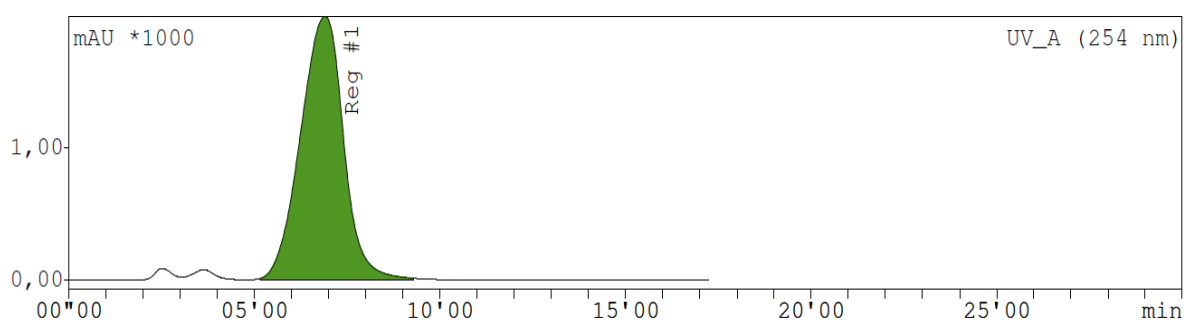
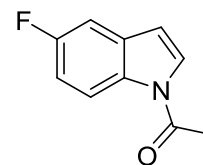




### 1-(5-fluoro-1H-indol-1-yl)ethan-1-one

HPLC chromatography, UV monitor

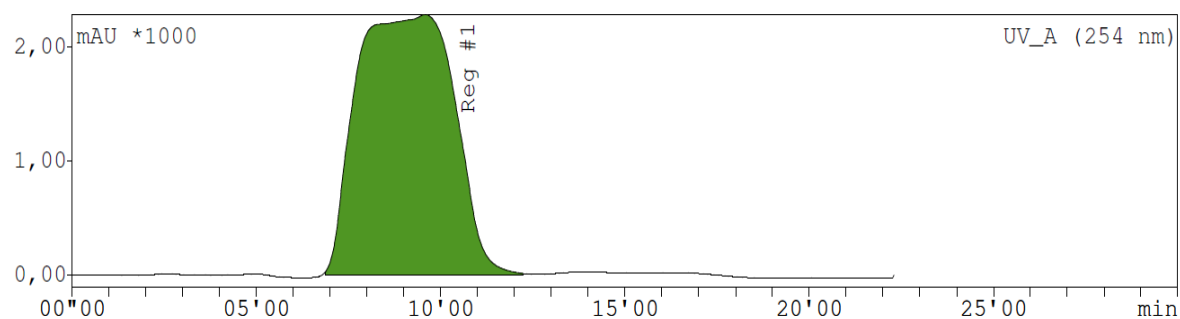
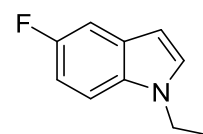
Mobile phase: 50% AcN, 50% 50 mM 3-morpholinopropane-1-sulfonic acid (MOPS), 1mL/min



### 1-ethyl-5-fluoro-1H-indole

HPLC chromatography, UV monitor

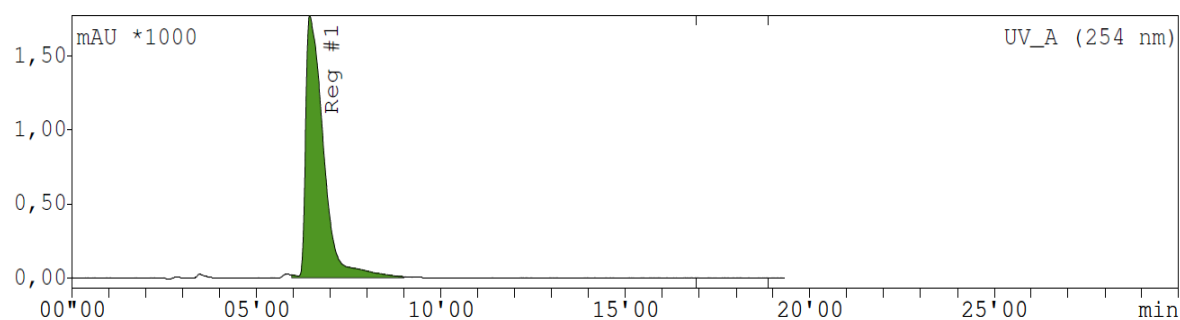
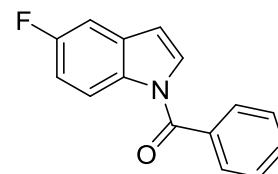
Mobile phase: 50% AcN, 50% 50 mM 3-morpholinopropane-1-sulfonic acid (MOPS), 1mL/min



### (5-fluoro-1H-indol-1-yl)(phenyl)methanone

HPLC chromatography, UV monitor

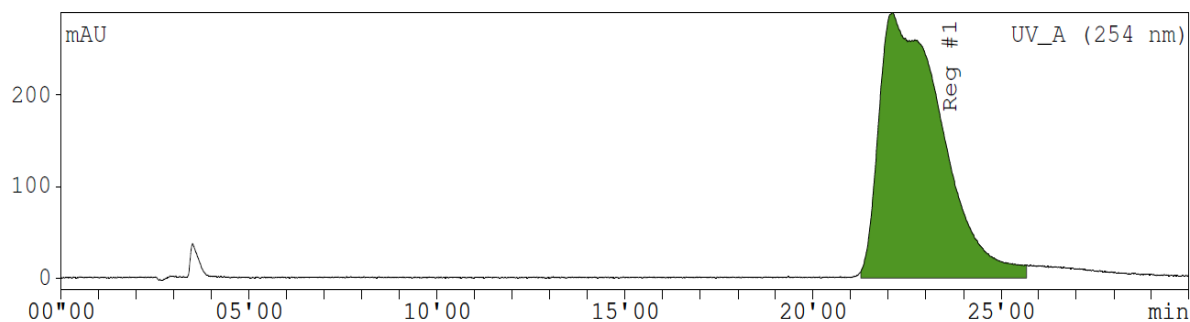
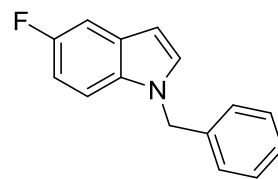
Mobile phase: 45% AcN, 55% 50 mM 3-morpholinopropane-1-sulfonic acid (MOPS), 1mL/min



### 1-benzyl-5-fluoro-1H-indole

HPLC chromatography, UV monitor

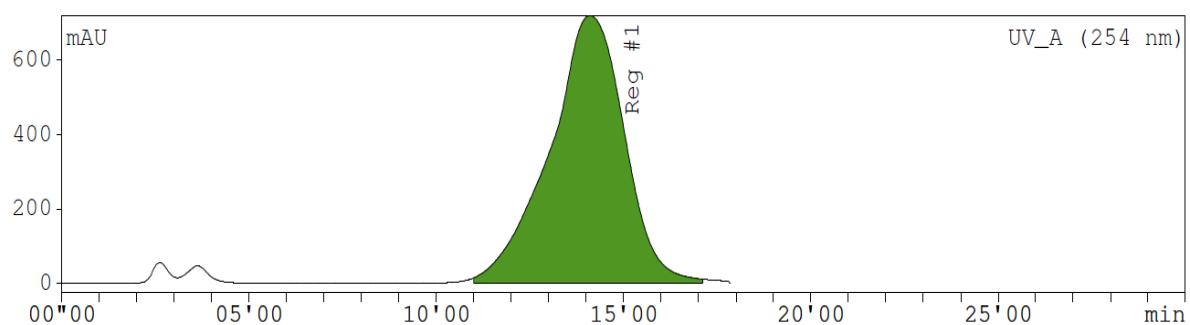
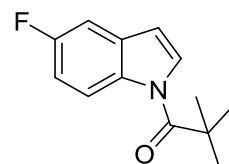
Mobile phase: 45% AcN, 55% 50 mM 3-morpholinopropane-1-sulfonic acid (MOPS), 1mL/min



### 1-(5-fluoro-1H-indol-1-yl)-2,2-dimethylpropan-1-one

HPLC chromatography, UV monitor

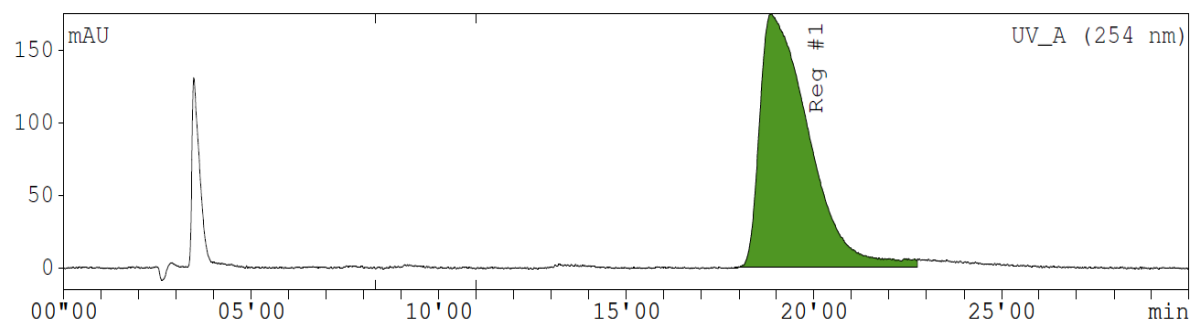
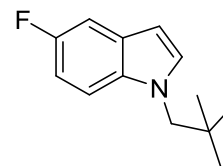
Mobile phase: 50% AcN, 50% 50 mM 3-morpholinopropane-1-sulfonic acid (MOPS), 1mL/min



### 5-fluoro-1-neopentyl-1H-indole

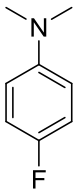
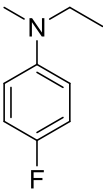
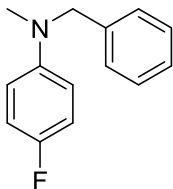
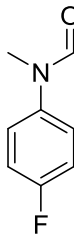
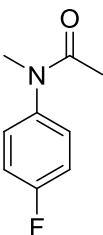
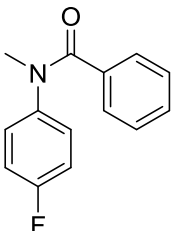
HPLC chromatography, UV monitor

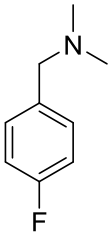
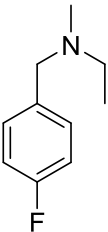
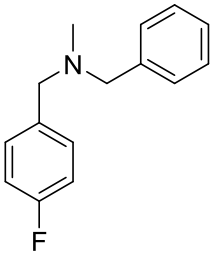
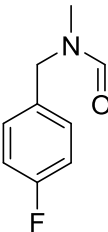
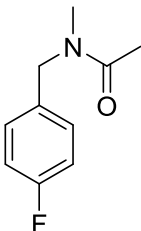
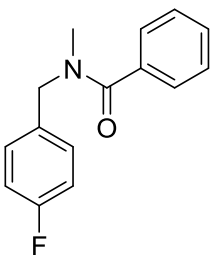
Mobile phase: 50% AcN, 50% 50 mM 3-morpholinopropane-1-sulfonic acid (MOPS), 1mL/min

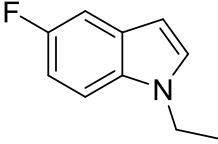
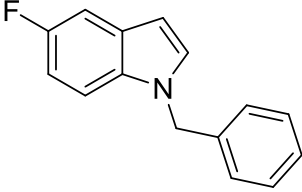
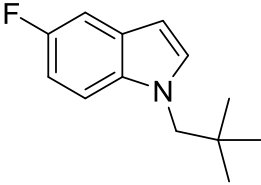
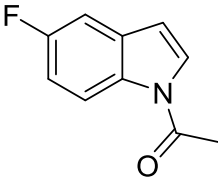
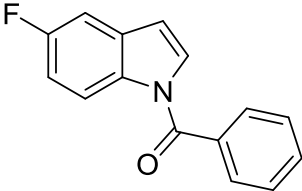
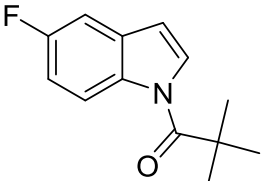


## TLC R<sub>f</sub>-values and RadioTLC chromatograms

RadioTLC was detected by Raytest miniGita beta detector GML.

	R <sub>f</sub> :		R <sub>f</sub> :	Solvent system
	0.81	1:48 MeOH:DCM	0.46	1:17 EtOAc:hexanes
	0.87	1:48 MeOH:DCM	0.49	1:17 EtOAc:hexanes
	0.92	1:48 MeOH:DCM	0.65	1:17 EtOAc:hexanes
	0.5	1:48 MeOH:DCM	baseline	1:17 EtOAc:hexanes
	0.5	1:48 MeOH:DCM	baseline	1:17 EtOAc:hexanes
	0.71	1:48 MeOH:DCM	0.25	1:17 EtOAc:hexanes

	Rf:	Solvent system
	0.35	2:23 MeOH:DCM
	0.26	2:23 MeOH:DCM
	0.50	1:24 MeOH:DCM
	0.52	2:23 MeOH:DCM
	0.64	2:23 MeOH: DCM
	0.25	1:3 EtOAc:Hex

	Rf:	Solvent system
	0.51	1:15 EtOAc:hexanes
	0.35	1:15 EtOAc:hexanes
	0.61	1:20 EtOAc Hex
	0.35	1:15 EtOAc:hexanes
	0.47	1:3 EtOAc:hexanes
	0.44	1:15 EtOAc:hexanes

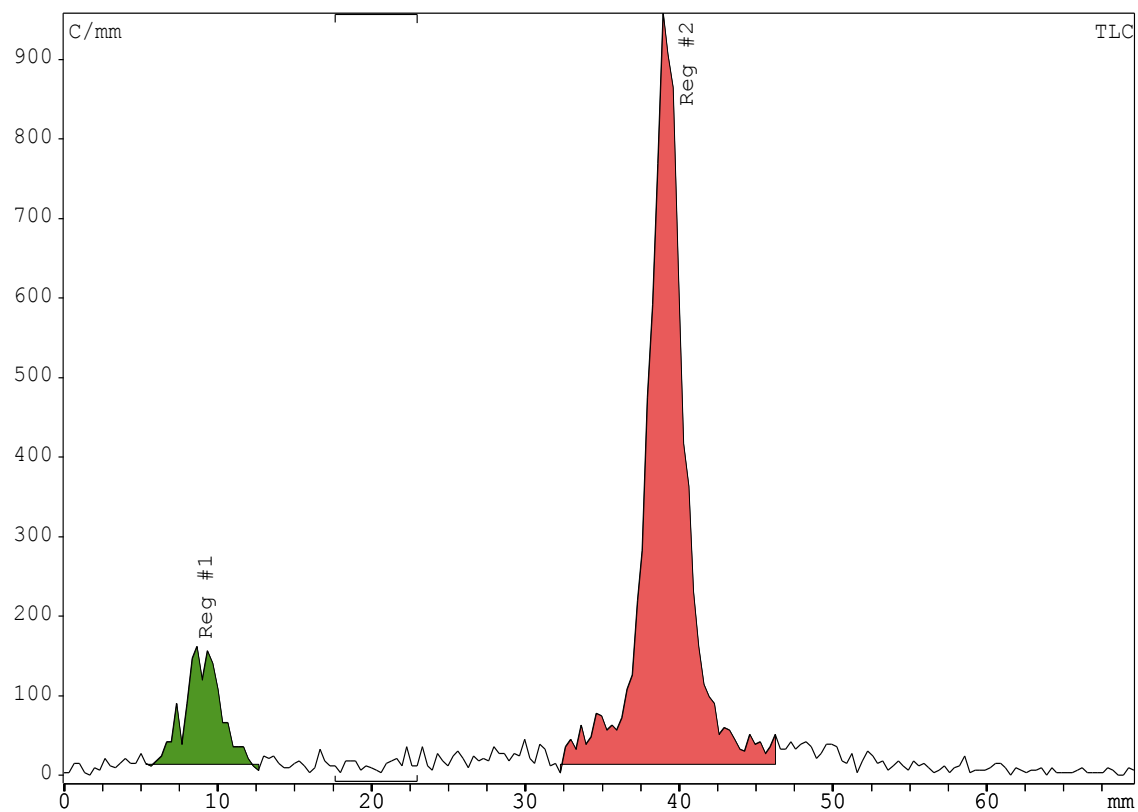


**Figure LXXIII Radiochemical incorporation into 1b)**

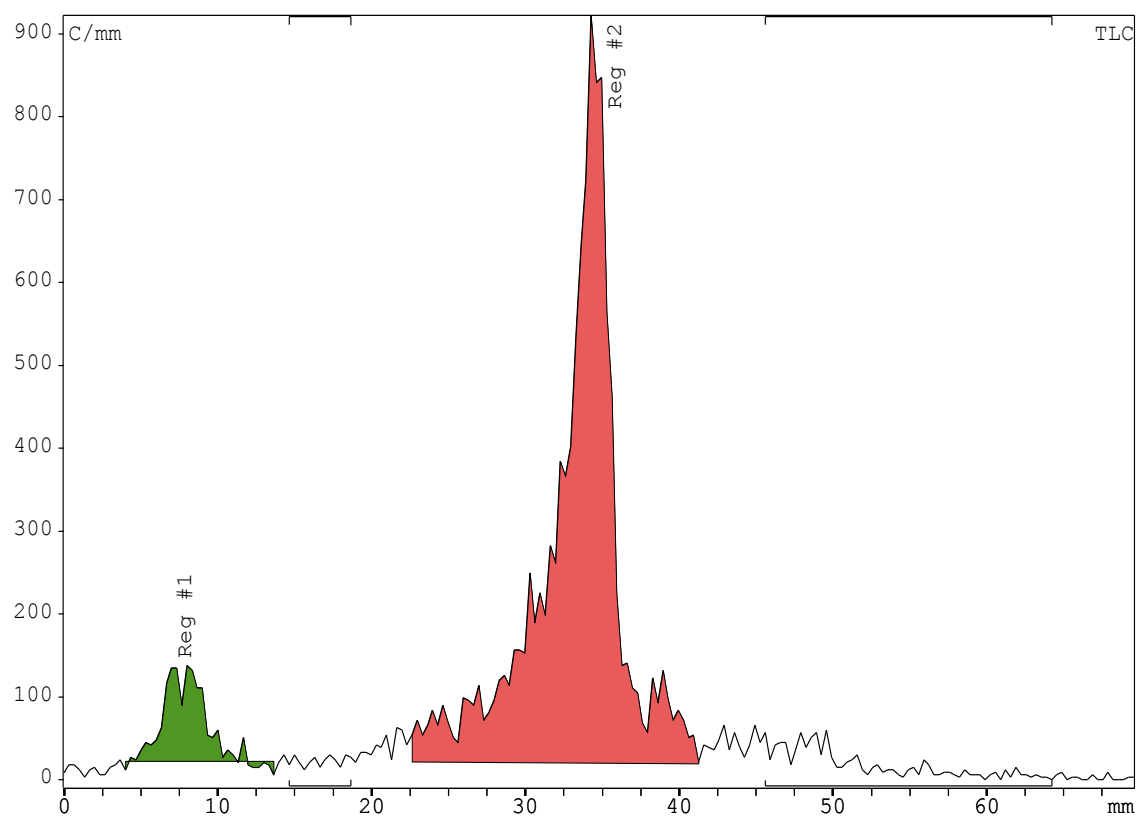


**Figure LXXIV Radiochemical incorporation into 2b)**

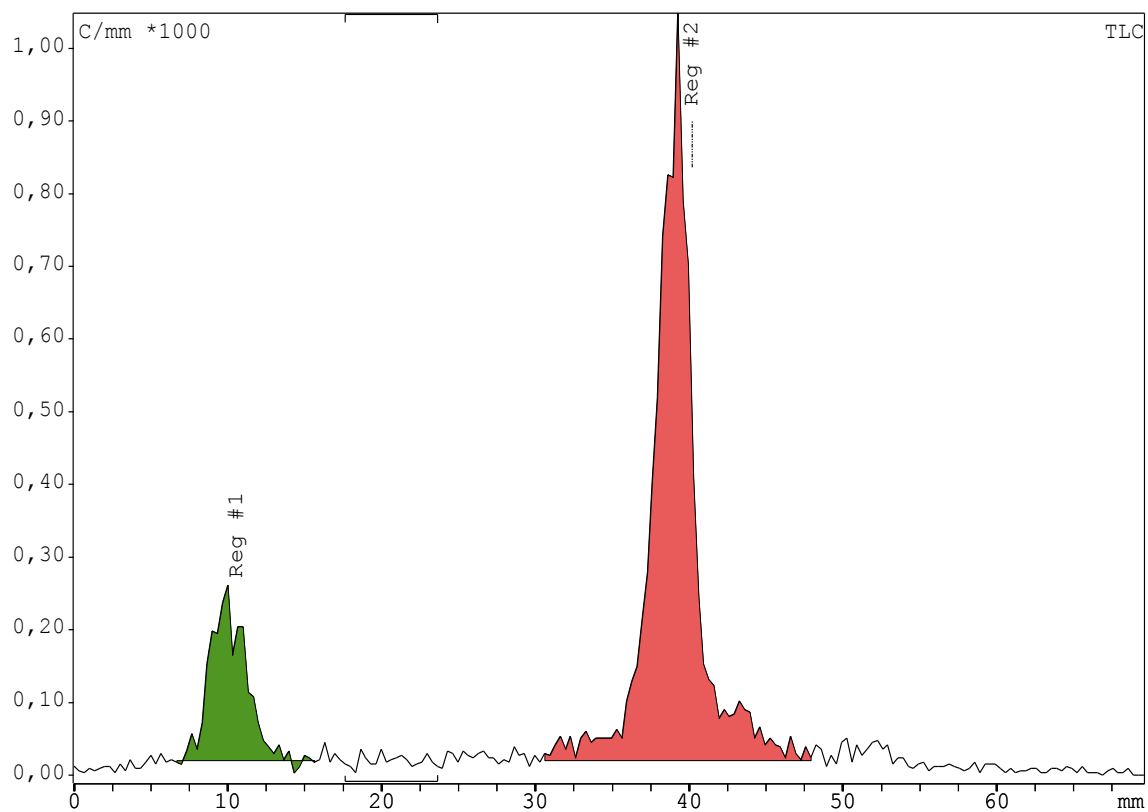


**Figure LXXV Radiochemical incorporation into 3b)**

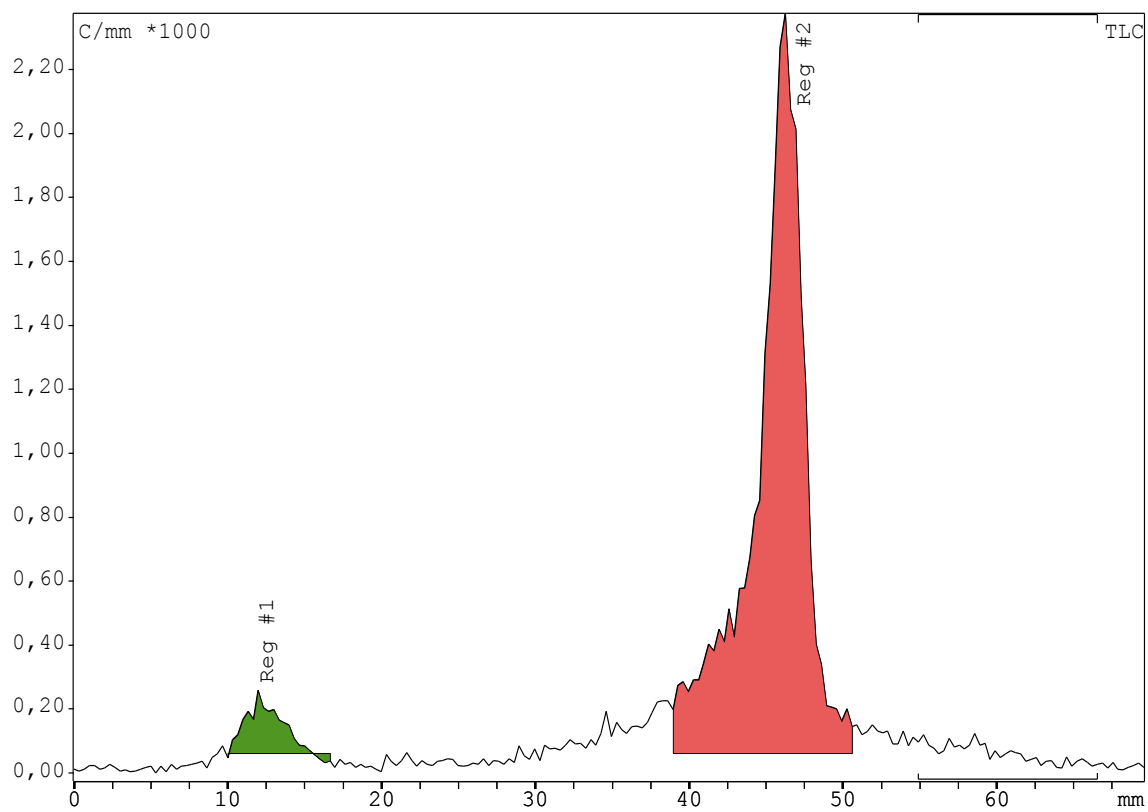


**Figure LXXVI Radiochemical incorporation into 4b)**

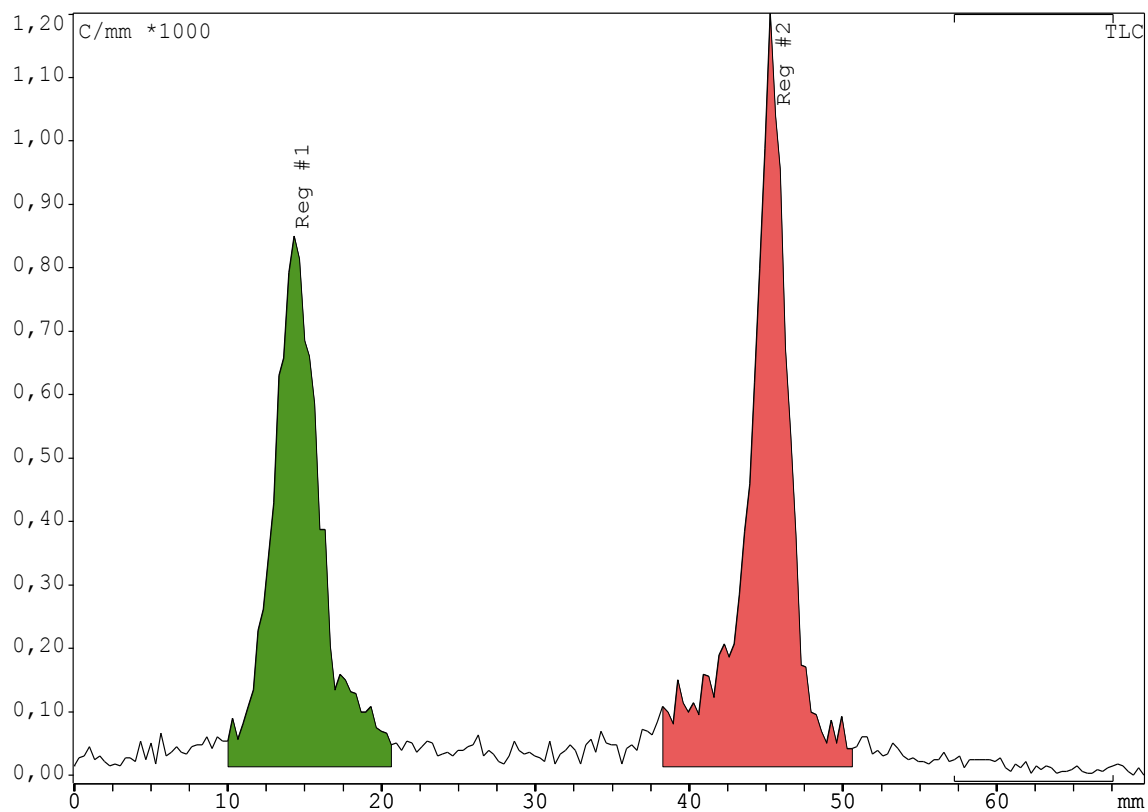


**Figure LXXVII Radiochemical incorporation into 5b)**

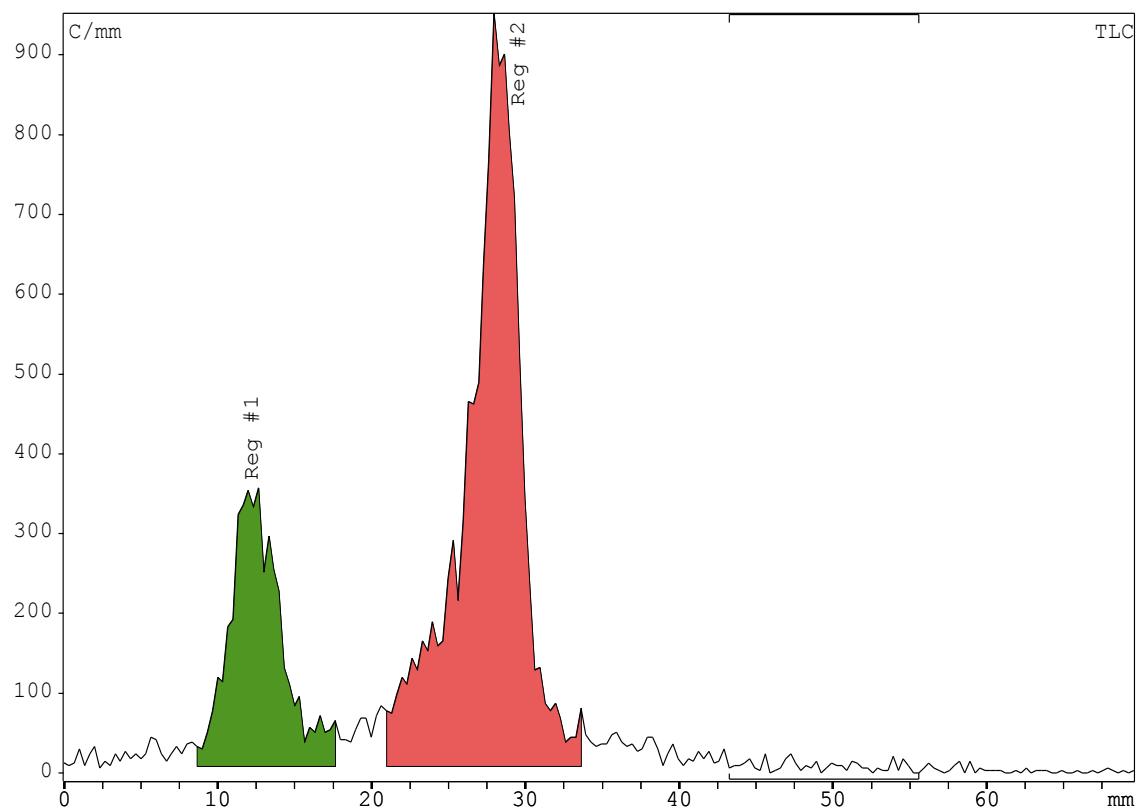


**Figure LXXVIII Radiochemical incorporation into 6b)**



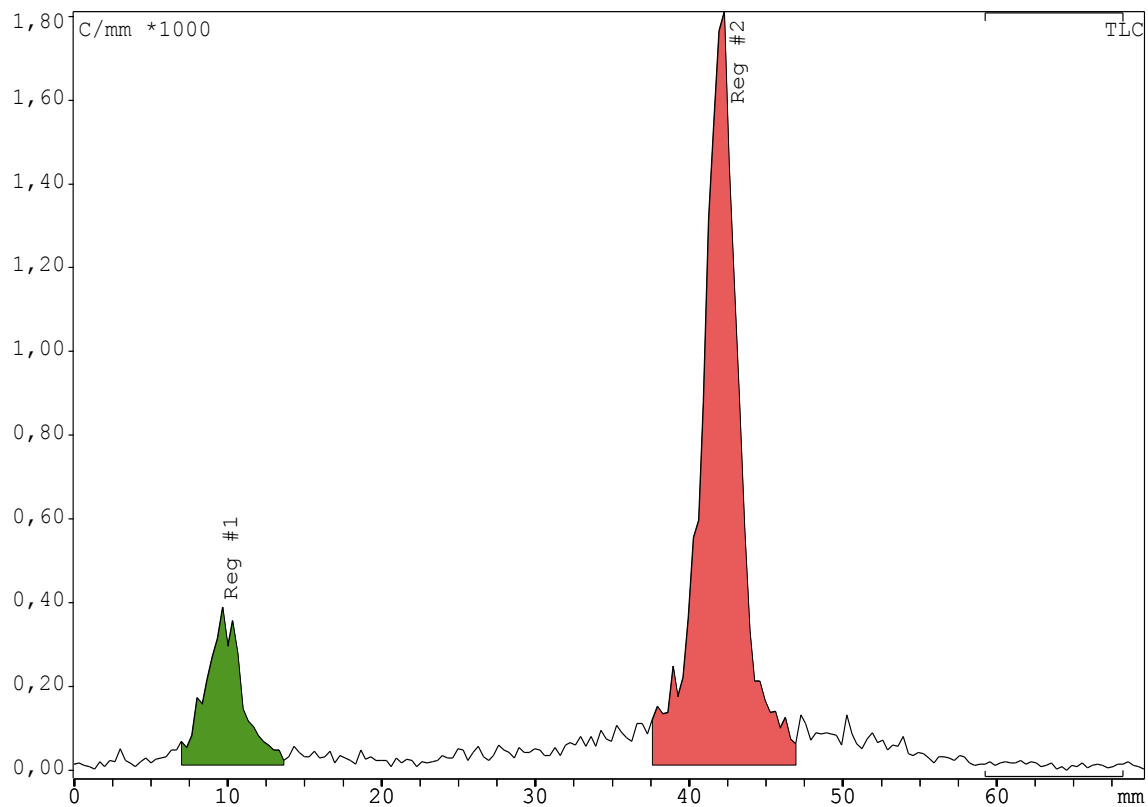


**Figure LXXIX Hydrolysis of 1b) into 1c)**

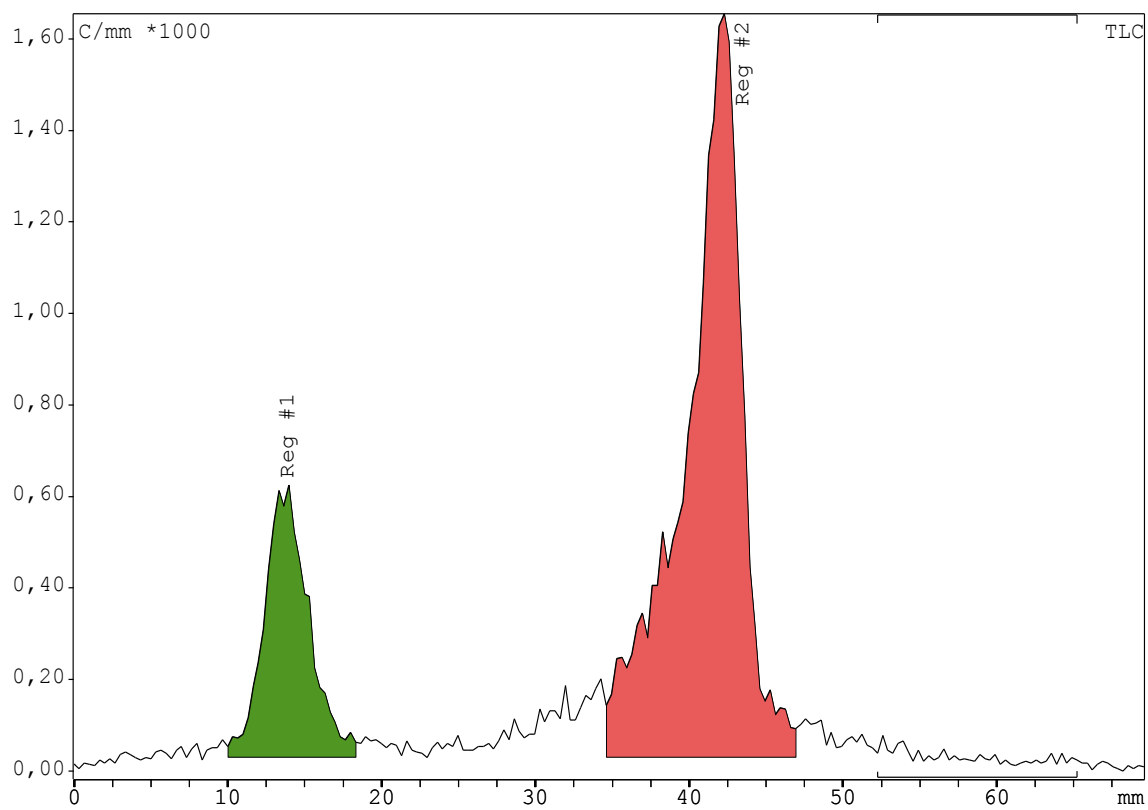


**Figure LXXX Hydrolysis of 4b) into 4c)**

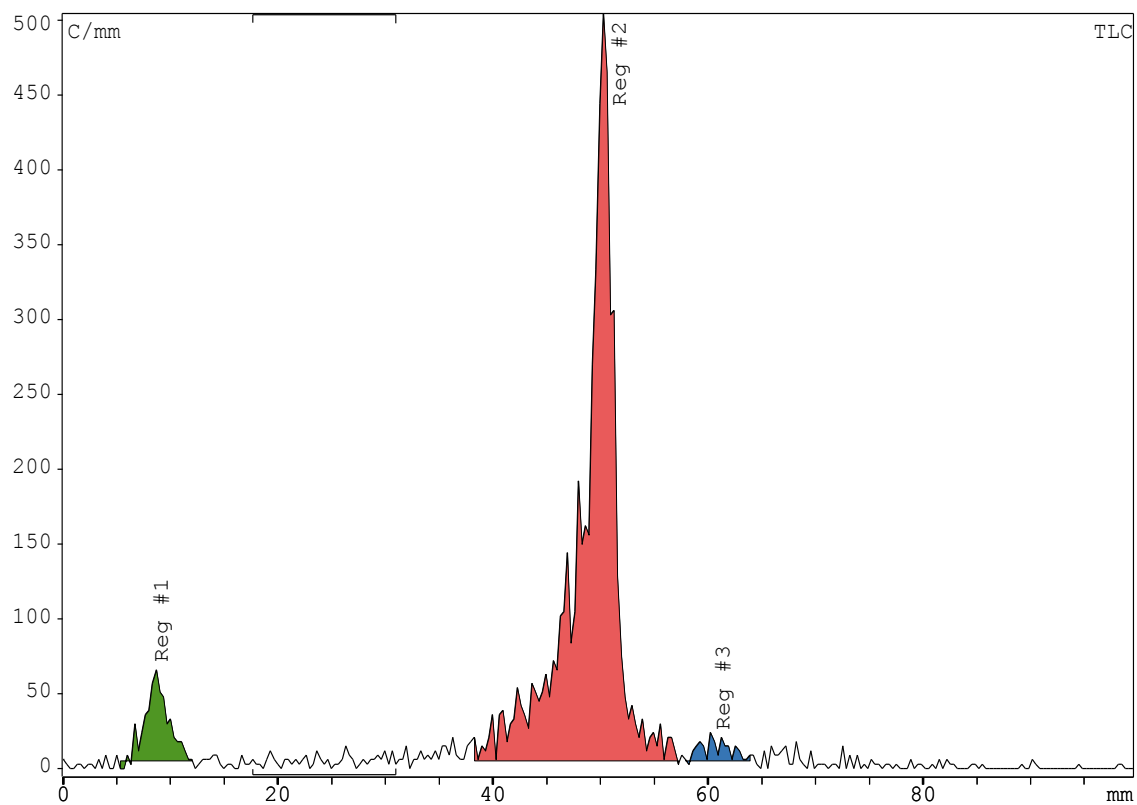


**Figure LXXXI compound of radiochemical incorporation competition of 43 vs 5a)**

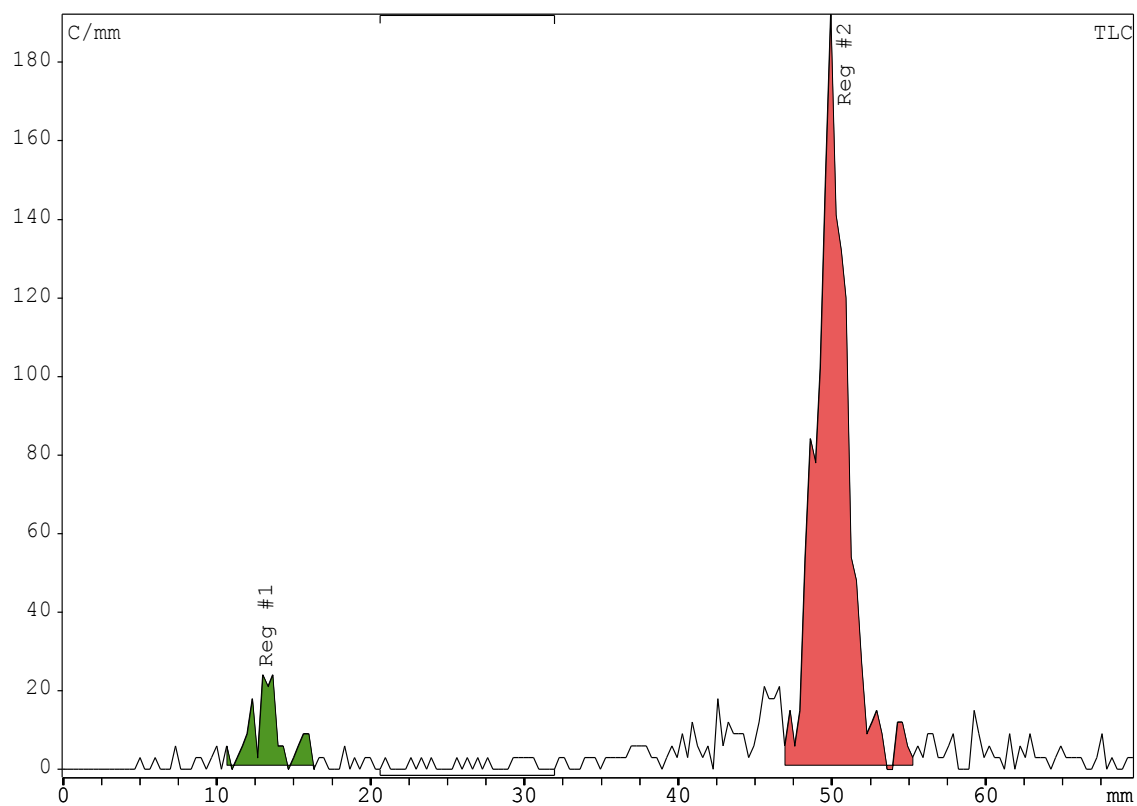


**Figure LXXXII Radiochemical incorporation into 4a) without 7f)**

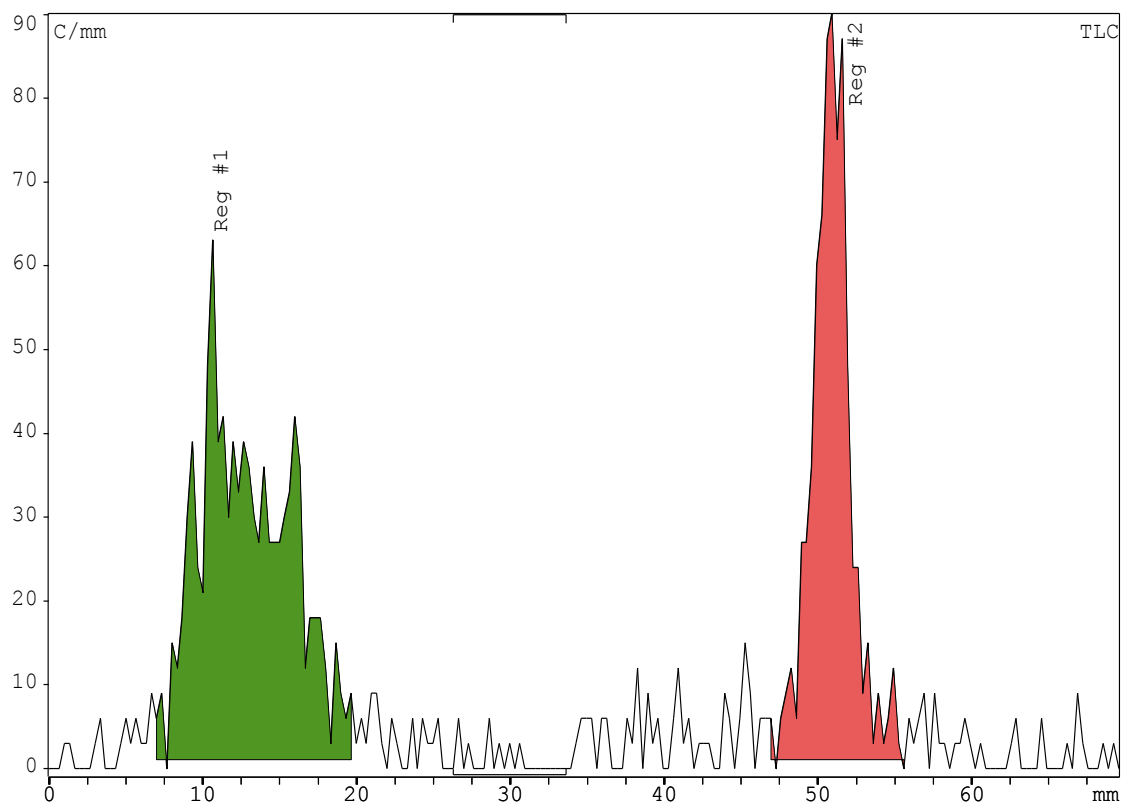


**Figure LXXXIII Radiochemical incorporation into 4a) together with 1 equivalent of 7f)**

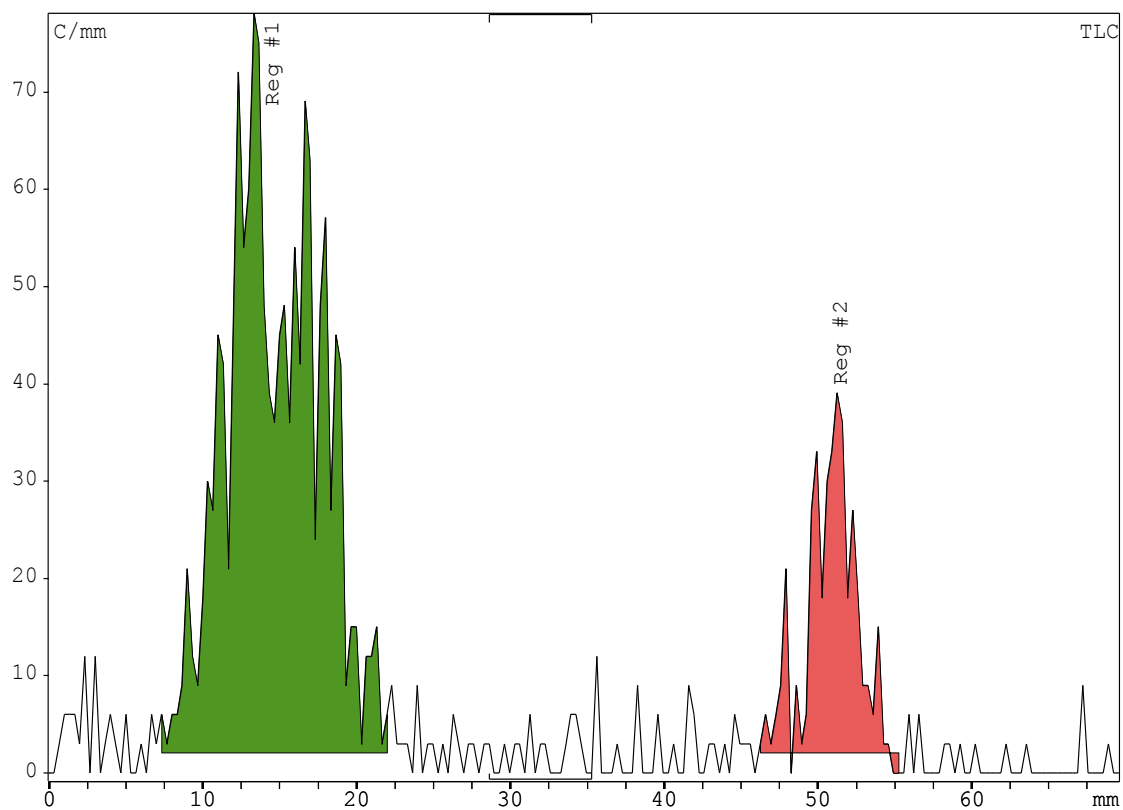


**Figure LXXXIV Radiochemical incorporation into 4a) together with 2 equivalents of 7f)**